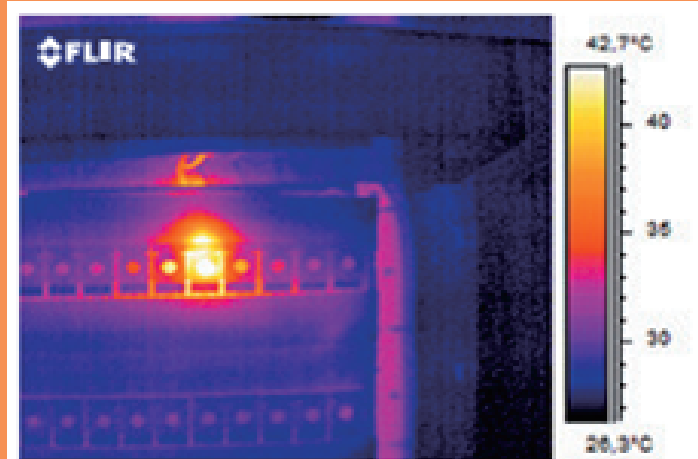
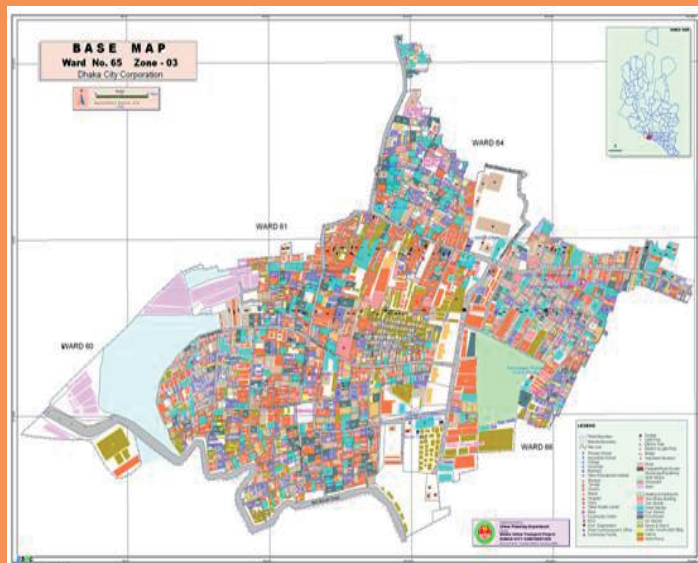
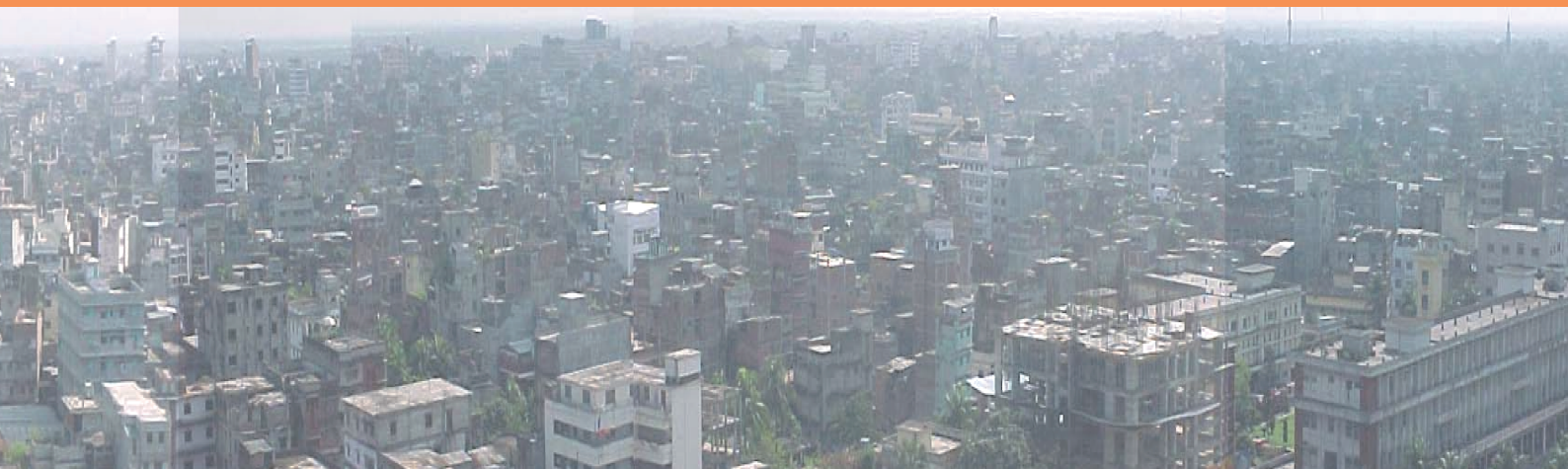


**BANGLADESH NETWORK
OFFICE FOR URBAN SAFETY**

BNUS ANNUAL REPORT-2014



One of the fuses is overheated, a potential





**BANGLADESH NETWORK
OFFICE FOR URBAN SAFETY**

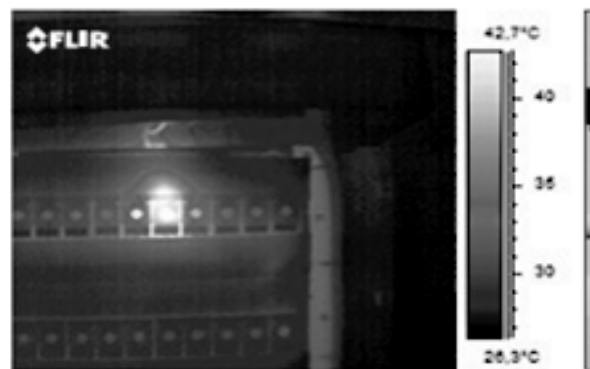


BNUS ANNUAL REPORT-2014

BANGLADESH NETWORK OFFICE FOR URBAN SAFETY BUET, DHAKA, BANGLADESH

Prepared By:

Mehedi Ahmed Ansary

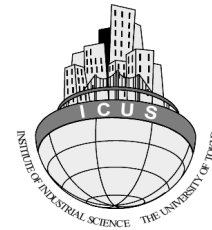


One of the fuses is overheated, a potential





**BANGLADESH NETWORK
OFFICE FOR URBAN SAFETY**

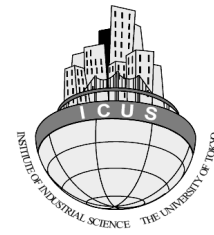


CONTENTS

PART-I: ASSESSMENT OF UNDERLYING CAUSES OF FIRE RISK IN OLD DHAKA: A CASE STUDY OF ISLAMBAG AREA OF WARD NO. 65 OF DHAKA SOUTH CITY CORPORATION	1
PART-II: MEASUREMENT OF VIBRATION ON PLOON TEXTILE BUILDING DUE TO FREQUENT MOVEMENT OF RAILS.....	19
PART-III: FOUR RECENT FIRE INCIDENCES IN AND AROUND DHAKA CITY	39
PART-IV: DISASTER MANAGEMENT SYSTEM OF DHAKA IN COMBATING MAN-MADE DISASTER IN THE LIGHT OF RECENT FIRES AND BUILDING COLLAPSES	45
PART-V: RESCUE OPERATION OF A 4-YEAR CHILD, JIHAD FROM AN ABANDONED DEEP TUBEWELL	61
PART-VI: GPR TESTING ON BALL MILL FOUNDATION.....	73
PART-VII: EARTHQUAKE RISK ASSESSMENT AND PLANNING FOR MANAGEMENT IN MYMENSINGH MUNICIPALITY, BANGLADESH	77
PART-VIII: EVALUATION OF LOAD CARRYING CAPACITY OF PRECAST CONCRETE PILES BASED ON CPT.....	101
PART-IX: MEASUREMENT OF VIBRATION ON UHA TRADE CENTER.....	127
PART-X: COMPARISON BETWEEN SMA AND MICROTREMOR MEASUREMENT AT JAMUNA BRIDGE SITES.....	143
PART-XI: MEASUREMENT OF SHEAR-WAVE VELOCITY AT DIFFERENT LOCATIONS OF DHAKA CITY USING SEISMIC REFRACTION	171
PART-XII: MEASUREMENT OF ELECTRICAL RESISTIVITY AT DIFFERENT LOCATIONS OF DHAKA CITY	191



**BANGLADESH NETWORK
OFFICE FOR URBAN SAFETY**



PART-I

ASSESSMENT OF UNDERLYING CAUSES OF FIRE RISK IN OLD DHAKA: A CASE STUDY OF ISLAMBAG AREA OF WARD NO. 65 OF DHAKA SOUTH CITY CORPORATION

**BANGLADESH NETWORK OFFICE FOR URBAN
SAFETY (BNUS), BUET, DHAKA**

Prepared By: Uttama Barua

Mehedi Ahmed Ansary

1. Introduction

Incident of fire is hazardous when it results in loss of human life and economy. In urban areas the effect of fire hazard is much more in comparison to other areas because of the development pattern and land use. In Dhaka, the capital city of Bangladesh, fire hazards cause huge life and economic loss every year (BSFCD). The causes behind such large scale fire hazards in the city are: violation of building codes and non-compliance with the Firefighting and Extinguishing Law, dense building concentrations, lack of safety measures, narrow roads, flammable building materials and electrical system as well as the lack of resources to raise awareness and response skills (BFSCD, 2003). Particularly in Old Dhaka, incidents of fire hazards are more frequent than any other part of the city. In this area, most of the buildings are of mixed use, where the ground floor and/or the first floor are used for small factories like chemical, plastic, rubber etc., mechanical shop, welding shops, warehouse and food shops, etc. Rests of the floors of the buildings are used for residential purpose mainly for the workers of the factories and shops. Thus, fire hazard vulnerability of Old Dhaka is very high.

In case of fire incidents in Dhaka city, firefighting is a very important job, but fire prevention is more crucial to prevent an actual fire accident from happening. In general, fire protection equipments and the use of fire fighting tools are given more emphasis, neglecting the importance of practicing fire preventive measures. The purpose of fire prevention plan is to eliminate the causes of fire and to prevent loss of life and property by fire (OSHCON, 2006), for which a clear understanding of underlying cause of fire are required to be identified to take initiatives thereby. Bangladesh, as a developing country, cannot afford the huge amount of loss caused by fire accidents every year in Dhaka city, particularly in Old Dhaka. So, this study aims at assessment of the reasons of fire risk in Old Dhaka to pave the way for the preparation of a fire prevention plan for Old Dhaka. In this study, Islambag area of Ward No. 65 (Figure 1) of Old Dhaka was selected for the assessment. The causes are that, fire incidents are very common phenomenon in this area and this area is one of most vulnerable areas to fire hazard because of its traditional land use and population density. Thus in this study, assessment of fire risk was done to find out potential underlying causes behind fire hazard in Islambag area of Ward 65 of Old Dhaka.



Figure 1: Study Area (Ward No. 65 of Dhaka city) (Source: Dhaka City Corporation)

2. Background of The Study

2.1 Reasons of Fire Hazard

The main reasons for any fire hazard are the sources of fire hazard and other factors accelerating the incident. So, for the assessment of the reasons of fire hazard, firstly it is required to understand its sources. Fires require fuel, an adequate oxygen supply, and an ignition source, i.e., the Fire Triangle, which when brought together, cause fires (Figure 2). Fire prevention can be accomplished by maintaining control over one or more of these three required elements (UoC, 2005).

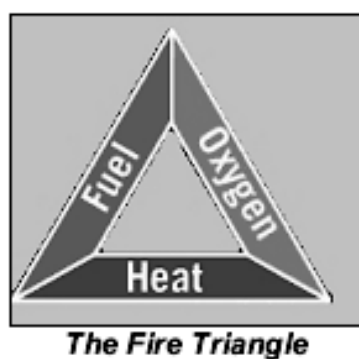


Figure 2: Fire triangle (Source: UoC, 2005)

2.1.1. Ignition Sources or Sources of Heat:

An ignition source is something that can cause an accelerant or flammable material to ignite, e. g. unsafe electrical conditions, machines and equipments, hot work, careless smoking etc (Margentino, & Malinowski, 1992). The ignition sources can pose a fire hazard if they are placed near the combustible materials (EHSS, 2011).

- **Unsafe Electrical Conditions:** The unsafe electrical conditions, e.g. damaged electrical conductors, overloaded sockets, extension cords, multiple plug adapters, faulty wirings, defective switches and outlets, blown fuses, low quality electrical equipment, malfunction of electrical devices, loose electrical connections etc, can all lead to electrical fires (OSHCON, 2006; EHSS, 2011). Use of unapproved electric cords or equipment in wet or damp locations may result in a short circuit (EHSS, 2011).
- **Machines and equipment:** Machines that are not lubricated properly can overheat and start a fire (EHSS, 2011).
- **Hot work:** Any operation involving open flames can present a fire hazard, e.g. welding (EHSS, 2011).
- **Careless Smoking:** Discarded smoking materials carelessly tossed can easily start a fire. (EHSS, 2011)

2.1.2. Sources of Fuel:

Anything that can burn is potential fuel for a fire or, in some cases, an explosion (Margentino, & Malinowski, 1992). Certain types of substances can ignite at relatively low temperatures or pose a risk of catastrophic explosion if ignited (OSHCON, 2006)

- **Combustible Materials:** Ordinary combustible materials, like paper, cardboard, wood, and products made from these materials can present a fire hazard when they are allowed to accumulate or are stored improperly (OSHCON, 2006; EHSS, 2011). Foam or plastic cups, utensils, materials close to heat sources burn rapidly and give off dense, toxic, black smoke (EHSS, 2011). Oily rags or other materials soaked in oil can spontaneously combust if placed in areas where the air does not circulate (EHSS, 2011).
- **Flammable Materials:** Some flammable liquids, such as xylene, toluene, benzene, and gasoline have a tendency to accumulate a static electric charge, which can release a spark that ignites the liquid (OSHCON, 2006; EHSS, 2011). The unsafe use, storage, dispensing, or disposal of flammable materials can be a prime source of fires and explosions (OSHCON, 2006; EHSS, 2011). Accumulation of vapors inside of storage areas of flammable liquids may also cause fire (EHSS, 2011).

- **Accelerants:** Accelerants are substances that increase the speed at which a fire spreads, e.g. gasoline, kerosene, oil, aerosol cans etc, which must be stored in approved containers and properly labeled (Margentino, & Malinowski, 1992). All accelerants are highly flammable or combustible, but not all highly flammable or combustible materials are accelerants (Margentino, & Malinowski, 1992).

2.1.3. Sources of Oxygen:

The main source of oxygen for a fire or explosion is in the general body of air. There are also other sources of oxygen, such as bottled oxygen, compressed air distribution systems and chemicals that release oxygen when heated (oxidizing agents) such as hydrogen peroxide etc (HSE, 2012).

2.1.4. Other Factors

Beyond the main sources of fire, there are other factors which are not responsible for ignition of a fire, but fire protection and ease of fire fighting to reduce loss depend on these factors.

2.1.4.1 Structural Condition:

Spreading of fire and success of fire rescue and firefighting operation largely depend on structural condition. The structural conditions includes, i.e. building material, condition of wall and roof, condition of exit door, condition of stair, etc.

2.1.4.2 Safety Measures:

Safety measures include, width of access road for the access of fire fighting vehicle, availability of fire fighting system and water source etc. Lack of safety measures prevent fire fighting and rescue operation resulting in increased life and property loss.

2.2 Applicability of Thermal Image in Identification of Fire Ignition Source

In this study, thermal image captured by thermal imaging camera has been used for identification of ignition sources of fire in the factories located in the study area. So it is required to understand its applicability in the study for the designated purpose.

2.2.1 The Thermal Imaging Camera and How It Works

A thermal imaging camera is a unique and non-contact tool utilizing infrared thermography which is the art of transforming an infrared image into a radiometric one allowing temperature values to be read from the image. Infrared radiation lies between the visible and microwave portions of the electromagnetic spectrum where heat or thermal radiation is its primary source. Thus the tool produces thermal image indicating the exact location of energy losses through scanning and visualizing the temperature distribution of entire surfaces quickly and accurately providing precise and convincing argumentation (FLIR, 2011a & 2011b).

2.2.2 Use of Thermal Images in Identification of Fire Ignition Source

From the literature review it could have been understood that, the main ignition sources of fire are unsafe electrical condition and overheated mechanical installations. Thermal imaging cameras are powerful and non invasive tools for monitoring and diagnosing these conditions, identifying problems early, allowing them to be documented and corrected before becoming more serious and more costly to repair (FLIR, 2011a).

2.2.2.1 Electrical Fault Detection through Thermal Image

Electrical devices are usually rated in power indicating the maximum amount of energy the device can consume without being damaged (Taib, Jadin, & Kabir, 2012). If an electrical equipment is operated above its specifications, this results in lower efficiency of the device, causing the energy to be spent in generating heat (FLIR, 2011b, Haidar, Asiegbu, Hawari, & Ibrahim, 2012, and Taib, Jadin, & Kabir, 2012). Faulty connections and wiring indicate a loose, over tightened or corroded connection with increased resistance and faulty fuses indicate its saturated capacity, which thus become warm (FLIR, 2011b). If the faulty electrical equipments are left unchecked, heat can rise to the point where connections start to melt resulting in sparks to start a fire (FLIR, 2011a & 2011b).

The radiated heat from an electrical device can be measured on the infrared spectral band of the electromagnetic spectrum using thermal imaging (FLIR, 2011b, Haidar, Asiegbu, Hawari, & Ibrahim, 2012). If the difference in temperature between similar components under similar loads exceeds 15 °C (~25 °F), it indicates requirement of immediate repairs (FLIR, 2011b). Thus, any of the electrical problems can be avoided with the use of a thermal imaging camera, helping to detect anomalies that would normally be invisible to the naked eye and to solve problems before production goes down or a fire occurs (FLIR, 2011b).

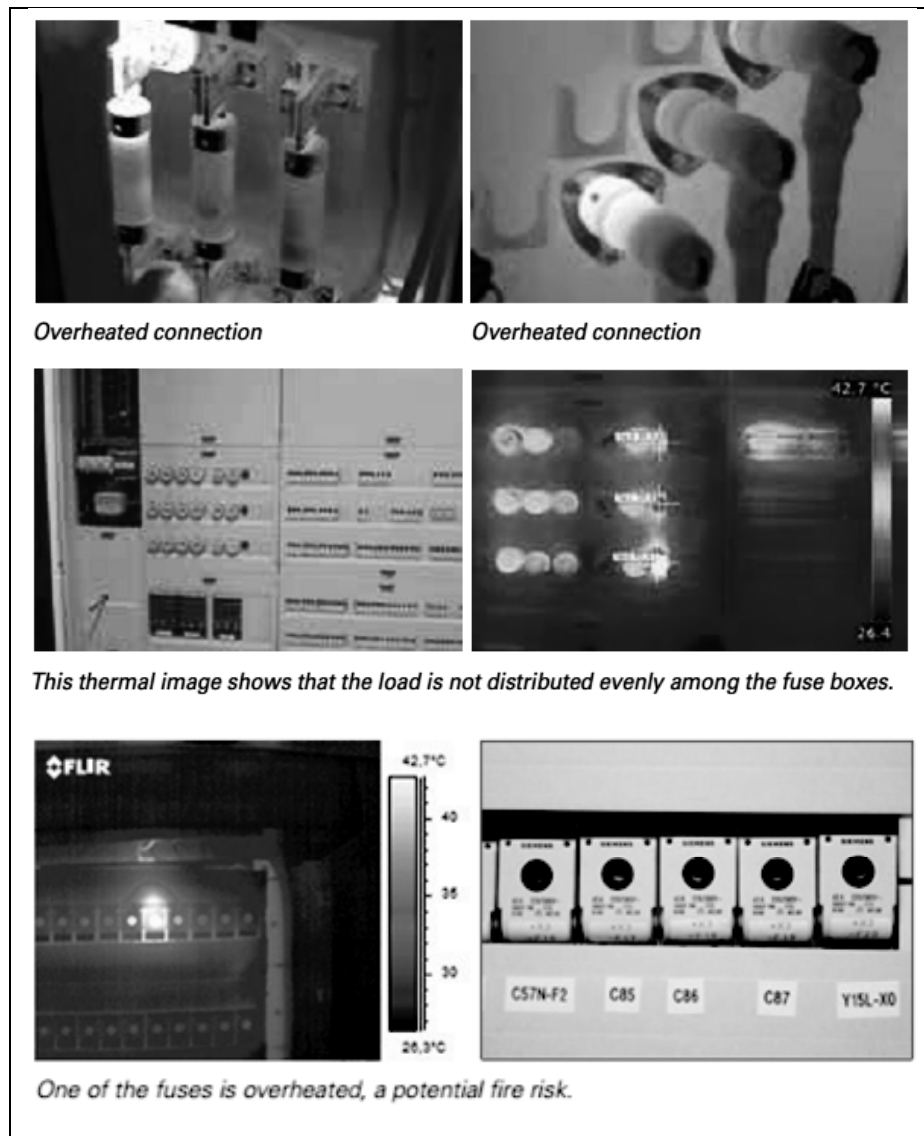


Figure 3: Use of thermal image in detecting faulty electrical instruments

(Source: FLIR, 2011a & 2011b)

2.2.2.2 Overheated Mechanical Installations

Mechanical systems heat up if there is a misalignment at some point in the system, or when mechanical components become worn and less efficient. Again, increased surface temperatures can be the result of internal faults. Excessive heat can also be generated by friction in faulty bearings due to wear, misalignment or inadequate lubrication. When these overheated machines come to contact with electrical equipments or any combustible or flammable materials, this results in fire to ignite. Thermal images help to inspect overheated mechanical installations in the factories. Interpretation of results should be based on comparison between components operating in similar conditions under similar loads (Source: FLIR, 2011b).

3. METHODOLOGY OF THE STUDY

The research has been conducted with the following methodology:

3.1 Study Design

In Old Dhaka fire incidents are very common, but for lack of knowledge about the reasons behind such frequent fire incidents proper initiatives for the fire prevention cannot be taken for the area. Thereby, objective of the study was defined to find out the causes of fire incidents in Old Dhaka. Then methodology of the study was defined based on literature review.

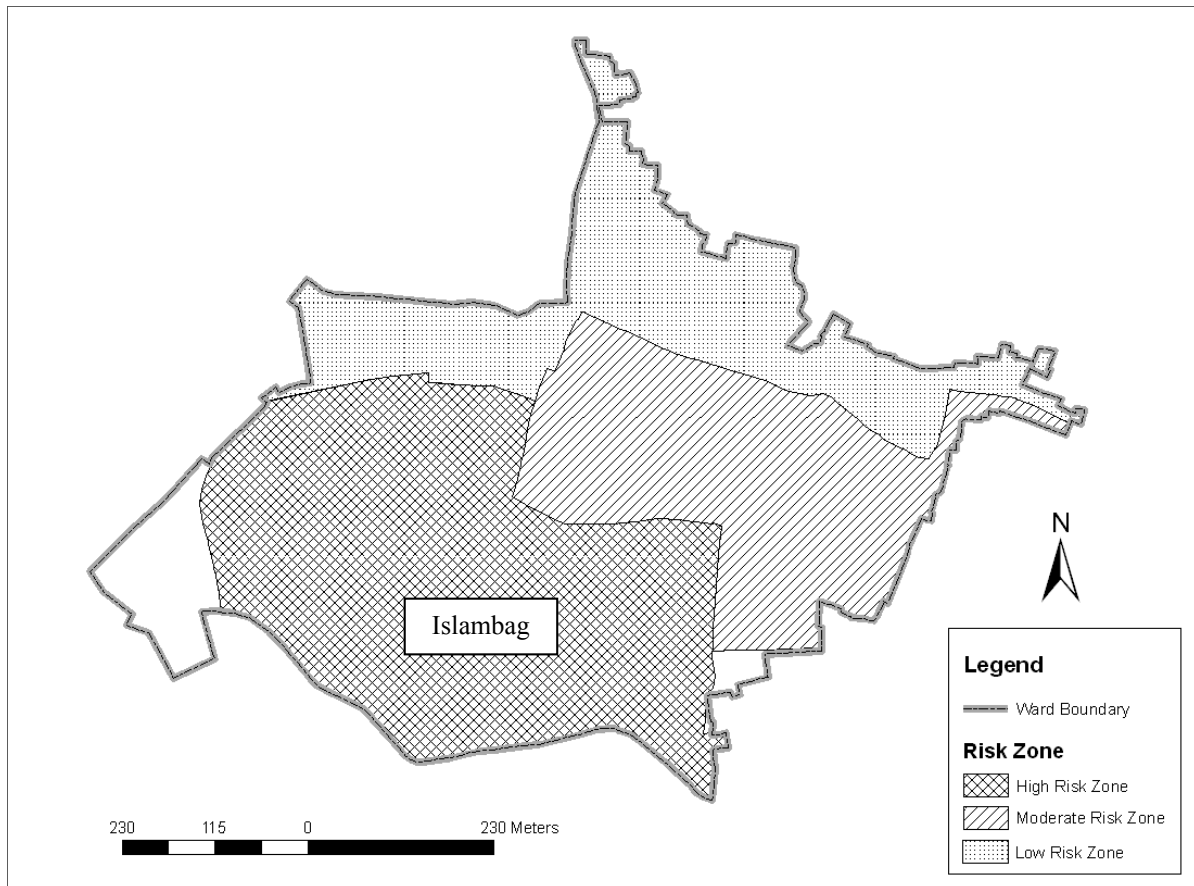


Figure 4: Fire risk zone in Ward 65

3.2 Study Area Selection

The Islambag area of Ward No. 65 of Old Dhaka is selected as the study area. The total area of Ward No. 65 is 118.1668 acres (0.478 Square Kilometer). Ward No. 65 is divided into three risk zones including high risk zone, moderate risk zone and low risk zone according to their land use from expert opinion (Figure 4). High risk zone is 52.84 acres (44.72%) where dominant land use are plastic processing industries; moderate risk zone is 30.89 acres (26.14%) where dominant land use are processing factory and different warehouse (plastic warehouse, cattle food storage etc), and low risk zone is 27.95 acres (23.65%) where dominant land use are residential use with commercial facilities (retail shop, office, bank and storage) (calculated from GIS). Islambag area lies in the high risk area as the livelihoods of the inhabitants of this area are primarily based on plastic processing industries like

plastic manufacturing, recycling and processing factories. This area also displays a high building density with multi-storey buildings and very few urban public spaces left. So, this area is selected as the study area.

3.3 Preparation of Questionnaire

For achieving the objectives, depending on the literature review a questionnaire for the study has been designed which has been modified on the basis of findings from pilot survey. The questionnaire is given in Appendix-A.

3.4 Sampling

In Islambag area twenty factories were selected as sample for the analysis through random selection.

3.5 Data Collection

3.5.1 Base Map Collection

A base map of the study area was collected from Dhaka City Corporation (DCC) office to become familiar with the environment of the study area.

3.5.2 Primary Data Collection

Field survey of the buildings was conducted on the basis of the DCC base map. The survey was conducted in the study area to find out the causes of fire incidents in the study area involving visual assessment and questionnaire survey.

3.6 Data Processing and Analysis

Information collected from the survey, have been inputted in MS Excel and then converted to SPSS 12 for processing and analysis.

3.7 Finding out Reasons behind Fire Hazard in the Study Area

The reasons behind fire hazard in the study area was assessed by identification and observation of the sources of fire hazard, i.e. ignition sources, sources of ignition, fuel and oxygen, assessment of structural condition, and identification and observation of availability of safety measures. Considering these factors, the methodology for fire hazard assessment was developed, which involves both questionnaire survey and visual assessment. According to the reasons, the assessment process has been divided into five segments:

- ***Assessment of the Ignition Sources:*** Through visual assessment and questionnaire survey, electrical conditions, condition of mechanical equipments, hot works and smoking condition were assessed. To detect unsafe electrical and mechanical conditions thermal images were used, which detect faults through thermal radiation, i.e. temperature difference.
- ***Assessment of the Fuel Sources:*** Through visual assessment and questionnaire survey, condition and storage of combustible materials, flammable materials and accelerants were assessed.

- **Assessment of the Oxygen Sources:** Through visual assessment and questionnaire survey, condition of ventilation and air circular system were for the oxygen source.
- **Assessment of Structural Condition:** Through visual assessment and questionnaire survey, the structural conditions, i.e. building material, condition of wall and roof, condition of exit door, condition of stair, etc were assessed.
- **Assessment of Safety Measures:** Through visual assessment and questionnaire survey, safety measures, i.e. width of access road for the access of fire fighting vehicle, availability of fire fighting system and water source etc were assessed.

3.8 Preparation of Final Report

All information and finding were gathered and presented by tables, graphs and maps to prepare the final report. Some recommendations based on the findings are provided to improve the overall conditions of Old Dhaka in the report.

4. Reasons of Fire Hazard in the Study Area

Fire hazards are mainly initiated in the factories or small scale industrial buildings in the study area. In this study, 20 number of buildings have been surveyed which are mainly factories or small scale industrial buildings. In the following section of the report, detailed findings from the survey have been described.

4.1 General Condition of the Buildings in the Study Area

Number of storey of the surveyed buildings ranged from one to seven. Table 1 shows the frequency of buildings surveyed with respect to occupancy and number of storey. Most of the surveyed buildings are plastic factory all of which are one storied. The buildings with greater than one floor are mainly of mixed use.

Table 1: Frequency of the building surveyed with respect to building occupancy and number of floors

Building occupancy \ No. of floors	No. of floors			Total
	1 Floor	2 Floors	Greater than 2 floors	
Welding Shop	1	0	0	1
Plastic Factory	7	0	0	7
Plastic Storage	1	0	0	1
Machine Shop	1	0	0	1
Welding shop and plastic storage	0	1	0	1
Welding shop and residential use	0	1	1	2
Machine shop and residential use	0	0	2	2
Plastic storage and residential use	0	0	1	1
Plastic factory and residential	0	0	1	1
Plastic shoe factory	1	0	0	1
Machine shop and plastic storage	0	1	0	1
Plastic shoe factory and residential	0	0	1	1
Total	11	3	6	20

4.2 Ignition Sources or Sources of Heat in the Study Area:

Figure 5 shows ignition sources of fire in the surveyed buildings with respect to number of buildings containing the source. The main ignition sources in the surveyed buildings are the unsafe electrical conditions. In the study area, the overhead electric supply pole and wires are arranged in much disorganized way, which may cause rapid spread of fire in the area. Almost all the surveyed buildings pose similar electrical unsafe conditions which include: improper wiring system, defective switches and outlets, defective fuses, cable conduit on wall not clipped properly and low quality electrical equipments, among which use of low quality equipments, defective wiring system, and defective cutouts and fuses are most common (Figure 5).

Among the surveyed buildings, plastic factories and machine shops contain machines and equipments. Most of the machines are not lubricated properly causing overheating. Thus, nine buildings among twenty have the problem of overheated machine (Figure 5). Moreover, for lack of proper maintenance, the machines and equipments used in the factories have a layer of oil cover which accelerates the possibility of ignition of fire. In these factories, the electric equipments and machines are observed in close proximity, which increase the risk of fire hazard.

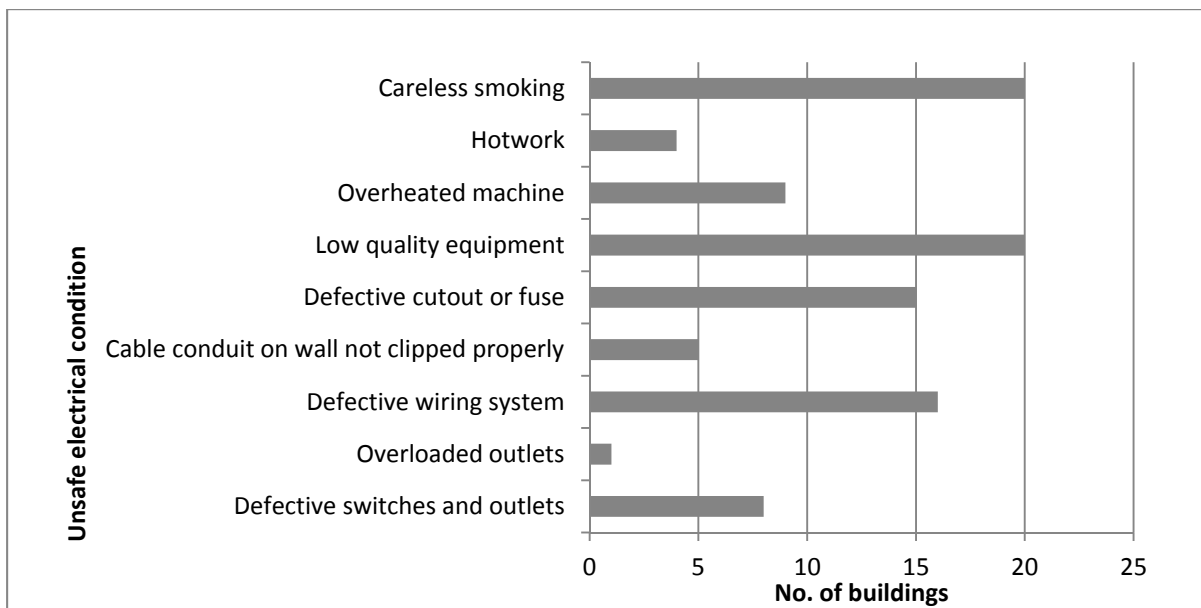


Figure 5: Fire ignition sources in the study area

In the welding shops, the operations involve hot works which produce open flame. In all the surveyed buildings, careless smoking is very common according to the workers. Other significant ignition source that was observed in one of the plastic storage is the use of candle light at the time of load shedding. Close proximity of the stored plastic materials and candle light may also cause a fire to initiate. One of these factors may contribute to ignition of fire in the buildings and the study area.

4.3 Sources of Fuel in the Study Area:

Figure 6 shows sources of fuel of fire in the surveyed buildings with respect to number of buildings containing the source. Most common combustible materials used, produced and preserved in the surveyed buildings are plastic products and materials soaked in oil (Figure 6). Others include oily rags or other materials soaked in oil. In plastic and shoe factories, flammable materials are used for plastic productions which are stored in an unsafe manner. In storages no flammable materials are required, but the plastics itself are combustible which are stored in the storages in an unsafe manner. Other accelerants used in the surveyed buildings include oil. In mechanical shops oil is used for proper functioning of the machines. Again close proximity of ignition sources and fuel sources increase the risk of fire hazard in the area.

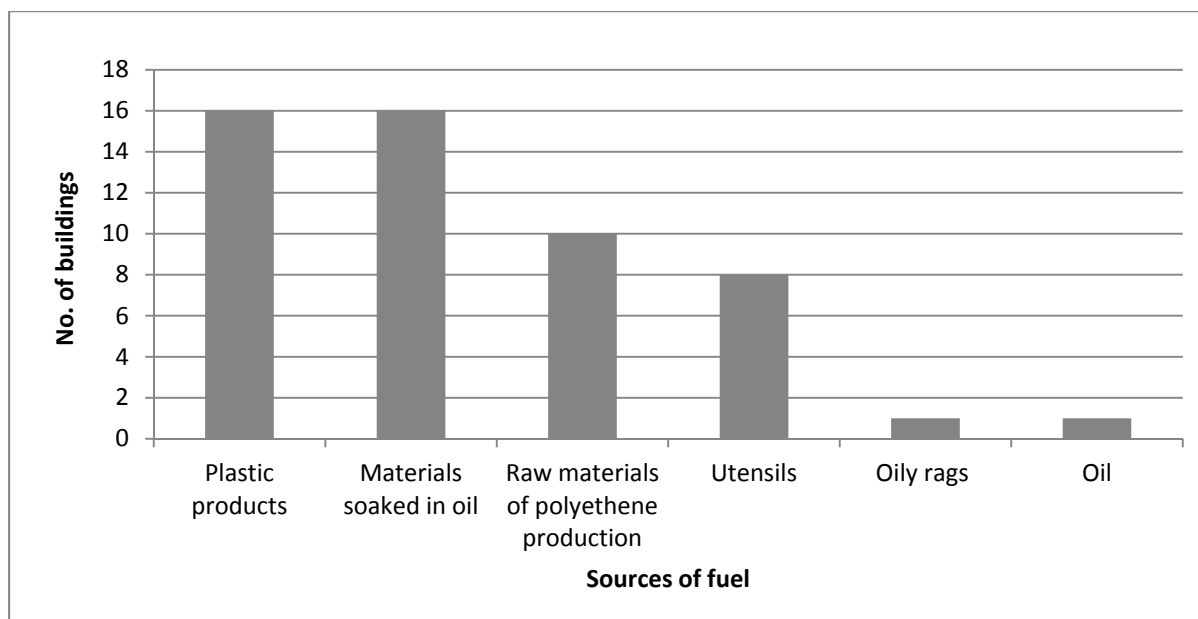


Figure 6: Sources of fuel of fire in the study area

4.4 Sources of Oxygen in the Study Area:

For assessment of sources of oxygen in the study area, the air circulation systems in the buildings were assessed. In plastic factories and storages, smoke and heat vents are installed, whereas in machine shop and welding shops there are no sufficient ventilation systems. Thus among twenty surveyed buildings thirteen buildings have smoke and heat vents, among which seven have sufficient ventilation. In storages of plastic materials, heat vents are mainly located in the walls which are mostly small in size, very few in numbers and are placed in distant locations. In plastic factories, heat vents are mainly located in the ceilings which are mostly large in size as the plastic production activity creates greater heat and smoke. In all the cases, smoke and heat vents are kept open. Thus among thirteen buildings, Thus, most of the buildings lack proper air circulation system, which may result in rapid spread of fire in the area.

4.5 Structural Condition in the Study Area:

Spreading of fire and success of fire rescue and firefighting operation largely depend on structural condition. The structural conditions includes, i.e. building material, condition of wall and roof, condition of exit door, condition of stair, etc. Figure 7 shows components of building structures in the surveyed buildings according to building material with respect to number of buildings. The structures made of brick have heat resistance time of three hours and concrete have heat resistance time of three hours (Brick Industry Association, 2008 and Beall, 1994). Thus the buildings with components made of brick are safe for fire hazard. The buildings of single storey are constructed with tin roof which are

highly vulnerable to fire. The buildings with two storeys are constructed with wooden roof and the second floors are constructed of tin and wood, which are also highly vulnerable to fire hazard.

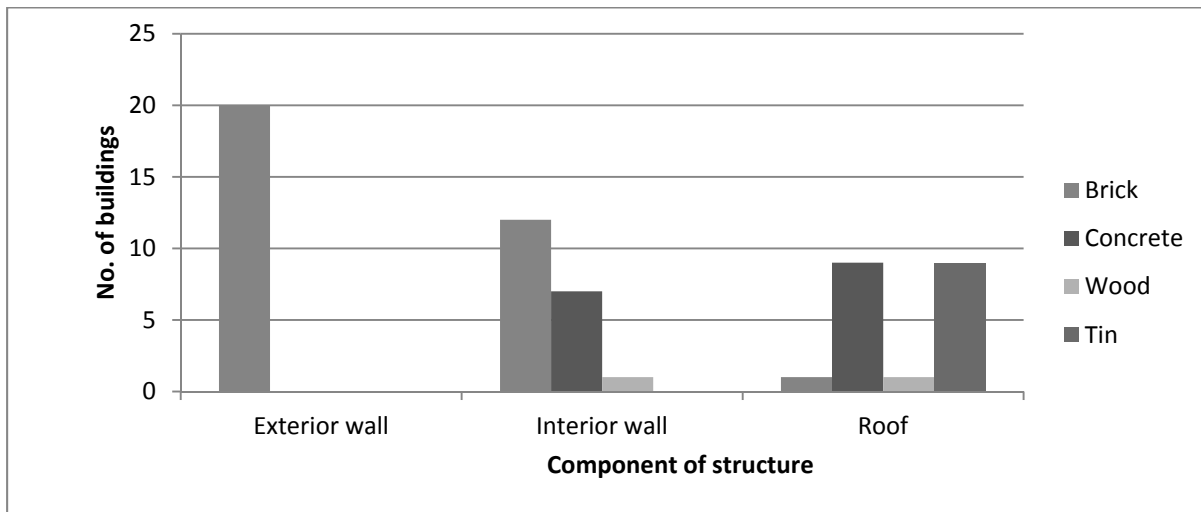


Figure 7: Component of structure with respect to material in the surveyed buildings

The minimum safe dimension of exit doors is minimum two feet width and minimum seven feet height, which is required for safe evacuation. In all of the factories, the exit doors are steel shutter, which are wide enough. Thus, sixteen out of twenty buildings have safe exits which are suitable for evacuation. Figure 8 shows condition of stairs in the surveyed buildings with respect to number of buildings. Among twenty surveyed buildings nine have stairs, among which seven buildings have concrete stair and two have steel stairs. Steel stairs are highly vulnerable to fire hazard due to its heat capacity. Stairs are the weakest part of a construction, whereas in the surveyed buildings the stairs are in deteriorated condition. Among nine buildings with stair, four do not have landing ventilation, three have obstruction in stairway and four have handrails. Thus, only two are suitable with respect to general condition of stair and seven are suitable with respect to dimension. So, conditions of the stairs are required to be improved. Thus, structurally the surveyed buildings are highly risky to fire hazard.

4.6 Availability of Safety Measures in the Study Area:

In most of the cases, width of access roads is on an average 15 ft. Thus, in case of any fire incident, fire vehicles will be able to enter the area through the adjacent roads, though they will have to continue the fire fighting operation on feet within the narrow access roads. Among twenty surveyed buildings, only two have fire fighting operation system. Again only six buildings among twenty have water source through underground and overhead tank due to their mixed use with residential use. Moreover, capacities of these water sources are not sufficient. According to Bangladesh National Building Code, buildings should have underground reservoir of 50000 liters and overhead reservoir of 25000 liters (BNBC, 2006). Thus, safety measures are not sufficient in the buildings.

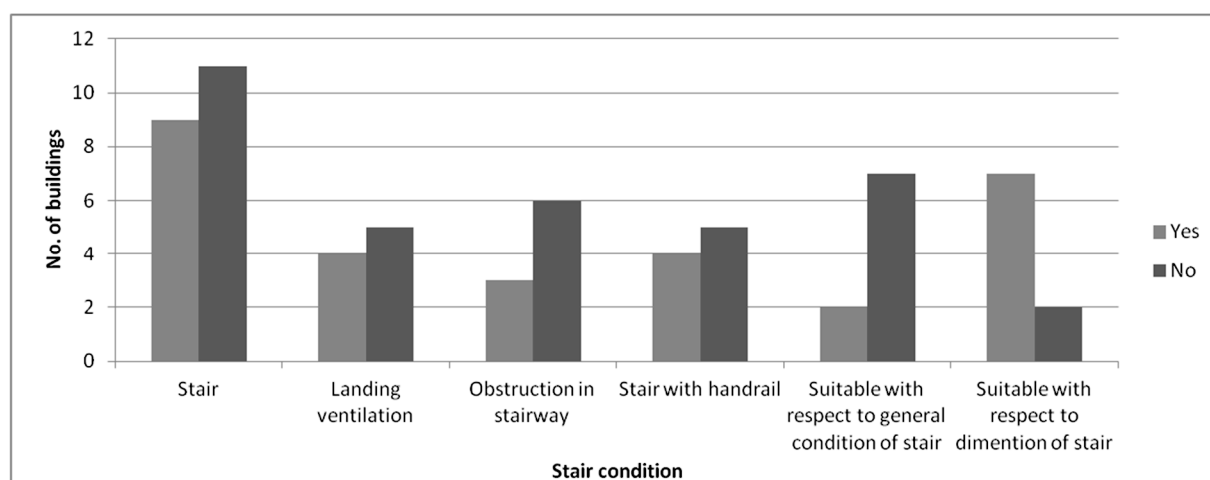


Figure 8: Condition of stair in the surveyed buildings

5. Prevention Strategy

Based on the findings of the study, fire prevention plan can be developed for the small scale industrial buildings of Old Dhaka to avoid any fire or explosion risks by eliminating either the potential ignition sources or potential fuel sources, or both (HSE, 2012). However, it is not possible to eliminate all the sources, so strategies can be developed to reduce fuel loads, eliminate ignition sources or prevent the fuel/ignition interaction by keeping potential ignition sources apart from potential fuel, then fire loss and human death and injury can be reduced (HSE, 2012). Particular strategies to prevent fire hazard in Old Dhaka are described below:

- Faulty electrical issues should be taken care of. The relevant strategies should include: correction and improvement of wiring system, replacement of damaged wiring, fuses, switches and plugs, avoid use of extension cords and ensure proper covering of all outlets, junction boxes and electrical panels.
- Machines and equipments should not be used by overloading their capacities to prevent overheating. Other measures should include: cleaning of all work areas of oil to prevent buildup and all power equipments should be turned off or unplugged after use.
- Hot works, i.e. welding or working with an open flame or other ignition sources, should be done in controlled and well-ventilated areas.
- Smoking should be strongly prohibited in the work place.
- Combustible or flammable materials should be kept in safe distance from the potential ignition sources and should be stored in safer places.
- Well ventilation in workplace should be ensured.

- Regular inspection in the factories should be ensured to keep the work place free of dust. The equipments should be kept in good working order, i.e., inspect electrical wiring and appliances regularly and keep motors and machine tools free of dust and grease. Electrical equipments should be turned off when not in use.
- Minimum fire protection instruments should be stored in the factories. Based on the type of source of a fire hazard, different fire protection instruments should be used, as some fire may be sensitive to certain types of fire extinguishers. Based on source of fire, fire incidents may be classified into five classes, for which certain extinguishing media may be required, which is shown in table 2.

Table 2: Classification of fire with respect to source and required extinguishing media

Class of fire	Materials causing the fire	Extinguishing media required and their characteristics	Extinguisher that should not be used
A	Ordinary combustible material: wood, paper, rags, rubbish, rubber and plastic.	Water and dry chemicals: Douse flames quickly and prevent spreading of fire.	
B	Flammable or combustible gases and liquids: gasoline, kerosene, thinners, paints, grease and similar materials.	Carbon dioxide, dry chemicals, foam and halogenated hydrocarbons: Limit supply of air. Water spray: to cool the containers which are likely to catch fire.	Water: Use of water may spread the fire.
C	Electric equipments	Carbon dioxide or dry powders: Non-conducting materials.	Water and foam: They may cause short circuiting, electric shock and damage to the equipment.
D	Metals: Magnesium sodium, titanium, potassium, zirconium.	Special extinguishing agents.	Normal extinguishing agents: Increase intensity of fire.

Source: Adopted from AmeriCares, n.d.

6. Conclusion

After an in depth assessment of the buildings with commercial and industrial use in Old Dhaka, it can be said that the buildings are vulnerable to fire hazard and the overall condition of buildings are not suitable for fire fighting. Although this study was not conducted on a large number of building samples, it represents the miserable condition of the buildings in Old Dhaka increasing the risk of fire hazards in the area. It is not possible to eliminate all the sources of fire hazard in the area, but at least some initiatives can be taken to minimize the loss. Thus, for improving the condition some fire prevention

strategies have been suggested in this study. For further development in the area, all buildings should follow the provision provided by Bangladesh National Building Code and Bangladesh Fire Service and Civil Defense during construction. To prevent violation of regulation strict inspection and actions are required from corresponding authority. The good practices of fire hazard prevention in the building codes of other countries need to be studied and adopted according to Bangladesh's context. In addition, to create public awareness, workshops and seminars may be arranged. Electronic and printing media can play an important role for increasing awareness. A pragmatic fire safety plan may be developed for all the buildings with the help of Bangladesh Fire Service department.

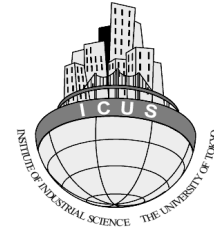
References

- Bangladesh Fire Service and Civil Defense (BFSCD). (2003). *Fire Fighting & Extinguishing Law*. Bangladesh National Building Code (BNBC). (2006). Published by HBRI-BIDS.
- AmeriCares. (n.d.). *Fire Prevention and Fire Safety: Health Worker Safety Training Module 5*. Retrieved October 11, 2014, from:
<http://www.americares.org/assets/downloads/pdf/modules/hws/HWS-5-fire-safety.pdf>
- OSHCN. (2006). *Sample Written Program for Fire Prevention Plan*. Occupational Safety and Health Consultation Program (OSHCN), Texas Department of Insurance, Division of Workers' Compensation, Publication No. HS03-013A (1-06). Retrieved October 11, 2014, from:
<http://www.tdi.texas.gov/pubs/videoresource/ofirepreventio.doc>
- EHSS. (2011). *Fire Prevention Planning*. Environmental, Health and Safety Services (EHSS), Virginia Polytechnic Institute and State University. Retrieved October 11, 2014, from:
http://www.ehss.vt.edu/uploaded_docs/200802261709470.Fire%20Prevention%20Planning.ppt
- UoC. (2005). *Basic Fire Prevention Measures*. Environmental Health and Safety, Division of Agriculture and Natural Resources, University of California, Safety Note #72. Retrieved October 11, 2014, from:
<http://safety.ucanr.org/files/1468.pdf>
- Margentino, M. R., & Malinowski, K. (1992). *Fire prevention and safety measures around the Farm*. Rutgers Cooperative Extension, University of New Jersey: document FS608. Retrieved October 11, 2014, from:
http://nasdonline.org/static_content/documents/1048/d000843.pdf
- HSE. (2012). *Guidance on the prevention and control of fire and explosion at mines used for storage and other purposes*. Great Britain: Health and Safety Executive (HSE). Retrieved October 11, 2014, from:
<http://www.hse.gov.uk/mining/festorage.pdf>

- Beall, C. (1994). Calculating Masonry's Fire Resistance. *Mag. Masonry Constr.*, 7(8), 372-391. Retrieved 24 November, 2014 from:
http://www.masonryconstruction.com/Images/Calculating%20Masonry%27s%20Fire%20Resistance_tcm68-1375295.pdf
- Brick Industry Association. (2008). Technical Note 16: Fire Resistance of Brick Masonry. Brick Industry Association, Reston, Virginia. Retrieved 24 November, 2014 from:
<http://www.gobrick.com/portals/25/docs/technical%20notes/tn16.pdf>
- FLIR. (2011a). Thermal Imaging Guidebook for Building and Renewable Energy Applications. FLIR Systems AB.
- FLIR. (2011b). Thermal Imaging Guidebook for Industrial Applications. FLIR Systems AB.
- Haidar, A., Asiegbu, G. O., Hawari, K., & Ibrahim, F. A. (2012). Electrical defect detection in thermal image. *Advanced Materials Research*, 433, 3366-3370. Retrieved 24 November, 2014 from:
<http://ro.uow.edu.au/infopapers/2315/>
- Taib, S., Jadin, M., S., & Kabir, S. (2012). Thermal Imaging for Enhancing Inspection Reliability: Detection and Characterization. In Prakash R., V. (Ed.). *Infrared Thermography*. InTech, ISBN: 978-953-51-0242-7. Retrieved 24 November, 2014 from:
<http://www.intechopen.com/books/infrared-thermography/thermal-imaging-forenhancing-inspection-reliability-detection-and-characterization>



**BANGLADESH NETWORK
OFFICE FOR URBAN SAFETY**



PART-II

MEASUREMENT OF VIBRATION ON PLOON TEXTILE BUILDING DUE TO FREQUENT MOVEMENT OF RAILS



**BANGLADESH NETWORK OFFICE FOR URBAN
SAFETY (BNUS), BUET, DHAKA**

Prepared By: Mehedi Ahmed Ansary

1. INTRODUCTION

Managing Director of Ploon Textiles Limited requested us for measurement of vibration on their factory building due to frequent train movement. This report presents the findings of the vibration test carried out at the site on April 18, 2014. Figure 1 shows the location of the surveyed building with sensor locations and Figure 2 show measurement of building vibration using Microtremor observation system.

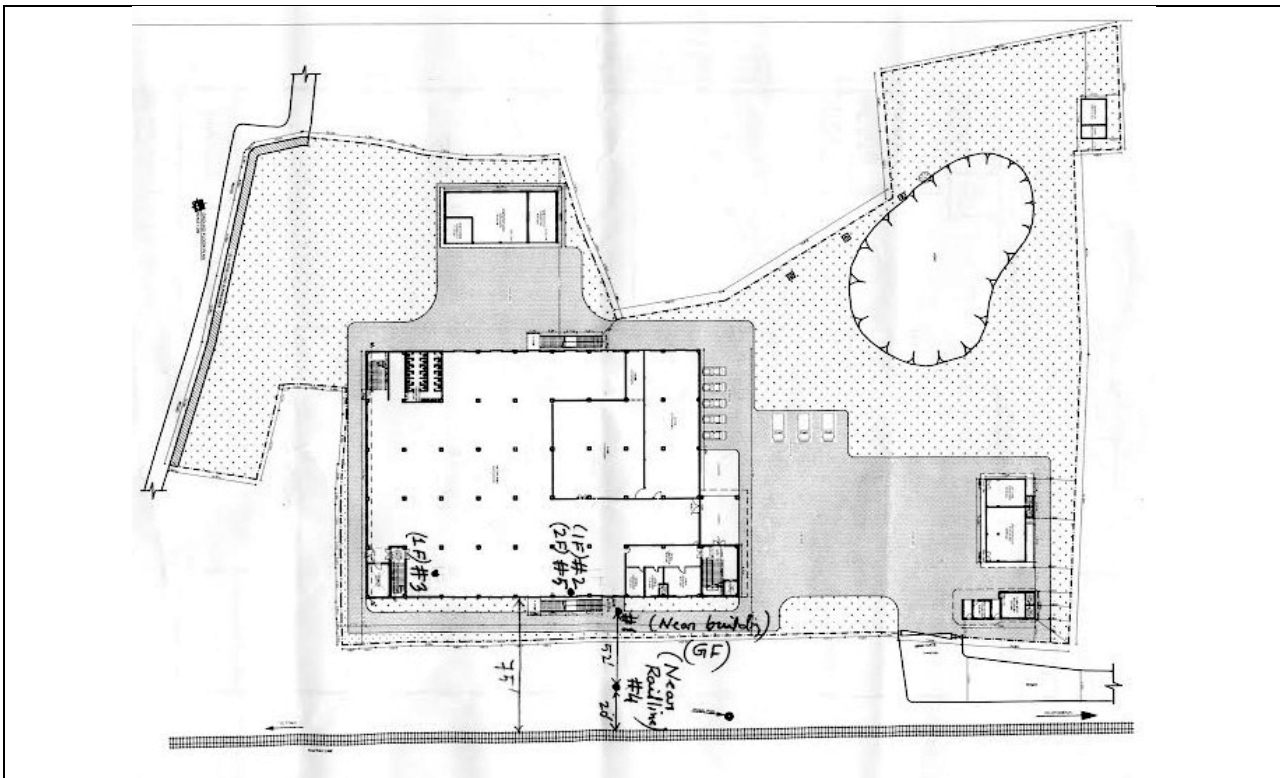


Figure 1: Location of Surveyed Building with Sensor Locations





Figure 2 Measurement of building vibration using Microtremor observation system

2. ACCEPTABLE VIBRATION LEVELS

Humans are very sensitive vertical vibration sensors, especially in environments like quiet buildings. An example of human comfort limit is the restriction on the acceleration - human begins to feel uncomfortable when the acceleration reaches about 0.02g:

$$\ddot{u} = 0,02g = 0,02 \cdot 981 = 196,2 \text{ mm/s}^2$$

Corresponding velocity at 16 Hz frequency is 1.96 mm/s.

According to [1], the allowable level of vibration acceleration at 16 Hz frequency is 28.0 mm/s², while the allowable level of vibration velocity at the same frequency is 0.28 mm/s. The allowable levels of vibration for public buildings according to [1] are shown in Table 1.

Table 1: Allowable levels of vibration for public buildings

Mean geometrical frequency [Hz]	Allowable vibration level along axes X, Y, Z			
	Acceleration		Velocity	
	<i>mm/s²</i>	dB	<i>mm/s</i>	dB
2	10,0	80	0,79	84
4	11,0	81	0,45	79
8	14,0	83	0,28	75
16	28,0	89	0,28	75
31,5	56,0	95	0,28	75
63	110,0	101	0,28	75

Figure 3 shows general limits of displacement amplitude for human beings, machine foundations, and buildings according to Winterkorn and Fang [2].

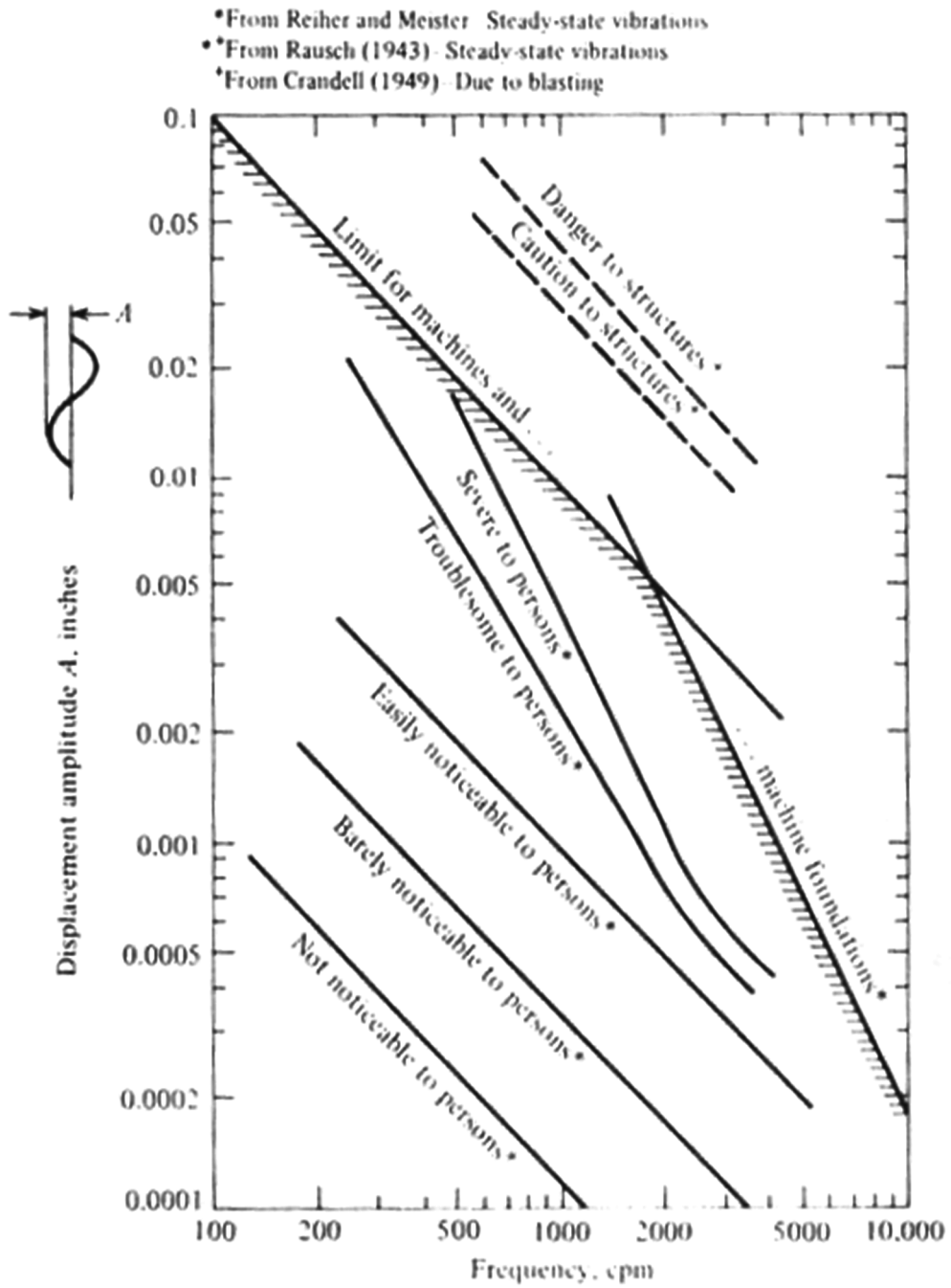
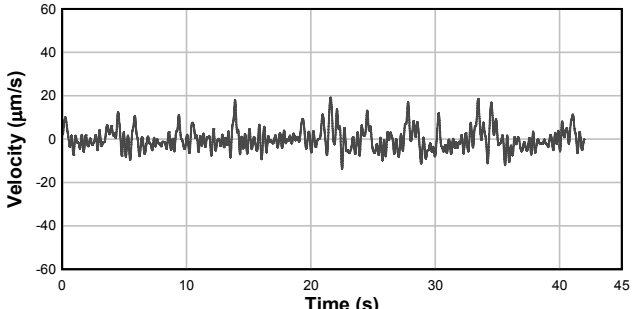
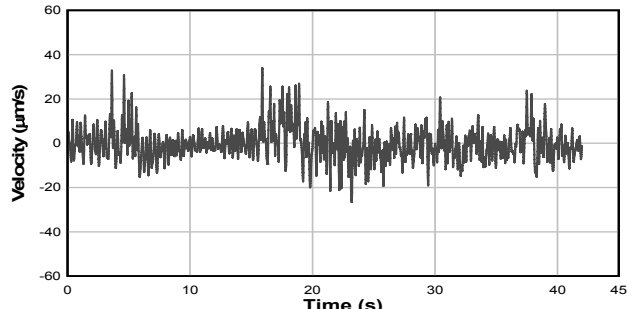
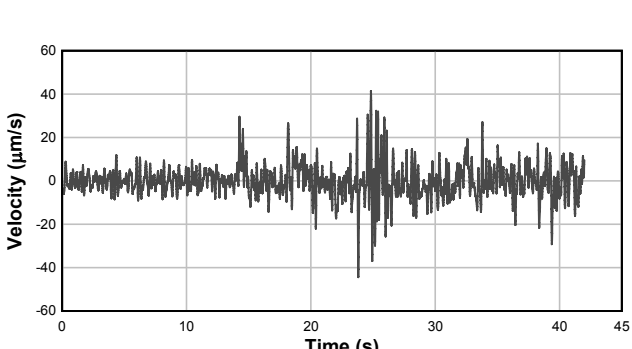
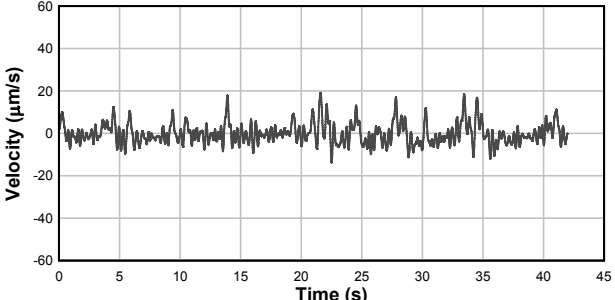
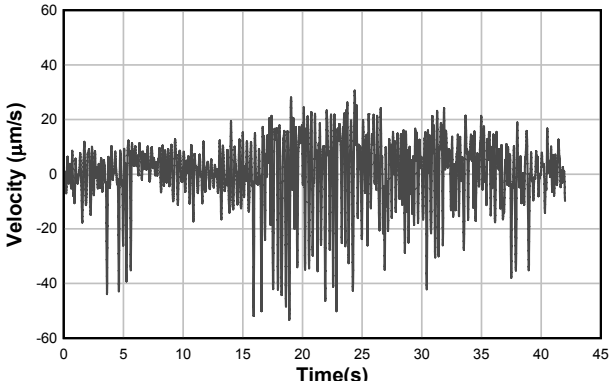
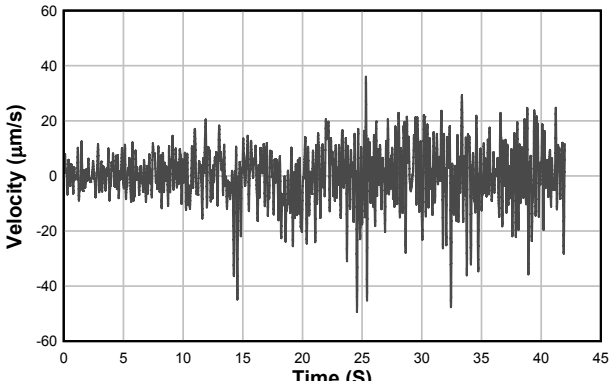


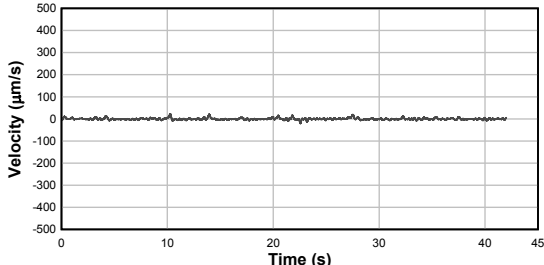
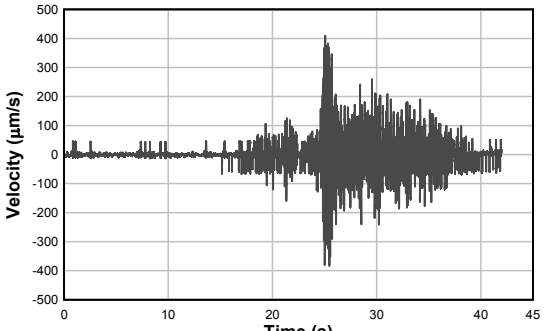
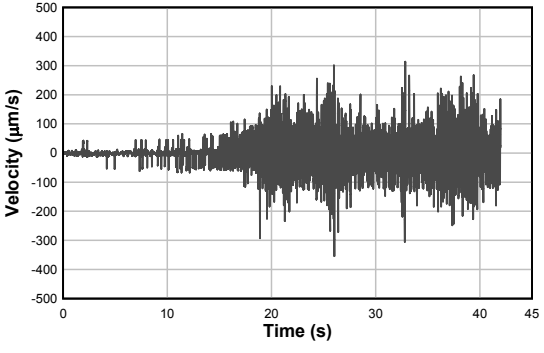
Figure 3 General limits of displacement amplitude for a particular frequency of vibration

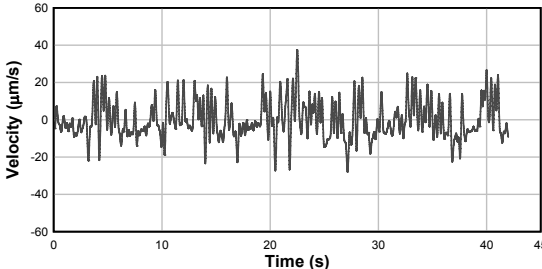
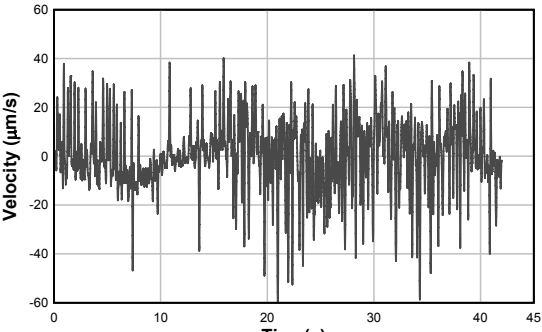
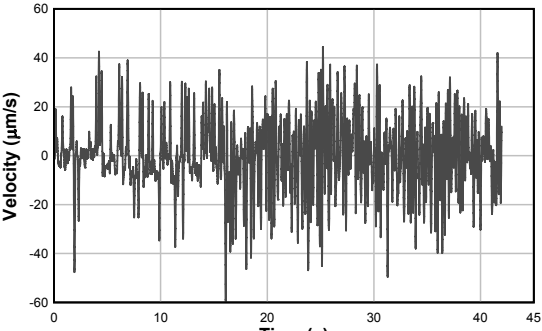
3. MEASUREMENT OF VIBRATION

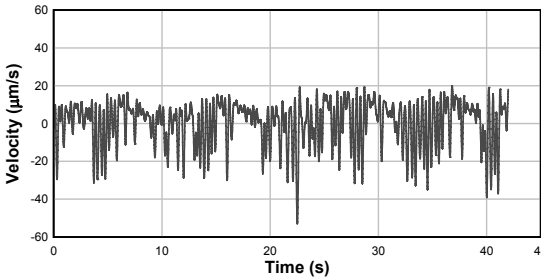
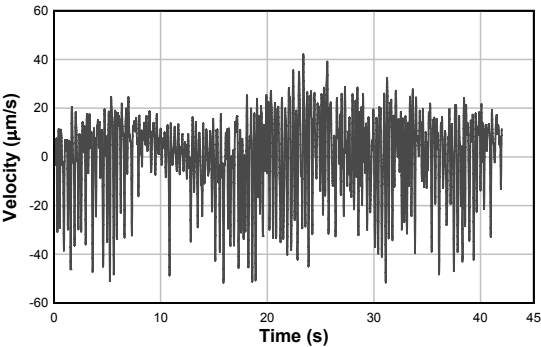
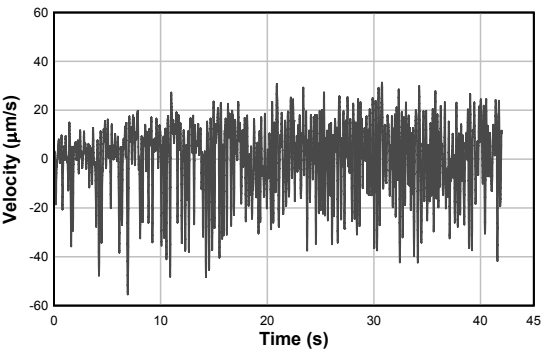
The BUET team conducted vibration test for the Pantaloon Textile building with and without rail movement. The measurement is conducted simultaneously at the ground near the rail line (sensor 4), at the building's ground floor (sensor 1), first floor (sensors 2 and 3) and at the top floor (sensor 5) of the building. In this report, the vibration data for the building which is located around 75 ft from the rail line is presented.

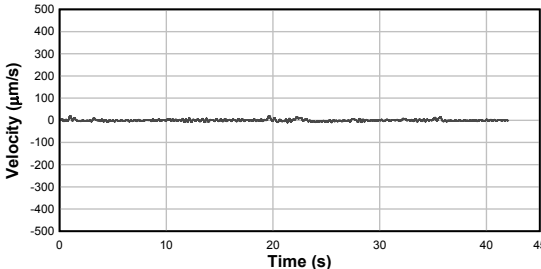
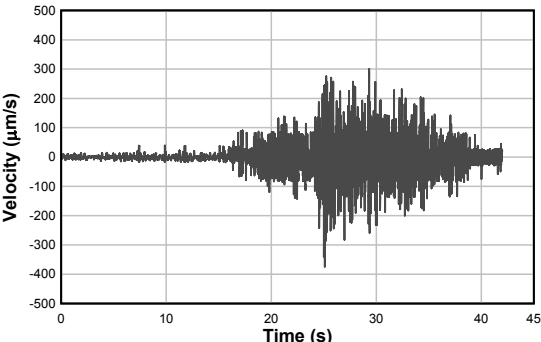
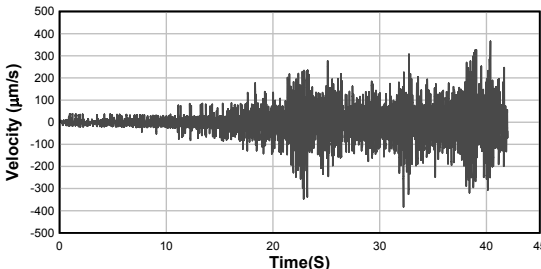
Location: 1X Measurement Mode	Time History	Maximum Velocity ($\mu\text{m/s}$)
Ambient noise		19.2
With noise 8 compartment train		34.0
With noise 15 compartment train		41.4

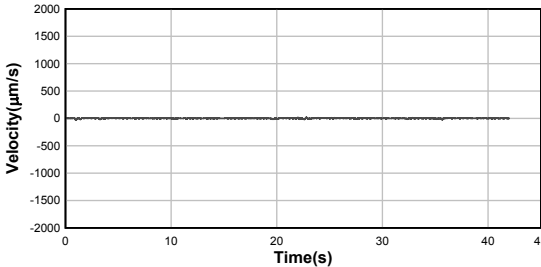
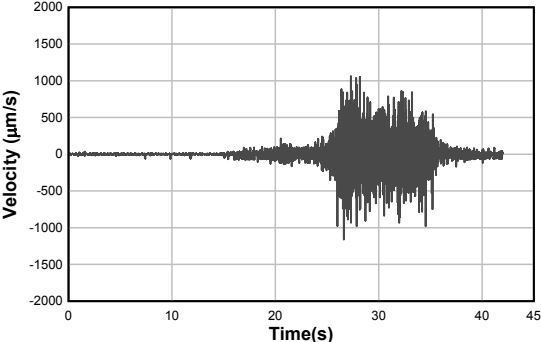
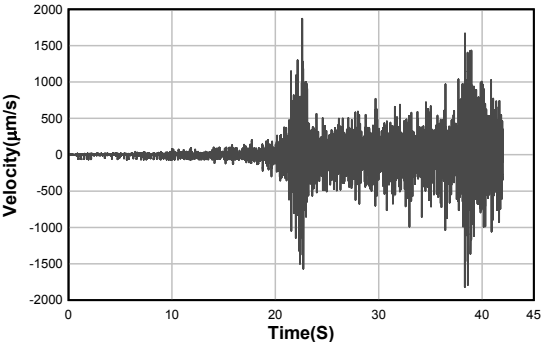
Location: 1Y Measurement Mode	Time History	Maximum Velocity ($\mu\text{m/s}$)
Ambient noise	 <p>A line graph showing velocity in micrometers per second on the y-axis (ranging from -60 to 60) against time in seconds on the x-axis (ranging from 0 to 45). The plot shows low-amplitude, high-frequency noise centered around zero, with most values between -10 and 10 micrometers per second.</p>	19.2
With noise 8 compartment train	 <p>A line graph showing velocity in micrometers per second on the y-axis (ranging from -60 to 60) against time in seconds on the x-axis (ranging from 0 to 45). The plot shows much higher amplitude noise than the ambient case, with several peaks reaching approximately 30 micrometers per second and troughs reaching -30 micrometers per second.</p>	53.4
With noise 15 compartment train	 <p>A line graph showing velocity in micrometers per second on the y-axis (ranging from -60 to 60) against time in seconds on the x-axis (ranging from 0 to 45). The plot shows high-amplitude noise, similar to the 8-compartment case, with a maximum peak of 49.3 micrometers per second.</p>	49.3

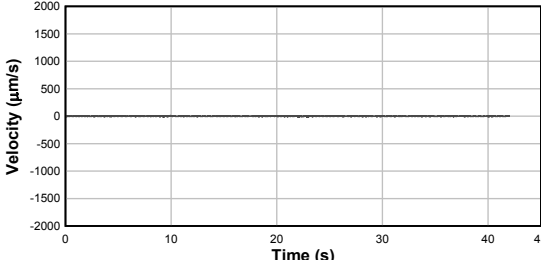
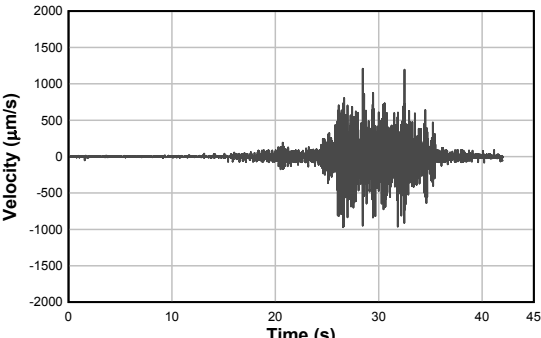
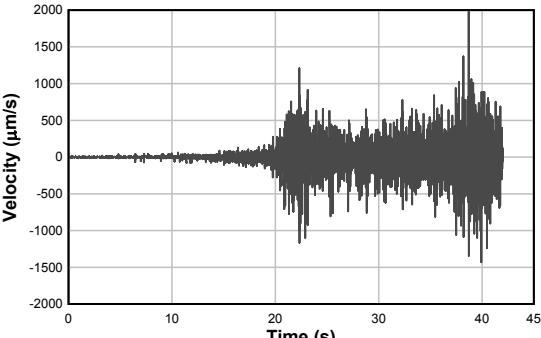
Location: 1Z Measurement Mode	Time History	Maximum Velocity ($\mu\text{m/s}$)
Ambient noise		22.7
With noise 8 compartment train		409.4
With noise 15 compartment train		354.4

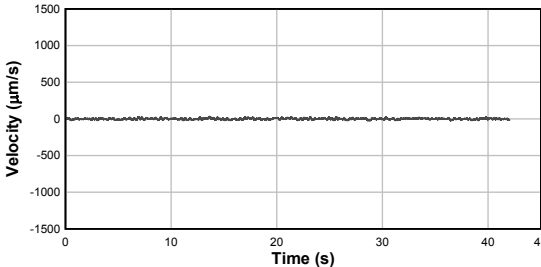
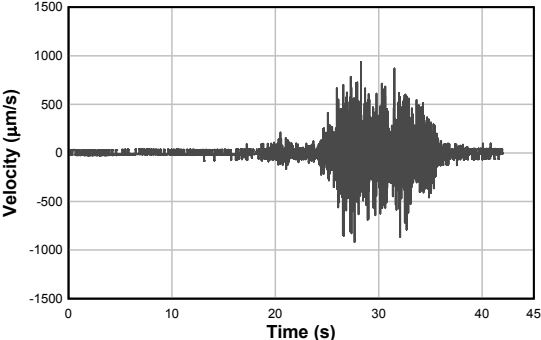
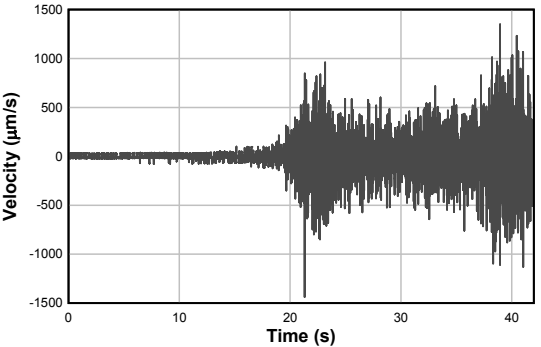
Location: 2X Measurement Mode	Time History	Maximum Velocity ($\mu\text{m/s}$)
Ambient noise	 <p>The plot shows a noisy signal fluctuating around zero. The y-axis is labeled 'Velocity ($\mu\text{m/s}$)' and ranges from -60 to 60. The x-axis is labeled 'Time (s)' and ranges from 0 to 45. The signal amplitude is generally below 20 $\mu\text{m/s}$.</p>	37.6
With noise 8 compartment train	 <p>The plot shows a noisy signal with a higher amplitude than the ambient noise. The y-axis is labeled 'Velocity ($\mu\text{m/s}$)' and ranges from -60 to 60. The x-axis is labeled 'Time(s)' and ranges from 0 to 45. The signal amplitude reaches approximately 40 $\mu\text{m/s}$.</p>	61.3
With noise 15 compartment train	 <p>The plot shows a noisy signal with the highest amplitude of the three. The y-axis is labeled 'Velocity ($\mu\text{m/s}$)' and ranges from -60 to 60. The x-axis is labeled 'Time (s)' and ranges from 0 to 45. The signal amplitude reaches approximately 45 $\mu\text{m/s}$.</p>	62.9

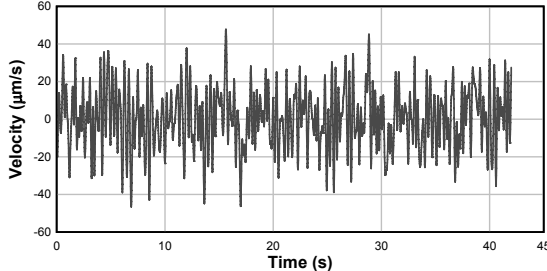
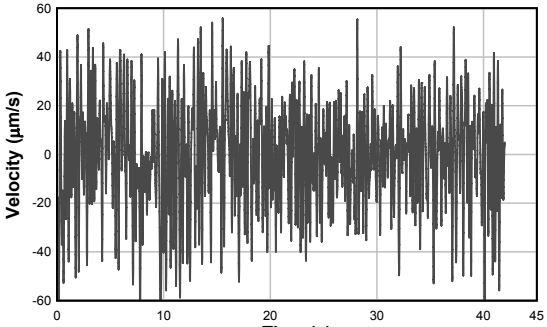
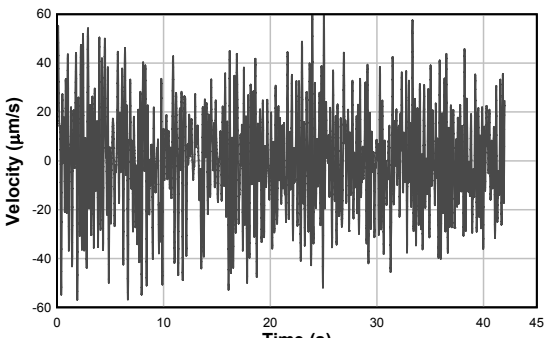
Location: 2Y Measurement Mode	Time History	Maximum Velocity ($\mu\text{m/s}$)
Ambient noise	 <p>The plot shows a highly oscillatory signal centered around zero. The y-axis is labeled 'Velocity ($\mu\text{m/s}$)' and ranges from -60 to 60. The x-axis is labeled 'Time (s)' and ranges from 0 to 45. The signal amplitude is generally between -20 and 20 $\mu\text{m/s}$.</p>	53.0
With noise 8 compartment train	 <p>The plot shows a highly oscillatory signal centered around zero. The y-axis is labeled 'Velocity ($\mu\text{m/s}$)' and ranges from -60 to 60. The x-axis is labeled 'Time (s)' and ranges from 0 to 45. The signal amplitude is generally between -40 and 40 $\mu\text{m/s}$.</p>	51.7
With noise 15 compartment train	 <p>The plot shows a highly oscillatory signal centered around zero. The y-axis is labeled 'Velocity ($\mu\text{m/s}$)' and ranges from -60 to 60. The x-axis is labeled 'Time (s)' and ranges from 0 to 45. The signal amplitude is generally between -40 and 40 $\mu\text{m/s}$.</p>	55.4

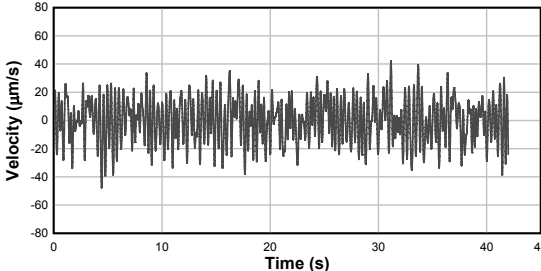
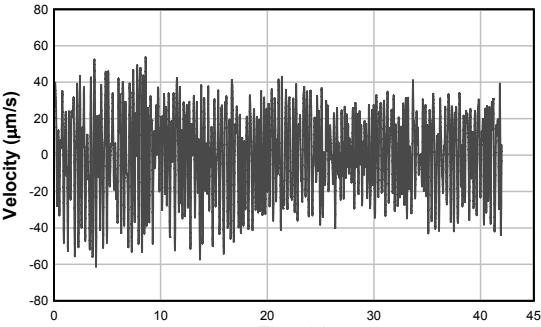
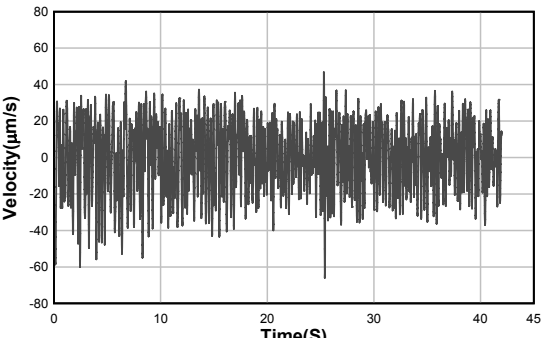
Location: 2Z Measurement Mode	Time History	Maximum Velocity ($\mu\text{m/s}$)
Ambient noise		20.3
With noise 8 compartment train		374.6
With noise 15 compartment train		382.7

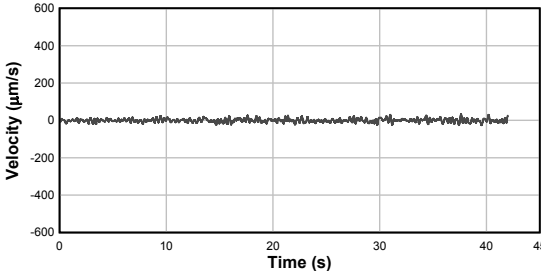
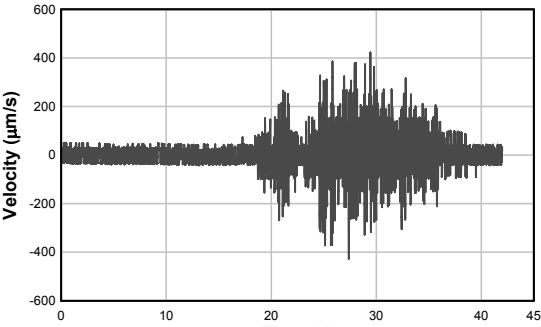
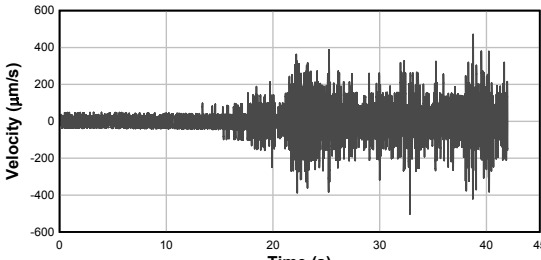
Location: 3X Measurement Mode	Time History	Maximum Velocity ($\mu\text{m/s}$)
Ambient noise	 <p>The plot shows a flat line at 0 $\mu\text{m/s}$ across the entire 45-second duration, indicating no significant noise.</p>	25.9
With noise 8 compartment train	 <p>The plot shows a significant noise spike between 20 and 40 seconds, with a maximum velocity of approximately 1159.2 $\mu\text{m/s}$.</p>	1159.2
With noise 15 compartment train	 <p>The plot shows a significant noise spike between 20 and 40 seconds, with a maximum velocity of approximately 1871.3 $\mu\text{m/s}$.</p>	1871.3

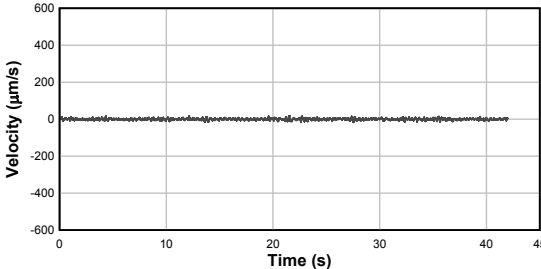
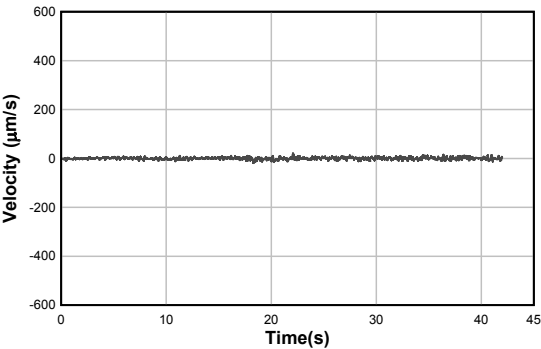
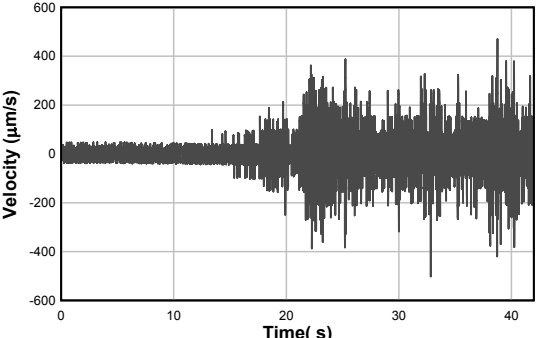
Location: 3Y Measurement Mode	Time History	Maximum Velocity ($\mu\text{m/s}$)
Ambient noise		12.0
With noise 8 compartment train		1207.7
With noise 15 compartment train		1980.6

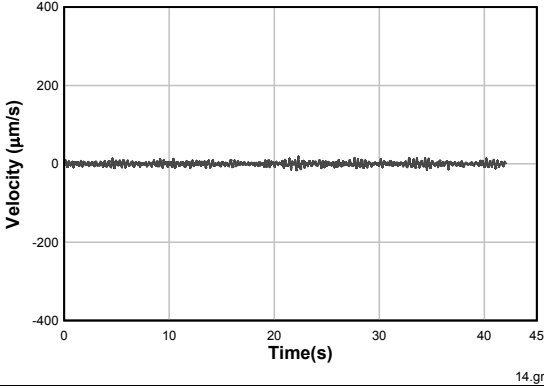
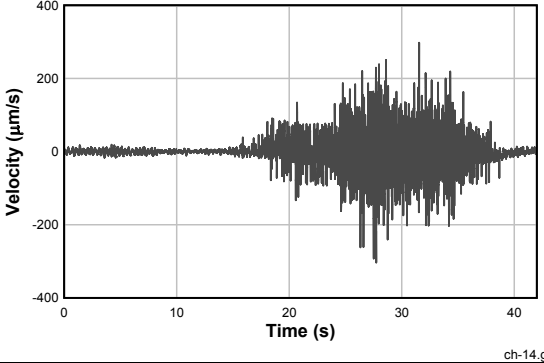
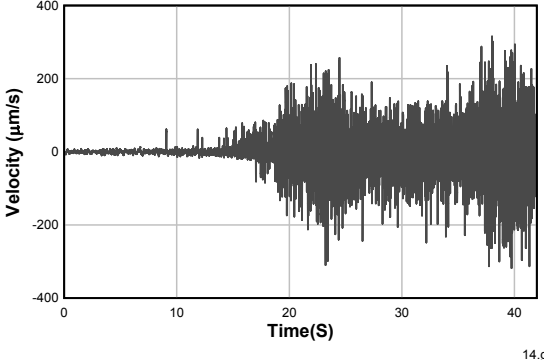
Location: 3Z Measurement Mode	Time History	Maximum Velocity ($\mu\text{m/s}$)
Ambient noise		30.8
With noise 8 compartment train		937.1
With noise 15 compartment train		1437.3

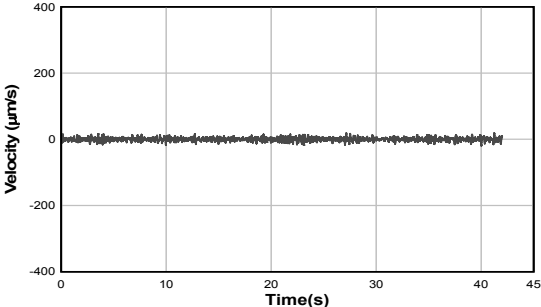
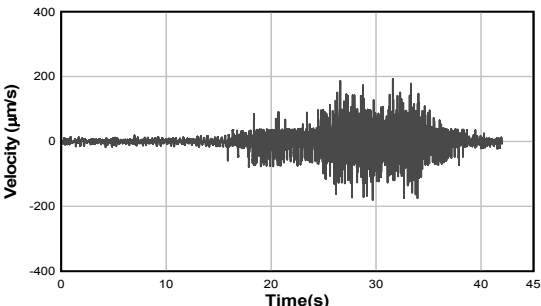
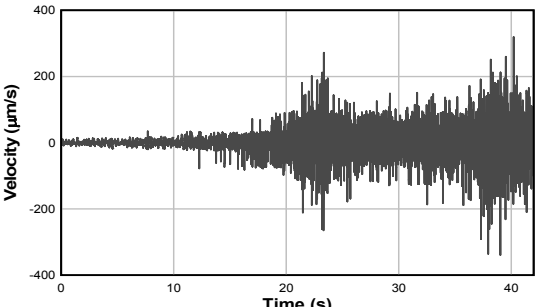
Location: 4X Measurement Mode	Time History	Maximum Velocity ($\mu\text{m/s}$)
Ambient noise	 <p>The plot shows a highly oscillatory signal with a peak-to-peak amplitude of approximately 60 $\mu\text{m/s}$. The x-axis is labeled 'Time (s)' and ranges from 0 to 45. The y-axis is labeled 'Velocity ($\mu\text{m/s}$)' and ranges from -60 to 60.</p>	47.7
With noise 8 compartment train	 <p>The plot shows a highly oscillatory signal with a peak-to-peak amplitude of approximately 60 $\mu\text{m/s}$. The x-axis is labeled 'Time (s)' and ranges from 0 to 45. The y-axis is labeled 'Velocity ($\mu\text{m/s}$)' and ranges from -60 to 60.</p>	64.8
With noise 15 compartment train	 <p>The plot shows a highly oscillatory signal with a peak-to-peak amplitude of approximately 60 $\mu\text{m/s}$. The x-axis is labeled 'Time (s)' and ranges from 0 to 45. The y-axis is labeled 'Velocity ($\mu\text{m/s}$)' and ranges from -60 to 60.</p>	62.5

Location: 4Y Measurement Mode	Time History	Maximum Velocity ($\mu\text{m/s}$)
Ambient noise	 <p>A line graph showing velocity fluctuations over time. The y-axis is labeled 'Velocity ($\mu\text{m/s}$)' and ranges from -80 to 80 with major ticks every 20 units. The x-axis is labeled 'Time (s)' and ranges from 0 to 45 with major ticks every 10 units. The plot shows a dense, irregular signal fluctuating around zero, with most of the amplitude contained within the -40 to 40 $\mu\text{m/s}$ range.</p>	47.8
With noise 8 compartment train	 <p>A line graph showing velocity fluctuations over time. The y-axis is labeled 'Velocity ($\mu\text{m/s}$)' and ranges from -80 to 80 with major ticks every 20 units. The x-axis is labeled 'Time (s)' and ranges from 0 to 45 with major ticks every 10 units. The plot shows a dense, irregular signal fluctuating around zero, with a wider range of amplitude than the ambient noise, reaching approximately -60 to 60 $\mu\text{m/s}$.</p>	61.3
With noise 15 compartment train	 <p>A line graph showing velocity fluctuations over time. The y-axis is labeled 'Velocity ($\mu\text{m/s}$)' and ranges from -80 to 80 with major ticks every 20 units. The x-axis is labeled 'Time(S)' and ranges from 0 to 45 with major ticks every 10 units. The plot shows a dense, irregular signal fluctuating around zero, with a range of amplitude similar to the 8-compartment train, reaching approximately -60 to 60 $\mu\text{m/s}$.</p>	66.0

Location: 4Z Measurement Mode	Time History	Maximum Velocity ($\mu\text{m/s}$)
Ambient noise	 <p>The plot shows velocity in $\mu\text{m/s}$ on the y-axis (ranging from -600 to 600) against time in seconds on the x-axis (ranging from 0 to 45). The signal is a low-amplitude, high-frequency noise centered around zero, with most values between -50 and 50 $\mu\text{m/s}$.</p>	33.3
With noise 8 compartment train	 <p>The plot shows velocity in $\mu\text{m/s}$ on the y-axis (ranging from -600 to 600) against time in seconds on the x-axis (ranging from 0 to 45). The signal is low-amplitude until approximately 20 seconds, then increases significantly in amplitude, reaching a peak of about 400 $\mu\text{m/s}$ around 30 seconds, before decreasing again.</p>	427.7
With noise 15 compartment train	 <p>The plot shows velocity in $\mu\text{m/s}$ on the y-axis (ranging from -600 to 600) against time in seconds on the x-axis (ranging from 0 to 45). The signal is low-amplitude until approximately 20 seconds, then increases significantly in amplitude, reaching a peak of about 500 $\mu\text{m/s}$ around 30 seconds, before decreasing again.</p>	502.0

Location: 5X Measurement Mode	Time History	Maximum Velocity ($\mu\text{m/s}$)
Ambient noise		18.0
With noise 8 compartment train		20.5
With noise 15 compartment train		502

Location: 5Y Measurement Mode	Time History	Maximum Velocity ($\mu\text{m/s}$)
Ambient noise	<p style="text-align: center;">without noise</p> 	18.9
With noise 8 compartment train	<p style="text-align: center;">With Noise 8 compartments</p> 	303.3
With noise 15 compartment train	<p style="text-align: center;">With Noise 15 Compartments</p> 	318.0

Location: 5Z Measurement Mode	Time History	Maximum Velocity ($\mu\text{m/s}$)
Ambient noise		20.1
With noise 8 compartment train		192.7
With noise 15 compartment train		339.5

4. REMARKS

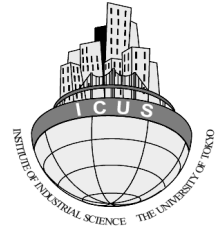
Condition	Measured value of building velocity (mm/s)					Allowable levels of vibration for public buildings from Table 1	Velocity at which vibration is dangerous to buildings (mm/s), from Figure 3	Comment
	NS	EW	UD	Maximum	Corresponding frequency (Hz)			
Ambient noise	0.05	0.05	0.03	0.05	3.0	0.65	-	No problem to buildings
With noise: 8 compartment train	1.16	1.21	0.94	1.21	3-15	0.28-0.65	75	May cause problem to buildings
With noise: 15 compartment train	1.87	1.98	0.38	1.98	6-15	0.28-0.35	75	May cause problem to buildings

References

1. Federal Sanitary Norm of Russian Federation (1996). “SN2.2.4/2.1.8.566-96 – The sanitary norms of industrial vibration, vibration of residential and public buildings, 1996”.
2. Winterkorn, H. F. and Fang, H. Y. (1975). Foundation Engineering Handbook publisher: Van Nostrand Reinhold.



**BANGLADESH NETWORK
OFFICE FOR URBAN SAFETY**



PART-III

FOUR RECENT FIRE INCIDENCES IN AND AROUND DHAKA CITY

**BANGLADESH NETWORK OFFICE FOR
URBAN SAFETY (BNUS), BUET, DHAKA**

**Prepared By: Uttama Barua
Mehedi Ahmed Ansary**

1. Blaze at a Chemical Shop in a Residential Building

A fire spread out at the hardware store named Mahfuz Sewing and Electric, a shop that sells accessories for garment factories in East Tejturi Bazar near Farmgate beside Tejgaon Women's College on April 10, 2014.

The fire, started at 2:45 PM at the ground floor of a 4 storied residential building seemed to be caused by exploding of a paint thinner drum. Flame spread in the whole shop and burnt the store owner and employees. The fire spread to the front of the store. Most of the victims were pedestrians and at least six of the injured are fighting for life with over 30 percent of their bodies burnt. Two university students and a minor boy are among the injured. Out of 11 victims 4 victims died of their injuries after being taken to Dhaka Medical College. On information, three fire fighting units rushed to the spot and doused the flame around 3:30pm.



Figure 1: Position of Shop



Figure 2: After doused fire



Figure 3: Victims at Hospital

2. Plastic Factory Fire

At the night of April 11, 2014 a fire attacks in a three-storey plastic factory building. The factory is situated at Rahmatganj in Old Dhaka's Lalbagh area.

The fire originated at the plastic factory housed in a three-storey tin-shed building near Rahmatganj Playground. Seven units of fire-fighters rushed to the spot and were trying to douse the blaze. As the factory was located at a congested area, that made it difficult for the fire-fighters to reach the spot and douse it. The fire that began around 8:00pm on the ground floor of factory building brought under control around 9:20pm. Several adjoining houses were also damaged in the fire.

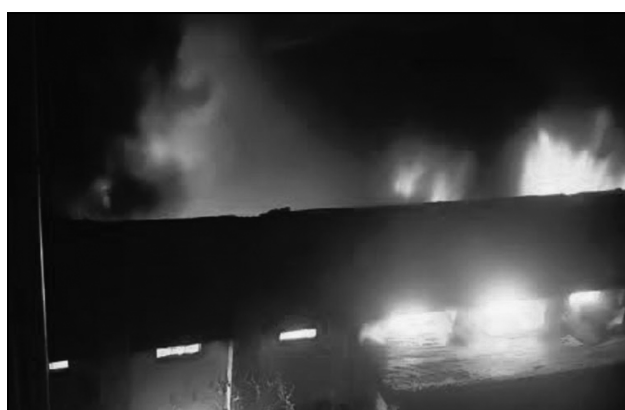


Figure 4: Fire Blaze



Figure 5: Fire fighters put out flames in the plastic factory at Lalbagh in Dhaka

3. OTOBI Furniture Factory Fire

A huge fire broke out at the OTOBI furniture factory at Birulia Union's Khagan area in Savar on the outskirts of the capital city Dhaka on 22nd April night. The fire broke out around 9:45pm and was brought under control around 3am. Ten units of Fire Service from Savar, Ashulia, Tongi, EPZ, Dhamrai and Dhaka Central stations rushed to the spot and brought the fire under control after five hours of frantic efforts.

At least thirty workers were injured when they were getting out of the factory while there around 400 workers was on duty in evening shift. No death was reported. The fire had gutted the entire factory, which was set up over 10 acres of land with corrugated tin roof over walls. It is assumed that an electrical short-circuit caused the fire. The fire spread quickly because of the stored furnitures and chemicals inside. Chemical-filled drums exploded frequently with

loud noise. The fire-fighting capacity inside the factory was inadequate and the fire service faced difficulty as it had to haul in water from outside.



Figure 6: Position of factory in Google Earth



Figure 7: Burning tin shades

4. Fire hazard at a blanket factory in Bakshibazar area

A devastating fire broke out at around 4:20 pm at a one storey tin-shed blanket factory ‘Kajal Woolen Mills Limited’, located beside the gate number-3 of Dhaka Central Jail at Bakshibazar in the capital on Friday, 7th November 2014, gutting the entire factory including the machineries. More than 150 workers were busy making blankets when the fire broke out. They were working to deliver an order of 2,214,000 blankets to the Disaster Management and Relief Ministry and 20,000 blankets for the jail authorities ahead of winter. In addition there were many blankets and raw materials stocked in the warehouse.

Soon after the fire incident, security in and around the central jail was beefed up. Around three platoons of police have been deployed around the jail to thwart any unpleasant incident. On information, eight firefighter units from fire service headquarters, Lalbagh and Polashi stations rushed to the spot and worked hard to douse the blaze. The fire was brought under control at about 6:00pm, but complete dousing of fire took two or three more hours.

However, none was injured in the incident and the fire did not affect the Dhaka Central Jail, because the main boundary wall was high enough to prevent fire entering the compound. The goods worth around 22 crore BDT has been burnt in the incident. More than two lakh and 21 thousand pieces of blankets were in the store in the factory.

The fire might have originated from an explosion of an electric bulb in the one-storied woolen mill. According to Md Maznu Mia, who was working in the cutting section of the factory, sparks from a machine lit the blankets on fire. The flames spread quickly due to the woolen materials.



Figure 8: Fire blaze



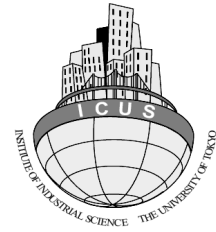
Figure 9: Fire fighting operation by local people



Figure 10: Fire fighting operation by fire fighting team



**BANGLADESH NETWORK
OFFICE FOR URBAN SAFETY**



PART-IV

DISASTER MANAGEMENT SYSTEM OF DHAKA IN COMBATING MAN-MADE DISASTER IN THE LIGHT OF RECENT FIRES AND BUILDING COLLAPSES

**BANGLADESH NETWORK OFFICE FOR
URBAN SAFETY (BNUS), BUET, DHAKA**

Prepared By: Uttama Barua

1. Background of the Study

Disasters occur when hazards meet vulnerability. Man-made disasters stem from man-made hazards, which cause due to human intent, negligence, or error; or involving a failure of a man-made system. In urban areas the effect of manmade hazards, especially fire hazard and building collapse, is much more in comparison to other areas because of the development pattern and land use. The development trend of Dhaka, the capital city of Bangladesh took place in a haphazard and unplanned manner with little or no attention to the issue of land use and structural planning. High-rise buildings are now being constructed in different parts of the city and most of them are without the provision of adequate safety. Thus, in the city, manmade hazards cause huge life and economic loss every year. The causes behind such hazards in the city are: violation of building codes and non-compliance with the legislations, dense building concentrations, incompatible landuse, narrow roads, flammable building materials and structural weakness of buildings, electrical system, lack of safety measures, institutional inefficiency, insufficient equipment support and lack of public awareness as well as the lack of resources to raise awareness and response skills. This study aims to explain the weakness of present disaster management system of Dhaka in combating man-made disaster in the light of recent fires in high rise buildings and collapse of buildings.

2. Recent Significant Fire Incidents in Dhaka

2.1 BSEC fire, 26 February and 24 December, 2007, and 31 October, 2014

A devastating fire broke out in the 11-storey building Bangladesh Steel and Engineering Corporation (BSEC) Bhaban at Karwan Bazaar in the capital at about 10.15 am on 26 February 2007. The building houses private satellite television channels NTV and RTV, and Bangla daily Amar Desh. Within minutes the fire engulfed the entire floor and gradually started to spread to the upper floors, trapping hundreds of people inside. It originated from a storehouse on the top floor as a result of electric short circuit. In BSEC building there were fire extinguishers, but people had no knowledge about how to use them. For not having fire lift or alternate stair, people rushed to the central stair case resulting in more disastrous situation. The first batch of fire-fighters came in BSEC from the Tejgaon fire station after half an hour of ignition. Twenty-five fire-fighting units from different fire stations arrived at the spot and worked frantically for more than six hours to bring the fire under control. Acute shortage of water and inadequate equipment hampered the rescue operation. The firemen had to bring in water from the nearby WASA Bhaban and the Sonargaon Hotel. Massive rescue efforts, including the first-ever airborne operation, were carried out when over 1,000 people were

evacuated from the building. Three persons were killed and more than 100 injured in this incidence. Ntv, Rtv and Amar Desh offices totally burnt and went off air.

On December 24 of the same year, another fire broke out in a room on the ground floor of the building. Even after the fire incidents on 2007 in BSED, no preventative or mitigation measures were taken in the building, causing fire for the third time in 2014 for the same reason, i.e. electric short circuit at storeroom of papers. The building caught fire for the third time at about 11:48 am on 31 October, 2014, which originated from a storehouse on the top floor. Twenty one fire-fighting units doused the flames after over two hours of frantic efforts, which included 100 fire fighters along with volunteers. The firemen had to bring in additional water-carrier trucks, for shortage of water in the spot. They used two long ladders to reach for the top floors of the building. Ambulances were stationed nearby along with additional water-carrier trucks. No casualties have been reported from the fire.

2.2 Bashundhara City Complex fire, 13 March, 2009

On 13th March 2009, Friday at around 1:45 pm, a hell fire engulfed the upper levels of 20 storey office cum shopping centre known as Bashundhara City Complex at Panthopath, Dhaka. The fire originated from the 17th floor, due to electric short circuit. Though Bashundhara City Complex had fire fighters, they had little training. Again, the building was equipped with sufficient fire detecting, suppressing, and evacuating systems but they were inactive during the fire. The fire alarm was defective which used to give false alarm, so the fighters of the building didn't care about those warnings. Thus, the fire fighters of the complex could do nothing. At Bashundhara City only one stairs leading to basement parking which act as fire exit, but this remains locked all the time and the escape route is occupied by trash, resulting in chaotic situation (Tabassum, Ahmed, & Romeo, 2014).

All fire fighting units of the capital and from its surroundings along with military, police and RAB personnel, took about six hours to tame the massive blaze that raged through the Tower. The hydrants were useless on the event as there was no water in the tank of the complex. Initially water was pumped from nearby Unique Trade Centre. The fire brigade brought a fire engine, but did not have enough hoses or water sources to tame the fire. Fire fighters claimed that the blaze was brought under control at about 7:00pm. Black plumes of smoke from the high rise spiraled upward, while blazing windowpanes, furniture, and other objects rained down on the pavement causing another fire in adjacent one storey furniture shop. The incident killed 7 and injured 20 people. The top six floors were totally gutted.

2.3 Nimtoli fire, 3 June, 2010

In 3rd June 2010, a devastating fire broke out in the densely-populated part of Old Dhaka called Nimtoli, which gutted eight buildings and over twenty shops. Initially it was thought that explosion of two transformers at Nimtoli started the fire but later it has been known the fire originated from an oil stove in five storey mixed use building with chemical warehouse. The fire spread very quickly because the chemicals exploded and flew all over. Fire killed at least 117 people and caused injury to a hundred people. Most of the affected peoples were women and children.

3. Recent Significant Incidences of Building Collapse in Dhaka

3.1 Phoenix, 25 February, 2006

On 25 February 2006, a five storied building undergoing remodeling construction for floors space-use collapsed without warning at the Tejgaon industrial area of Dhaka city. Initially the building was used as warehouse for factory machines and equipments of Phoenix Fabrics a year ago. It was being converted into a 500 bed specialized hospital in joint collaboration with Mount Elizabeth Hospital, Singapore. There were also showrooms of Phoenix Fabrics and Phoenix Electronics on the ground and first floors and a number of tin-shed rooms on the rooftop. Experts blamed faulty and unplanned construction, and increased concentrated vertical load for the collapse. Soldiers, police, fire officials and hundreds of volunteers rushed to the scene to pull out victims trapped under the caved-in Phoenix Building in the city's congested industrial area. Cleaning of the concrete debris and rescue operation took a few days for lack of proper logistics. As consequence of the incident, 20 people died and 40 were injured.

3.2 Begunbari, 1 June, 2006

A five-storey building toppled onto three tin-shed houses at Begunbari area in the Tejgaon area of the city at 11 pm on 1 June. From the way the five-storied structure fell down, it appears there was no proper plan for the building, nor was any rule or code followed during its construction. The building was built on land filled with garbage instead of soil. Some heavy construction materials were stored in the top floor of the building. Moreover the foundation was not design properly. And it is also patently clear that the workmanship and engineering as well as the materials that went into the making of that house were also of very poor quality. FSCD, Police, AFD, BDRCS, Ansar, community volunteers all were involved in the search and rescue operations, but still the collapsed building could not be removed. Narrow Access route made the response work difficult. This incident resulted death to 23 people.

3.3 Rana Plaza, 24 April, 2013

“Rana Plaza” is located at Dhaka-Aricha highway near Savar bus stand, collapsed on 24 April, 2013 at around 9:30 am. The building housed five garment factories (New Wave Button, New Wave Styles, Ethar Tex, Phantom Apparels and Phantom Tex) employing around 5,000 people, 300+ shops, and a bank. Rana Plaza was a 9-storied industrial building with a single basement. Instead of Rajuk, local municipality (Savar) gave the owner permission to construct a five storey commercial building with one basement in 2005 and later allowed the owner to extend it up to nine storey, without considering the structural design, though the foundation of the building was of 5 storey (Odhikar, 2013; Osman, Khan, Hossain, & Khan, 2013; Rahman, & Ansary, 2013). Moreover, the building was converted from commercial to industrial use and Power Generators were placed at the higher floors (Rahman, & Ansary, 2013).

A day prior to the fateful day, on 23 April 2013, cracks developed on some pillars and a few floors of the building following a jolt. After inspection of industrial police, they requested the building authorities to close the building and to suspend operations of the factories. However, the building owner and top-management of the garment factories ignored the warning and forced the workers to work in the morning of 24th April. An official statement of the Bangladesh Garment Manufacturers and Exporters Association cited 3,122 workers to be in the building at the time of the collapse. This resulted in the high death toll of 1,127 at the end of the rescue operation on 14 May 2013, one of the world’s deadliest industrial disasters (Osman, Khan, Hossain, & Khan, 2013). Right after the collapse, members of the Bangladesh Army, Fire Service and Civil Defence, Police, BGB, pedestrians and also members of various social welfare organizations had begun rescue operations. Armed Forces Division (AFD) of Bangladesh coordinated the search and rescue operation. Thus around 2438 could be rescued, however badly injured (Odhikar, 2013).

4. Recent Acts and Policies Regarding Urban Development in Bangladesh

4.1 Building Construction Act 1952

The Act provided regulations regarding setbacks, building heights etc. in urban areas and provided prevention of haphazard construction of buildings.

4.2 The Town Improvement Act (TI), 1953

It is the first statute which recognized the need for planning approach and created a special agency for development such as preparation of master plans, improvement schemes, and their implementations.

4.3 Building Construction Rules, 2008

These rules seek to control development plot-by-plot and case-by-case by imposing conditions on setbacks, site coverage, Floor Area Ratio (FAR), construction of garages, access to plot, provision of lift, land use of that particular plot and height of building. It helps to control the density of an area and manage the growth providing rules of building coverage area, allowable floor space and relation among building height - road width and plot size. The Rule provided more authority to RAJUK for responsibility to monitor the development of the city, spread out the responsibilities to various actors, and spell out responsibilities of building designers, structural engineers, site supervisors and their penalties etc.

4.4 Bangladesh National Building Code (BNBC), 2014

The purpose of the Code is to establish minimum standards for design, construction, quality of materials, use and occupancy, location and maintenance of buildings within Bangladesh in order to safeguard, within achievable limits, life, limb, health, property and public welfare.

4.5 Land Development Rules for Private Housing, 2004

This is a legal instrument for controlling land development in private sector housing. It provides procedures and guidelines for land development protecting the environment, spelling out land for community facilities, amount of land to be sold out, school sites, road hierarchy and importantly planning standards.

5. Recent Acts and Policies Regarding Disaster in Bangladesh

5.1 Disaster Management Act, 2012

The Act is enacted to create the legislative tool and legal basis for disaster risk and emergency management, along with mandatory obligations and responsibilities on Ministries, committees and appointments. The main aims of the Act include development of mitigation, response and recovery strategies, and establishment of institutional framework for disaster management. The Act addressed manmade disasters in some activities.

5.2 Disaster Management Bureau Strategic Plan, 2005-2006

The purpose of the Plan is to provide a statement of key strategies for the provision of Disaster Management Policy and Plan. It provided seven strategic goals for the purpose.

5.3 National Disaster Management Policy, 2008

The Policy is formulated to define the national perspective on disaster risk reduction and emergency management, and to describe the strategic framework and national principles of disaster management in Bangladesh. The policy proposed some actions based on seven strategic goals.

5.4 National Plan for Disaster Management, 2010-2015

The Plan which aims to give direction, vision and goal for the disaster management initiatives along with implementation including all stakeholders and considering all hazards under seven strategic goals. It provides the overall guideline for the relevant sectors and the disaster management committees at all levels to prepare and implement their area specific plans. It addresses fire and infrastructure collapse as hazard for Bangladesh.

5.5 Standing Orders on Disaster, 2006

The SOD has been prepared to make the concerned persons understand their duties and responsibilities regarding disaster management at all levels, and accomplishing them, describing the detailed roles and responsibilities of committees, Ministries and other organizations in disaster risk reduction and emergency management, and establishes the necessary actions required in implementing Bangladesh's Disaster Management Model. All Ministries, Divisions/Departments and Agencies shall prepare their own Action Plans in respect of their responsibilities under the Standing Orders for efficient implementation. The National Disaster Management Council (NDMC) and Inter-Ministerial Disaster Management Coordination Committee (IMDMCC) will ensure coordination of disaster related activities at the National level. Coordination at District, Thana and Union levels will be done by the respective District, Thana and Union Disaster Management Committees. The Disaster Management Bureau will render all assistance to them by facilitating the process.

5.6 Fire Prevention and Extinction Act, 2003 and Rules, 2014

The Act and Rules include provision for preparedness and responsibilities of fire brigade, license, clearance and occupancy, and general arrangement for fire fighting with respect to occupancy.

6. Bangladesh Fire service and Civil Defence

BFSCDA is the legitimate authority responsible for managing fire along with other disasters in Bangladesh. The present Fire Service and Civil Defense has been established in 1980 with amalgamation of the then Fire Service Directorate, Civil Defense Directorate and The Rescue Department of Roads and Highway. At present the department is running under the Ministry of Home Affairs. In Dhaka city there are total 79 fire stations, and a training complex, which is located in Mirpur-10, where mock drills and training programs are organized by co-ordinating, the officers, trained volunteers, government and NGOs, to response properly after a disaster. Table 1 shows class wise number of fire stations in Dhaka city, table 2 shows class wise manpower of the fire stations, and table 3 shows equipments available in the fire stations according to class. Other fire fighting equipments include: special water truck (with capacity

8000/ 11000 liters), foam tender, chemical tender, cold cut, foam making generator, water mist, and ground monitor. Equipments for rescue includes: emergency tender, smoke ejector, lifting air bag, hydraulic cutter, hydraulic speeder, breathing apparatus, air line breathing apparatus, chopping hammer, door opener, pipe squeezer, chains, and reciprocating. These numbers are very insignificant with respect to the population of Dhaka city. Thus, the institution is characterized by weak equipment, poor technology, and inadequate manpower.

Table 1: Fire stations in Dhaka

Fire station type	No. of fire station
Class A	21
Class B	30
Class C	23
River fire station	5
Total	79

Table 2: Manpower in fire stations

Designation	Fire station			
	Class A	Class B	Class C	River fire station
Senior station officer	1	0	0	0
Station officer	1	1	1	1
Sub-station officer	0	1	0	0
Leader	3	2	1	1
Driver	5	4	2	3
Fireman	22	16	10	8
Other staff	3	3	2	0
Total	35	27	16	13

Table 3: Equipments in fire stations

Equipment	Fire station			
	Class A	Class B	Class C	River fire station
Water truck	1	1	1	0
Pump truck	1	1	0	0
Helping truck	1	0	0	0
Potable pump	3	2	1	1
Ambulance	1	0	0	0
Fire float	0	0	0	1
Speed boat	0	0	0	1

Despite their limited resources and capacity, the BFSCD has taken various steps to reduce loss of lives and properties at the time of disasters, especially fire. The main activity of BFSCD is to keep themselves standby as first responder for fire fighting, fire prevention, search & rescue,

to render first aid, to send the serious casualties to hospital, to provide fire safety for the VIP's, and issue silence fire safety. BFSCD is also responsible to take necessary initiatives for raising awareness among people. Mass communication through poster, leaflet, speech, seminar, workshop etc, and training and drill programs in institutional, residential, and commercial buildings, on fire fighting rescue operation, first aid, send the serious casualties to hospital, safe escape from building through escape route, response according to plan etc, are some of the initiatives to raise awareness among people as well as to make them resilient and prepared for any kind of disaster. In some case, people or institutions can apply to BFSCD to organize or take part in the training program accordingly. Moreover, the total manpower of the agency is not adequate in respect to necessity, and community people are the first responder for any kind of disaster. Realizing the fact, CDMP has initiated volunteer training program which aims to strengthen the capacity of the city dwellers to face, manage and operate the plan effectively at the event of any disaster through BFSCD. For this purpose, CDMP has procured light equipments for search and rescue operations and ICT devices. Training to the community volunteers enables them to render their service more efficiently in the mitigation of earthquake disaster especially for collapsed structure search and rescue, fire fighting and first aid before and after the arrival of professionals. Thus, Fire Service and Civil Defence has aimed to train 62,000 Urban Community Volunteer. Already 19,500 volunteers have been trained by this time. On the other hand, for disaster resilience in slum areas, BFSCD provides training to the slum dwellers, where 600 volunteers have already been trained.

7. Strengths and Weaknesses of Present Disaster Management System of Dhaka in Combating Man-Made Disaster

7.1 Prevention and Mitigation Measures

The Acts and Policies regarding urban development are the means to control development, which are meant to ensure safety from manmade hazards, i.e. fire hazard and infrastructure collapse. Even though, haphazard and unplanned development violating the regulations are going on, which result is devastating disasters. From the case studies, it could be observed that in all of the cases of building collapse, the buildings were constructed violating the rules of setback, FAR, building material, structural fitness, etc and most importantly they were constructed without permission from concerning authority. Even after taking clearance, they did not build the building according to the approved design. Even use of some buildings are change which result in increased vertical load. This was evident in the cases of Phoenix building collapse, 2006 and Rana Plaza collapse, 2013. Internal roads in most of the areas are

narrow which do not comply with the legislations, especially in old part of Dhaka. Thus, the main problems regarding these acts and policies are that, these are not exercised properly, for lack of manpower regular monitoring cannot be ensured, and the concerning authorities also lack modern technology for data management. The existing manpower of RAJUK is not sufficient to monitor and enforce the building code properly.

The Disaster Management Act, 2012 enacted arrangement of instruments regarding fire prevention and mitigation according to risk of different occupancy buildings, along with restriction on preservation and use of combustible and flammable materials without proper safety measures in residential area, but the act lacks specific provision prevention and mitigation measures. National Disaster Management Policy, 2008 proposes development of a standard guideline, preparation, and implementation of hazard specific risk reduction plan for manmade hazards under fifth strategic goal, i.e. expanding risk reduction programming across hazards and sectors. On the other hand the National Plan for Disaster Management, 2010-2015 does not include risk reduction plan for manmade hazards. The plan addresses strategies to strengthen national capability to reduce the risks of manmade hazards (including infrastructure collapse and fire) under the fifth strategic goal. The strategies include: reduction of the incidence of disasters in the manufacturing industry by developing guidelines and risk reduction plans for chemical and technological hazards and increasing awareness of community, and strengthen Bangladesh Fire Service and Civil Defence providing better equipped with latest fire fighting technology including training. Guidelines and risk reduction plans for chemical and technological hazards have not been prepared yet. Again, awareness activities are very inefficient because of lack of integration at the community level. In most of the cases, people are not aware of the manmade hazards, though they know about the consequences. The incident of the collapse of Rana Plaza caused due to negligence and lack of awareness of the respective authorities, for which they did not take the warning seriously.

To prevent and mitigate fire incident, Fire Prevention and Extinction Act, 2003 and Rules, 2014, and Bangladesh National Building Code (BNBC), 2014 have enforced legislation for license, clearance and occupancy certificate to ensure fire safety, indicating the provision for punishment for any discrepancy by BFSCD. In Bangladesh National Building Code (BNBC), 2014, fire zones have been defined with respect to occupancy class. In most of the cases, different activities are carried out without license, clearance and occupancy certificate, or violating the permitted license, clearance and occupancy certificate. Most of the buildings do not comply with the building code, i.e. use of low quality electric equipments, unsafe electric

wiring system and unsafe storage of flammable and combustible materials. Thus, most of the fire incidents are ignited from electric short circuit, and spread by flammable and combustible materials and chemicals. The evidence of such incidence can be observed in case of BSEC fire (2007 and 2014). Even after the fire incidents on 2007 in BSED, no preventative or mitigation measures were taken in the building, causing fire for the third time in 2014 for the same reason, i.e. electric short circuit at storeroom of papers. For limitation of manpower in BFSCD, regular monitoring and inspection cannot be done.

7.2 Preparedness Measures

In the Disaster Management Act, 2012 responsibilities of different committees, groups and councils at different levels, and Disaster Management Bureau for preparedness purpose have been specified. Moreover the act addressed establishment of National Disaster Volunteer Committee, and National Disaster Management Research and Training Institute for proper preparedness. The Act entitled establishment of fund for arrangement of different instruments to ensure proper preparedness. The Act enacted arrangement of instruments necessary for preparedness for fire hazard and building collapse, and safe escape along with proper marking, according to risk and occupancy load of different occupancy buildings. The Act skipped community level preparedness issues and most importantly the awareness initiatives which are very important for fire hazard and building collapse. Again, most of the stakeholders are unaware of their responsibility stated in the act, plan or SOD. For financial preparedness, formation of three funds has been stated in National Disaster Management Policy, 2008 including, National Risk Reduction Fund, National Disaster Response and Recovery Fund, and Disaster Management Fund, but details about the funds arrangement and allocation are absent. The National Plan for Disaster Management, 2010-2015 does not include plan for manmade hazards specifying preparedness strategies.

To ensure proper preparedness, Fire Prevention and Extinction Act, 2003 and Rules, 2014 have defined the responsibilities and activities of brigade including response activities, awareness activities for officer, government and mass people, training programs for officials, volunteers and general people, arrangement and preservation of necessary equipments. In reality, the respective authorities do not have sufficient manpower, equipments and vehicles to carry on the rescue operation (Osman, Khan, Hossain, & Khan, 2013). Fire service authority can provide equipment support for firefighting up to 10th floor, but there are high rise buildings beyond this height in Dhaka city (Islam, & Adri, 2008).

Moreover, in these rules and acts along with Bangladesh National Building Code (BNBC), 2014, fire fighting floor plan has been made mandatory for different occupancy class buildings, which should include, permanent and potable fire fighting system, emergency and alternative stair, lift and fire lift, smoke and heat detection system, alarm system, emergency light, exit sign, fire command station, transformer and generator room, fire fighting and pump house, riser point and hoes cabinet, sprinkler head, water spray projector head, safety lobby, means of escape, water source and reservoir, minimum width of road, etc. In reality, people are not aware of the facts and thus the plans are not prepared thereby. The buildings do not have stair with proper sign. Moreover, the exits remains locked all the time and the escape route is occupied by trash. This incident was evident in case of Bashundhara City Complex fire, 2009. From the case studies it could be observed that fire extinguishers are not preserved in the buildings. Even though some buildings are equipped with sufficient fire detecting, suppressing, and evacuating systems, people have no knowledge about how to use them, and they also remain deactivate and defective , i.e. Bashundhara City Complex fire, 2009; BSEC fire incident, 2007. People of the city also do not have any training and not even the minimum perception about how to respond or cope with the fire when an accident occurs. General people are not trained for response to and rescue from the incidents. Again, regular training for volunteers is absent (Osman, Khan, Hossain, & Khan, 2013). Even though some buildings have fire fighters, they lack proper and regular training, i.e. Bashundhara City Complex fire, 2009.

7.3 Response Measures

In the Disaster Management Act, 2012 responsibilities of different committees, groups and councils at different levels, and Disaster Management Bureau for preparedness purpose have been specified. Moreover the act addressed establishment of National and Local Level Disaster Response Coordinator Group integrating different stakeholders in the committee for proper response during and after a disaster at different level. The Act specified activities immediately after a disaster including declaration of disaster affected area and activities of different stakeholders, ensuring uninterrupted movement of fire fighting and rescue team. The Act enacted arrangement of instruments regarding search and rescue according to risk of different occupancy buildings. Thus the act could properly address the response issues properly. The National Plan for Disaster Management, 2010-2015 defines responsibility of different stakeholders to prepare plan at different levels including response activities, but it does not include plan for manmade hazards specifying response strategies.

The buildings do not have stair with proper sign, and the exits remains locked all the time and the escape route is occupied by trash, which worsen the scenario. This incident was evident in case of Bashundhara City Complex fire, 2009. For not having fire lift or alternate stair, people rush to the central stair case resulting in more disastrous situation. This happened in BSEC fire (2007), where people rushed to central staircase to go out off the building. Though in some buildings fire extinguishers are preserved, but for lack of knowledge and training people cannot use those at the time of necessity. This situation was observed in BSEC fire (2007). Various fire fighting equipments are sometimes provided at the individual building but they are inferior in number, and in many cases located in the isolated places and people do not know how to use these equipments. As a result, the equipment does not provide any benefit at the time of emergency.

The prime challenges that the authority usually face after a fire call is to reach the spot rapidly considering the low mobility in the road way and to manage water for fire fighting. To ensure proper response, Fire Prevention and Extinction Act, 2003 and Rules, 2014 have ruled to keep the roads clear for easy movement of fire fighting vehicles, but it is not followed properly. Narrow access roads hamper the movement of fire vehicles and make the response work difficult, especially in Old Dhaka. The crowd of curious people is also another problem that is usually had to face by the fire fighters during their work. Sometimes the crowd becomes too large that they even clog the movement of fire fighting vehicles towards the target location. The crowd and road blockage results in delay of fire fighting vehicles to reach at the spot. According to the rules and acts, the brigade will be responsible for fire fighting, rescue, first aid and transfer the injured to hospital through ambulance service. There is no provision of water for emergency situation, which result in delay in the fire fighting operation, i.e. Bashundhara City Complex fire, 2009; BSEC fire, 2007 and 2014. For lack of sufficient equipments, rescue operations are delayed (From case studies). Since Fire Service and Civil Defence's only aerial ladder cannot gain access beyond 13th floor, six floors of the 20-storey mall-cum-office tower remained out of the fire fighters' reach to be left in ruins, in Bashundhara City Complex fire incident in 2009.

Moreover, in the rules and acts along with BNBC, 2014, provision for trained fire safety officers has been enforced for buildings to ensure immediate response. In case of Rana Plaza collapse in 2013, the rescue operation was hampered for absence of training and guidance,

weak chain of command, and lack of coordination (Osman, Khan, Hossain, & Khan, 2013). Even though some buildings have fire fighters as provision, they cannot response to the situation properly for lack proper and regular training, i.e. Bashundhara City Complex, 2009. In any incident, general people play the role of first responder, though they do not have the required knowledge, training or experience, i.e. Phoenix building collapse, 2006, Rana Plaza collapse, 2013. After the incident of Rana Plaza collapse in 2013, fifty percent of the volunteers were general and untrained people. They also helped the injured to various hospitals, delivered dead bodies to the relatives, arranged for the burial of unidentified bodies and financially helped the affected (Odhikar, 2013).

7.4 Relief and Recovery Measures

The Disaster Management Act, 2012 entitled establishment of fund for ensuring relief after occurrence of a disaster and arrangement of instruments regarding first aid according to risk of different occupancy buildings, which is not done in reality. The National Plan for Disaster Management, 2010-2015 defines responsibility of different stakeholders to prepare plan at different levels including relief and recovery activities, but it does not include plan for manmade hazards. Management system for relief has not been stated in any of the acts or rules. In case of Rana Plaza collapse in 2013, aids were raised from government, foreign organizations along with aids from general people. For lack of proper management many of the victims either did not get the defined amount of aid or did not get it at all. Rather some other people received aid instead with fake ID (Moazzem, Afros, & Sehrin, 2014). Again, Fire Prevention and Extinction Act, 2003 and Rules, 2014 have ruled to investigate the causes and results of any fire incident afterwards, for taking necessary actions accordingly. Whenever a fire occurs or building collapse, the authorities are usually asked to investigate the fire, pay exemplary compensation to the survivors as well as to the families of those that died, take immediate steps to improve health and safety in the industry, as well as take legal action against those found responsible for criminal negligence in allowing the existence of such unsafe conditions. This activity is done efficiently after every incident because of the involvement of mass media.

8. Conclusion

The real city is a safe city that ensures the security of living and livelihood of its citizens. Safety issues should be given high priority in the urban areas because of the involvement of huge population in a limited geographical space. Dhaka is growing in an unplanned manner and

unfortunately the authorities have very limited control over the development trend. The safety issues in the large urban areas, like Dhaka are not highly emphasized from the city planning perspective in Bangladesh. In most cases, immediately after any large scale fire and building collapse, the issue of urban safety is highly discussed by local newspapers but with the progress of time, the issue ultimately fades away from people's memory. As a result, the government shows an attitude of reluctance in taking further. At present, the authority of this metropolitan city has no contingency plan and sufficient preparation to avoid manmade hazards. The city authority has no proper equipment and adequate trained manpower to combat fire. Again, at present BFSCDA is working as the emergency service providing organization and the authority has very limited involvement to the planning decision. The city authorities like RAJUK, City Corporation etc. are also characterized by weak institutional capacity. The existing legal provisions are also limited and needed to be modified for proper enforcement. To overcome the situation, these shortcomings should be minimized and safety issues should be addressed from the individual building premises to the city planning level.

References

- Alam, N. (2010). Collapse of 4 storied building in Begunbari---A pictorial case study. BFSCD. (n.d.). Bangladesh Fire Service and Civil Defence (BFSCD). Retrieved on 27 December, 2014, from: <http://www.fireservice.gov.bd/>
- Islam M. M., & Adri N. (2008). Fire Hazard Management of Dhaka City: Addressing Issues Relating to Institutional Capacity and Public Perception. *Jahangirnagar Planning Review*, 6:57–67.
- Moazzem, K. G., Afros, A. & Sehrin, F. (2014). *Post-Rana Plaza Developments: Rana Plaza Tragedy and Beyond: A Follow Up on Commitments and Delivery: Monitoring Report on Rana Plaza Tragedy*. Center for Policy Dialogue (CPD) in collaboration with Canada Fund for Local Initiative (CFLI).
- Odhikar. (2013). *Broken Dreams: A Report on the Rana Plaza Collapse*. Fact finding report, Odhikar.
- Osman, M. S., Khan, M. A. A. M., Hossain, M. A. & Khan, A. I. (2013). *Search and Rescue Roles of Fire Service and Civil Defence and Urban Community Volunteers in Rana Plaza: A Rapid Assessment*. CDMP, Ministry of Disaster Management and Relief.
- Rahman, N. & Ansary, A. A. (2013). *Savar Building Tragedy in Bangladesh: Way Forward*. Presented at USMCA conference.

Tabassum, S., Ahmed, S., & Romeo, T. M. (2014). An Investigation on Fire Safety of Air-conditioned Shopping Centers at Dhaka City. *Asian Journal of Applied Science and Engineering*, 3(2), 20-34.



**BANGLADESH NETWORK
OFFICE FOR URBAN SAFETY**



PART-V

RESCUE OPERATION OF A 4-YEAR CHILD, JIHAD FROM AN ABANDONED DEEP TUBEWELL

**BANGLADESH NETWORK OFFICE FOR
URBAN SAFETY (BNUS), BUET, DHAKA**

**Prepared By: Uttama Barua
Mehedi Ahmed Ansary**

The Incident

On Friday evening, 26 December, 2014, Jihad was playing with two of his playmates in a playground at the Shahjahanpur Railway Colony. At one moment of playing, Jihad fell into a pipe adjacent to the playground at about 4 pm. He did not see the pipe as its mouth was covered only with an empty jute sack, which was just wide enough to fit the boy and too narrow for an adult to pass through. Seeing the incident, his playmates informed the local people and his family about the incident. Several women had heard Jihad scream from down the pipe. Jihad's father Nasiruddin works as a security guard at the Motijheel School and College. Jihad is the youngest among his parents' three children. They live in the same colony. Residents said the deep tubewell was declared abandoned when it stopped delivering water. A new deep tubewell and pump were being installed near it by the Bangladesh Railway. Locals said another child nearly had a similar accident on the previous day in the same pipe where Jihad fell. One of his legs went inside the pipe accidentally, but the locals saved him. From the surface, the pipe is 17 inches wide for around 300 feet underground. It is followed by a 'submersible pump' and filter. After that, the pipe is three inches wide and has gone over 300 feet underground. Jihad was sitting on the pump at about 300 feet depth.

Response to Rescue Jihad

Getting the news, three units of firefighters arrived at the scene around 4 pm and started the rescue efforts, and were assisted by Dhaka WASA, railway, RAB, police and other volunteer agencies. Jihad, kept responding for six hours since the launch of the rescue operation. Rescuers said they spoke to the boy several times and provided him with some food, juice, bottled milk and fresh oxygen. They also sent a torch down the pipe as the evening fell. But Jihad got weaker after spending long hours in the cold, dark and damp underground.

The fire brigade personnel employed various techniques one after another. Between 4pm and 7:30pm, the firefighters repeatedly tried to bring up the child by using the rope line, but failed every time as he could not hold on to the rope for long enough. Firstly the rescuers tried to pull up the boy with thin nylon rope, but the rope got lighter after pulling up around 10 feet. Afterwards, they dropped a thick rope with a torch and the boy had held it but released after some time. Thus the fire-fighters made five abortive attempts to bring the boy, 'Jihad', up using rope. After 7:30pm, the fire-fighters sent down a sack and asked Jihad to sit on it. That plan also failed as the child fell again after being pulled up for a while.



Figure: Initiation of rescue operation



Figure: Rescue effort using rope



Figure: Rescue effort using sack

Their attempts to save the boy were facing obstruction as the hole was not that wide and had another three inches wide pipe inside the first one. At about 8.20 pm the fire service brought their crane in the spot to uproot the inner pipe. Then after 11 pm, the rescue team was able to pull up the 350 feet long pipe, three inches in diameter that went inside the first one using the crane to create more space.



Figure: Uprooting of internal pipe

Rescuers then planned to send one of their men down the pipe with a camera and light. A man named Bashir Uddin Ahmed volunteered to go down into the well at around 11:30pm to bring out the child. He took all the preparations to follow through with the plan, but ultimately he was not allowed to go down considering safety issues because the experts wanted to observe the situation down the well through the camera first.

Soon after that, a team from BUET's mechanical engineering department arrived at the scene with an alternative plan to save the boy. After consulting them, Fire Service and Civil Defence Director tried the BUET team's plan. One of the team members, BUET student Tanvir Arafat Dhrubo said they planned to use another pipe, smaller in diameter, which would have a 'catcher' at the end. After it reaches Jihad, the mouth of the 'catcher' would open up and get a hold of boy and bring him up, he said. The work to build the 'catcher' started near the scene. Meanwhile, the Directorate General of Health Services kept a medical team standby from Dhaka Medical College and Hospital with a fully equipped ambulance at the spot to meet Jihad's emergency needs once he is rescued.

Nine hours after Jihad fell; Dhaka WASA sent a waterproof camera to get visual inside the pipe. The rescuers lowered the borehole camera down the pipe and searched for an hour without success. In the first attempt, the borehole camera identified a piece of cloth, sandals, pieces of cork sheet, a common lizard and pieces of paper around 250 meter down. The camera completed its slide into the hole around 2:00am but there was no sign of the boy. After that, Jihad's existence down the pit was denied by professionals known for their skills. Abu Sayeed Raihan, joint director of National Security Intelligence, termed the news of Jihad's falling in the shaft as "rumor" after seeing images sent by Dhaka WASA camera. Confusions grew when the State Minister for Home Affairs Asaduzzaman Khan Kamal, at about 2:45am Saturday

declared that there was no boy trapped in the well and the entire episode might be a 'rumor' saying, "...I'm sure there's nobody down there".

Shahjahanpur police picked up Jihad's father Nasir Uddin moments after the announcement. Police picked him up around 3am on Saturday saying journalists would pester him if he were at the scene. But at the police station, he was told that his son was not spotted by a camera sent down the pipe. The law keepers suspected Jihad had been hidden somewhere else. They questioned Jihad's father suspecting the whole thing was staged. He was threatened and tortured in the name of RAB to tell the 'truth'. Police confined Nasir for 12 hours.

At this stage, rescuers doubted same but did not give up. DG Khan said they would continue their search until they were absolutely sure. "Though we can't see any human being there, we are not wrapping up our operation. We will remove the debris to be certain," he said. But optimism slowly gave way to frustration and outrage. They decided to send the camera again, after clearing the debris. Thus, in a second attempt, non-government experts sent another camera around 4:00am. It got obstructed again after reaching 240 feet. After that the rescue operation slowed down.

In the morning, the rescuers tried to send the catcher they prepared to the bottom of the well in a bid to pull out the boy allegedly trapped inside the well shaft. A camera has also been attached with the case made with iron rods. Despite their renewed efforts since 9:30am, the fire fighters, who have been conducting rescue operation since yesterday, failed to send the "catcher" at the bottom till 11:00am.

The Fire Service closed the rescue operation at 2:30pm on Saturday; 23 hours after the rescue operation had started. Fire Service DG Brigadier General Ali Ahmed Khan made the announcement at 2:40pm after the rescuers failed to detect any human body inside the tube-well, using high-tech camera and catcher. He said: "We have tried several times, but could not detect the location of the boy. Experts from different organizations also could not find any specific evidence in this regard. However, we continued the rescue efforts as the parents requested us. We are now handing over the operation to railway engineers. They will take further step in this regard and the fire fighters will help them if necessary. We are thanking all for their efforts and expressing our sorrow and shock for the family members of the ill-fated boy".

Rescue of the Child by Locals

When sophisticated instruments failed to even locate Jihad, ten volunteers eventually succeeded to bring him out using a simple handmade tool. The volunteers were unknown to each other before the operations and had been with the rescue team since Thursday night. They also volunteered during last year's Rana Plaza tragedy in Savar. Three of the volunteers lead the rescue operation and planned to make a metal-rod cage seeing the rescue method of fire service. They are Shafiqul Islam Faruq, Shah Muhammad Abdullah Al-Moon and Sujon Das Rahul. Faruq, who financed and led the drive, is a businessman while Moon, a diploma engineer, is working for a private firm and Rahul is studying at a private polytechnic institute. They made the instrument with a net, a close circuit camera, a torch, a tri-stand and a cleat tied to a 600-feet-long rope. They attached the manual cable TV camera binding it with an iron rope. The device was named 'mechanical capsule'. The volunteers claimed that it was possible to rescue the boy on Friday night, but they were not allowed to do that. They had the chance to use it only after the fire service declared postponement of the operation.



Figure: Mechanical capsule

At 2.30 pm on Saturday, 27 December 2014, the volunteers started their rescue operation by slowly lowering the cage into the pipe. After sliding down around 100 feet it got stuck into something. Later, they pulled the cage around ten feet up and then dropped it again. This time, it started going down fast. They started releasing the rope slowly. He said the cage was stuck again at the spot where Jihad's body was found. At one stage about 250 feet down the pipe, the camera captured the boy's image, spurring the private rescuers on. They could see on the camera that the head of the boy was upward and an arm was on his forehead. The rescuers then pulled the body up, which was tied up with wires. Water was traced 235-240 feet down the hole. Jihad was found 5-7 feet down from there. Thus the volunteers rescued the kid at 3:00pm by their brave effort within half an hour. They however, gave some credit to the fire service personnel for extending help to them. Many of the fire service officers stood by them when they were conducting the operation, and they used the crane of fire service. The recovery ended the story with an unsettling combination of human ingenuity and neglect. DG Khan was quick to take credit saying Jihad was rescued with everyone's help. But the 'success' turned out to be an embarrassment for the Fire Service.



Figure: Rescue operation by volunteers



Figure: Jihad after rescue

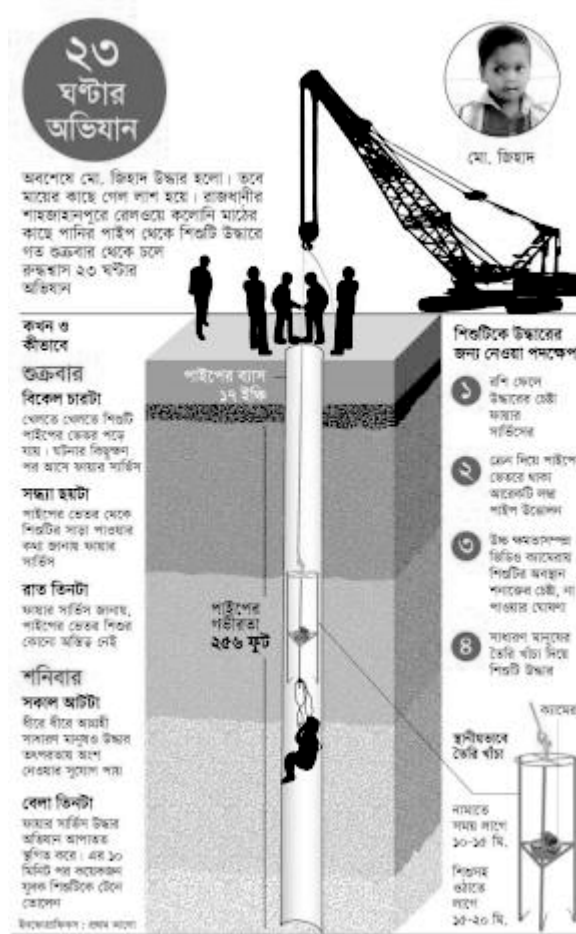


Figure: Overall 23 hours rescue effort of Jihad

Declaration of Death of Jihad

After pulling out Jihad, he was taken to Dhaka Medical College and Hospital where doctors announced him dead. Doctors said the boy had died several hours before he was brought there. Jihad's body bore bruise marks apparently from the fall; Dr Riaz Morshed said adding there were evidences of him falling into water as well. Later, the body was sent to the college morgue for an autopsy. The autopsy was performed by Habibuzzaman Chowdhury along with Forensic Department Assitant Professor AKM Shafiuzzaman Khair and lecturer Pradip Kumar Biswas.

After post-mortem of the four-year-old child, Dhaka Medical College and Hospital's Forensic Department chief Habibuzzaman Chowdhury said that internal and external injury marks were found on the boy's head, which were caused during his fall into the abandoned deep tube-well. Rust particles were found under Jihad's fingernails, proving that the boy desperately tried to hold on to the wall of steel pipe, used to reinforce the shaft, during the plunge. "The presence of water inside the boy's stomach, respiratory system and lungs indicates that his death was

caused by drowning. We have come to the conclusion that the child drowned in the water within two hours of his fall inside the pipe. Even if there were no water, the [head] injury itself could prove fatal for him.” said Habibuzzaman Chowdhury.

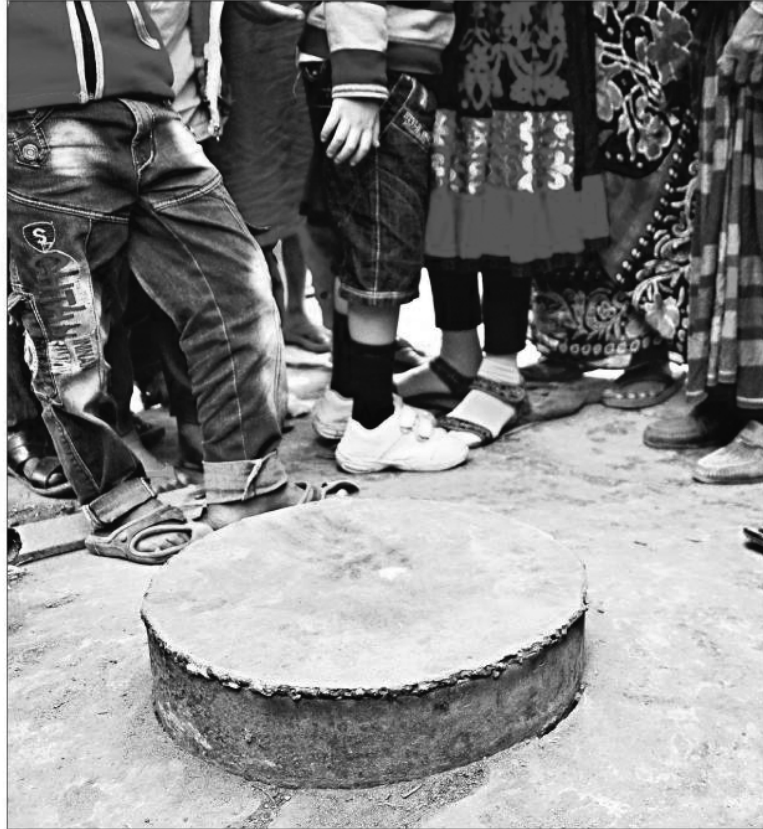
Shahjahanpur Police Sub-Inspector Abu Jafar said the body has been handed over to the family around 9:45am Sunday at the end of the post-mortem. The child was buried his ancestral village of Nagerpara in Shariatpur's Gosairhat upazila and buried there. Several thousand people attended his janaza before the burial.

Aftermath of the Incident

At the time of rescue operation in Friday, 26 December, 2014 at night, Jahangir Alam, who was in charge of the project, was suspended following the incident, while the project contractor firm, SR House, which was installing a new deep tube-well at the site, was blacklisted.

Nasir Fakir, the father of Jihad was released on Saturday afternoon after his son's body was recovered from the pit. The state minister and the police chief claimed law enforcers picked up him with a good intent to inquire about the lost kid. But they could not explain why the man was held in police station for so long.

The locals and volunteers marched in processions at Shajahanpur and in front of DMCH demanding immediate withdrawal of the junior minister for his ‘irresponsible’ remarks about the incident. Angry over the authorities' slow move to rescue Jihad, locals demonstrated against State Minister and officials of the Fire Service. They also expressed anger citing that the rescue operation has been delayed as different government bodies gave contradictory opinions and suggestions over the issue. By then, agitated locals vandalized shops around the accident spot and WASA's temporary establishments. Later, police tried to calm the situation, but agitated mob threw brick chips at police. To maintain law and order, police charged batons and dispersed the protesters. After Jihad's rescue, authorities welded the pipe's entrance with an iron plate.



রাজধানীর শাহজাহানপুর রেলওয়ে কলোনির যে অরক্ষিত পাইপটিতে পড়ে শিশু জিহাদ মারা গেছে, সেটির মুখ বন্ধ করে দেওয়া হয়েছে। এখানে জিহাদ স্মরণে স্মৃতিস্তম্ভ নির্মাণের দাবি করছে এলাকাবাসী। ছবিটি গতকাল তোলা ● প্রথম আলো

Figure: Sealed pipe's entrance after rescue operation

Nasir filed a case against Abdus Salam, owner of the construction company responsible for setting the pipe, and Jahangir Alam, Railway senior sub-assistant engineer around Saturday midnight bringing charges of negligence. Two writs were filed with the High Court seeking a number of directives, including asking the government to give adequate compensation to Jihad's family and take actions against officials who failed to rescue the boy.

Comments on the Incident and the Rescue Operation

The accident was the result of negligence on the part of the contractor and the railway that were supposed to keep the abandoned well sealed but they left it open. Open manholes on various city roads have become virtual death traps for the commuters, but the civic bodies are hardly taking any notice of this, alleged city dwellers. More than 100 manholes remain open on various roads in the capital for years, posing serious threat to public particularly for pedestrians. Careful strategy and prompt action are the two things required, which only well-trained professionals can undertake. There was veritable lack of discipline and coordination among the

civil defence people at the site with apparently no chain of command. The confusion at the scene over how best to deal with the situation, whether or not there was, in fact, a child stuck in the hole at all, and even the depth of the hole with estimates ranging from 400 to 700 feet, demonstrates how unprepared we are when it comes to handling emergencies. While rescue operations started within half an hour of the accident, the next several hours were wasted over many short-sighted attempts to recover the child. Even though the expectation of the rescue team to drag a frightened four-year-old boy up 600 feet using a rope was unrealistic, they repeatedly pursued the same method after the first failed attempt.

To say the least, the rescue effort was unplanned and disorganized, with no control over the large number of onlookers. Police were having trouble with the large number of onlookers gathered there at the time of rescue operation. Shahjahanpur Police Station OC Mehedi Hasan said the huge gathering of onlookers was hindering the rescue. Moreover, State Minister for Home Affairs Asaduzzaman Khan Kamal, WASA Director General Engineer Taksim A Khan, DMP Commissioner Benazir Ahmed, BNP Standing Committee member Mirza Abbas and Dhaka University Vice-Chancellor AAMS Arefin Siddique visited the scene at the time of rescue operation in Friday, 26 December, 2014, which added more chaos in the scene. It is high time that the government seriously considers a thorough reworking of its rescue preparedness and take full-scale measures to guarantee a systematic and effective response to emergencies in the future.

Moreover the deceit resorted to and the hint of conspiracy that the authority ‘discovered’ in the matter was uncalled for. The callous and insensitive behavior of the government agencies involved in the rescue effort worsened and slowed down the rescue operation. Not only the Fire Brigade failed to handle the situation, the behavior and utterances of persons in positions of responsibility, including the state minister for home also confounded the situation. And how does the government explain the extremely cruel treatment meted out by the police to a father who was not sure at that time what his son's fate would be? One wonders what his fate would have been had Jihad's body not been recovered. To keep him in custody for 12 hours without food is cruel and betrays a government that is prone to see conspiracy in every event.



**BANGLADESH NETWORK
OFFICE FOR URBAN SAFETY**



PART-VI

GPR TESTING ON BALL MILL FOUNDATION



**BANGLADESH NETWORK OFFICE FOR
URBAN SAFETY (BNUS), BUET, DHAKA**

Prepared By: Mehedi Ahmed Ansary

1.0 Introduction

The General Manager of a cement company has approached us for undertaking non-destructive testing on existing Ball Mill foundation at their cement plant site at Meghnaghat, Sonargaon, Narayanganj. It has been agreed that the terms of reference of the work would be limited to non-destructive testing of Ball Mill foundation using Ground Penetrating Radar (GPR). Testing at the plant site was carried out on August 30 and September 2, 2014. The report indicated the probability of void and possible location void. The cement company injected ConbextraEP10 (M) by high pressure pumping through drilled holes. 2nd time GPR test at the plant was done on December 10, 2014 after the first grouting. Significant improvement by grouting was observed in the 2nd time GPR Test. However, still there were small voids indicated near the first grouting points. The cement company again injected ConbextraEP10 (M) by high pressure pumping through drilled holes. 3rd time GPR test was performed at the site on December 19, 2014 after second grouting. This report is the outcome of the 3rd GPR tests after second time grouting.

2.0 NDT Using Ground Penetrating Radar (GPR)

Ground Penetrating Radar (GPR) is a near-surface geophysical technique that can provide high resolution scan of the dielectric properties of the earth. GPR works by sending a tiny pulse of energy (Electromagnetic Energy) into a material and recording the strength and the time required for the return of any reflected signal. A series of pulses over a single area make up what is called a scan. Reflections are produced whenever the energy pulse enters into a material with different electrical conduction properties or dielectric permittivity from the material it left. The strength, or amplitude, of the reflection is determined by the contrast in the dielectric constants and conductivities of the two materials.

Signal of 400 MHz has been used to investigate the machine foundation. All data were collected in simple line and point scan format. The direction of arrow in site plan and data collection grids indicates the starting and ending point GPR scan. The attached pictures and drawings show the results of those investigations.

3.0 Data Collection

GPR data were collected using 400 MHz with a GSSI SIR-3000 control unit. Data were collected in simple line scan format. Figure 1 shows the schematic diagram of the ball mill foundation plan. Figure 2 shows the GPR scan lines with scan ID. The direction of arrow in site plan and data collection grids is indicating the starting point of GPR scan.

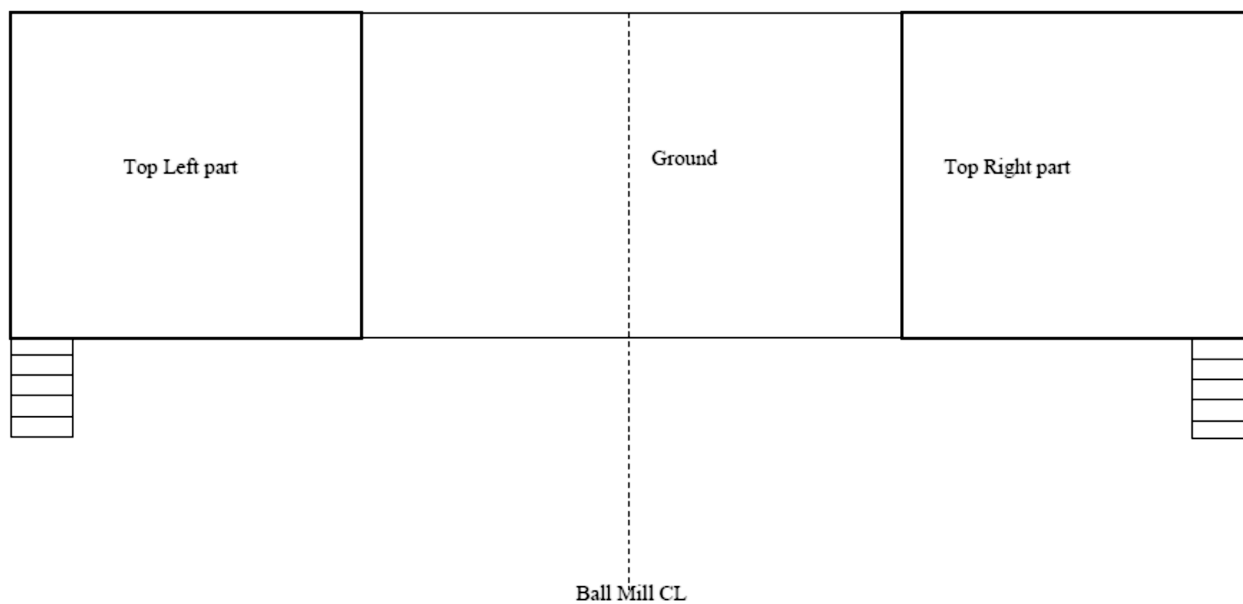


Figure 1: Ball mill foundation plan (*note: drawing is not in scale*)



Figure 2: Data collection grid lines (*note: drawing is not in scale*)

4.0 Data Processing

The collected data sets were processed by specialized software program RADAN. Three basic kind of processing tools were used in order to calculate accurate depth, to remove noise and to improve display for documentation purpose.

Time-Zero Correction: A corrected Time-Zero provides a more accurate depth calculation because it sets the top of the scan to a close approximation of the ground surface. Timezero corrections also remove the section of data that occurs before direct wave.

Infinite Impulse Response (IIR): Often used to remove noise.

Finite Impulse Response (FIR): Background noise, often seen as horizontal banding, may be removed using the FIR Filter.

5.0 Findings of Ground Penetrating RADAR (GPR) after First Grouting

The results of 400 MHz GPR data are presented below. These scan data don't show any clear contrast within the foundation area except scan ID 05 and 06. Figure 3 shows the comparison of reflectogram at the same line before and after grouting. After second time grouting, 3rd GPR test data clearly shows the absence of any void or crack in the foundation.

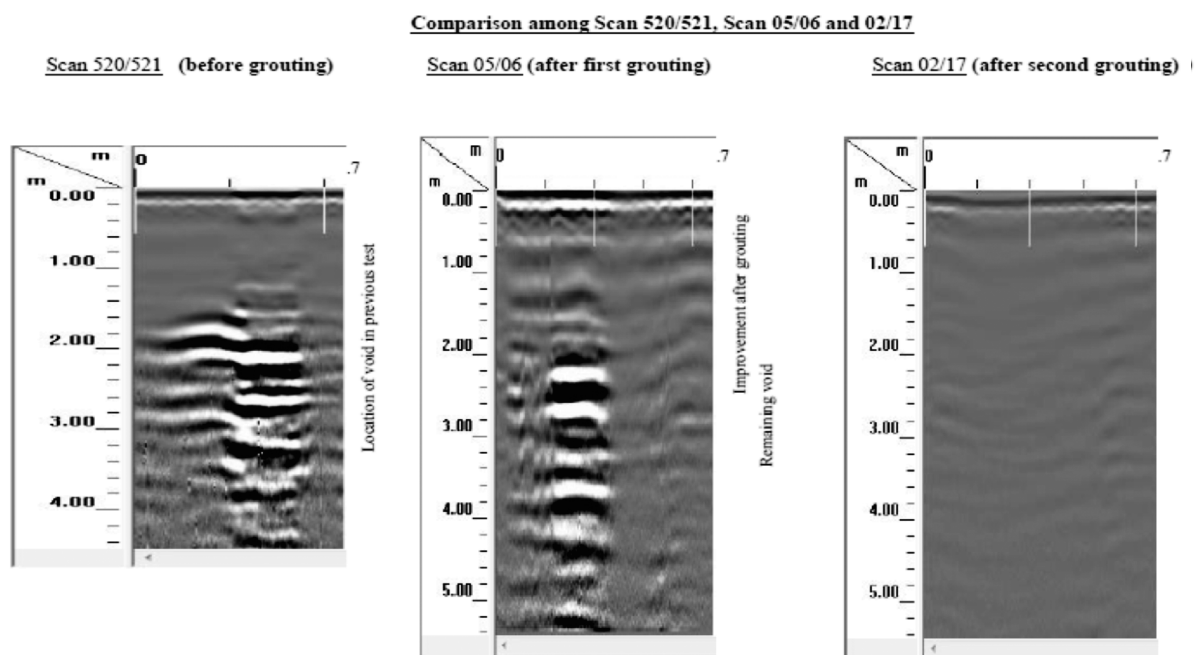
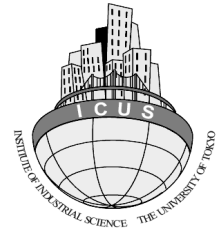


Figure 3: Comparison of reflectogram before and after grouting



**BANGLADESH NETWORK
OFFICE FOR URBAN SAFETY**



PART-VII

EARTHQUAKE RISK ASSESSMENT AND PLANNING FOR MANAGEMENT IN MYMENSINGH MUNICIPALITY, BANGLADESH

**BANGLADESH NETWORK OFFICE FOR
URBAN SAFETY (BNUS), BUET, DHAKA**

**Prepared By: Uttama Barua
Mehedi Ahmed Ansary**

1. Introduction

Earthquake is one of the most destructive natural hazards. It can occur at any time without any warning and can destroy buildings, infrastructure and above all lead to human loss and tragedy. Again urban earthquake risk is rapidly increasing, particularly in developing countries, because of high rate of urbanization, faulty land-use planning and construction, inadequate infrastructure and services, and environmental degradation (Erdik, 2006). There are three basic stages to reduce urban earthquake risk: evaluation (understanding the underlying problem and its magnitude), planning (taking actions to solve it), and implementation (realizing the proposed actions) (Villacis, 2000). Earthquake risk evaluation is the first step for quantification of the effects of the earthquake on the physical and social environment (Guragain, Jimée, & Dixit, 2008; Erdik, 2006).

Total elimination of risks may be difficult and impractical, so disaster management through proper hazard assessment is very essential to reduce loss of lives and sufferings of people. Realizing the importance of damage estimation, different studies have been undertaken for hazard specific damage estimation, i.e. flood (Smith, 1994; Herath, Dutta, & Musiake, 1999; Renyi, & Nan, 2002; Dutta, Herath, & Musiake, 2003; Kang, Su, & Chang, 2005; Koshimura et al, 2009; Middelman-Fernandes, 2010; Pistrika, 2010; Poser, & Dransch, 2010), earthquake (Park, Ang, & Wen, 1985; Cret et al, 1993; Kanamori, Hauksson, & Heaton, 1997; Kircher et al, 1997a; Kircher et al, 1997b; Eguchi et al, 1997; Whitman et al, 1997; Rojahn et al, 1997; Yamazaki, Noda, & Meguro, 1998; Dolce et al, 2003; Spence et al, 2003; Aleskerov et al, 2005; Bird et al, 2006; Miura et al, 2008; Brunner, Lemoine, & Bruzzone, 2010), hurricane (Pinelli et al, 2004; Watson Jr, & Johnson, 2004; Ginger et al, 2007), landslide (Alexander, 1986; Petrucci, Pasqua, & Gullà, 2010), etc.

Different studies related to earthquake damage estimation have been carried out covering different aspects. Park, Ang, & Wen (1985) proposed a method for evaluating structural damage of reinforced concrete buildings under random earthquake excitations. Yamazaki, Noda, & Meguro (1998) studied early earthquake damage assessment systems in Japan to provide future direction in the process. Cret et al (1993) presented earthquake damage estimation and decision analysis for emergency shut-off of city gas networks using fuzzy set theory. Whitman et al (1997) summarizes the development of a Geographic Information System (GIS) based regional earthquake loss estimation methodology for the United States funded as part of a four-and-one-half year project by the Federal Emergency Management

Agency (FEMA) through the National Institute of Building Sciences (NIBS). Kircher et al (1997a & 1997b) described building damage functions that were developed for the FEMA/NIBS earthquake loss estimation methodology. Rojahn et al (1997) developed and/or updated methodology for estimation of damage due to ground shaking, estimation of damage due to collateral loss causes such as fault rupture, ground failure, inundation, and fire following earthquake, estimation of time to restore damaged facilities to pre-earthquake usability, and estimation of deaths and injuries, for implementation in a geographic information system (GIS) application, or in a non-GIS software application, such as a relational database management system or spreadsheet for Salt Lake County, Utah (ATC-36). Eguchi et al (1997) described the development, operation and application of the first real-time loss estimation system to be utilized by an emergency services organization. Kanamori, Hauksson, & Heaton (1997) studied the then real-time seismology and earthquake hazard mitigation. Spence et al (2003) compared estimated loss from two different approaches (using predicted macro-seismic intensity, and the spectral displacement) with actual observed losses in the Kocaeli event at two different locations for estimating future losses. Dolce et al (2003) presented damage scenarios relevant to the building stock of the town of Potenza, Southern Italy. Bird et al (2006) presented a framework for resolving issues that, the assessment of building damage caused by liquefaction-induced ground deformations requires the definition of building capacity and vulnerability as a function of the demand, as well as damage scales to describe the state of the damaged building; within the context of earthquake loss estimations, where large variations in building stock and ground conditions must be considered. Brunner, Lemoine, & Bruzzone (2010) presented a novel method that detects buildings destroyed in an earthquake using pre-event VHR optical and post-event detected VHR SAR imagery at individual building level.

The earthquake records of Bangladesh suggest that the country is prone to massive earthquake in near future (The Daily Star, 2008). The active faults are gaining energy, which can be indicated by the occurrences of historical earthquakes in and around the country and long-term silences of happening potential earthquake (seismic-gap) across the region (The Daily Star, 2008). The country is divided into three earthquake zones and Mymensingh municipality lies in the northeastern zone which is designated as the most earthquake prone area of Bangladesh (Sarker, Ansary, Rahman, & Safiullah, 2010 and Ali, 1998). So, earthquake preparedness in Mymensingh Municipality has become necessary for which, earthquake damage estimation is

a must. This study aims at estimation of earthquake damage in Mymensingh municipality and preparation of risk management plan on its basis.

2. Study Area Profile: Mymensingh Municipality

Mymensingh Municipality is located in the district headquarters of Mymensingh District of Dhaka division and is situated on the right bank of the old river Brahmaputra (Mymensingh Municipality, 2012), which is shown in Figure 1. The municipality lies in the northeastern zone of Bangladesh which is designated as the most earthquake prone area of Bangladesh (Sarker, Ansary, Rahman, & Safiullah, 2010 and Ali, 1998). For this reason, this municipality was selected as the study area of this study. It is one of the oldest towns established in 1869 having an area of 21.73 sq km. The municipality is divided into 21 wards and 85 mahallahs (BBS, 2001a,b). Mymensingh is one of the rapidly growing and densely populated secondary towns of Bangladesh, with an estimated present population (night time) of 0.414 million in the municipal area (Mymensingh Municipality, 2012). Number of buildings in this municipality is 46,055 and average family size is 5.6 (Mymensingh Municipality, 2012). About 60.4 percent population of the Pourashava is literate, of which 66.4 percent are male and 53.4 percent are female (BBS, 2001a,b). The principle occupations of the adult males in the Pourashava are in the business and service areas.

3. GIS based RADIUS Methodology for Earthquake Damage Estimation in Mymensingh Municipality

For the efficient seismic risk management and for the establishment of efficient and effective mitigation schemes; advanced, multidisciplinary and integrated methodological tools are required to estimate the likely emergency response resource needs and socioeconomic impacts of large earthquakes in urban areas (Pitilakis, & Kalliopi, 2011). For the purpose, different methods and tools have been developed from different perspectives, some of which integrate information from existing building inventory and site seismicity (Alam, Tesfamariam, & Alam, 2012). These methods can be broadly grouped into: probabilistic methods based on secondary information and deterministic methods with detailed quantitative analysis (Guragain, Jimee, & Dixit, 2008). Bayraktarli, Yazgan, Dazio, & Faber (2006) utilized Bayesian Probabilistic Networks (BPN's) for earthquake risk management on the basis of a generic and indicator based risk assessment framework. Korkmaz (2009) introduced a probabilistic-based methodology for earthquake disaster risk assessment and evaluation for Turkey. Lang, Molina-Palacios, & Lindholm (2008) utilized CSM-Based Tool SELENA for damage estimation which

takes into account epistemic uncertainties in all types of input data by a logic-tree computation scheme. Sarris, Loupasakis, Soupios, Trigkas, & Vallianatos (2010) developed a GIS based application for the purpose considering a localized model. Rashed, & Weeks (2003) developed GIS methodology for same through a spatial analytical procedure combining elements from the techniques of spatial multicriteria analysis and fuzzy logic. In U.S., several methodologies and standards have been developed, such as Hazard- United States (HAZUS) and Applied Technology Council (ATC), which provide comprehensive earthquake loss estimation methodology for post-earthquake assessment (Korkmaz, 2009). In Nepal six different methodologies have been used for evaluation of earthquake risk: KVERMP (Kathmandu Valley Earthquake Risk Management Program) methodology, RADIUS (Risk Assessment Tools for Diagnosis of Urban Areas against Seismic Disasters) methodology, GIS (Geographic Information System) in Grid, SLARIM (Strengthening Local Authorities in Risk Management) methodology (GIS based), community watching (Community Based Disaster Risk Management Program) and HAZUS (Hazards-United States) methodology (Guragain, Jimee, & Dixit, 2008). The overall comparison of various loss estimation processes is summarized in table 1.

Among these processes RADIUS is more convenient to use for its simple methodology and it does not require detail technical knowledge on earthquake engineering (Guragain, Jimee, & Dixit, 2008). But, the process has become more and more complex in terms of handling a large amount of spatial data with subsequent analysis (Guragain, Jimee, & Dixit, 2008). So, GIS based RADIUS (GBR) has been developed integrating RADIUS with GIS to simplify the process (RADIUS, 2000). RADIUS initiative was launched in 1996 by the secretariat of the International Decade for Natural Disaster Reduction (IDNDR 1990-2000) of the United Nations to develop seismic risk assessment and management tools to reduce the effects of seismic disasters in urban areas, particularly in developing countries (RADIUS, 2000 and Villacis, 2000). Under RADIUS initiative, a methodology was developed by GeoHazards International for implementation of case studies in nine cities around the world. Based on nine case studies, OYO Group, Japan (OYO Corporation and OYO International and coded by Geosoft Technical Support Singapore and Risk Management Software India) developed a computer program in excel, for earthquake damage estimation, providing a basis for similar efforts as a first step of earthquake risk management for other cities in developing countries to understand the seismic vulnerability of cities, to raise awareness and encourage the start of disaster prevention programmes (GHI, 2004 and RADIUS, 2000). Figure 2 shows general flow

of GIS based RADIUS methodology along with required inputs and generated output. It requires input of a simple data set which is organized in GIS. After analyzing in RADIUS, the results can be represented in GIS maps to show the spatial distributions of the seismic damage states (Alam, Tesfamariam, & Alam, 2012). So, in this study GIS based RADIUS methodology was followed for earthquake damage estimation in Mymensingh Municipality. This study was conducted in November, 2013.

Damage estimation in GIS based RADIUS is generally carried out by subdividing the study area (Alam, Tesfamariam, & Alam, 2012). So, firstly the area of Mymensingh municipality is divided into equal-sized square grids in GIS, where the grid size is defined 1 sq.km. Then the input values are assigned to each of the grids to obtain spatially distributed outputs in RADIUS. RADIUS tool only requires total night-time population of the study area from which day-time population and population distribution in each mesh is calculated by predefined factors in the tool. In RADIUS methodology, building inventory is required in different format. In Mymensingh municipality, data on total number of buildings, grid by grid number of buildings and grid by grid percentage of buildings of each class are collected and calculated in GIS and then inputted in RADIUS. In table 2 classifications of building types used in RADIUS and building stock in Mymensingh Municipality in terms of percentage are described. Weight of each mesh is defined based on relative building density and population density in each mesh unit. Categories of mesh weight in RADIUS are: 0 (none), 1 (low), 2 (average), 3 (high) and 4 (very high).

For hazard assessment, five ground classifications have been adopted in the RADIUS tool, based on the surface soil. They are: hard rock, soft rock, medium soil, soft soil and unknown soil (for the convenience of the users). It is used to evaluate the site amplification ratio in earthquake scenario study. Again, different seismic scenarios for the municipality are determined on the basis of past earthquake history of the study area. Tectonically, Bangladesh lies in the north eastern Indian plate and at the junction of three tectonic plates—the Indian plate, the Eurasian plate and the Burmese microplate (Akhter, 2010). OYO International Corporation (OIC) proposed four earthquake scenarios for Bangladesh, where each scenario was set as a maximum possible earthquake occurring within each of the five major fault zones (CDMP, 2009b). The history of severe earthquake in Mymensingh municipality is described in table 3. A powerful earthquake needs at least 100-150 years to be originated for a particular region (CDMP, 2009b) and it is overdue for Mymensingh municipality, as 129 years and 117 years

have passed by since earthquake from Madhupur Fault and Dauki fault hit the region respectively (Table 3). So, scenarios of earthquakes generated from these two faults are considered as scenario earthquakes for damage estimation in Mymensingh municipality (Table 4).

The time of occurrence for the scenario earthquake are specified 2 am and 2 pm, because the casualty count depends on whether the earthquake occurs during night or day (Alam, Tesfamariam, & Alam, 2012). In RADIUS tool, two seismic intensity scales are adopted: Modified Mercalli Intensity (MMI) peak ground acceleration (PGA), where PGA is calculated by one of three of the most popular attenuation formulas and converted to MMI using the empirical formula of Trifunac and Brady (1975) (Table 5). Average MMI for Dauki and Madhupur earthquake scenarios in Mymensingh municipality are 5.95 and 6.35 respectively. So, earthquake from Madhupur fault will have greater impact on the area. For Dauki and Madhupur earthquake scenarios, the north-eastern and south-western part of the area will have greater probable intensity respectively.

The tool gives vulnerability curves for each of the building categories, which show the relationship between the mean damage rate and seismic hazard (MMI or PGA). Combining all the factors with the calculated seismic intensity distribution, building damage of Mymensingh municipality is estimated. Casualties (injury and death) are calculated in RADIUS from the number of damaged buildings. It varies with the time of earthquake occurrence: the day (6 am – 6pm) and night (6pm – 6am) as, the number of inhabitants residing inside buildings during the earthquake are normally not the same during day and night time (Alam, Tesfamariam, & Alam, 2012). Thus earthquake damage estimation was done in RADIUS tool.

4. Results and Discussion

4.1 Estimated Damage in Mymensingh Municipality

Total number of damaged building for Dauki and Madhupur earthquake scenarios are 1174 and 2023 respectively. So, building damage is greater for Madhupur earthquake scenario. Figure 3 shows mesh-by-mesh damaged building count in Mymensingh municipality for two scenario earthquakes. For Dauki earthquake scenario, most of the meshes contain 35 to 55 damaged building each, where building damage ratio is between 2.00 and 2.80, and for Madhupur earthquake scenario, most of the meshes contain 60 to 100 damaged building each, where building damage ratio is between 3.14 and 4.97. Though impact from Madhupur earthquake

scenario is greater; higher damaged building count and damage ratio can be observed in almost same areas for two scenario earthquake events. Again, for both scenario earthquakes casualty is greater for earthquake event occurrence at night and it is higher for Madhupur earthquake scenario. Figure 4, 5, and 6 represent mesh-by-mesh death count, severe injury count, and moderate injury count in Mymensingh municipality for two earthquake scenarios occurring at day or night. Though casualty from Madhupur earthquake scenario (night-time occurrence) is greater; higher casualty (death and injury) can be observed in almost same areas for two scenario earthquake events and two occurrence times.

4.2 Use of the Estimated Damage: Earthquake Risk Management Planning

Earthquake risk can be reduced by coordinating and focusing on risk management activities to maintain community safety, to reduce physical damage and socio-economic disruption and; to reduce potential impact of large earthquakes on urban societies by timely and correct action after a disastrous earthquake (Pitilakis, & Kalliopi, 2011). Chile's earthquake (2010) was larger but less destructive than Haiti's (2012) which represent the importance of disaster preparedness in preventing possible disastrous events or at least minimizing their impacts on the society (Wayman, 2010 and Bapat, 2010). The preparation of earthquake preparedness plans based on the assessment of the impact of earthquakes and the minimization of their consequences are the most important tasks of civil protection (Pitilakis, & Kalliopi, 2011).

The results of GIS based RADIUS analysis emphasize the importance of earthquake risk reduction in Mymensingh municipality. So, the estimated damage can be regarded as a preliminary estimation for earthquake risk management in the municipality. The results give the spatial idea about the potential losses, which can be integrated mainly in preparedness, response and recovery steps of earthquake disaster management. From the damage maps, potential risky areas in the municipality can be found out to take mitigation steps respectively. It will guide to improve the seismic performance of existing structures, improve safety in school buildings, and help the decision makers to integrate seismic resistance into new construction processes. From the damaged buildings count in the municipality, distribution of internal displaced people can be estimated, which will further guide to take preparedness through earthquake shelter planning. Casualties (death and injury) caused by the seismic events are the main social damage parameters (Alam, Tesfamariam, & Alam, 2012). Overall damage scenario will help to increase awareness among the local people of the municipality about the earthquake risk, to increase preparedness for earthquake, to take part in the preparation of earthquake preparedness plan, and most importantly to improve emergency response planning

and capability. The results also provide a preliminary estimation of severe and moderate injury for the decision makers to plan and to be prepared for taking actions according to the requirement and guide the first responders for quick response during a disaster, e.g. first aid, hospital requirement, emergency treatment requirement etc. It will also help the authority to immediately take decision to repair or retrofit vulnerable buildings and to take preparation for long-term community recovery after an earthquake. Thus, the estimated earthquake damage of Mymensingh municipality will help to guide the future development activities of the municipality.

5. Conclusion

GIS based RADIUS methodology is very useful for quick earthquake damage estimation to take immediate steps for earthquake disaster risk management, though it has some limitations. For its simple methodology, its function and accuracy is limited (GISdevelopment, n.d.), where quantification of this uncertainty in the results is not addressed within the framework (Alam, Tesfamariam, & Alam, 2012). To simplify the methodology, fragility functions generalize both reinforced concrete (RC) and masonry buildings, which does not match with the real-life scenario (different damage pattern for a particular seismic activity) and thus develops some uncertainty and similar uncertainty can be observed for building occupancy classes (Alam, Tesfamariam, & Alam, 2012). Another fact is that earthquakes and their impacts differ widely, which is not considered in the methodology. So the results cannot be used for detailed analysis: exact engineering analysis, site specific earthquake analysis etc and for exact engineering decision making (GISdevelopment, n.d.). So, the tool should be used for only preliminary estimation, where further validation and more detailed studies should be done (RADIUS, 2000). It is hoped that the results of the earthquake risk assessment in Mymensingh municipality will assist the decision makers to understand the risk of the municipality to earthquake, to take initiatives for earthquake risk management in the municipality, to promote awareness among the local people to contribute in the management process and most importantly to assist starting preparedness programmes for future earthquake disasters in Mymensingh municipality.

References

1. Akhter, S.H. (2010). Earthquakes of Dhaka. In M. A. Islam & S. U. Ahmed, *Environment of Capital Dhaka: Plants, Wildlife, Gardens, Parks, Open Spaces, Air, Water, Earthquake* (Volume 6 of Dhaka celebration series, 1608-2008, pp. 401-426). Dhaka, Bangladesh.
2. Alam, M.N., Tesfamariam, S., & Alam, M.S. (2012). GIS-Based Seismic Damage Estimation: Case Study for the City of Kelowna, BC. *Natural Hazards Review*, 14(1), 66-78.
3. Aleskerov, F., Say, A.I., Toker, A., Akin, H.L., & Altay, G. (2005). A cluster-based decision support system for estimating earthquake damage and casualties. *Disasters*, 29(3), 255-276.
4. Alexander, D. (1986). Landslide damage to buildings. *Environmental Geology and Water Sciences*, 8(3), 147-151.
5. Ali, M.H. (1998). *Earthquake Database and Seismic Zoning of Bangladesh*. Bangkok. Retrieved October 20, 2013 from:
<http://www.cridlac.org/digitalizacion/pdf/eng/doc12294/doc12294.htm>
6. Bangladesh Bureau of Statistics. (2001a). *Population Census, 2001: Zilla series, Mymensingh Zila*. Bangladesh Bureau of Statistics, Planning Division, Ministry of Planning, Government of Peoples Republic of Bangladesh, Dhaka, Bangladesh. Retrieved October 20, 2013 from:
<http://www.bbs.gov.bd/WebTestApplication/userfiles/Image/Wing/Census%20Wing/Zila%20Series/mymensing.pdf>
7. Bangladesh Bureau of Statistics. (2001b). *Population and Housing Census, 2001. Community Report, Mymensingh Zila*. Bangladesh Bureau of Statistics, Planning Division, Ministry of Planning, Government of Peoples Republic of Bangladesh, Dhaka, Bangladesh. Retrieved October 20, 2013 from:
http://www.bbs.gov.bd/WebTestApplication/userfiles/Image/Wing/Census%20Wing/Community%20Series/mym_u_sum.pdf
8. Bangladesh Bureau of Statistics. (2012). *Population and Housing Census, 2011. Community Report, Mymensingh Zila*. Bangladesh Bureau of Statistics, Planning Division, Ministry of Planning, Government of Peoples Republic of Bangladesh, Dhaka, Bangladesh. Retrieved October 20, 2013 from:
<http://www.bbs.gov.bd/webtestapplication/userfiles/image/census2011/dhaka/mymensingh/Mymensingh%20at%20a%20glance.pdf>

9. Bapat, A. (2010). Re-Orientation of Disaster Management Plans in Asian Countries in View of Recent Earthquakes in China, Haiti and Chile. *Asian Disaster Management News*, 16 (1), 20-21. Retrieved May 20, 2014, from:
http://www.adpc.net/v2007/Downloads/2010/Jun/Newsletter_V16No1_2010.pdf
10. Bayraktarli, Y.Y., Yazgan, U., Dazio, A., & Faber, M.H. (2006). Capabilities of the Bayesian probabilistic networks approach for earthquake risk management. In *First European Conference on Earthquake Engineering and Seismology* (Vol. 3, No. 8, pp. 1-10). Retrieved October 20, 2013 from:
http://129.132.120.202/Publications/bayraktarli_1458.pdf
11. Bird, J.F., Bommer, J.J., Crowley, H., & Pinho, R. (2006). Modelling liquefaction-induced building damage in earthquake loss estimation. *Soil Dynamics and Earthquake Engineering*, 26(1), 15-30.
12. BNBC. (1993). *Bangladesh National Building Code*.
13. Brunner, D., Lemoine, G., & Bruzzone, L. (2010). Earthquake damage assessment of buildings using VHR optical and SAR imagery. *Geoscience and Remote Sensing, IEEE Transactions on*, 48(5), 2403-2420.
14. CDMP. (2009a). *Report on Earthquake Vulnerability Assessment of Dhaka, Chittagong and Sylhet City Corporation Area*. Dhaka, Bangladesh: Comprehensive Disaster Management Programme (CDMP), Ministry of Food and Disaster Management, Government of the People's Republic of Bangladesh.
15. CDMP. (2009b). *Report on Risk Assessment of Dhaka, Chittagong and Sylhet City Corporation Area*. Dhaka, Bangladesh: Comprehensive Disaster Management Programme (CDMP), Ministry of Food and Disaster Management, Government of the People's Republic of Bangladesh.
16. Cret, L., Yamazaki, F., Nagata, S., & Katayama, T. (1993). Earthquake damage estimation and decision analysis for emergency shut-off of city gas networks using fuzzy set theory. *Structural Safety*, 12(1), 1-19.
17. Dolce, M., Masi, A., Marino, M., & Vona, M. (2003). Earthquake damage scenarios of the building stock of Potenza (Southern Italy) including site effects. *Bulletin of Earthquake Engineering*, 1(1), 115-140.
18. Dutta, D., Herath, S., & Musiaka, K. (2003). A mathematical model for flood loss estimation. *Journal of hydrology*, 277(1), 24-49.
19. Earthquake in Bangladesh. (2008). *The Daily Star*. Retrieved October 27, 2013, from:
<http://www.scribd.com/doc/6956055/Earthquake-in-Bangladesh>

20. Eguchi, R.T., Goltz, J.D., Seligson, H.A., Flores, P.J., Blais, N.C., Heaton, T.H., & Bortugno, E. (1997). Real-time loss estimation as an emergency response decision support system: the early post-earthquake damage assessment tool (EPEDAT). *Earthquake Spectra*, 13(4), 815-832.
21. Erdik, M. (2006). Urban Earthquake Risk. *Geohazards*, 17. Retrieved October 27, 2013, from:
<http://dc.engconntl.org/geohazards/17>
22. FEMA. (1999). *Earthquake Loss Estimation Methodology: HAZUS 99: User's Manual*. Federal Emergency Management Agency (FEMA), Washington, DC. Retrieved October 20, 2013 from:
http://www.geodata.lib.ncsu.edu/fema/hazus/Manuals_FINAL/.../AVUserManual.pdf
23. FEMA. (2004). *HAZUS: The Federal Emergency Management Agency's (FEMA's) Methodology for Estimating Potential Losses from Disasters*. Federal Emergency Management Agency (FEMA), Washington, DC. Retrieved October 20, 2013 from:
<http://www.geohaz.org/news/images/publications/QuitoRiskManagementProject.pdf>
24. GHI. (2004). *RADIUS Introduction*. GeoHazards International (GHI). Retrieved October 20, 2013 from:
<http://www.geohaz.org/projects/radius.html>
25. Ginger, J.D., Henderson, D.J., Leitch, C.J., & Boughton, G.N. (2007). Tropical Cyclone Larry: Estimation of wind field and assessment of building damage. *Australian Journal of Structural Engineering*, 7, 209-224.
26. GISdevelopment. (n.d.). *GIS Development*. Retrieved October 27, 2013, from:
http://www.gisdevelopment.net/application/natural_hazards/overview/nho0017pf.htm
27. Guragain, R., Jimée, G., & Dixit, A.M. (2008). Earthquake Awareness and Effective Planning Through Participatory Risk Assessment: An Experience from Nepal. In *Proceedings of 14th World Conference on Earthquake Engineering (14WCEE)* (pp. 12-17). Retrieved October 27, 2013, from:
www.14wcee.org/Proceedings/files/07-0086.PDF
28. Herath, S., Dutta, D., & Musiake, K. (1999). Flood damage estimation of an urban catchment using remote sensing and GIS. In *Proc. the Eighth International Conference on Urban Storm Drainage*. Retrieved February 11, 2015, from:
<http://www.adrc.asia/publications/TDRM2003June/10.pdf>

29. Kang, J.L., Su, M.D., & Chang, L.F. (2005). Loss functions and framework for regional flood damage estimation in residential area. *Journal of Marine Science and Technology*, 13(3), 193-199. Retrieved February 11, 2015, from:
<http://jmst.ntou.edu.tw/marine/13-3/193-199.pdf>
30. Kanamori, H., Hauksson, E., & Heaton, T. (1997). Real-time seismology and earthquake hazard mitigation. *Nature*, 390(6659), 461-464.
31. Kircher, C.A., Nassar, A.A., Kustu, O., & Holmes, W.T. (1997a). Development of building damage functions for earthquake loss estimation. *Earthquake spectra*, 13(4), 663-682.
32. Kircher, C.A., Reitherman, R.K., Whitman, R.V., & Arnold, C. (1997b). Estimation of earthquake losses to buildings. *Earthquake spectra*, 13(4), 703-720.
33. Korkmaz, K.A. (2009). Earthquake Disaster Risk Assessment and Evaluation for Turkey. *Environmental Geology*, 57(2), 307-320. Retrieved October 27, 2013, from:
<http://link.springer.com/article/10.1007/s00254-008-1439-1#page-1>
34. Koshimura, S., Oie, T., Yanagisawa, H., & Imamura, F. (2009). Developing fragility functions for tsunami damage estimation using numerical model and post-tsunami data from Banda Aceh, Indonesia. *Coastal Engineering Journal*, 51(03), 243-273.
35. Lang, D.H., Molina-Palacios, S., & Lindholm, C.D. (2008). Towards Near-Real-Time Damage Estimation Using A CSM-Based Tool for Seismic Risk Assessment. *Journal of Earthquake Engineering*, 12 (S2), 199-210. Retrieved October 27, 2013, from:
http://www.saferproject.net/doc/publications_safer/jee_hazturk_ii.pdf
36. LGED. (2012). *Digital Map*. Local Government Engineering Department (LGED), Dhaka, Bangladesh. Retrieved May 20, 2013, from:
<http://www.lged.gov.bd/ViewMap.aspx>
37. Mattingly, S. (2000). Advances in Seismic Risk Management in Developing Countries. *Bulletin of the New Zealand Society for Earthquake Engineering*, 33(3), 286-302. Retrieved October 27, 2013, from:
<http://www.nzsee.org.nz/db/Bulletin/Archive/33%283%290286.pdf>
38. Middelmann-Fernandes, M.H. (2010). Flood damage estimation beyond stage–damage functions: an Australian example. *Journal of Flood Risk Management*, 3(1), 88-96.
39. Miura, H., Midorikawa, S., Fujimoto, K., Pacheco, B.M., & Yamanaka, H. (2008). Earthquake damage estimation in Metro Manila, Philippines based on seismic performance of buildings evaluated by local experts' judgments. *Soil Dynamics and Earthquake Engineering*, 28(10), 764-777.

40. Muhit, A., Roy, C., Rahman, A. and Ahamed, T. (2011). Municipal Solid Waste Mapping of Mymensingh Town Using GIS ArcView. *Bangladesh Research Publication Journal* 5(3): 271-281. Retrieved October 27, 2013, from:
<http://www.bdresearchpublications.com/admin/journal/upload/09221/09221.pdf>
41. Mymensingh Municipality. (2012). *About Mymensingh Pourashava*. Retrieved November 9, 2013, from:
<http://www.mymensinghmunicipality.gov.bd/>
42. Okazaki, K. (2000). *RADIUS Initiative for IDNDR-How to Reduce Urban Seismic Risk*. In 12th World Conference on Earthquake Engineering, Auckland, New Zealand. Retrieved October 27, 2013, from:
<http://www.iitk.ac.in/nicee/wcee/article/2528.pdf>
43. Park, Y.J., Ang, A.H.S., & Wen, Y.K. (1985). Seismic damage analysis of reinforced concrete buildings. *Journal of Structural Engineering*, 111(4), 740-757.
44. Petrucci, O., Pasqua, A.A., & Gullà, G. (2010). Landslide damage assessment using the Support Analysis Framework (SAF): the 2009 landsliding event in Calabria (Italy). *Advances in Geosciences*, 26(26), 13-17. Retrieved February 11, 2015, from:
<http://www.adv-geosci.net/26/13/2010/adgeo-26-13-2010.pdf>
45. Pinelli, J.P., Simiu, E., Gurley, K., Subramanian, C., Zhang, L., Cope, A., & Hamid, S. (2004). Hurricane damage prediction model for residential structures. *Journal of Structural Engineering*, 130(11), 1685-1691.
46. Pistrika, A. (2010). Flood damage estimation based on flood simulation scenarios and a GIS platform. *Eur Water*, 30, 3-11.
http://www.ewra.net/ew/pdf/EW_2010_30_01.pdf
47. Ptilakis, K. D., & Kalliopi, G. K. (2011). Seismic Risk Assessment and Management of Lifelines, Utilities and Infrastructures. *Santiago*, 10, 13. Retrieved October 27, 2013, from:
<http://www.vce.at/SYNER-G/pdf/publications/5ICEGE-Ptilakis%20-%20theme%20lecture.pdf>
48. Poser, K., & Dransch, D. (2010). Volunteered geographic information for disaster management with application to rapid flood damage estimation. *Geomatica*, 64(1), 89-98.
49. Rashed, T., & Weeks, J. (2003). Assessing Vulnerability to Earthquake Hazards through Spatial Multicriteria Analysis of Urban Areas. *International Journal of Geographical Information Science*, 17(6), 547-576. Retrieved October 27, 2013, from:
http://sustsci.aaas.org/files/rashed_weeks_ijgis2003.pdf

-
50. RADIUS. (2000). *Risk Assessment Tools For Diagnosis of Urban Areas against Seismic Disasters*. Retrieved October 27, 2013, from:
<http://www.geohaz.org/projects/radius.html>
51. Renyi, L., & Nan, L. (2002). Flood area and damage estimation in Zhejiang, China. *Journal of environmental management*, 66(1), 1-8.
52. Rojahn, C., King, S.A., Scholl, R.E., Kiremidjian, A.S., Reaveley, L.D., & Wilson, R.R. (1997). Earthquake damage and loss estimation methodology and data for Salt Lake County, Utah (ATC-36). *Earthquake Spectra*, 13(4), 623-642.
53. AUDMP. (2005). *Community-based Earthquake Risk Management in Dhaka City*. Community empowerment for earthquake preparedness, Safer Cities 15, AUDMP. Retrieved October 27, 2013, from:
www.adpc.net/AUDMP/library/safer_cities/15.pdf
54. Sarker, J.K., Ansary, M.A., Rahman, M.S., & Safiullah, A.M.M. (2010). Seismic Hazard Assessment for Mymensingh, Bangladesh. *Environmental Earth Sciences*, 60(3), 643-653.
55. Sarris, A., Loupasakis, C., Soupios, P., Trigkas, V., & Vallianatos, F. (2010). Earthquake Vulnerability and Seismic Risk Assessment of Urban Areas in High Seismic Regions: Application to Chania City, Crete Island, Greece. *Natural Hazards*, 54(2), 395-412. Retrieved October 27, 2013, from:
<http://soupios.chania.teicrete.gr/papers/naturalHazard2009-serisk.pdf>
56. Smith, D.I. (1994). Flood damage estimation- A review of urban stage-damage curves and loss functions. *Water S. A.*, 20(3), 231-238.
57. Spence, R., Bommer, J., del Re, D., Bird, J., Aydinoğlu, N., & Tabuchi, S. (2003). Comparing loss estimation with observed damage: a study of the 1999 Kocaeli earthquake in Turkey. *Bulletin of Earthquake Engineering*, 1(1), 83-113.
58. Villacis, C.A., & Cardona, C.N. (1999). Guidelines for the Implementation of Earthquake Risk Management Projects. *Geo hazards International*. Palo Alto, California. Retrieved October 27, 2013, from:
<http://www.gripweb.org/gripweb/sites/default/files/Guidelines%20for%20the%20Implementation%20of%20Earthquake%20Risk%20Management%20Projects.pdf>
59. Villacis, C.A. (2000). *RADIUS – An IDNDR Project on Urban Earthquake Risk Management*. In 12th World Conference on Earthquake Engineering, Auckland, New Zealand. Retrieved October 27, 2013, from:
www.iitk.ac.in/nicee/wcee/article/2819.pdf

60. Watson Jr, C.C., & Johnson, M.E. (2004). Hurricane loss estimation models: Opportunities for improving the state of the art. *Bulletin of the American Meteorological Society*, 85(11), 1713-1726.
61. Wayman, E. (2010). Chile's Quake Larger But Less Destructive Than Haiti's. *Earth*. Retrieved October 27, 2013, from:
www.earthmagazine.org/article/chiles-quake-larger-less-destructive-haitis
62. Whitman, R.V., Anagnos, T., Kircher, C.A., Lagorio, H.J., Lawson, R.S., & Schneider, P. (1997). Development of a national earthquake loss estimation methodology. *Earthquake Spectra*, 13(4), 643-661.
63. Yamazaki, F., Noda, S., & Meguro, K. (1998). Developments of early earthquake damage assessment systems in Japan. In *Proceedings of ICOSSAR* (Vol. 97, pp. 1573-1580).
<http://ares.tu.chiba-u.jp/~papers/paper/ICOSSAR/ICOSSAR1997-1Early.pdf>

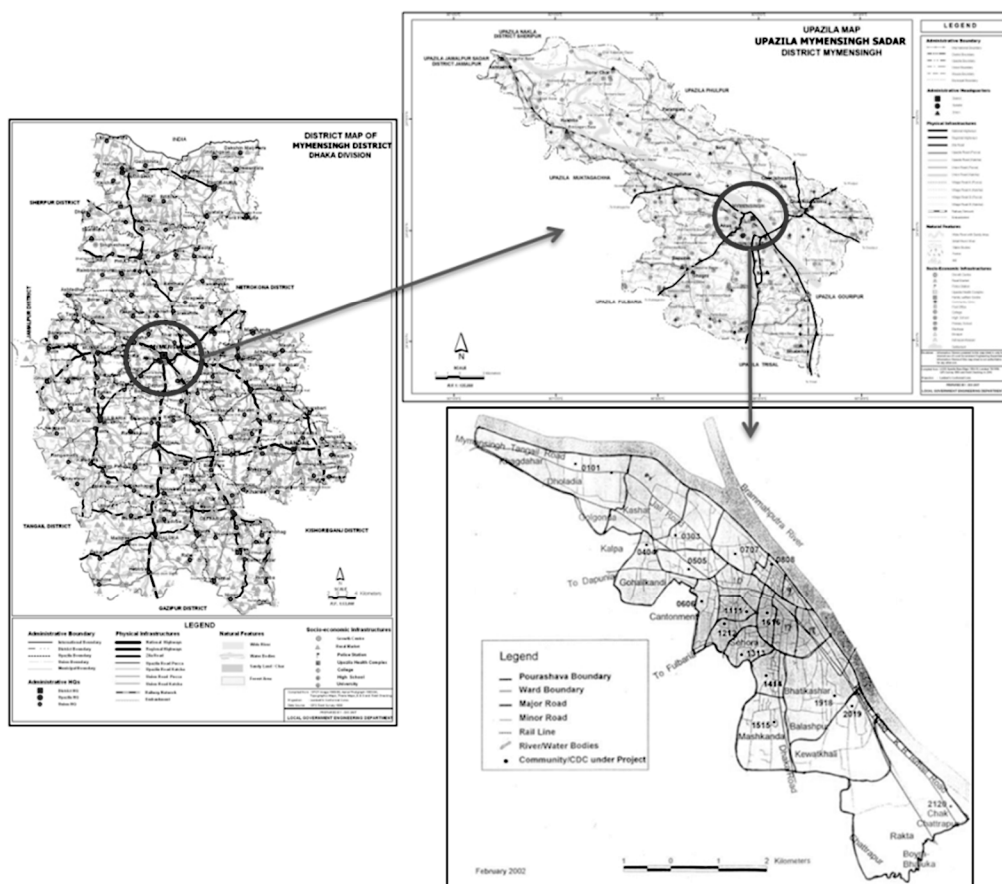


Figure 1: Location Map of Mymensingh Sadar Upazila in Mymensingh District (Source: LGED, 2012 and Muhit, Roy, Rahman, and Ahamed, 2011)

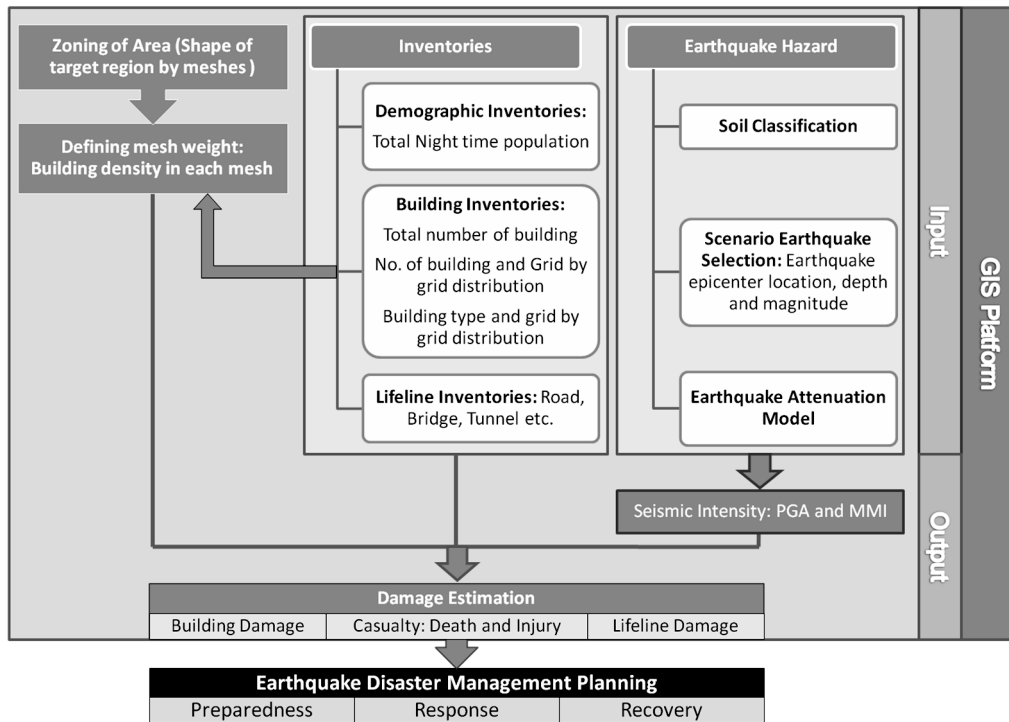


Figure 2: Process of earthquake damage estimation in GIS based RADIUS methodology

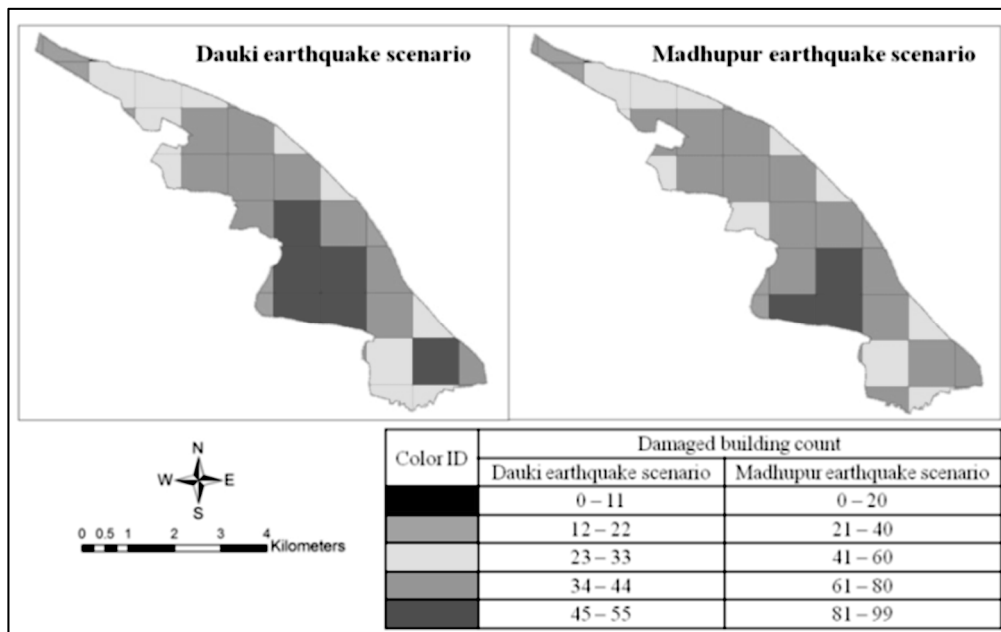


Figure 3: Mesh-by-mesh damaged building count in Mymensingh municipality for two scenario earthquakes (Dauki and Madhupur)

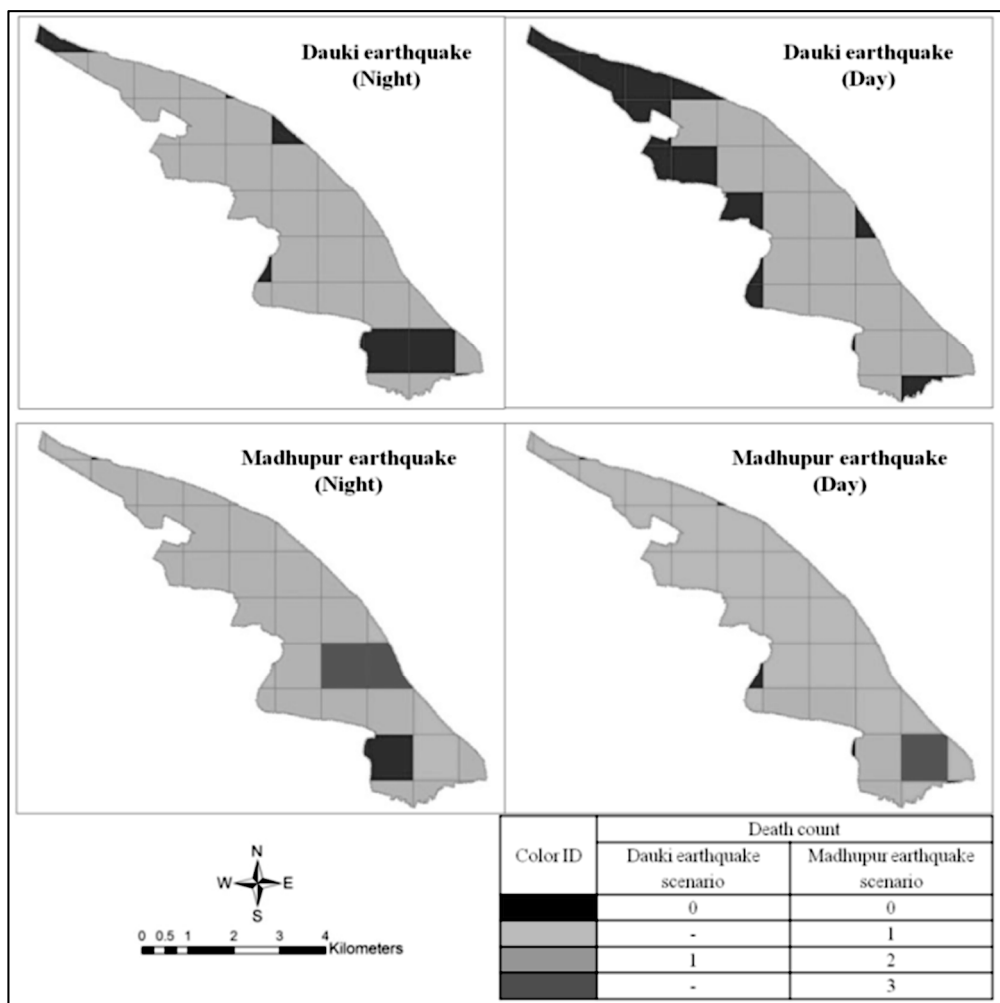


Figure 4: Mesh-by-mesh death count in Mymensingh municipality for two scenario earthquakes (Dauki and Madhupur) at two occurrence times (2am and 2pm)

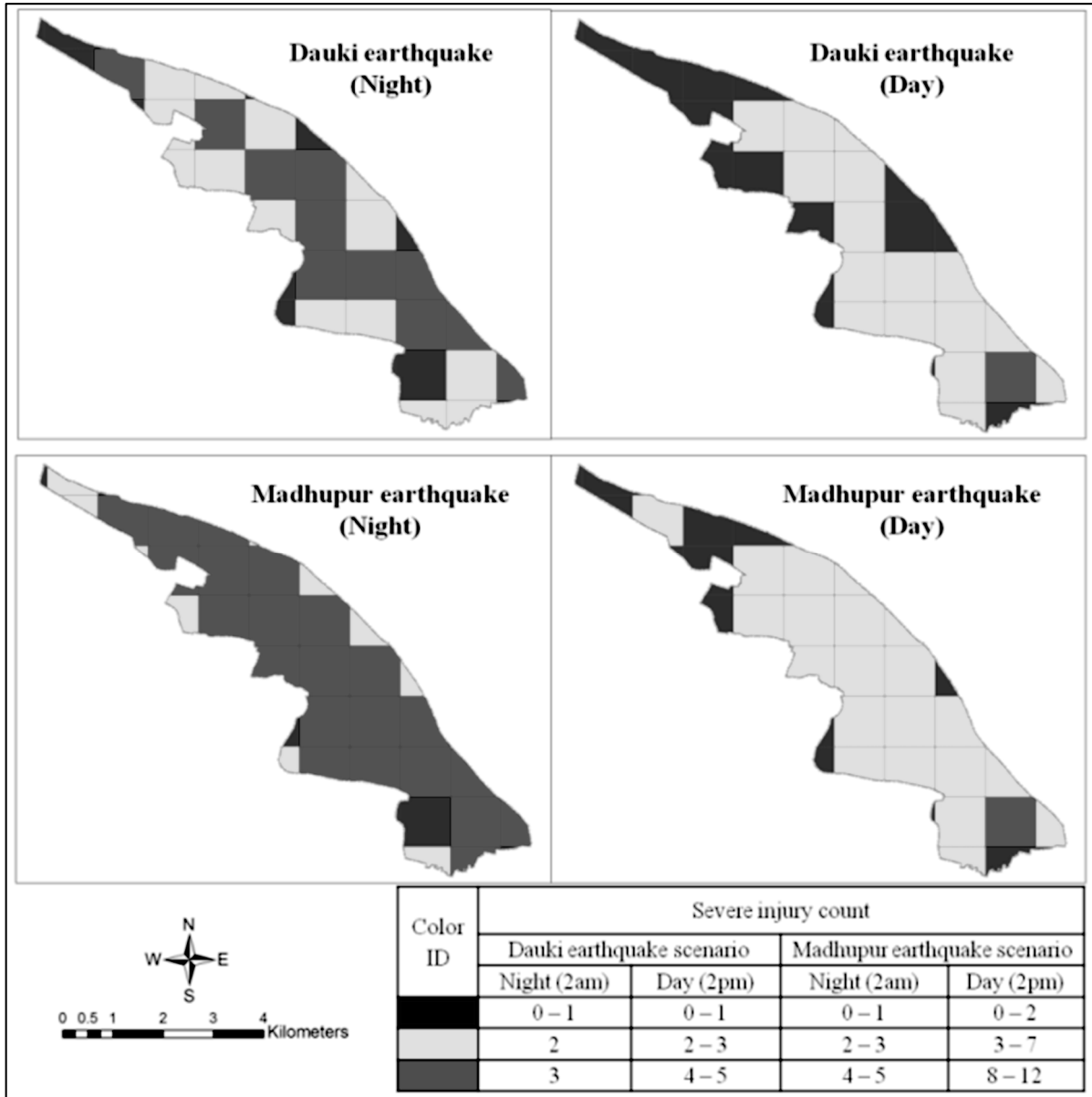


Figure 5: Mesh-by-mesh severe injury count in Mymensingh municipality for two scenario earthquakes (Dauki and Madhupur) at two occurrence times (2am and 2pm)

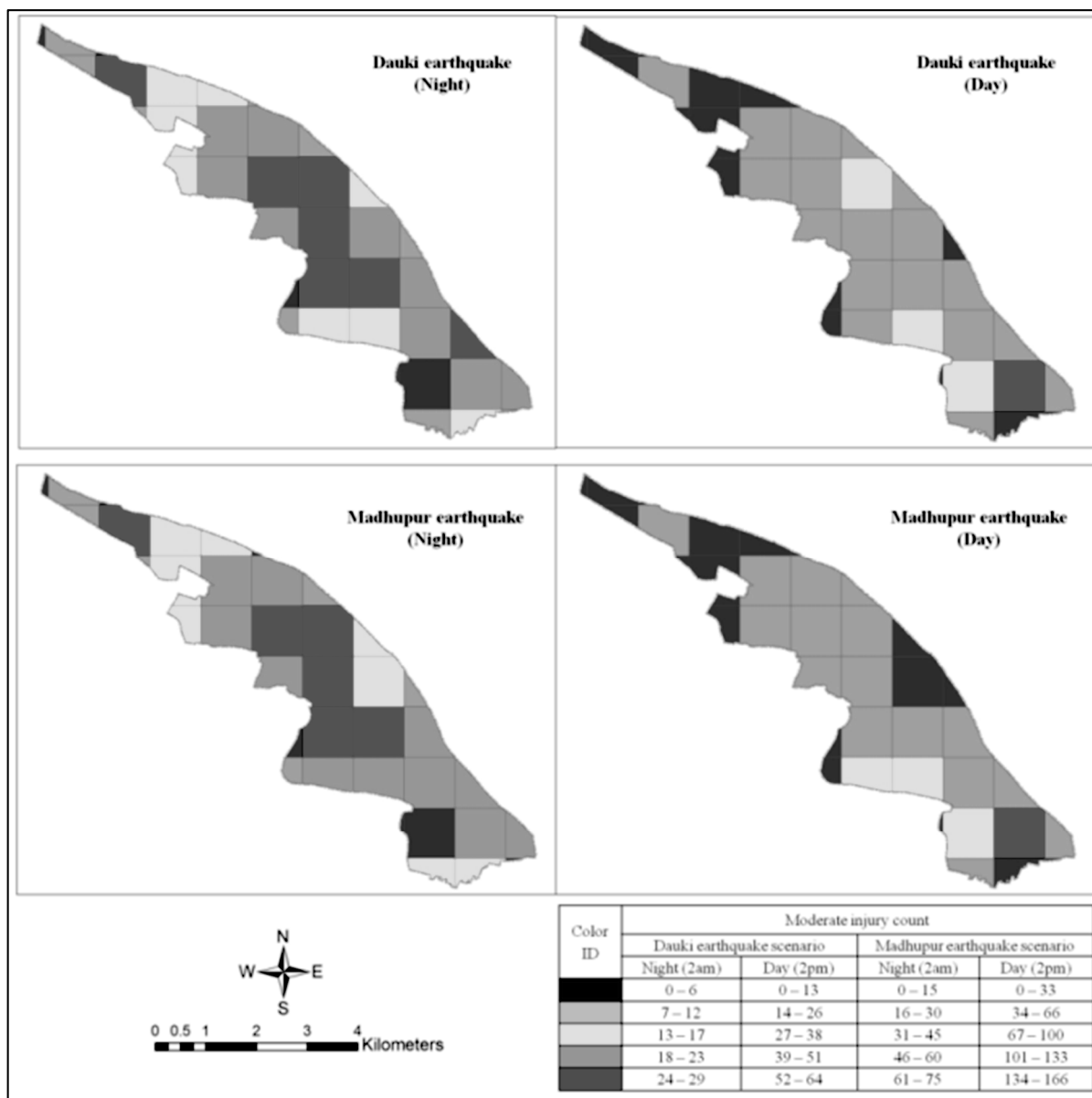


Figure 6: Mesh-by-mesh moderate injury count in Mymensingh municipality for two scenario earthquakes (Dauki and Madhupur) at two occurrence times (2am and 2pm)

Table 1: Comparison of earthquake loss estimation methodologies (Source: Guragain, Jimee, & Dixit, 2008)

Methodology	Stakeholders involvement			Motivation to community	Accuracy	Resource required	Possibility of use in developing countries
	Professionals	Authorities	Community				
Community Watching	Low	Medium	High	High	Low	Low	Yes
HAZUS	High	Low	Low	Low	High	High	Yes
RADIUS	Medium	High	Medium	High	Medium	Low	Yes
GIS based RADIUS	High	Low	Low	Low	Medium-high	High	Yes

Table 2: Classifications of building types used in RADIUS and percentage in Mymensingh Municipality (Source: adopted from RADIUS, 2000)

Building class in RADIUS	Type	Definition	Defined height	Building stock in Mymensingh Municipality (%)
Residential 1	Informal construction	Mainly slums and row housing made from unfired bricks, mud mortar, loosely tied walls and roofs	n.d.	29.14
Residential 2	Unreinforced masonry (URM)-reinforced concrete composite construction	Substandard construction, not complying with the local building code provisions	up to 3 stories	42.05
Residential 3	URM-reinforced concrete composite construction	Old, deteriorated construction, not complying with the latest building code provisions	4-6 stories	1.27
Residential 4	Engineered reinforced concrete construction	Newly constructed multistory buildings for residential and commercial purposes	n.d.	9.94
Educational 1	School buildings	Generally, the percentage of this type of building should be very low	up to 2 stories	1.89
Educational 2	School buildings	Generally, the percentage of this type of building should be very low	higher than 2 stories	0.27
Medical 1	Hospitals	Generally, the percentage of this type of building should be very low	Low- to medium-rise	0.19
Medical 2	Hospitals	Generally, the percentage of this type of building should be very low	High-rise	0.0
Commercial	Shopping centers	n.d.	n.d.	12.53
Industrial	Industrial facilities	n.d.	n.d.	2.72

Table 3: History of earthquake in Mymensingh municipality (Source: Akhter, 2010 and The Daily Star, 2008)

Year	Name of earthquake	Magnitude	Origin	Comment
1822	Kishoreganj	7.1	Kishoreganj	Caused severe damage
1846	Mymensingh	6.4	Mymensingh	Three foreshocks occurred Many structures were damaged
1885	Bengal	7.0	Madhupur Fault	one of the most severe earthquakes eleven aftershocks occurred
1897	Great Indian	8.7	Dauki Fault	one of the most powerful and destructive earthquakes in recorded history
1923	Meghalaya	7.1	Meghalaya	Hundreds of aftershocks occurred
2008	Mymensingh	5.1	Madhupur Fault	Caused heavy damage

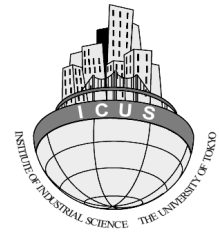
Table 4: Earthquake scenarios for Mymensingh municipality

Scenario	Dauki earthquake scenario	Madhupur earthquake scenario
Occurrence time	2am and 2pm	2am and 2pm
Earthquake Magnitude (Mw)	8.0	7.5
Depth to top of fault (km)	3	10
Earthquake direction relative from reference mesh	North-east	South-west
Earthquake distance (km) to reference mesh	87.9	58.3

Table 5: Attenuation equations and empirical formula adopted in RADIUS (Source: RADIUS, 2000)

Equation	Source	Attenuation Equation
1	Joyner & Boore (1981)	$PGA = 10^{[(0.249 \times M) - \text{Log}(D) - (0.00255 \times D) - 1.02]}$ $D = \sqrt{E^2 + 7.3^2}$
2	Campbell (1981)	$PGA = 0.0185 \times \exp(1.28 \times M) \times D^{-1.75}$ $D = E + [0.147 \times \exp(0.732 \times M)]$
3	Fukushima & Tanaka (1990)	$PGA = [10^{[(0.41 \times M) - \text{Log}_{10}\{R + 0.032 \times 10^{(0.41 \times M)}\}}] - 0.0034 \times (R + 1.30)] \div 980$
Trifunac (1975)	& Brady	$\log(PGA \times 980) = (0.3 \times MMI) + 0.014$, Or, $MMI = \frac{\log(PGA \times 980)}{0.3} - 0.014$

E = Epicentral distance, R = Hypocentral distance, M = Earthquake magnitude, PGA unit ‘g’



PART-VIII

**EVALUATION OF LOAD CARRYING
CAPACITY OF PRECAST CONCRETE PILES
BASED ON CPT**



**BANGLADESH NETWORK OFFICE FOR
URBAN SAFETY (BNUS), BUET, DHAKA**

**Prepared By: Mominur Rahman
Mehedi Ahmed Ansary**

1 GENERAL

The study location is at a site in Siddhirganj. In this site seven CPT and twelve SPT have been carried out. In this chapter pile capacity has been estimated from CPT and SPT methods discussed in chapter 2.

2 GEOLOGY OF THE PROJECT

According to geological map of Bangladesh published in 1990 geological characteristics of Siddhirganj is described. Geology of this location is alluvial silt – light to medium grey, fine sandy to clayey silt. Commonly poorly stratified; average grain size decreases away from main channels. Chiefly deposited in flood basins and interstream areas. Unit includes small backswamp deposits and varying amounts of thin, interstratified sand, deposited during episodic or unusually large floods. Illite is the most abundant clay mineral. Most areas are flooded annually. Included in this unit are thin veneers of sand spread by episodic large floods over flood-plain silts. Historic pottery, artefacts, and charcoal (radiocarbon dated 500-6000 yrs. B.P.) found in upper 4 m.

3 SUBSOIL INVESTIGATION BASED ON SPT

Figure 1 represents the site plan showing the five sections of soil profiles, location of twelve bore holes for SPT values and location of seven CPT points. Figures 2-6 describe the five soil profile sections having twelve bore holes which exhibit SPT values with depth, visual soil classification and thickness of soil layers. RL of the site is not the same. RL is 5.7m for bore hole no. 02, 03,04, 05, 06, 07, 08, 09, 10, 11 and RL is 4.0m and 5.3m for bore hole no. 12 and 01 respectively.

The soil of the site is very erratic in nature. The predominant soil of the whole site is clay and the thickness of the clay layers varies drastically among the bore holes. The maximum and minimum thickness of clay layers is 26m and 12m respectively when total depth of all bore holes is 26m. For bore hole no. 05 and 06, soil of 26m depth is clay; for bore hole no. 3, 8, 9, 11 and 12 the maximum 6m top soil is either fine sand or nonplastic silt when the soil of the remaining depth is clay; for bore hole no. 1, 7 and 10 the maximum 16m top soil is clay when the soil of the remaining depth is nonplastic silt and clay; for bore hole no. 4, the 8m top soil

is fine sand, clay and nonplastic silt when the soil of the remaining depth is clay; for bore hole no. 2, the 2m top soil is nonplastic silt, then 18m depth is clay, then 2m depth is nonplastic silt and the remaining depth is clay.

4 SUBSOIL INVESTIGATION BASED ON CPT

Figure 7-13 presents cone tip resistance, shaft friction, friction ratio and soil classification for seven different locations. The total depth of the soil profile tested for CPT data is variable and the maximum total depth is 22m. From seven CPT points it is seen that the soil of the whole site is erratic and the predominant soil of the site is cohesive soil. For soil profiles as shown in Figures 7, 10 and 12, the plus and minus 18m top soil is cohesive soil (clay, silty clay) and the remaining soil of the profiles is cohesionless soil (nonplastic silt, silty sand). For soil profiles as shown in Figures 8, 9 and 13, the 2m top soil is fine sand and the remaining soil of the profiles is cohesive soil (clay, silty clay) except 1m nonplastic silt existing in the soil profile as shown in Figure 13. For soil profile as shown in Figure 11, the 2m top soil is fine sand, the bottom soil below 19.5m depth is nonplastic silt and the remaining 17.5m middle soil of the profile is cohesive soil (clay, silty clay).

5 INTERPRETATION OF SOIL PROFILE FROM CPT

In this report, soil classification chart by Robertson and Campanella as presented in Article 2.5 is used to identify the soil layers. This method is selected since it is simple and provides output that can be easily understood. Douglas and Olsen chart shows the soil classification change (diagonally) from SP to SM to ML to CL to CH as the cone tip resistance decreases and friction ratio increases. Douglas and Olsen (1981) method demonstrates that the CPT classification charts cannot provide an accurate prediction of soil type based on soil composition, but rather serve as a guide to soil behavior type. Figures 7-13 present CPT as well as soil classification after Robertson and Campanella.

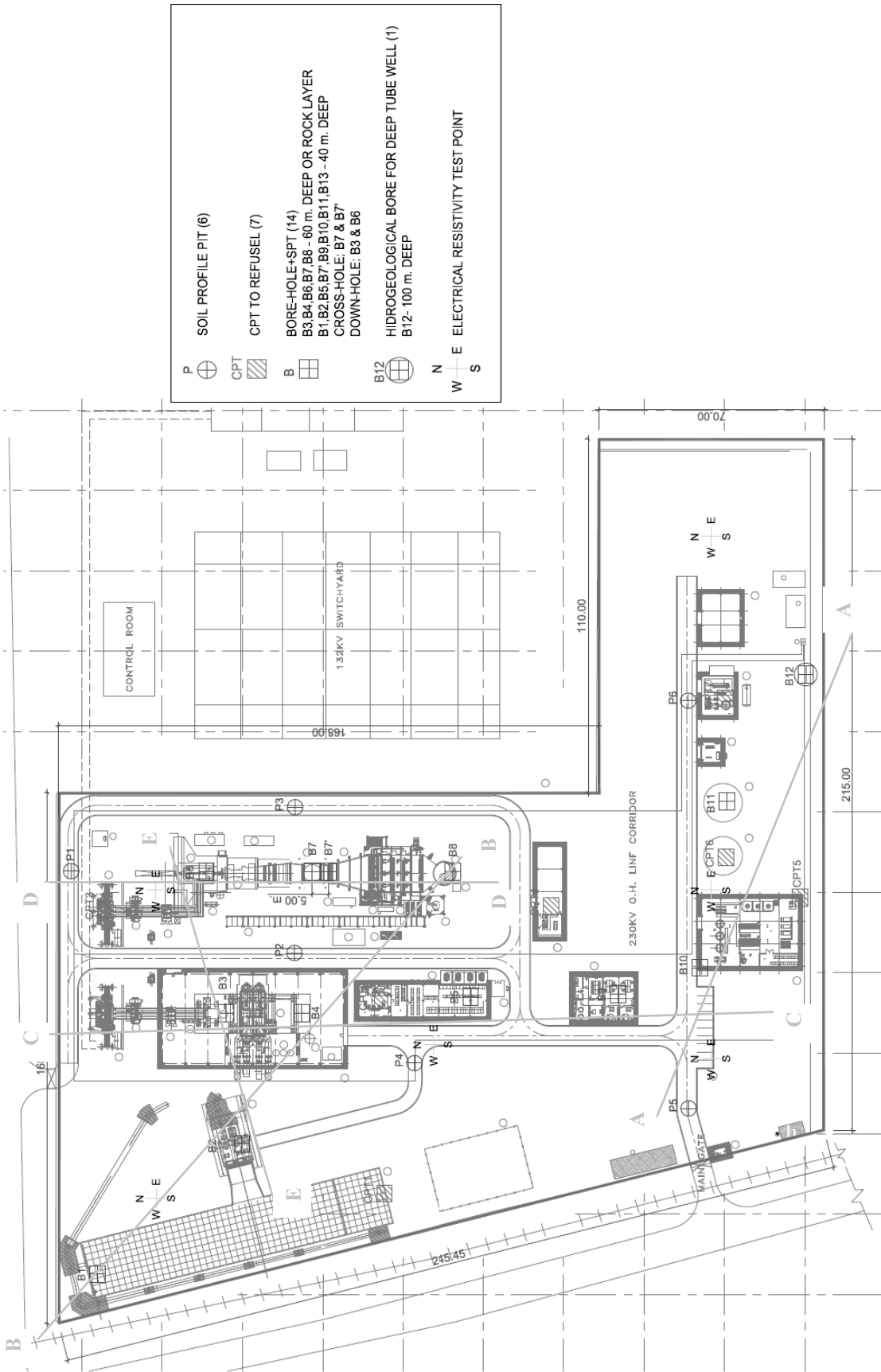


Figure 1. Layout of bore holes and sections

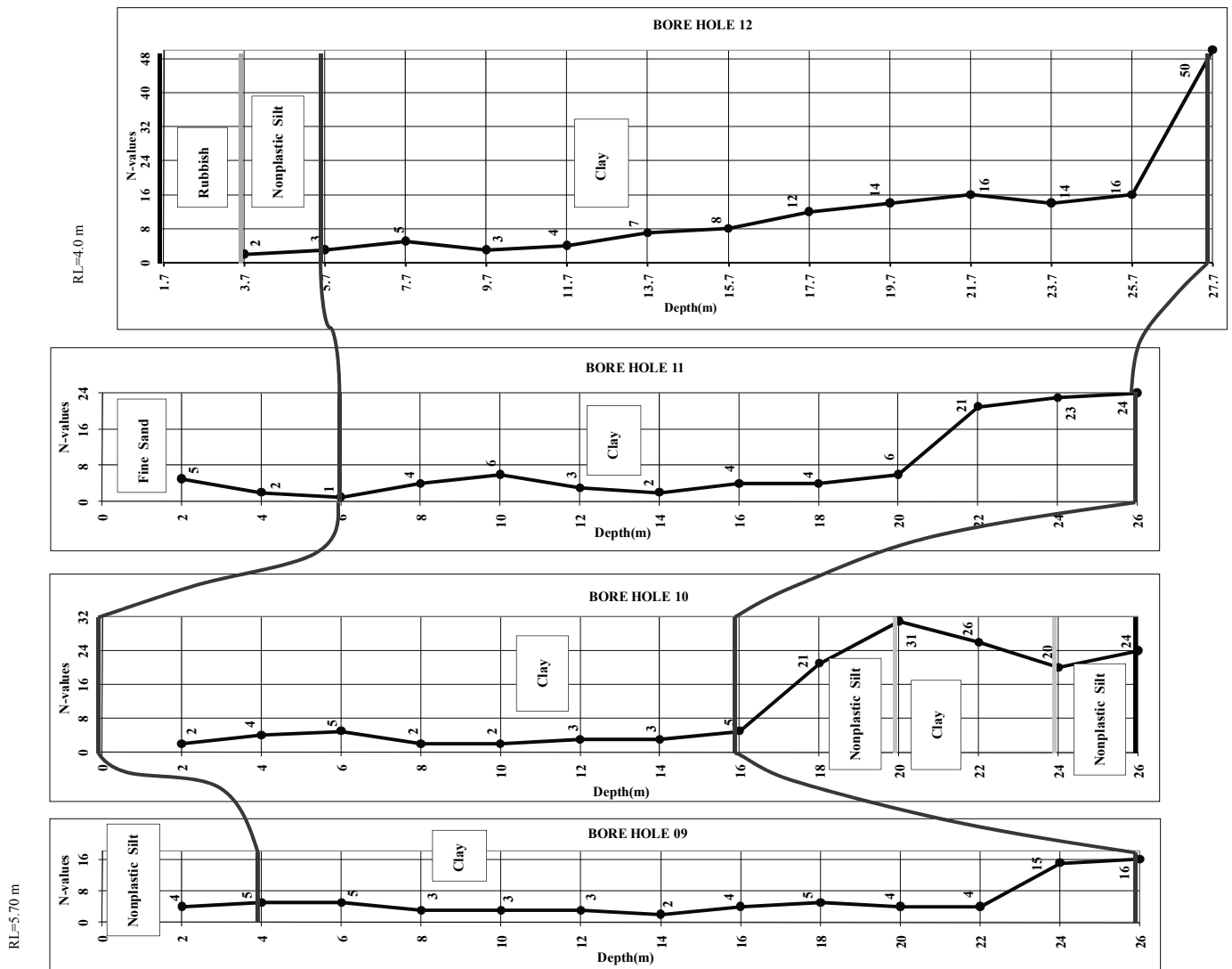


Figure 2. Geotechnical Characterization, Section-AA

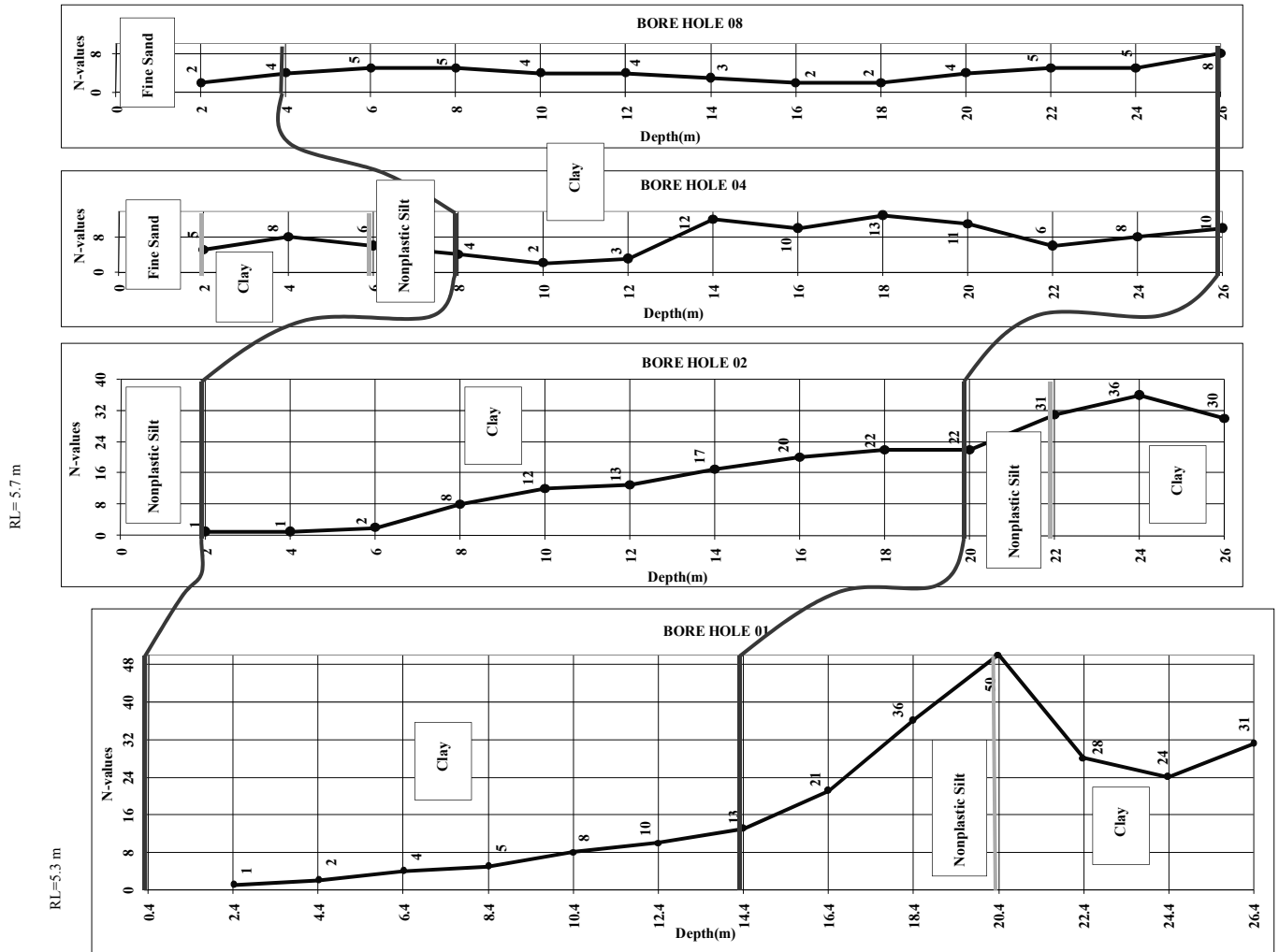


Figure 3. Geotechnical Characterization, Section-BB

RL=5.70 m

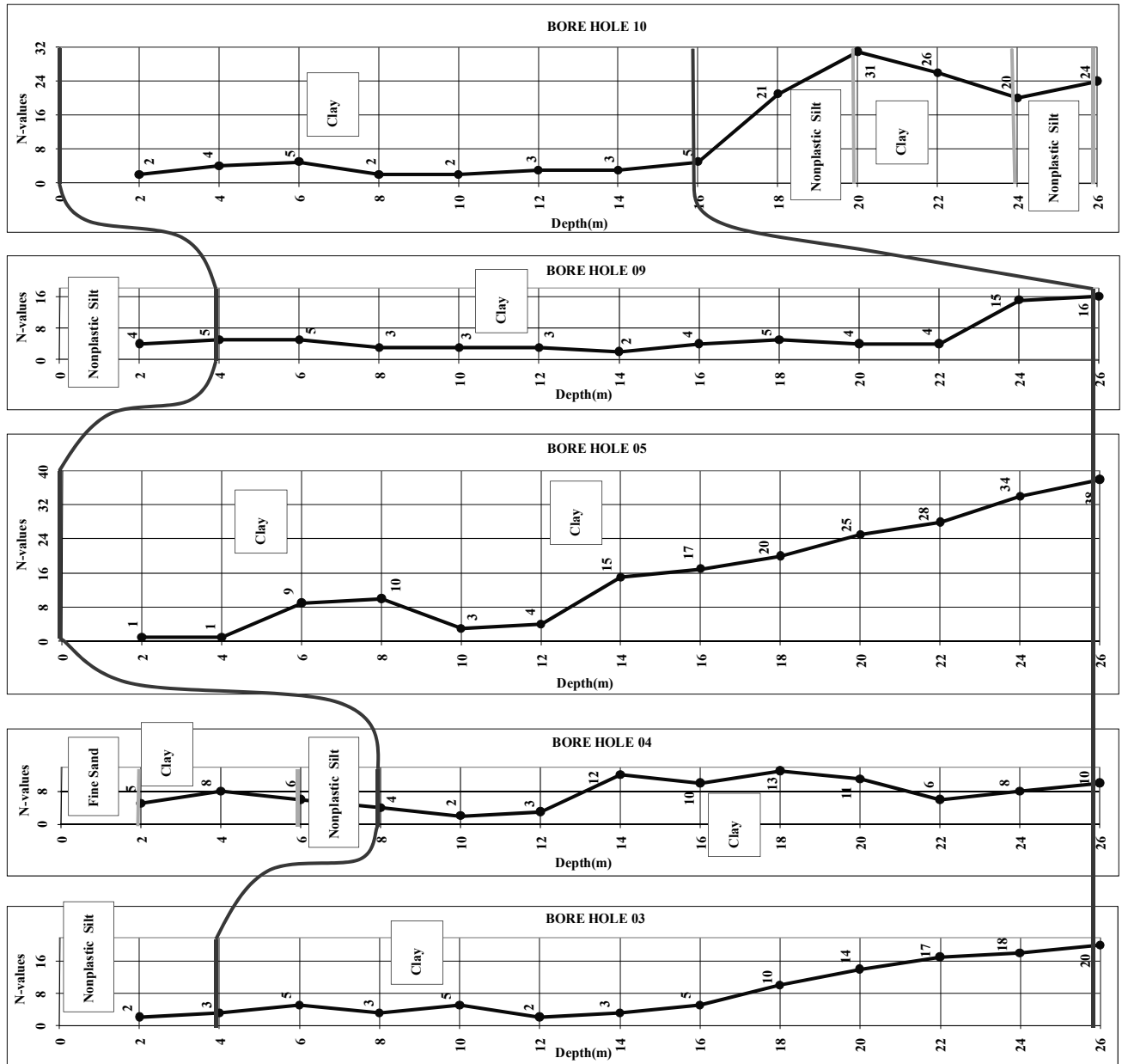


Figure 4. Geotechnical Characterization, Section-CC

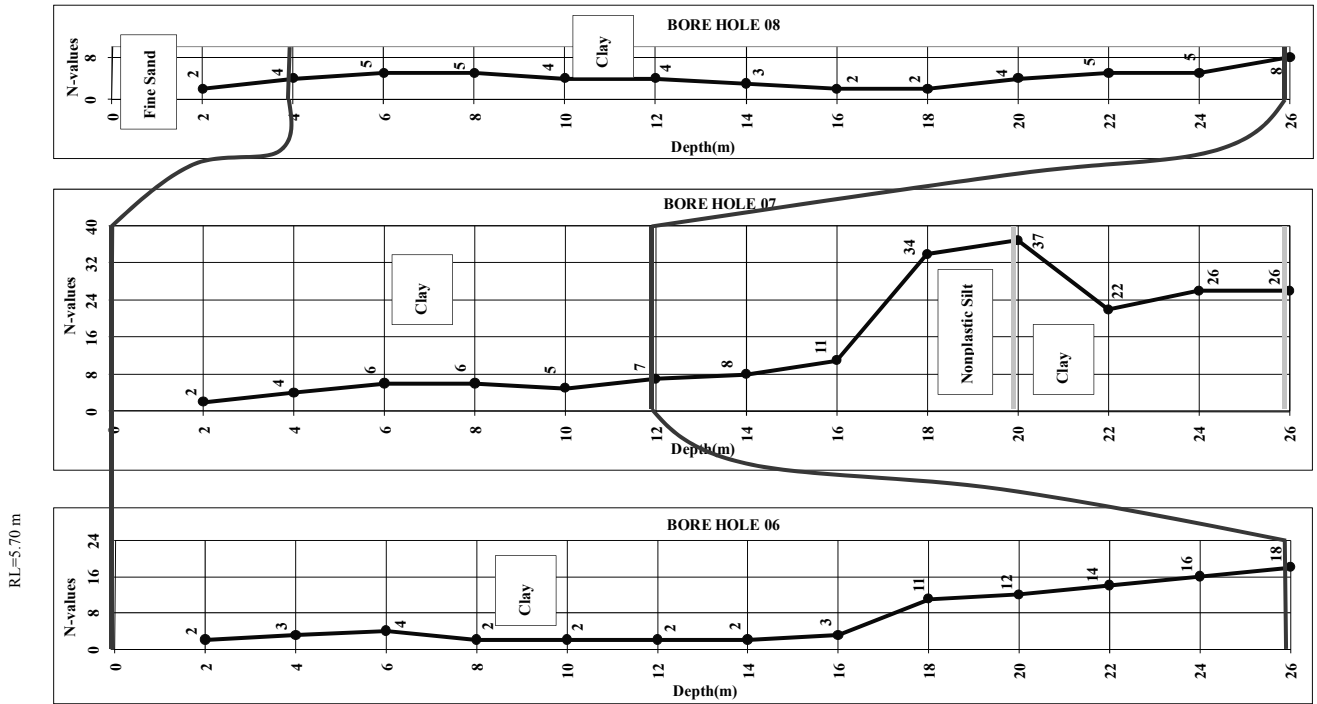


Figure 5. Geotechnical Characterization, Section-DD

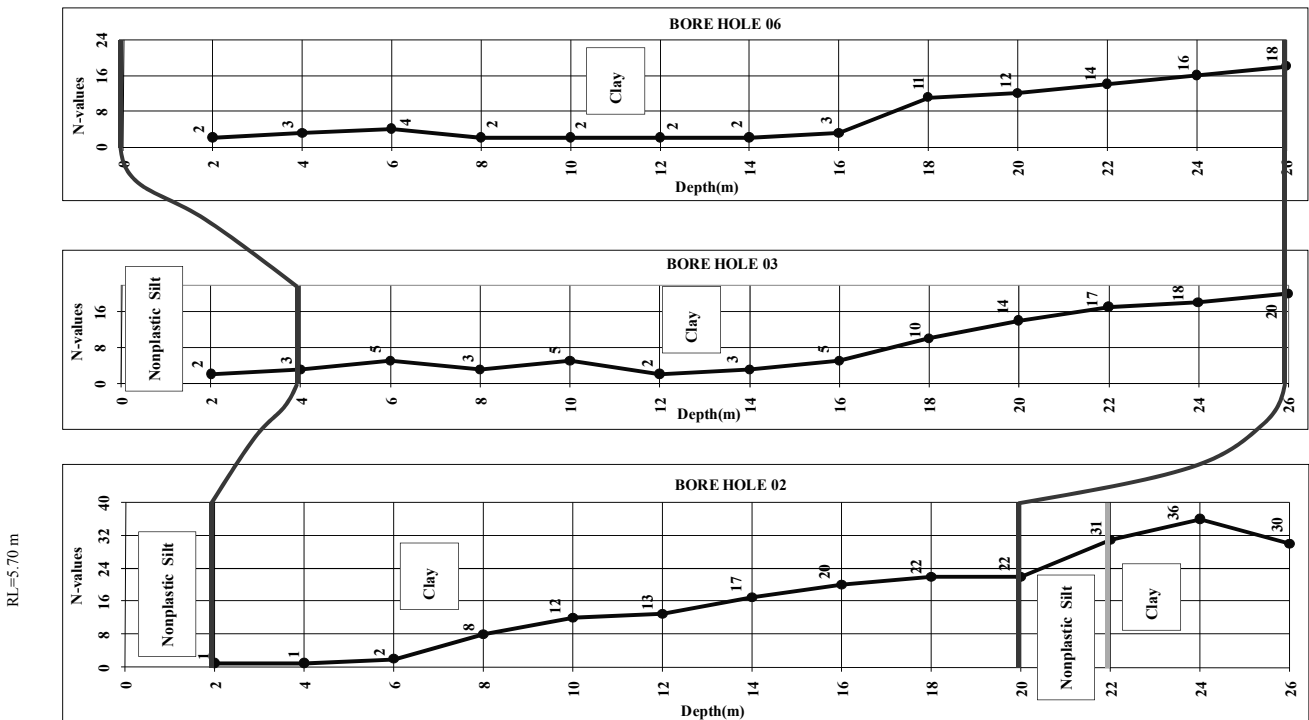


Figure 6. Geotechnical Characterization, Section-EE

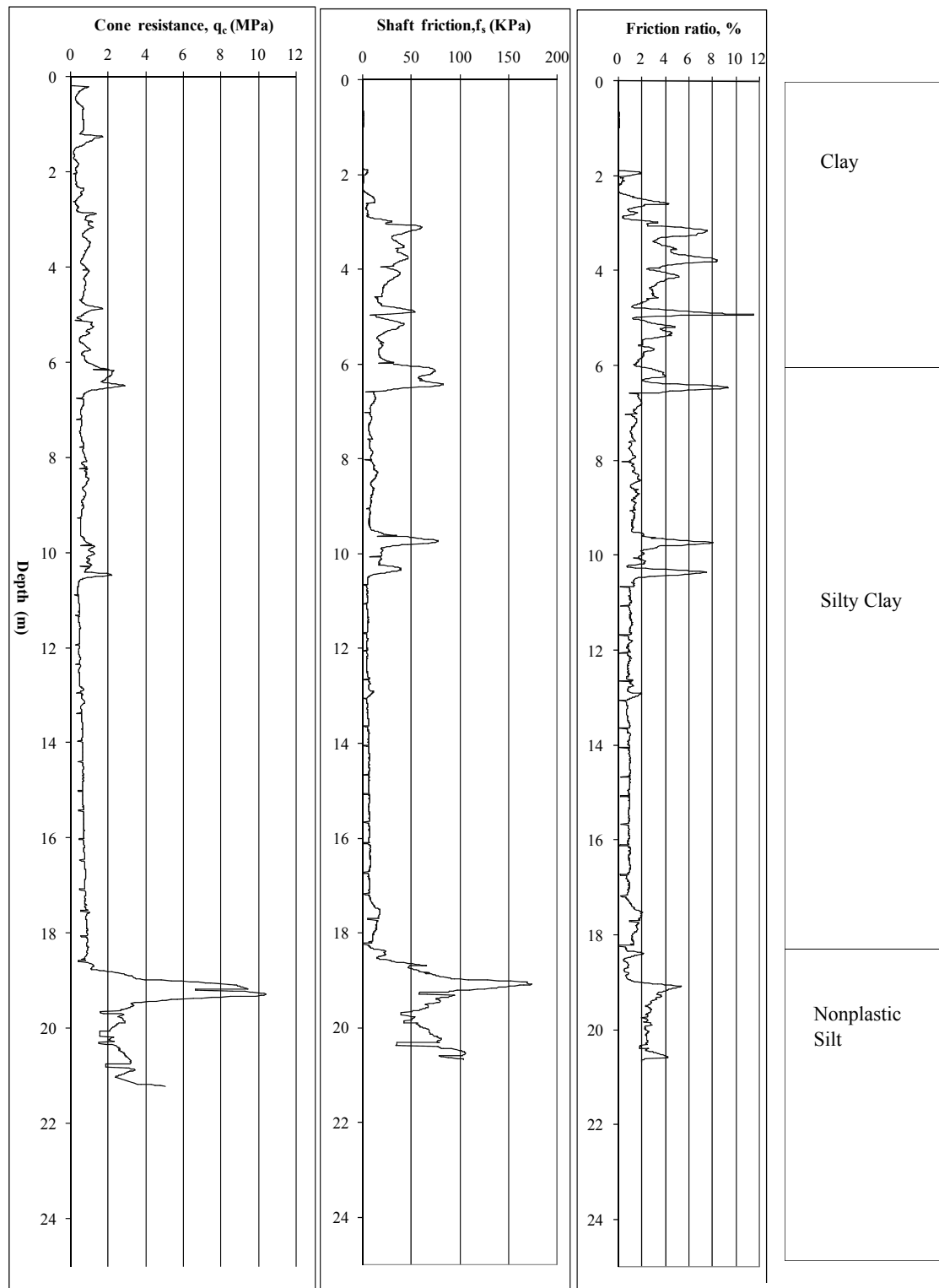


Figure 7 Cone Tip Resistance, Shaft Friction and Friction Ratio with Depth

Soil Classification based on CPT (after Robertson and Campanella)

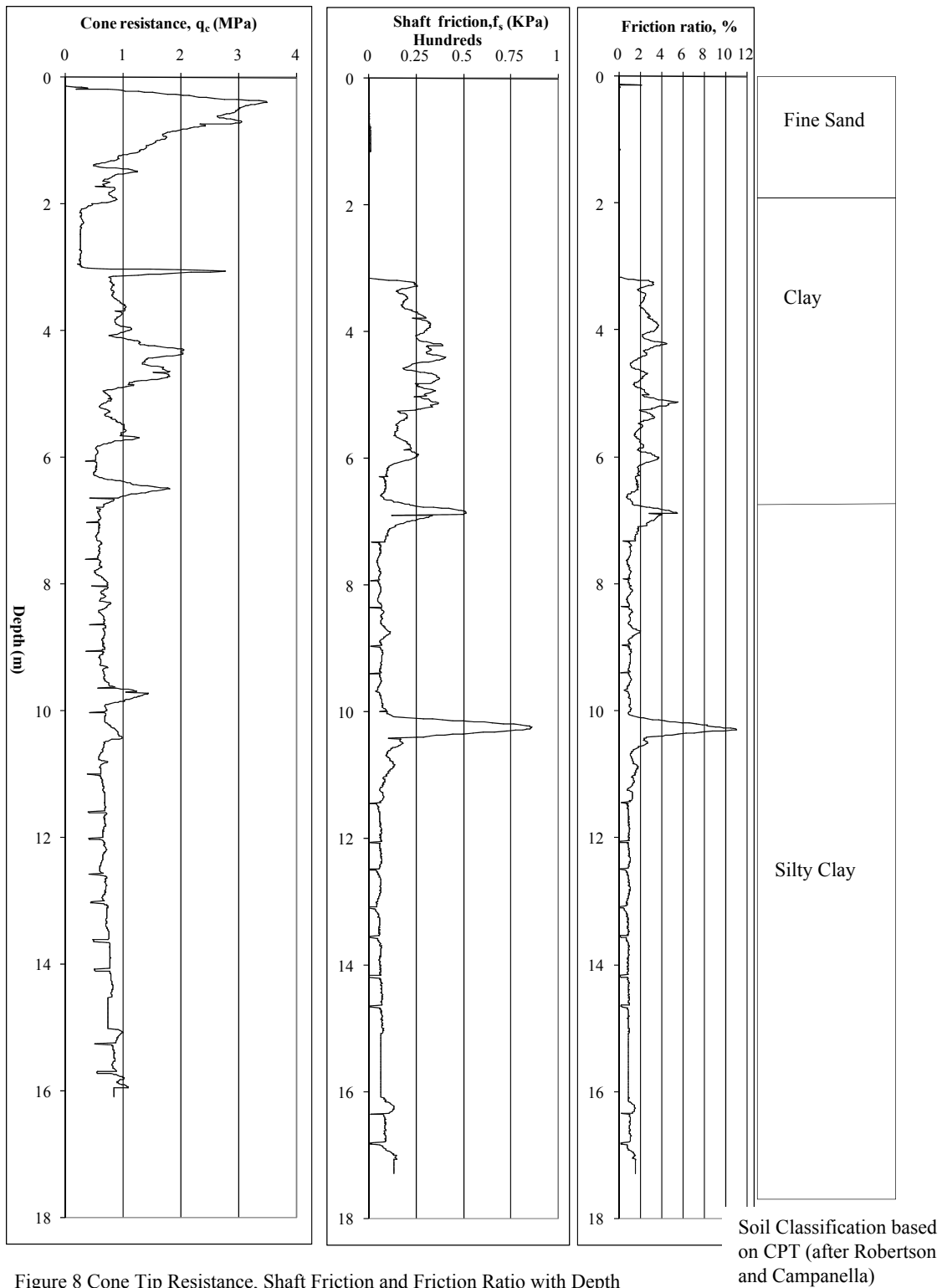


Figure 8 Cone Tip Resistance, Shaft Friction and Friction Ratio with Depth

Soil Classification based on CPT (after Robertson and Campanella)

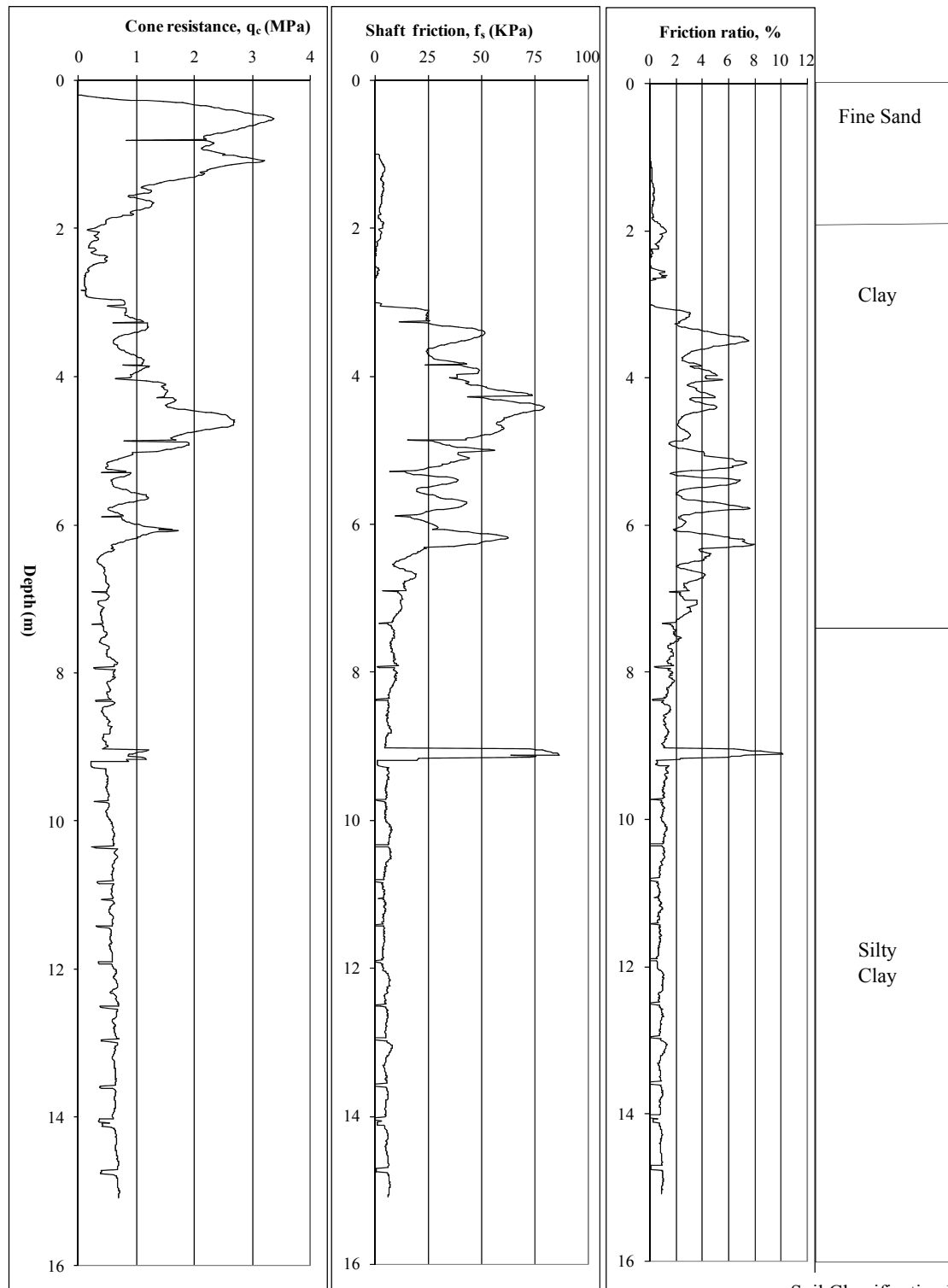


Figure 9 Cone Tip Resistance, Shaft Friction and Friction Ratio with Depth

Soil Classification based on CPT (after Robertson and Campanella)

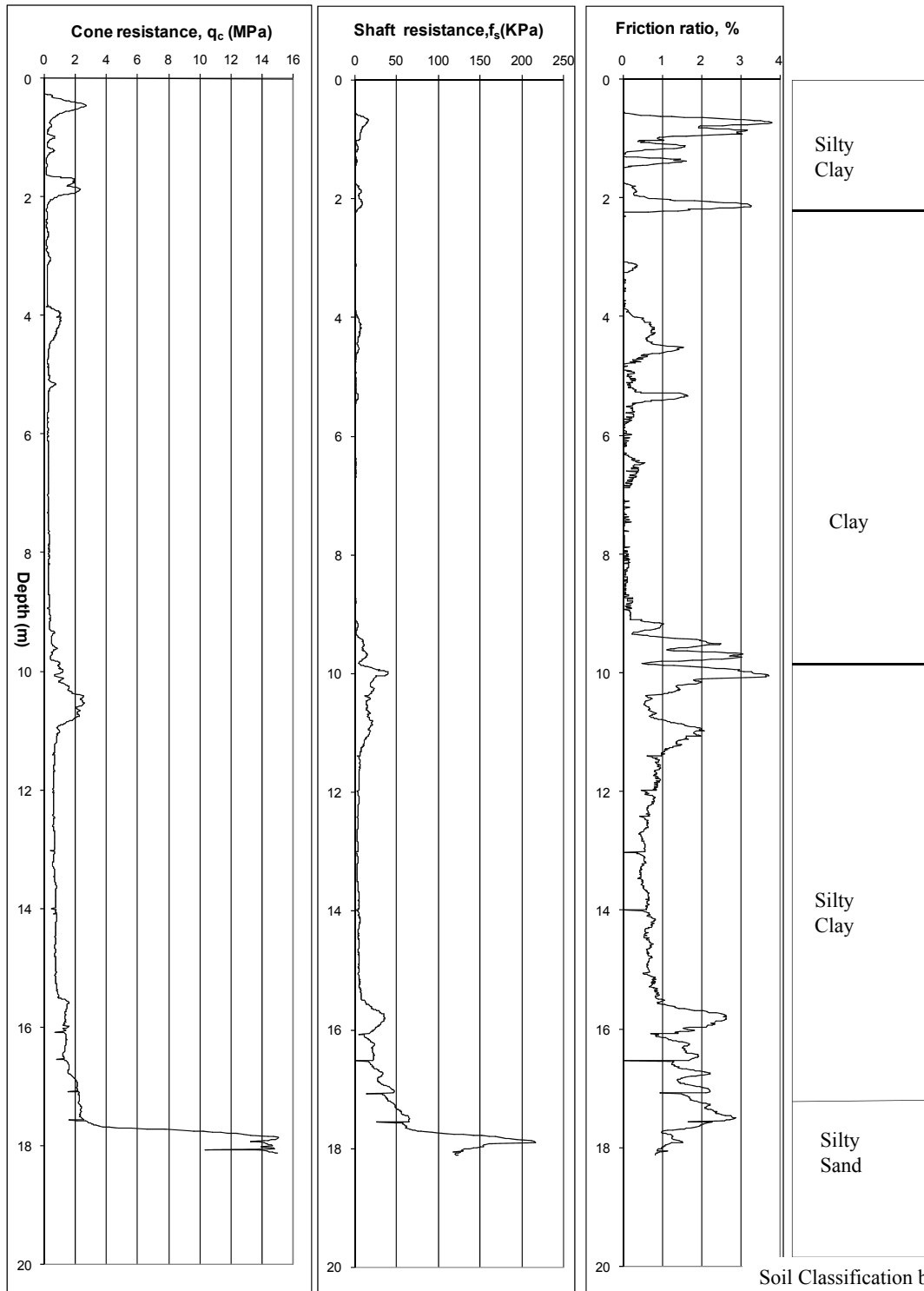


Figure 10 Cone Tip Resistance, Shaft Friction and Friction Ratio with Depth

Soil Classification based on CPT (after Robertson and Campanella)

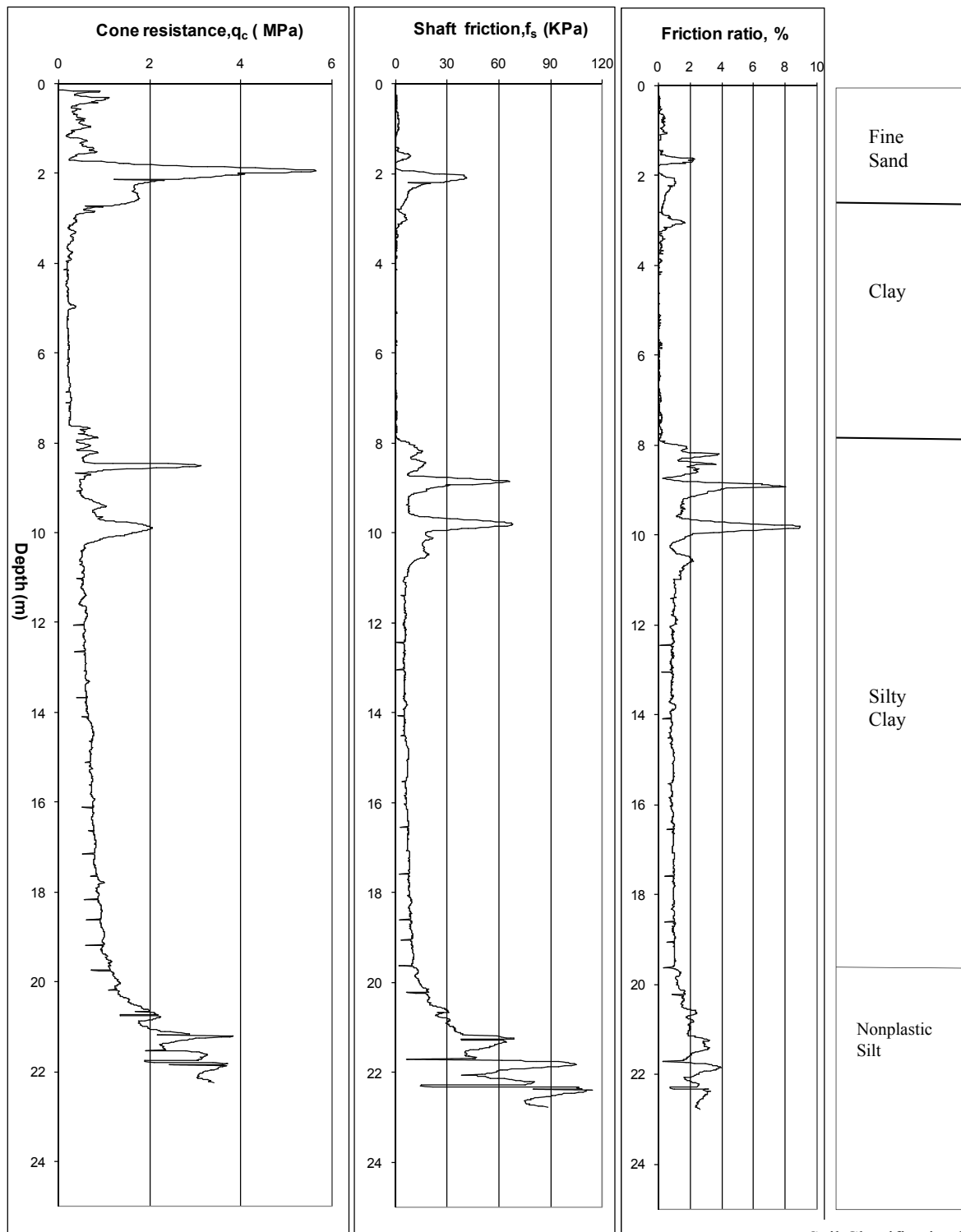


Figure 11 Cone Tip Resistance, Shaft Friction and Friction Ratio with Depth

Soil Classification based on CPT (after Robertson and Campanella)

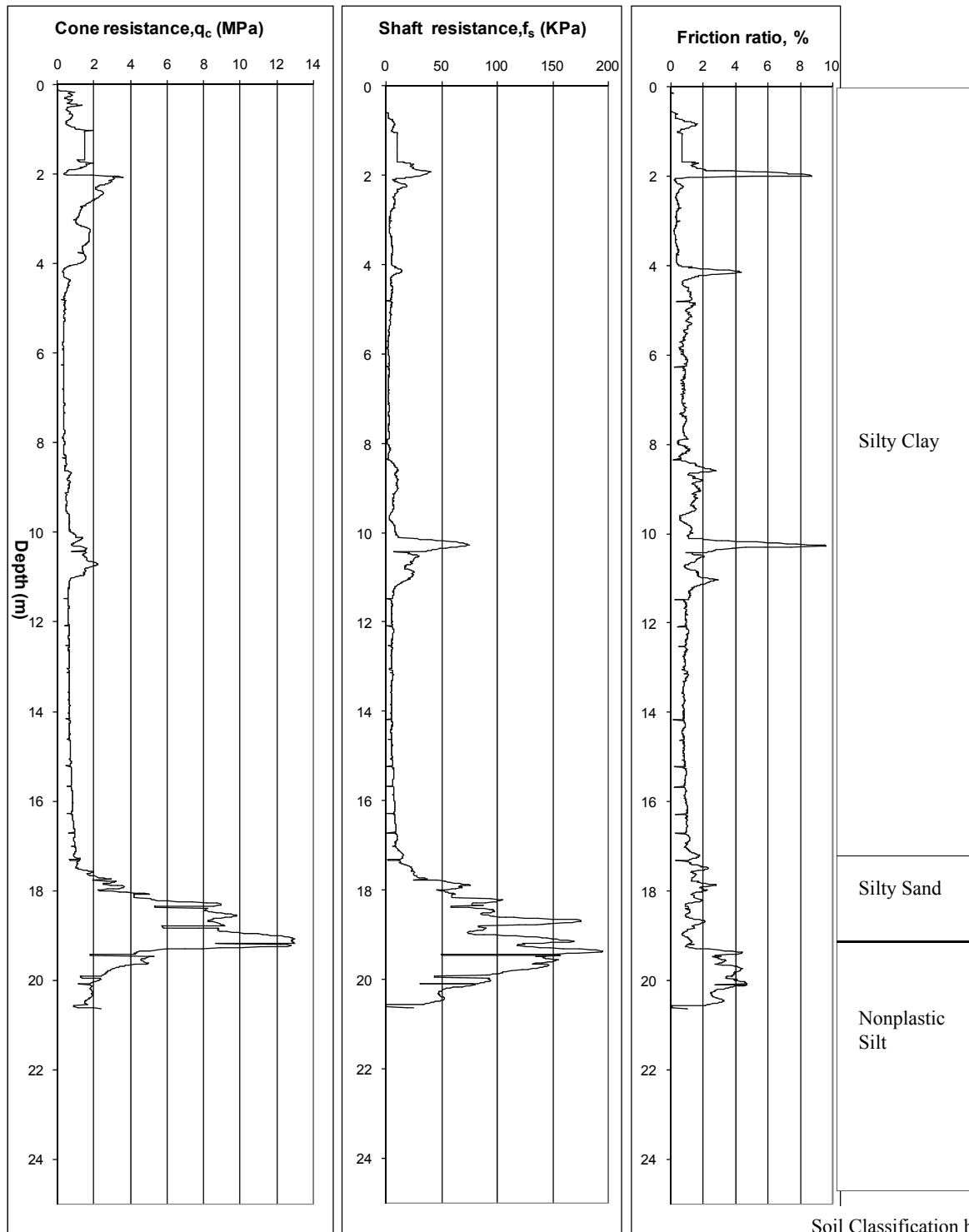


Figure 12 Cone Tip Resistance, Shaft Friction and Friction Ratio with Depth

Soil Classification based on CPT (after Robertson and Campanella)

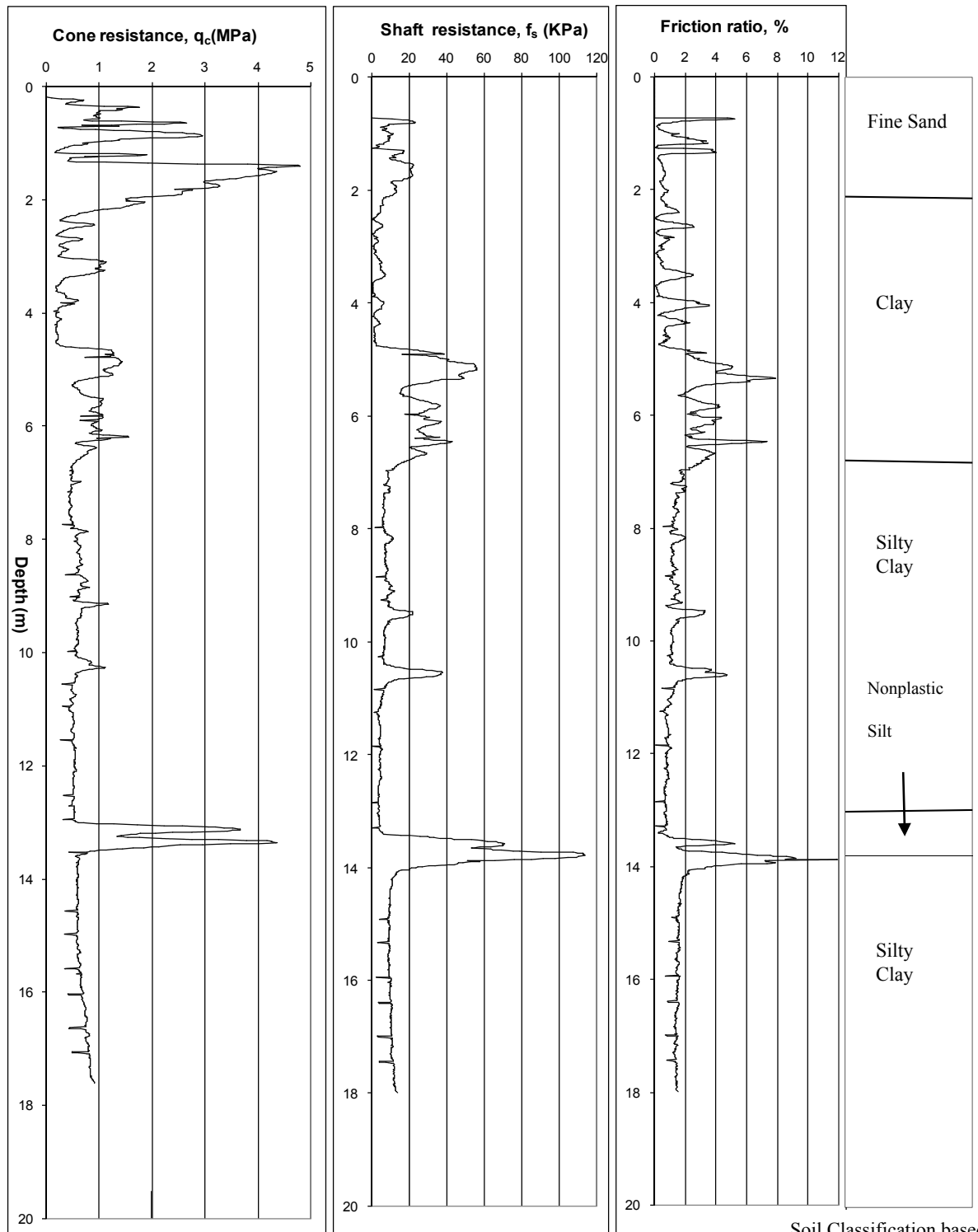


Figure 13 Cone Tip Resistance, Shaft Friction and Friction Ratio with Depth

Soil Classification based on CPT (after Robertson and Campanella)

3.6 CHARACTERIZATION OF THE INVESTIGATED PILES

Seven square precast RC concrete piles depending on depth and soil characteristics are considered in the current study. A summary of the characteristics of the investigated piles is presented in Table 1. The piles are categorized based on the predominant soil type, pile type and pile splicing..

Table 1: Seven precast piles investigated based on pile type, soil type, and pile splicing

355mm Square Precast Pile Length	Pile Type		Predominant Soil Type			Splicing of Pile	
	Friction	End-bearing	Cohesive	Cohesionless	Both	Yes	No
21m	1	1	1	0	0	1	0
15m	1	0	1	0	0	0	1
14m	1	0	1	0	0	0	1
20.5m	0	1	0	0	1	1	0
22m	1	0	1	0	0	1	0
20m	1	0	1	0	0	1	0
17m	1	0	1	0	0	0	1

Note: 1 = Yes, 0=No

3.7 PREDICTED PILE CAPACITY USING SPT AND CPT DATA

Only seven piles depending on depth and soil characteristics are used in the analyses and most of the piles are identified as friction piles. To predict the ultimate axial load capacity of the piles, the methods used are the Schmertmann, de Ruiter and Beringen, Bustamante and Gianeselli, Tumay and Fakhroo, Aoki and De Alencar, Price and Wardle, Philipponnat, and Penpile method. The ultimate load capacity for each pile is also predicted from the soil properties (soil boring close to the pile) using the SPT data. The ultimate load carrying capacity predicted by these methods (Q_p) using the CPT data is compared to the pile capacity (Q_m) obtained from the SPT data. Table 2 summarizes the results of the analyses conducted on the investigated piles. Among the data presented in Table 2 are: the pile size, type, length, the predicted ultimate load carrying capacity from CPT, the predicted ultimate load carrying capacity from SPT, average ultimate pile capacity for each pile and standard deviation for each pile.

The predicted ultimate load carrying capacity (Q_p) consists of pile tip capacity (Q_t) and pile shaft resistance (Q_s). Comparison between the pile capacities Q_t , Q_s , and Q_p predicted by the

CPT methods and the pile capacities Q_t , Q_s , and Q_m predicted by the SPT method. The results of five friction piles, one friction and end-bearing pile and one end-bearing pile are shown in these figures. Inspection of these figures shows that the ratio Q_t/Q_p for the 5 piles is relatively small, which is consistent with the previous classification of these piles as friction piles (pile capacity is derived mainly from the shaft resistance). On the other hand, the ratio Q_t/Q_p for 1 pile is relatively large and hence this pile is considered as end bearing pile (pile capacity is derived mainly from the pile tip capacity).

The ratio Q_t/Q_p for 1 pile is almost one and hence this pile is considered as friction and end bearing pile (pile capacity is derived mainly from the shaft resistance and pile tip capacity). These figures also find out the method giving the maximum/minimum ultimate end bearing capacity, the maximum/minimum ultimate shaft friction capacity, and the maximum /minimum total ultimate pile capacity for seven piles.

Table 3.2: Results of the analyses conducted on square reinforced concrete piles at a site in Siddhirganj.

Pile and Soil Identification	Pile ID	TP1, 355mm Square Precast RC Concrete Pile (Spliced)		TP2, 355mm Square Precast RC Concrete Pile		Increase or decrease of pile capacity compared with arithmetic mean (in %)			
		Q _s	Q _t	Q _u	Q _s	Q _t	Q _u	TP1	TP2
	Pile Length(m)		21		15				
	Embedded Length(m)		21		15				
	Pile Classification	Friction and end bearing		Friction					
	Predominant Soil	Cohesive		Cohesive					
Methods of Predicting Pile Capacity by Cone Penetration Test (CPT)	Predicted Ultimate Load (KN)	Q _s	Q _t	Q _u	Q _s	Q _t	Q _u		
	Schmertmann	453	450	903	240	94	334	2	-25
	de Ruiter & Beringen	478	450	928	394	56	450	5	1
	LCPC	905	221	1126	673	62	735	28	64
	Tumay & Fakhroo	1028	417	1445	722	93	815	64	82
	Aoki & De Alencar	257	303	560	261	54	315	-37	-30
	Price & Wardle	263	157	420	129	33	162	-52	-64
	Philipponnat	528	210	738	397	50	447	-16	0
	Penpile	280	56	336	142	23	165	-62	-63
	Pile Capacity by SPT		847	630	1477	540	61	601	67
Arithmetic Mean		881		447					
Standard Deviation		390		219					

Q_s: Pile shaft capacity (friction), Q_t: Pile tip capacity (end-bearing), Q_u: Total ultimate capacity(Q_s+Q_t)

Table 3.2: Results of the analyses conducted on square reinforced concrete piles at a site in Siddhigangaj, continued

Pile and Soil Identification	Pile ID	TP5, 355mm Square Precast RC Concrete Pile			TP6, 355mm Square Precast RC Concrete Pile			TP7, 355mm Square Precast RC Concrete Pile			Increase or decrease of pile capacity compared with arithmetic mean (in %)		
		Friction			Friction			Friction					
		Cohesive			Cohesive			Cohesive					
		Q _s	Q _t	Q _u	Q _s	Q _t	Q _u	Q _s	Q _t	Q _u			
Pile Length(m)		22			20			17					
Embedded Length(m)		22			20			17					
Pile Classification		Friction			Friction			Friction					
Predominant Soil		Cohesive			Cohesive			Cohesive					
Predicted Ultimate Load (KN)		Q _s	Q _t	Q _u	Q _s	Q _t	Q _u	Q _s	Q _t	Q _u	TP5	TP6	TP7
Schmertmann		333	321	654	497	434	931	318	98	416	-10	-5	-15
de Ruiter & Beringen		435	321	756	663	434	1097	508	59	567	5	12	15
LCPC		738	164	902	1239	272	1511	667	42	709	25	55	44
Tumay & Fakhroo		909	310	1219	1045	406	1451	1036	90	1126	69	49	129
Aoki & De Alencar		316	183	499	381	248	629	260	56	316	-31	-36	-36
Price & Wardle		189	112	301	389	152	541	142	34	176	-58	-45	-64
Philippomat		470	148	618	673	278	951	380	44	424	-15	-3	-14
Penpile		206	40	246	387	108	495	175	24	199	-66	-49	-59
Pile Capacity by SPT		749	554	1303	697	479	1176	461	20	481	80	20	-2
Arithmetic Mean		722			976			490					
Standard Deviation		347			351			275					

Q_s: Pile shaft capacity (friction), Q_t: Pile tip capacity (end-bearing), Q_u: Total ultimate capacity(Q_s+Q_t)

3.8 APPLICABILITY OF THE VARIOUS METHODS USED FOR PREDICTING PILE CAPACITY

Evaluating the performance of different pile capacity prediction methods is not an easy task. In this study, an evaluation scheme using only analytical criteria is considered in order to observe the performance of different CPT methods for predicting the ultimate axial capacity of piles. The arithmetic mean and standard deviation of piles at seven locations(such as TP1, TP2, TP3, TP4, TP5, TP6 and TP7) for each method are calculated. The best applied method among nine methods is the one which is closer to the mean of nine methods.

Ultimate pile capacities of piles at six locations calculated by Schmertmann method and de Ruiter and Beringen method are closer to mean of nine methods than any other methods except Philipponnat method. All the values at six locations determined by these two methods are lying within plus and minus of one standard deviation.

Ultimate pile capacities for piles at five locations calculated by Schmertmann method tend to underpredict the ultimate pile capacity by not more than 25% in comparison with the mean of nine methods. This method uses sleeve friction, f_s to calculate ultimate friction capacity of pile and sleeve friction is lower in clayey soil which is predominant as shown in Figure 3.8. Ultimate pile capacities for piles at two locations calculated by this method tend to overpredict the ultimate pile capacity. According to CPT values as shown in Figure 3.10, this method exhibits 35% higher pile capacity than the mean of nine methods. In Figure 3.10 the bearing stratum of the pile is dense silty sand where high cone tip resistance exists. The ultimate end bearing capacity estimated by this method shows the largest value because of not applying any reduction factor to cone tip resistance like only Tumay and Fakhroo method. Besides this, ultimate shaft friction capacity by this method is lower, because cone shaft friction exhibits lower value in predominant clayey soil. Philipponnat method estimates better results for piles at all locations of this site fortunately, though it does not consider the consistency of cohesive soil (soft or hard) to determine the ultimate shaft friction capacity, Q_s of pile and assumes the same empirical factor for all types of clay.

de Ruiter and Beringen method also exhibits relatively better performance. Ultimate pile capacities of piles at six locations calculated by this method are closer to mean of nine methods. Ultimate pile capacity at CPT4 location is 46% higher than the mean of nine methods. In this method no reduction factor is imposed in sandy soil to calculate ultimate end-bearing capacity like Schmertmann method. This method assumes the larger empirical factor for soft clay and the lower empirical factor for stiff

clay to calculate the ultimate shaft capacity of pile. Ultimate pile capacities for piles at seven locations calculated by de Ruiter and Beringen method tend to overpredict the pile capacity. The maximum value has been observed at CPT4 location as shown in Figure 3.10.

The performance of Bustamante and Gianeselli method (LCPC/LCP method) is not satisfactory at this study. This method overpredicts the pile capacity by 24%-64% and the values at three locations are lying beyond one standard deviation. This method for the French Highway Department is based on the analysis of 197 pile load tests with a variety of pile types and soil conditions. It utilizes cone tip resistance, q_c instead of shaft friction, f_s to determine the ultimate shaft friction capacity, Q_s . To calculate shaft friction capacity it shows much larger value in clayey soil which is predominant at all seven CPT locations.

Tumay and Fakhroo method overpredicts the pile capacity excessively and pile capacities for piles at six locations are beyond one standard deviation. In this method no reduction factor is assumed for cone tip resistance, q_c to calculate the ultimate end bearing capacity. Same adhesion factor is used both for cohesive and cohesionless soil to calculate the ultimate shaft friction capacity of pile and this factor becomes very high when sleeve friction is very low.

Aoki and De Alencar method underpredicts the pile capacity and the results show the moderate performance. This method assumes the identical empirical factor for both clayey and sandy soil to find out the ultimate end bearing capacity of pile. It does not consider the consistency of cohesive soil (soft or hard) to determine the ultimate shaft friction capacity, Q_s of pile and assumes the same empirical factor for all types of clay.

Both Price and Wardle method and Penpile method tend to underpredict the pile capacity seriously and show the values beyond one standard deviation. Those are very conservative to calculate the pile capacity. Penpile method uses empirical factor 0.25 for clay and 0.125 for sand to calculate the end bearing capacity of pile when Price and Wardle method utilizes 0.35 for both types of soil. Both method uses sleeve friction, f_s to determine the shaft friction capacity.

The results of pile capacity have been estimated for different depths at seven locations using SPT values. Arithmetic mean and standard deviation at different depths for those seven locations have also been estimated. Ultimate pile capacities based on SPT values show the wide variation. Pile capacities at five locations overpredict or underpredict the pile capacity satisfactorily. The rest of the piles at two

locations overpredict the pile capacity beyond one standard deviation. The soil of this site is very erratic and the thickness of soil layers varies drastically throughout the soil layer. SPT is not reliable for cohesive soil which is predominant for the whole site.

3.9 CONCLUDING REMARKS

In this chapter five soil profile sections having twelve bore holes describe SPT values with depth, visual soil classification and thickness of soil layers. Cone tip resistance, sleeve friction, friction ratio and soil classification at seven different locations are presented graphically. The results of the analyses based on SPT and CPT data are conducted on square reinforced concrete piles at a site in Siddhirganj. Applicability of eight CPT methods are focused to predict the ultimate axial compression load carrying capacity of piles. The static analysis using the SPT method is applied to evaluate the load carrying capacity for seven locations of the site. Ultimate pile capacity predicted by various methods of CPT are compared graphically with the one predicted by SPT data. The pile size, type, length, the predicted ultimate load carrying capacity from CPT, the predicted ultimate load carrying capacity from SPT, average ultimate pile capacity, and standard deviation are presented in tabular form. The arithmetic mean and standard deviation are calculated in order to observe the performance of different CPT methods for predicting the ultimate axial capacity of piles. The four CPT methods, which are de Ruiter and Beringen method, Philipponnat method, Schmertmann method and Aoki and De Alencar method show better performance than the currently used method based on SPT.

REFERENCES

- Abedin, M. Z. et al. (1998). “ Ultimate Capacity of a Low Cost Pile Foundation in Soft Ground” , Proceedings of Conference on Low and Low Medium Cost Housing Development, 9-10 July, 1998, Kuching, Sarawak, Malaysia.
- Ansary, M. A. et al. (1999). “ Status of Static Pile Load Tests in Bangladesh” , Proceedings of the Eleventh Asian Regional Conference on Soil Mechanics and Geotechnical Engineering, Seoul, Korea.
- Aoki, N. and de Alencar, D.(1975). “An Approximate Method to Estimate the Bearing Capacity of Piles”, *Proceedings of the 5th Pan-American Conference of Soil Mechanics and Foundation Engineering*, Buenos Aires, VI. 1, pp. 367-376.
- Bandini, P. and Salgado, R. (1998). "Methods of Pile Design Based on CPT and SPT results", Proceedings of 1st International Conference on Site Characterization (P. Robertson and P. Mayne ed.), Balkema, Rotterdam, pp. 967 - 976.
- Bowles, J.E.(1982). “Foundation Analysis and Design”, McGraw-Hill, Inc., New York, p.816.
- Briaud, J-L and, Tucker, L.M.(1988). “Measured and Predicted Axial Response of 98 Piles”,

- Journal of Geotechnical Engineering, ASCE, Vol. 114, No. 8, pp. 984-1001.
- Briaud, J-L et al. (1986). "H.M. Development of An improved Design Procedure for Single Piles in Clays and Sands", Report No. MSHDRD-86-050-1, Mississippi State Highway Department, Jackson, MS, p. 192.
- Bullock, P.J. et al.(2005). Side shear set-up I; Test piles driven in Florida. *ASCE Journal of Geotechnical and Environmental Engineering*. 131 (3) 292-300
- Bustamante, M., and L. Gianeeselli(1982). "Pile Bearing Capacity Predictions by Means of Static Penetrometer CPT", *Proceedings of the 2nd European Symposium on Penetration Testing*, ESOPT-II, Amsterdam, Vol. 2, pp. 493-500.
- Clisby, M.B. et al.(1978). "An Evaluation of Pile Bearing Capacities", Volume I, Final Report, Mississippi State Highway Department.Campanella, R.G., et al. (1989). "Use of In Situ Tests in Pile Design", *Proceedings of International Conference on Soil Mechanics and Foundation Engineering*, pp. 199 - 203.
- de Ruiter, J., and F.L. Beringen.(1979). "Pile Foundations for Large North Sea Structures", *Marine Geotechnology*, Vol. 3, No. 3, pp. 267-314.
- Douglas, J.B. and Olsen, R.S.(1981). "Soil Classification Using Electric Cone Penetrometer, Symposium on Cone Penetration Testing and Experience", *Geotechnical Engineering Division, ASCE, St. Louis*, pp. 209-227.
- El-Sakhawy N.R. et al. (2008)," Prediction of the Axial Bearing Capacity of Piles by Five -Cone Penetration Test Based Design Methods" ,(IAMAG),India.
- Eslami, A., and Fellenius, B.H.(1997). "Pile Capacity by Direct CPT and CPTU Methods Applied to 102 Case Histories", *Canadian Geotechnical Journal*, Vol. 34, pp. 886-904.
- FDOT. (2010). Standard specifications for road and bridge construction 2010. Section 455-2.2.1. Florida Department of Transportation, Tallahassee, Florida.
- Fellenius, B. H., and Eslami, A. (2002). "Soil Profile Interpreted from CPT Data", *Geotechnical Engineering Conference. Asian Institute of Technology. Bangkok. Thailand*.18 p.
- Fellenius, B. H., (1991). Summary of pile capacity predictions and comparison with observed behavior. *American Society of Civil Engineers, ASCE, Journal of Geotechnical Engineering*, Vol. 117, No. 1, pp. 192 - 195.
- Fellenius B.H. (2008). Effective Stress Analysis and Set-up Capacity of Piles in clay. *Geotechnical Special Publication No. 180*.ASCE
- Hu, Z. (2007). Updating Florida Department of Transportation's (FDOT) pile/shaft design procedures based on CPT & DTP data. Ph.D. dissertation, University of Florida, Gainesville, Florida.
- Lambe, W.T. and Whitman, R.V. (1986). *Soil Mechanics, SI Version*, John Wiley and Sons, Korea.

- Lehane, B.M. et al.(2005). CPT based design of driven piles in sand for offshore structures. UWA Report, GEO: 05345.
- Long, J.H. and Wysockey, M.H.(1999). “Accuracy of Methods for Predicting Axial Capacity of Deep Foundations”, ASCE Geotechnical Special Publication GSP 88, OTRC '99 Conference, Analysis, Design, Construction, and Testing of Deep Foundations, Austin, TX, pp. 180-195.
- Lunne, T. et al. (1997). “Cone Penetration Testing in Geotechnical Practice”, Blackie Academic and Professional, London.
- Meyerhof, G. G. (1956). "Penetration Tests and Bearing Capacity of Cohesionless Soils", *Journal of Geotechnical Engineering*, ASCE, 82(1), 1- 19.
- Paikowsky, G.S. (2004). Load and resistance factor design (LRFD) for deep foundations. NCHRP Report 507.
- Philipponnat, G.(1980). “Methode Pratique de Calcul d’un Pieu Isole a l’aide du Penetrometre Statique”, *Revue Francaise de Geotechnique*, 10, pp. 55-64.
- Price, G. and Wardle, I.F.(1982). “A Comparison Between Cone Penetration Test Results and the Performance of Small Diameter Instrumented Piles in Stiff Clay”, *Proceedings of the 2nd European Symposium on Penetration Testing*, Amsterdam, Vol. 2, pp. 775-780.
- Robertson, P.K. and Campanella, R.G.(1984). “Guidelines for Use and Interpretation of the Electric Cone Penetration Test”, Hogentogler & Company, Inc., Gaithersburg, MD, Second Edition, p. 175.
- Robertson, P.K. (1990). Soil classification using the cone penetration test. *Canadian Geotechnical Journal* 27(1): 151-158.
- Robertson, P. K., and Campanella, R. G., (1989). Guidelines for use, interpretation, and application of CPT and CPTU. *Soil Mechanics Series*, No. 105, UBC, Dept. of Civil Engineering.
- Schmertmann, J.H.(1978). “Guidelines for Cone Penetration Test, Performance and Design”, U.S. Department of Transportation, Report No. FHWA-TS-78-209, Washington, D.C., p.145.
- Skempton, A.W.(1951). “The Bearing Capacity of Clays”, *Proceedings Building Research Congress*, Vol. 1, pp. 180-189.
- Sumanta H. and Sivakumar B.(2008),”Reliability measures for pile foundations based on CPT test data”,NRC Canada.
- Terzaghi, K. and Peck, R. B. (1948). *Soil Mechanics in Engineering Practice*, John Wiely and Sons Inc., New York, N.Y.
- Terzaghi, K. and Peck, R. B. (1967). *Soil Mechanics in Engineering Practice*, 2nd Edition, John Wiely and Sons Inc., New York, N.Y.

- Togliani G.(2008). “Pile Capacity Prediction for in Situ Tests”, *Proceedings ISC-3. Taiwan*, 1187-1192. Taylor & Francis Group, London, UK.
- Tomlinson, M. J. (1971). Some effects of pile driving on skin friction, *Proceedings of the Conference on the Behavior of Piles*, Institution of Civil Engineers, London, 107-14.
- Tomlinson, M. J. (2001). *Foundation Design and Construction*. 7th ed., Pearson Education Ltd, Essex, 99 - 154.
- Tumay, M.T.(1994). “Implementation of Louisiana Electric Cone Penetrometer System (LECOPS) for Design of Transportation Facilities”, Executive Summary, Report No. FHWA/LA-94/280 A&B. LTRC, Baton Rouge, LA.
- Tumay, M.T., and Fakhroo, M.(1982). “Friction Pile Capacity Prediction in Cohesive Soils Using Electric Quasi-Static Penetration Tests”, Interim Research Report No. 1, Louisiana Department of Transportation and Development, Research and Development Section, Baton Rouge, LA, 275 p.
- Zhang, Z. and M.T. Tumay (2003). “Nontraditional Approaches in Soil Classification Derived from the Cone Penetration Test,” ASCE Special Publication No. 121 on Probabilistic Site Characterization at the National Geotechnical Experimentation Sites, ISBN 0-7844-06693, pp. 101-149.
- Zhou, J. et al. (1982). " Prediction of Limit Load of Driven Pile by CPT,” *Penetration Testing, Proc. 2nd European Symp. Penetration Testing, ESOPT II, Amsterdam, Vol. 2*, pp. 957-961.



**BANGLADESH NETWORK
OFFICE FOR URBAN SAFETY**



PART-IX

MEASUREMENT OF VIBRATION ON UHA TRADE CENTER

**BANGLADESH NETWORK OFFICE FOR
URBAN SAFETY (BNUS), BUET, DHAKA**

Prepared By: Mehedi Ahmed Ansary

1. INTRODUCTION

Landlord of Uha Trade Center, Tejgaon requested us for measurement of vibration on their building due to a roller movement in a nearby road construction project at Hatirjheel.

This report presents the findings of the vibration test. Figure 1 shows the location of the surveyed building with sensor locations and Figure 2 shows the measured building, the roller and the measurement of building vibration using Microtremor observation system.

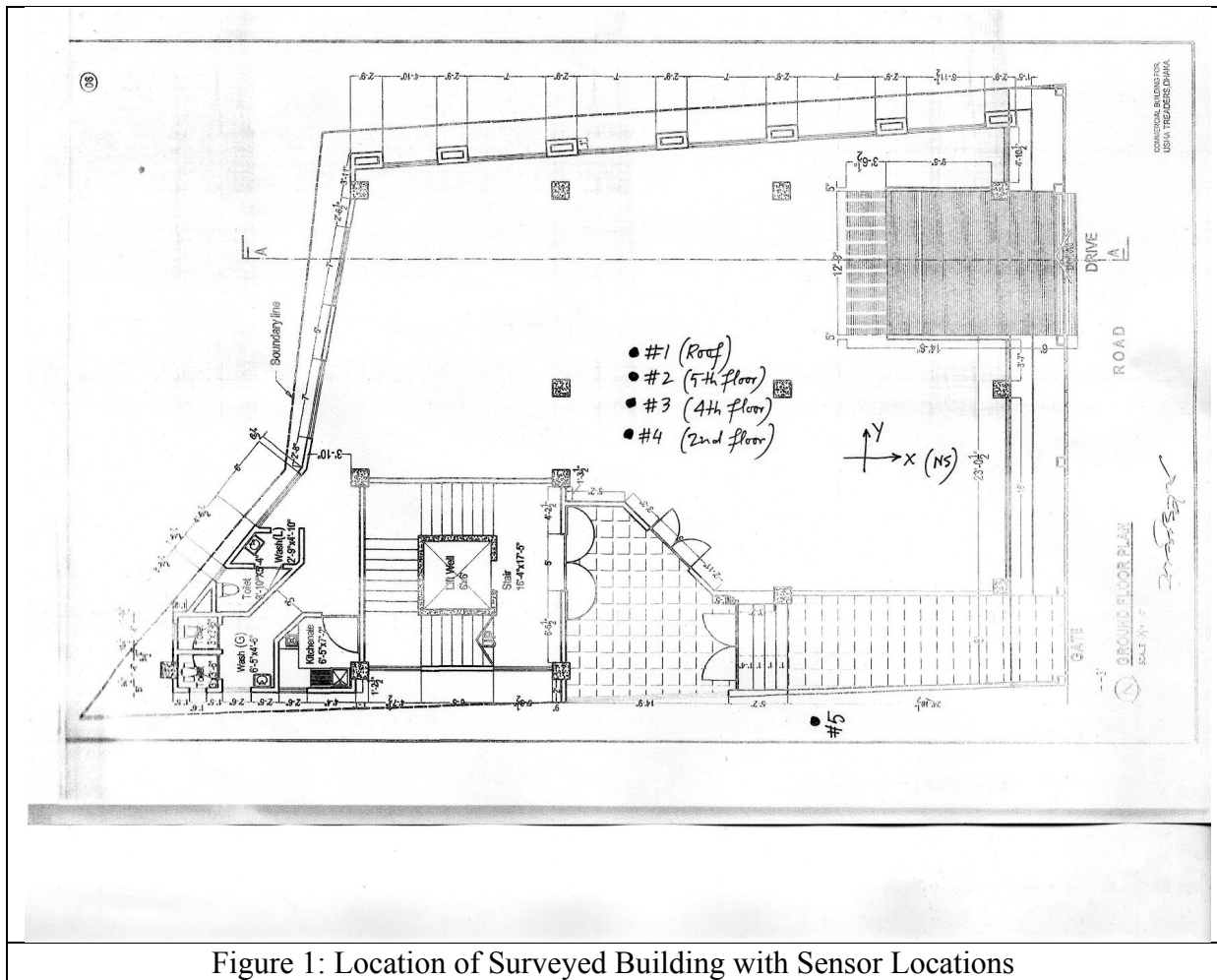


Figure 1: Location of Surveyed Building with Sensor Locations



Figure 2 Measurement of building vibration using Microtremor observation system

2. ACCEPTABLE VIBRATION LEVELS

Humans are very sensitive vertical vibration sensors, especially in environments like quiet buildings. An example of human comfort limit is the restriction on the acceleration - human begins to feel uncomfortable when the acceleration reaches about 0.02g:

$$\ddot{u} = 0,02g = 0,02 \cdot 981 = 196,2 \text{ mm/s}^2$$

Corresponding velocity at 16 Hz frequency is 1.96 mm/s.

According to [1], the allowable level of vibration acceleration at 16 Hz frequency is 28.0 mm/s², while the allowable level of vibration velocity at the same frequency is 0.28 mm/s. The allowable levels of vibration for public buildings according to [1] are shown in Table 1.

Table 1: Allowable levels of vibration for public buildings

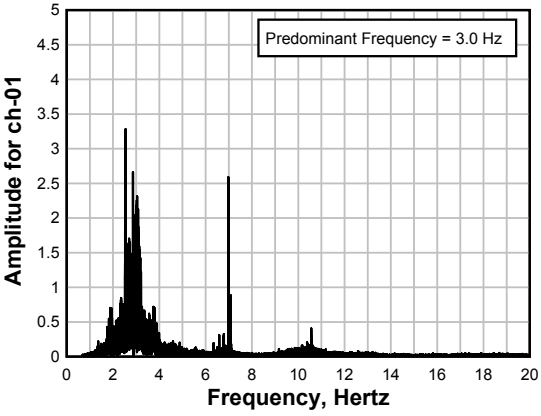
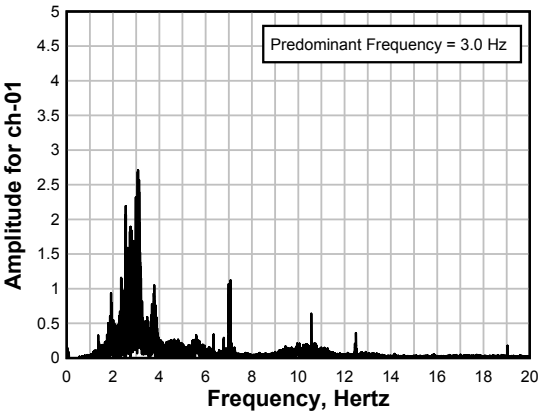
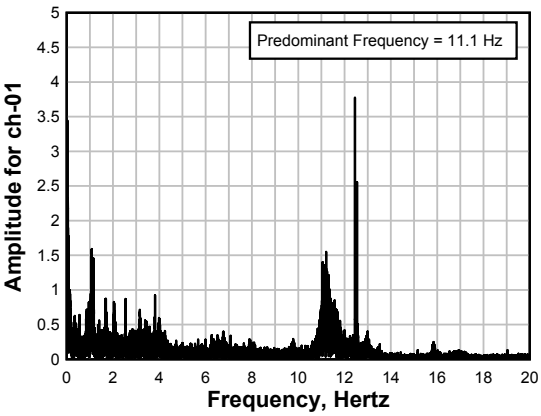
Mean geometrical frequency [Hz]	Allowable vibration level along axes X, Y, Z			
	Acceleration		Velocity	
	<i>mm / s²</i>	dB	<i>mm / s</i>	dB
2	10,0	80	0,79	84
4	11,0	81	0,45	79
8	14,0	83	0,28	75
16	28,0	89	0,28	75
31,5	56,0	95	0,28	75
63	110,0	101	0,28	75

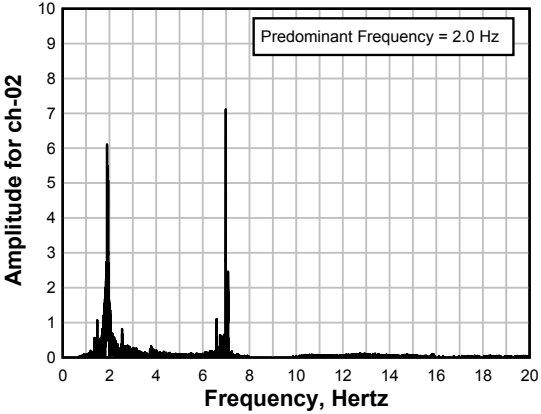
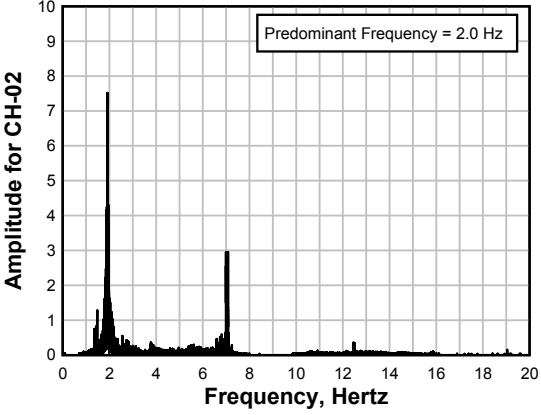
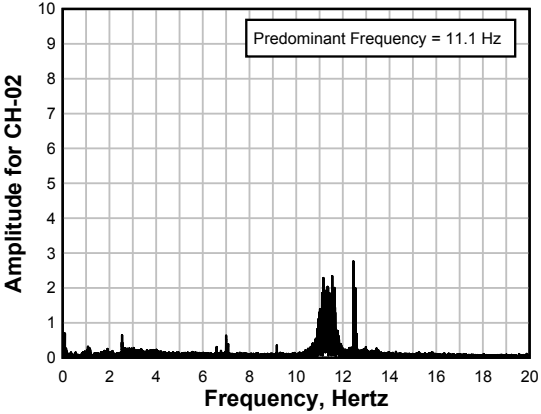
3. MEASUREMENT OF BUILDING VIBRATION

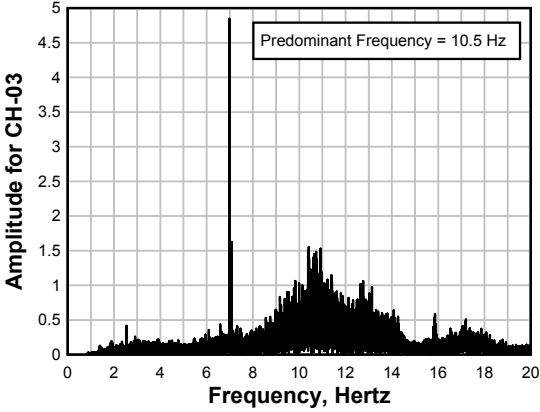
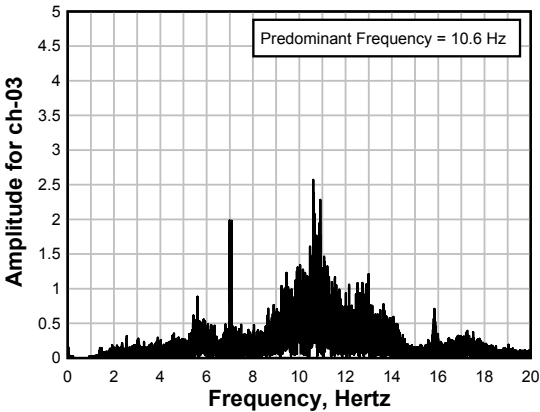
The BUET team conducted vibration test for the BRAC Bank located at Usha Trade Center at ambient state, with generator and with roller movement. The measurement is conducted simultaneously at the ground (sensor 5), at the building's 2nd floor (sensor 4), 3rd floor (sensor 3), 5th floor (sensor 2) and at the roof (sensor 5) of the building. The Fourier Spectra of the measured vibrations and corresponding predominant frequencies are shown in the next few pages.

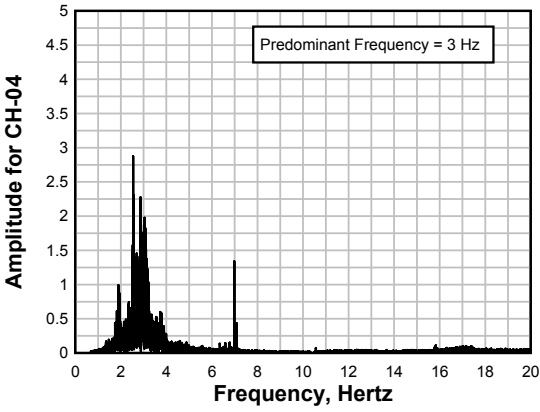
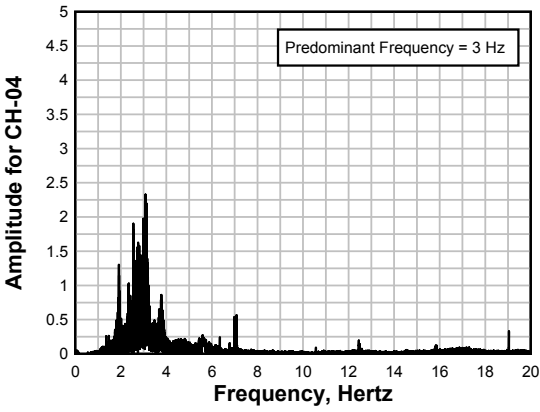
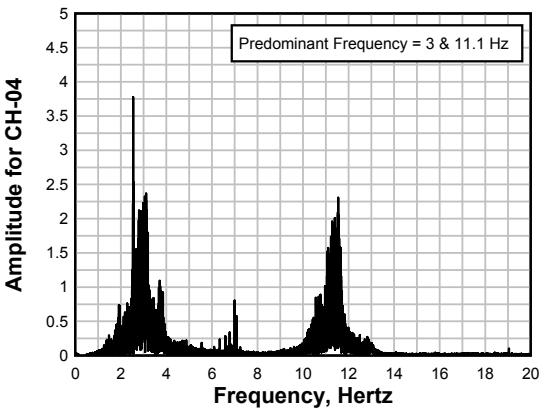
In the following table, the amplitude of vibration at different vibration state for the building which is located around 400 ft from Hatirjheel area where a 5 ton roller is working, is presented.

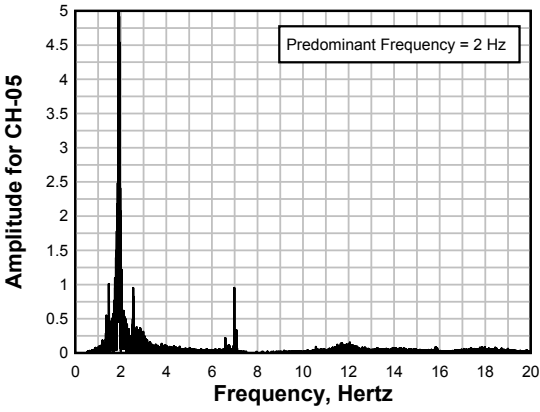
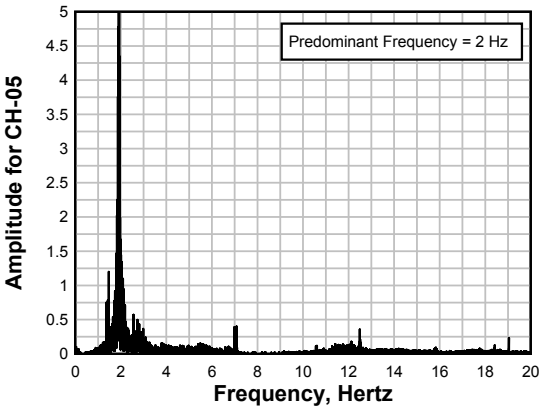
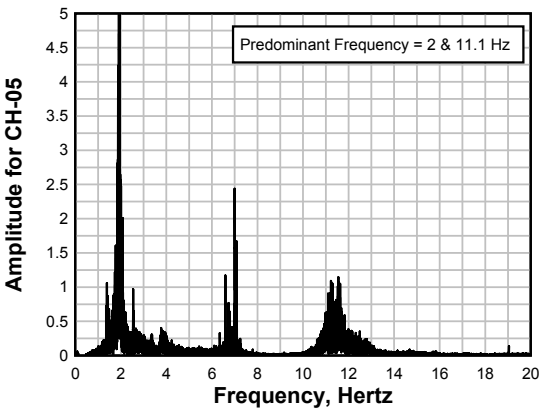
Condition	Measured value of building velocity (mm/s)					Allowable levels of vibration for public buildings from Table 1	Comment
	X	Y	Z	Maximum	Corresponding frequency (Hz)		
Ambient noise	0.08	0.11	0.25	0.25	7-11	0.28-0.32	No problem to the building
With Generator running in the basement	0.11	0.09	0.35	0.35	7-12	0.28-0.32	May cause slight problem to the building
With Generator running in the basement and a 5 ton Roller working about 400 ft away	0.14	0.15	0.90	0.90	11	0.28	May cause problem to the building

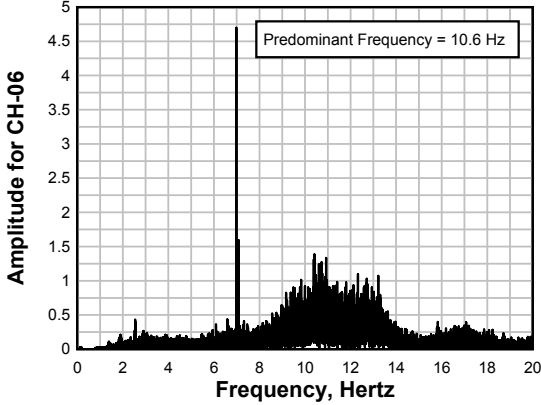
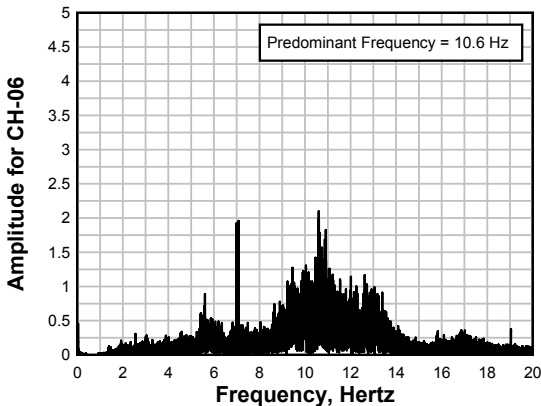
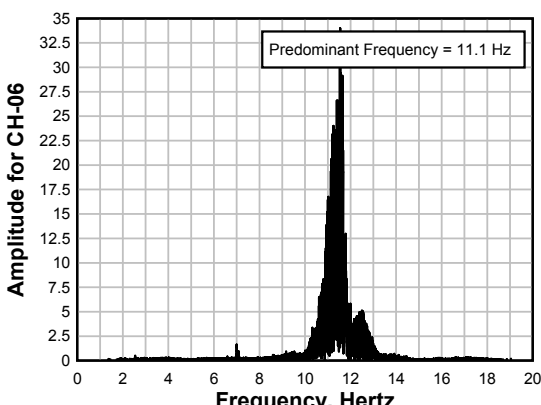
Location: 1X (Roof) Measurement Mode	Fourier Spectrum	Predominant Frequency
Ambient noise	<p style="text-align: center;"> tes20150204_1158.xls tes20150204_1158 </p>  <p style="text-align: center;"> Amplitude for ch-01 Frequency, Hertz </p> <p style="text-align: right;">FFT</p>	3
With Generator running in the basement	<p style="text-align: center;"> tes20150204_1237.xls tes20150204_1237 </p>  <p style="text-align: center;"> Amplitude for ch-01 Frequency, Hertz </p> <p style="text-align: right;">FFT3</p>	3
With Generator running in the basement and a 5 ton Roller working about 400 ft away	<p style="text-align: center;"> tes20150204_1451.xls tes20150204_1451 </p>  <p style="text-align: center;"> Amplitude for ch-01 Frequency, Hertz </p> <p style="text-align: right;">FFT6</p>	11.1

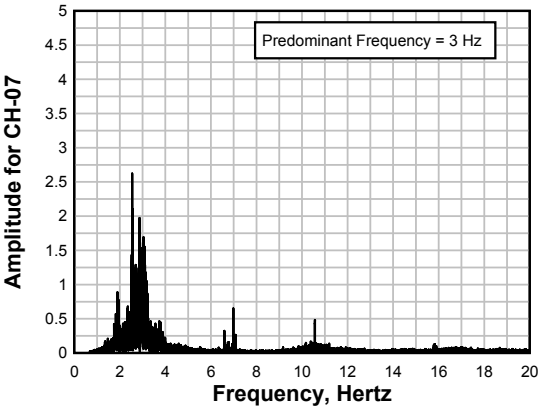
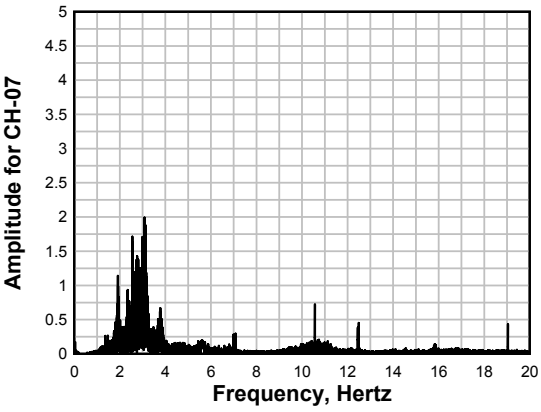
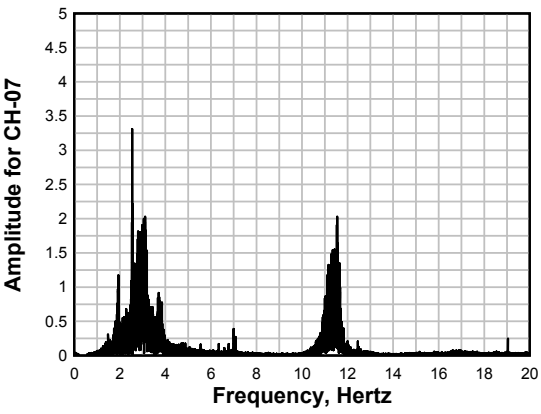
Location: 1Y (Roof) Measurement Mode	Fourier Spectrum	Predominant Frequency
Ambient noise	<p style="text-align: center;">tes20150204_1158.xls tes20150204_1158</p> 	2
With Generator running in the basement	<p style="text-align: center;">tes20150204_1237.xls tes20150204_1237</p> 	2
With Generator running in the basement and a 5 ton Roller working about 400 ft away	<p style="text-align: center;">tes20150204_1451.xls tes20150204_1451</p> 	11.1

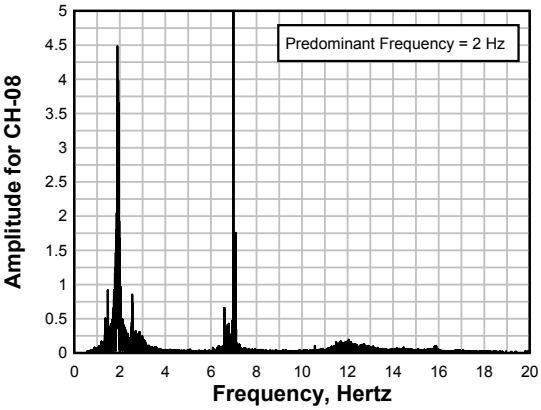
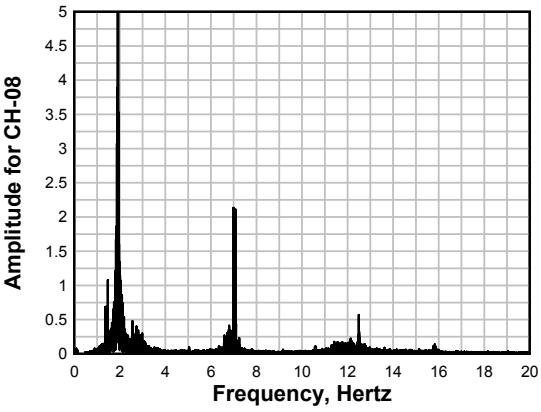
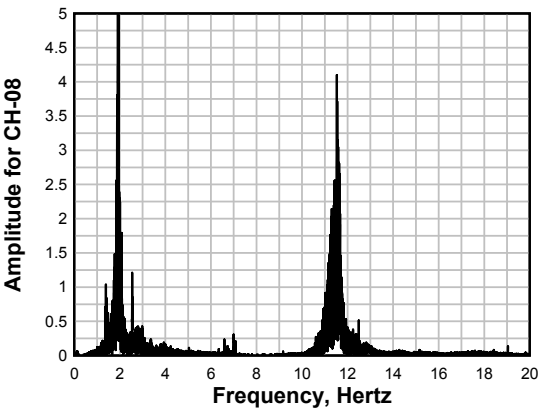
Location: 1Z (Roof) Measurement Mode	Fourier Spectrum	Predominant Frequency
Ambient noise	<p style="text-align: center;"> tes20150204_1158.xls tes20150204_1158 </p> 	7 & 10.5
With Generator running in the basement	<p style="text-align: center;"> tes20150204_1237.xls tes20150204_1237 </p> 	7 & 10.6
With Generator running in the basement and a 5 ton Roller working about 400 ft away	White noise	-

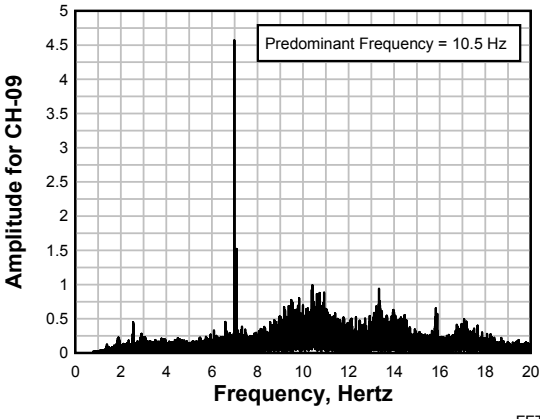
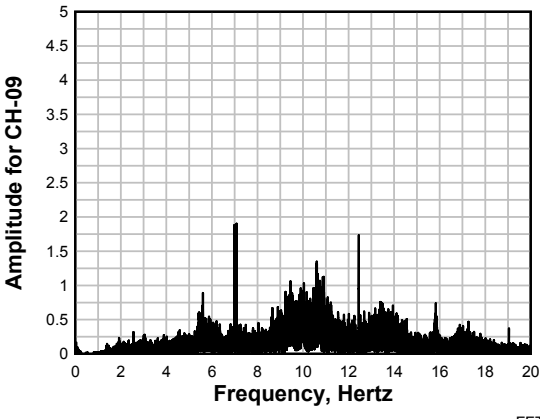
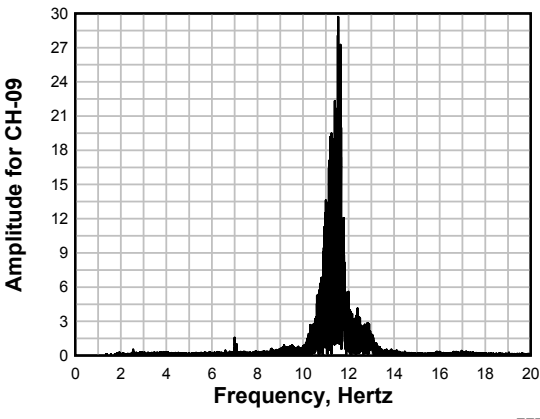
Location: 2X (5th floor) Measurement Mode	Fourier Spectrum	Predominant Frequency
Ambient noise	<p style="text-align: center;">tes20150204_1158.xls tes20150204_1158</p>  <p style="text-align: right;">FFT</p>	
With Generator running in the basement	<p style="text-align: center;">tes20150204_1237.xls tes20150204_1237</p>  <p style="text-align: right;">FFT3</p>	
With Generator running in the basement and a 5 ton Roller working about 400 ft away	<p style="text-align: center;">tes20150204_1451.xls tes20150204_1451</p>  <p style="text-align: right;">FFT6</p>	

Location: 2Y (5 th floor) Measurement Mode	Fourier Spectrum	Predominant Frequency
Ambient noise	<p style="text-align: center;">tes20150204_1158.xls tes20150204_1158</p> 	
With Generator running in the basement	<p style="text-align: center;">tes20150204_1237.xls tes20150204_1237</p> 	
With Generator running in the basement and a 5 ton Roller working about 400 ft away	<p style="text-align: center;">tes20150204_1451.xls tes20150204_1451</p> 	

Location: 2Z (5th floor) Measurement Mode	Fourier Spectrum	Predominant Frequency
Ambient noise	<p style="text-align: center;">tes20150204_1158.xls tes20150204_1158</p> 	
With Generator running in the basement	<p style="text-align: center;">tes20150204_1237.xls tes20150204_1237</p> 	
With Generator running in the basement and a 5 ton Roller working about 400 ft away	<p style="text-align: center;">tes20150204_1451.xls tes20150204_1451</p> 	

Location: 3X (4th floor) Measurement Mode	Fourier Spectrum	Predominant Frequency
Ambient noise	<p style="text-align: center;">tes20150204_1158.xls tes20150204_1158</p>  <p style="text-align: right;">FFT</p>	
With Generator running in the basement	<p style="text-align: center;">tes20150204_1237.xls tes20150204_1237</p>  <p style="text-align: right;">FFT4</p>	
With Generator running in the basement and a 5 ton Roller working about 400 ft away	<p style="text-align: center;">tes20150204_1451.xls tes20150204_1451</p>  <p style="text-align: right;">FFT7</p>	

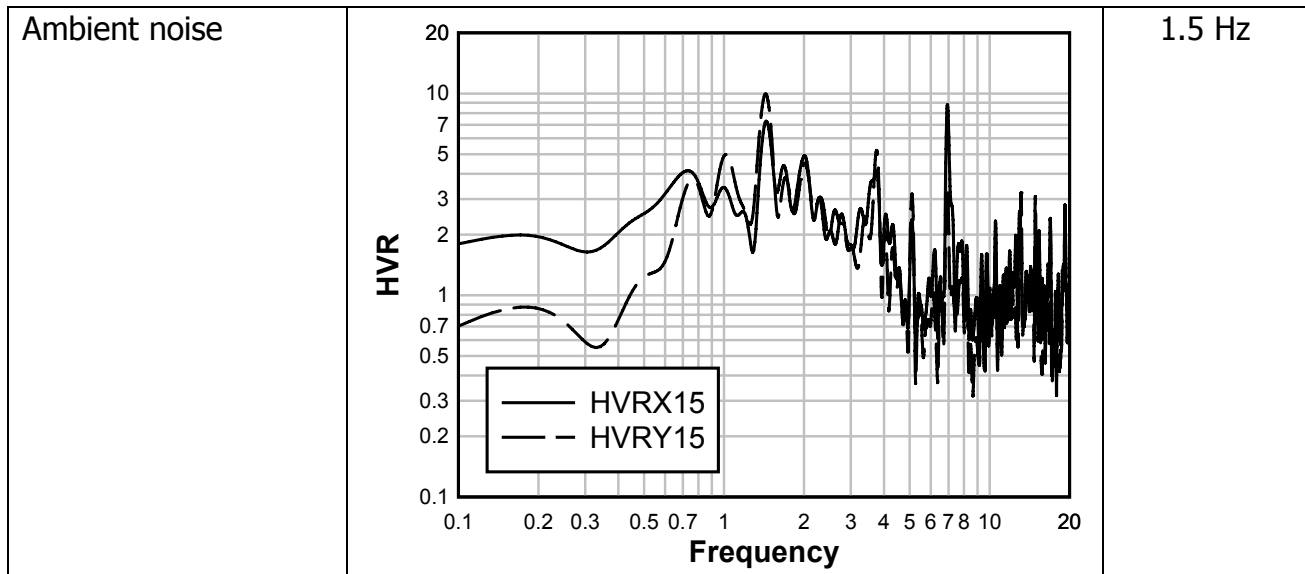
Location: 3Y (4 th floor) Measurement Mode	Fourier Spectrum	Predominant Frequency
Ambient noise	<p style="text-align: center;">tes20150204_1158.xls tes20150204_1158</p> 	
With Generator running in the basement	<p style="text-align: center;">tes20150204_1237.xls tes20150204_1237</p> 	
With Generator running in the basement and a 5 ton Roller working about 400 ft away	<p style="text-align: center;">tes20150204_1451.xls tes20150204_1451</p> 	

Location: 3Z (4 th floor) Measurement Mode	Fourier Spectrum	Predominant Frequency
Ambient noise	<p style="text-align: center;">tes20150204_1158.xls tes20150204_1158</p> 	
With Generator running in the basement	<p style="text-align: center;">tes20150204_1237.xls tes20150204_1237</p> 	
With Generator running in the basement and a 5 ton Roller working about 400 ft away	<p style="text-align: center;">tes20150204_1451.xls tes20150204_1451</p> 	

4. MEASUREMENT OF GROUND VIBRATION

The ground vibration is also measured and computed predominant frequency is presented in the following figure.

Location: Ground Measurement Mode	H/V Ratio	Predominant Frequency
--------------------------------------	-----------	-----------------------



5. REMARKS

- The predominant frequency of the building in X direction (NS) is around 3 Hz and along Y direction is around 2 Hz.
- The predominant frequency of the ground is around 1.5 Hz.
- Additional frequency (around 11 Hz) is generated by a 5 ton roller working in the Hatijheel area.
- The amplitude of vibration caused by the roller is greater than the *allowable levels of vibration for public buildings, but is not high enough to cause damage to the building.*

References

1. Federal Sanitary Norm of Russian Federation (1996). "SN2.2.4/2.1.8.566-96 – The sanitary norms of industrial vibration, vibration of residential and public buildings, 1996".
2. Winterkorn, H. F. and Fang, H. Y. (1975). Foundation Engineering Handbook publisher: Van Nostrand Reinhold.



PART-X

COMPARISON BETWEEN SMA AND MICROTREMOR MEASUREMENT AT JAMUNA BRIDGE SITES



**BANGLADESH NETWORK OFFICE FOR URBAN
SAFETY (BNUS), BUET, DHAKA**

Prepared By: Mehedi Ahmed Ansary

1. INTRODUCTION

An agreement has been signed on July 2014 between Bangladesh Bridge Authority (BBA) and Bureau of Research, Testing, and Consultation (BRTC), Bangladesh University of Engineering and Technology (BUET) for Consultancy Service for the Seismic Instrumentation Monitoring of Bangabandhu Bridge. The BUET Consultant team has visited different free-field sites of Strong Motion Devices as listed in the Inception Report (2014) and the Bridge site between November 10 and 23, 2014 and has carried out microtremor study both array and stand alone measurements. This report has presented the findings of those study carried out at those free-field sites tabulated in Table 1.

Table 1 Free-field Instruments

Model	Type	Location
ETNA	Triaxial Accelerometer (NS, EW, Vertical) plus Digital Recorder	LGED, Bogra
ETNA		LGED, Natore
ETNA		West-End of Bridge
ETNA		East-End of Bridge
ETNA		Police Staff College, Mirpur
ETNA		Hazicamp, Dhaka
ETNA (Portable)		BUET

2. BACKGROUND

The geotectonic set-up of Bangladesh suggests high probabilities of damaging future earthquakes and the possibility of rarer but extraordinarily large earthquakes that can cause damage far from their epicenters. Thus continuous watch of earthquake motion is necessary to predict and monitor the occurrence of earthquake disaster.

Using microtremor for site response has been widely popular among developing countries and also in lower seismic areas. Kanai and Tanaka (1954) initially studied the applicability of Microtremor and they had some limitations regarding the analysis. Afterward, based on their studies Nogoshi and Igarashi (1971) introduced a method of using horizontal and vertical spectral amplitude of Microtremor readings which was later modified and popularized by Nakamura (1989). Nakamura customized the new technique using the horizontal-to-vertical spectral ratio which is widely known as **H/V Method**. Investigations have been going in general still now and more improvements are taking place around the world consequently.

Microtremor is a type of short term vibration, preferably termed as “Ambient Vibration” for this special phenomenon, coming from lower amplitude. Generally, the vibrations can be caused due to natural occurrences and sometimes caused by disturbance commenced by mankind. It is renowned for the ease of using. It can be simply used in places of low seismicity and still give a good number of information. Moreover it is inexpensive which makes it more convenient for developing country like ours where resources are short. It can be really useful to obtain the key parameters in the site response studies (site period, local site effects), soil-structure interaction studies, seismic hazard studies, site geological conditions estimation (peak period of amplification) etc.

3. OBJECTIVE OF THE STUDY

In this study, the main objective is to report the preliminary factors that can give some perception about the site response of the ground. Moreover, knowing one or two parameters, that hold the fundamental feature of the site response, can be helpful to resolve further seismic response characteristics of surface ground and Bridge structures.

Monitoring the variation of the frequency is an important feature to perceive. The reasons of those variations should be observed closely. These variations can mainly occur due to the placement of the apparatus, time of data recording, soil condition, weather conditions, surrounding environment and especially traffic conditions. These variations, while comparing with relevant data, give a definitive point of view of the stability of the site. It also points out the obstacles to be covered up while examining at another sites.

So, to summarize, the overall objectives are:

- Experimental determination of predominant frequency of site
- Investigational assessment of soil for vulnerability

Throughout this whole report these objectives have been pursued with the help of microtremor (MT) equipment and convenient locations have been selected.

4. OUTCOME OF THE STUDY

The H/V ratio method in the microtremor analysis is widely used for microzonation study and local effects studies. But this research mainly emphasizes on observing and analyzing site response of soils and structures due to ambient noise at various times of a day using H/V ratio technique. Measurement done using this microtremor method can give valuable information about the natural frequency, amplification factor and even weak points on all types of soil and structure.

In this study, H/V ratio technique for microtremor data analysis has been used to investigate resonance criteria for ground. This approach is able to determine the weak points of ground, bridge structure and weak points of ground and structure to estimate the real earthquake damage before an earthquake. The results therefore, can be used for earthquake disaster mitigation. Estimation of damage can be done quickly and accurately. Possible types of preparatory study in highly seismic region are very promising for disaster prevention activities in the future.

Again, the comparison studies can indicate the effects of surroundings. These results shed light on the fact that soil and structure react differently while some factors are changed. Thus, these factors have a great influence over the behavior of damage due to seismic hazards. So, if the nature of change is identified, manners of damage can be perceived too.

If weak points of ground and structures can be detected in advance by investigating the durability of various structures and ground, damage can be decreased by taking appropriate countermeasures. In addition, if seismic characteristics of ground and structures are already known, seismic intensity distribution of the area can be precisely estimated.

Occurrence of earthquake damage depends upon strength, period and duration of seismic motions. These parameters, of course, depend upon earthquake itself but they are also strongly influenced by the seismic response characteristics of surface ground and structures. So, there are a lot of scopes to investigate using this H/V ratio method for microtremor data analysis.

5. METHODOLOGY

Spectral contents of microtremor can be normally influenced by the near-surface geological structures. For example due to soft soil layer resonant amplification is produced. This phenomenon leads to amplification at the fundamental S-wave resonance frequency of the soil layer (Nakamura, 1989). Also, it should be kept in mind that, source characteristics are usually unknown in microtremor studies. Moreover, microtremor consists of shear, Rayleigh and Love wave. So, using H/V ratio provides more stable measure for site related properties. Stability check of microtremor data, effects of processing of raw data and analysis of calculated results are discussed. After analyzing and checking the H/V curves, interpretation of the results (predominant frequency, peak type of H/V curve) are discussed.

One of the most widely used methods for site response estimation using ambient vibration measurements is the so-called Nakamura's technique (1989). This technique, initially introduced by Nogoshi and Igarashi (1971), consists in taking the ratio between the Fourier spectra of the horizontal and vertical components of the ambient vibrations. Many studies (Ohmachi *et al.* 1991, Field and Jacob 1993b) confirmed that these ratios (H/V ratios) are very stable, and on soft soil sites they exhibit a clear peak that is correlated with the fundamental resonant frequency. Regarding the amplitude of the peak, there are still a lot of debates. According to Konno and Ohmachi (1998) there is a good correlation between the amplitude of the H/V peaks and the S-wave site amplification, while other researchers (Lermo and Chavez-Garcia, 1994) suggests that there is no good correlation between the H/V peaks and site transfer function. Lachet and Bard (1994) proposed that the good match at the fundamental frequency is due to horizontal-vertical polarization of the Rayleigh waves, an interpretation that is in agreement with the early Japanese studies (Kudo, 1995).

Using microtremor H/V method gives a benefit for low seismological areas for recording the data and investigates them at ease. Taking data in different time period is the singular field activity here. After that, only transforming those time domain data and using some software to analyze them will give us enough outcomes to study further for assessing site effects. Due to the insufficiency of adequate reference sites, especially in flat areas where exposed rock sites are not found, the traditional H_S/H_R method cannot be used generally. Hence, approach to the microtremor H/V method, which requires no reference sites, is the only convenient path. There are so many procedures that can be followed for this research. In this experiment, a simple and widely used method has been used with some modifications. The following flow chart (Figure 1) shows the outline of the methodology.

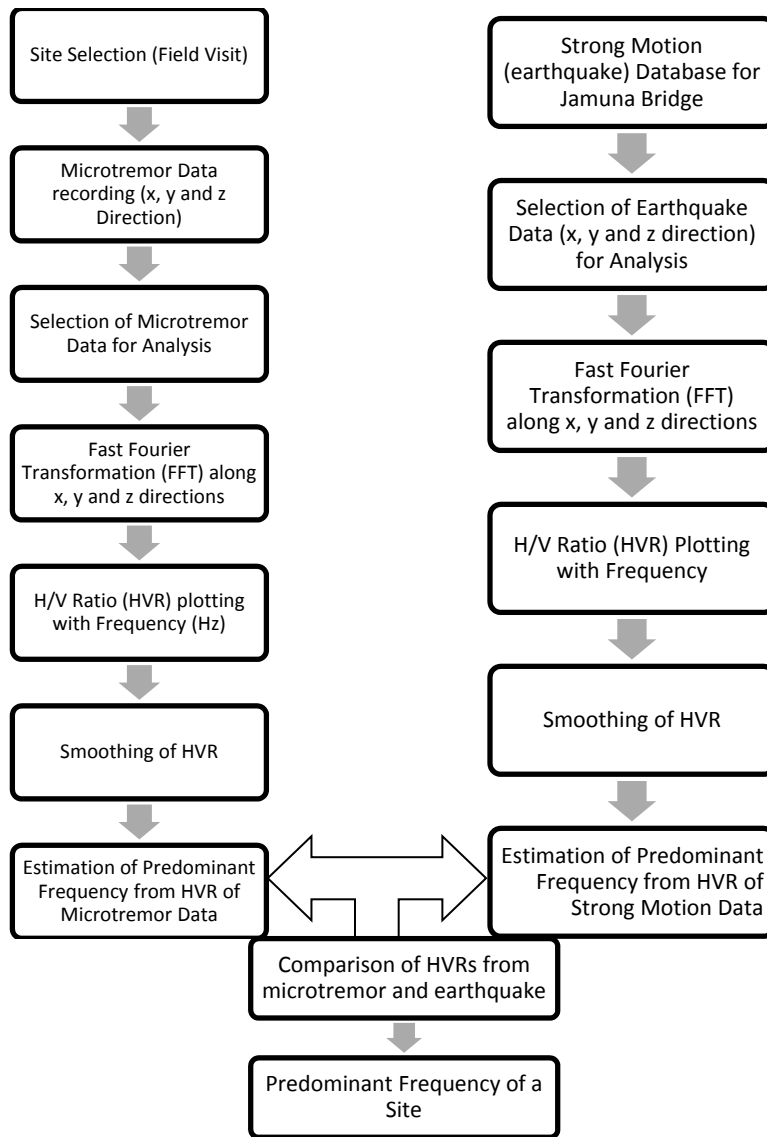


Figure 1 Flow Chart for Methodology of Microtremor and Strong Motion Data Analysis

6. DATA COLLECTION AND EQUIPMENT USED FOR THIS STUDY

Data are collected from various field stations. They are situated in BUET, Police Staff College, Hazi Camp, LGED of Bogra and Natore, East and West part of Jamuna Bridge as shown in Table 1. There are some preinstalled devices in these places, where ground excitation due to earthquakes have been already recorded. As there are memory cards so the data can be collected with two or three month intervals. On 10 November 2014, prerecorded data from BUET, Police Staff College and Hazi Camp have been collected. Field vibration data has also been collected from these places using microtremor array technique. Five sensors have been used to collect field vibration data from one site.

On 20 November 2014, the BUET team has collected data from Natore and Bogra LGED. Similarly on 21 November 2014, data has been collected from East and West side of Jamuna bridge. Ground vibration data using microtremor array technique has been collected from all those sites. Ground vibration has also been collected next to the west bridge abutment. In all sites, microtremor data has been collected for 30 minutes. The data are collected at various time periods for specific time duration. This is mainly done to minimize the consequence of any kind of interruption that can distort the results.

Microtremor measurement apparatus includes Geodas 15-HS equipment (data logger and laptop), five sensors, cable, battery, and GPS. Mtobs.exe software has been used to record microtremor data. Sensors comprise three components, which can record the horizontal motion (in Latitude and Longitude directions) and the vertical motions (up and down). Microtremor sensor sensitivity is 2, 95,900 lm/s/V. The converting speed is 50 kHz. The sampling frequency was 100-500 Hz. Velocity time history field microtremor data have been recorded in Mtobs.exe software with suitable number of observation channels, observation length, observation frequency, specific low or high pass filter code, amplification ratio, observation latitude and longitude, observation time, and observation channel mode. For each location, three sensors have been used.

7. DATA INTERPRETATION

7.1 BOGRA LGED

The data are collected at various time periods for specific time duration. This is mainly done to minimize the consequence of any kind of interruption that can distort the results.

The following Figure 2 shows time history microtremor (MT) data of 80 seconds duration. These MT data were recorded at Bogra LGED. Time history data is not suitable to estimate dynamic properties. Movements of the Earth's surface generated by the whole ambient seismic background noise, and their corresponding Fourier spectra for frequencies above 1 Hz, are usually recorded by MT. Transformation of time domain data to frequency domain data is required with Fourier transformation. Therefore FFT has been used and compared with actual earthquake data. Figure 1 shows the ground wave velocity recorded in three channels of MT. Ch1, ch2 and ch3 respectively represent x, y and z component of ground wave velocity in $\mu\text{m/s}$. Peak velocity is recorded in ch3 or in Z direction with a value of $20\mu\text{m/s}$.

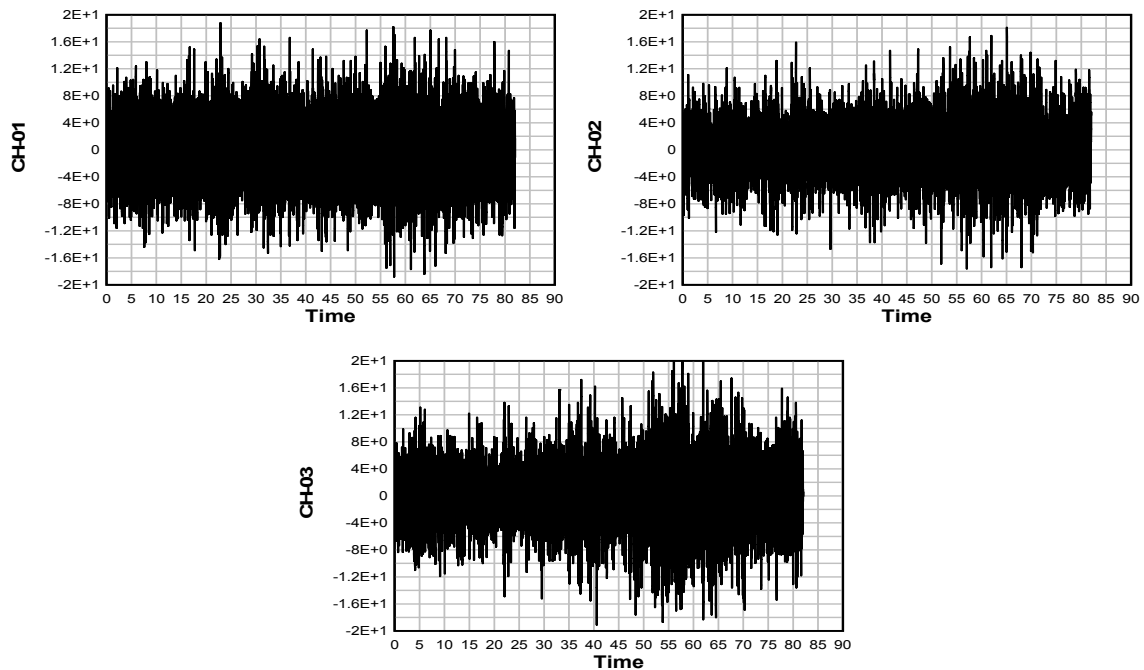


Figure 2 Microtremor Time History data at Bogra, LGED

Figure 3 shows Earthquake (EQ) data recorded by triaxial accelerometer on 22 June 2004. Here time is in Second and ground acceleration is in cm/s^2 . The figure shows that the highest ground acceleration was in north-south (n-s) direction with a value of 20 cm/s^2 . The duration of the EQ was 41 seconds. The peak acceleration in east-west (e-w) and Up-down (u-d) was 16 and 4 cm/s^2 respectively.

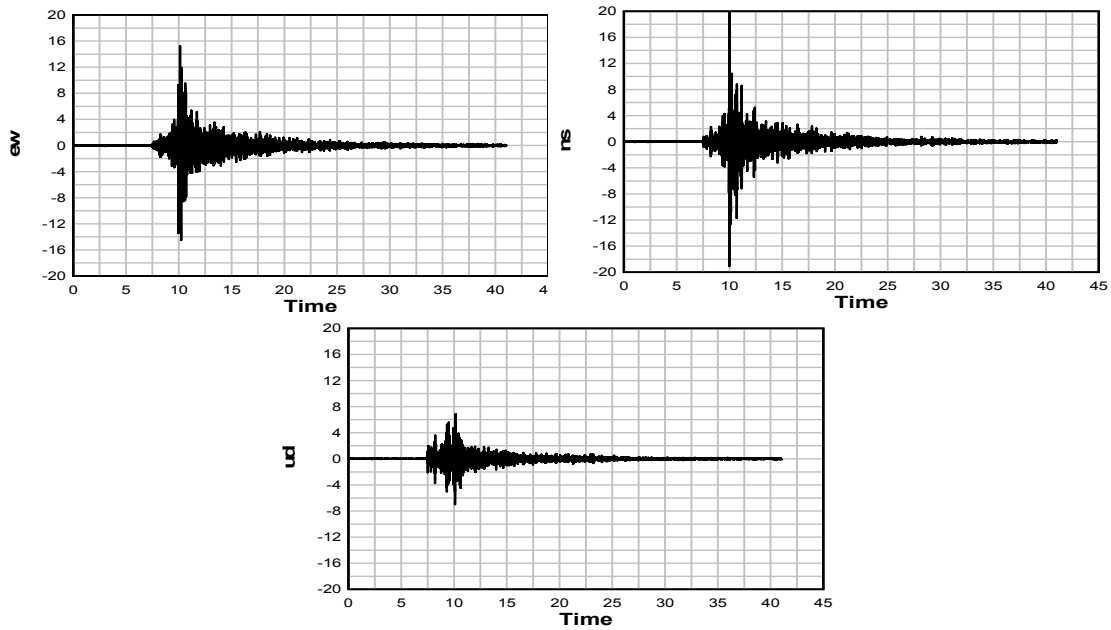


Figure 3 Earthquake Time History data at BOGRA (22-06-2004)

Figure 4 shows Earthquake (EQ) data recorded by triaxial accelerometer on 14Feb 2006. The Figure shows that the highest ground acceleration was in e-w direction with a value of 2.4 cm/s². The duration of the shaking was 75 seconds. The peak acceleration in n-s and up-down (u-d) was 1.8 cm/s² and 0.7 cm/s² respectively.

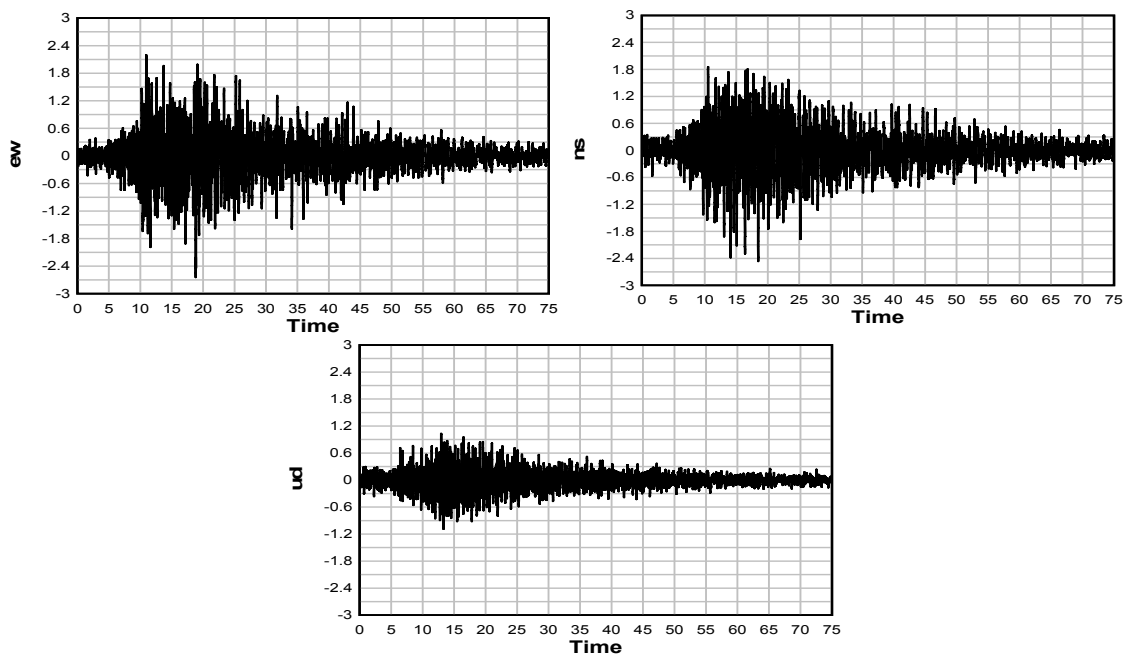


Figure 4 Earthquake Time History data at BOGRA (14-02-2006)

Figure 5 shows Earthquake (EQ) data recorded by triaxial accelerometer at 27 July 2008. The figure shows that the ground acceleration in both e-w and n-s direction was equal with a value of 18 cm/s².

The duration of the shaking was 70 seconds. After that the vibration gradually dissipated. The peak displacement in u-d was 8 cm/s².

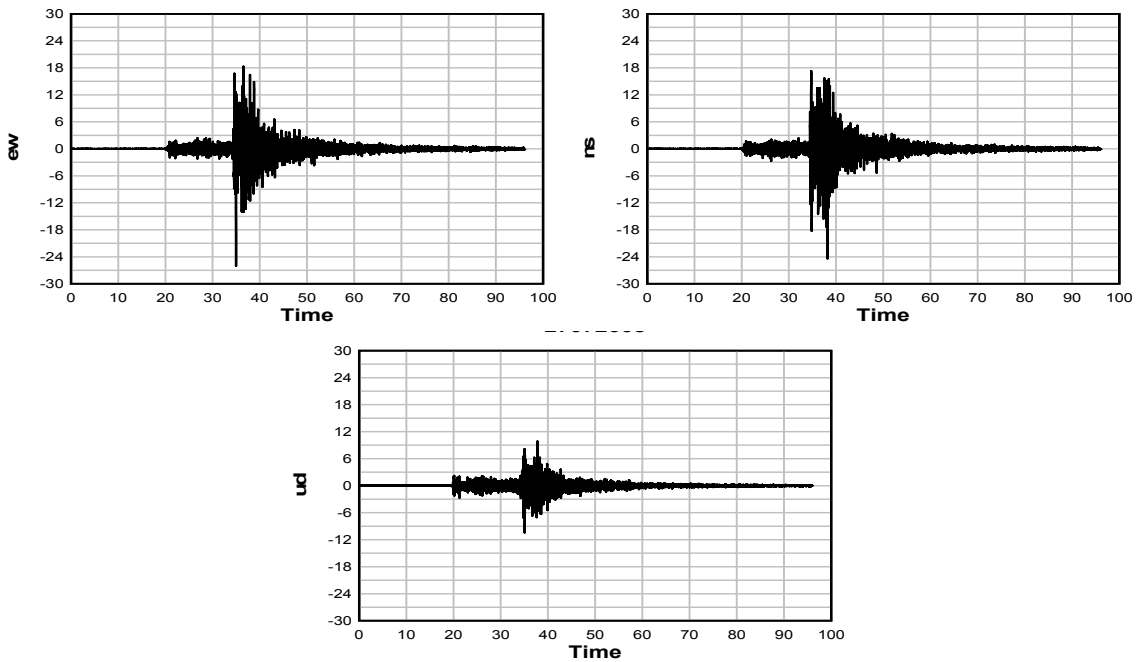


Figure 5 Earthquake Time History data at BOGRA (27-07-2008)

Figure 6 shows comparison of horizontal to vertical ratio (HVR) of MT and EQ data. HVR of EQ data is average of 11 different earthquakes. HVR of MT is also average of 5 data. Comparison of earthquake and MT HVR shows similar overall trend. For both cases predominant frequency ranges between 1 and 2 hz.

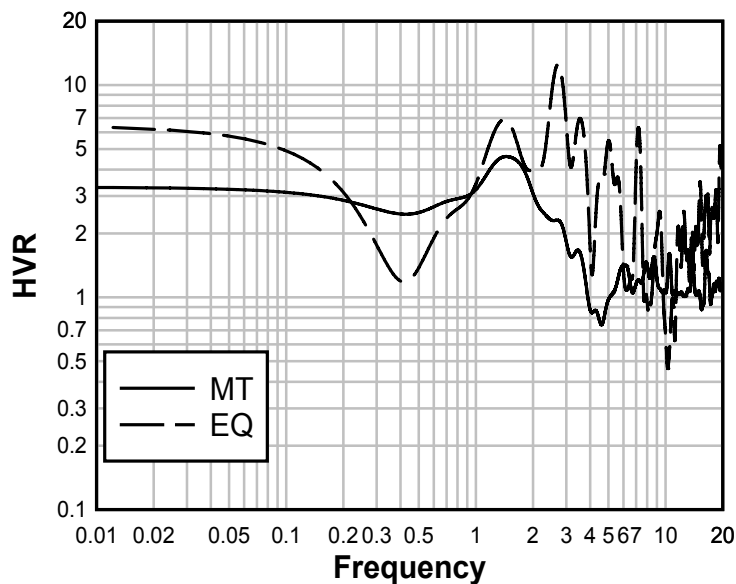


Figure 6 HVR vs Frequency plot of MT and EQ

7.2 BUET CAMPUS

Figure 7 shows Earthquake (EQ) data recorded by triaxial accelerometer on 18 September 2005 at BUET campus. Ground acceleration in both e-w and n-s direction was equal with a value of 1.8 cm/s^2 . The duration of the shaking was 40 seconds. After that the vibration gradually dissipated. The peak acceleration in u-d direction was 8 cm/s^2 .

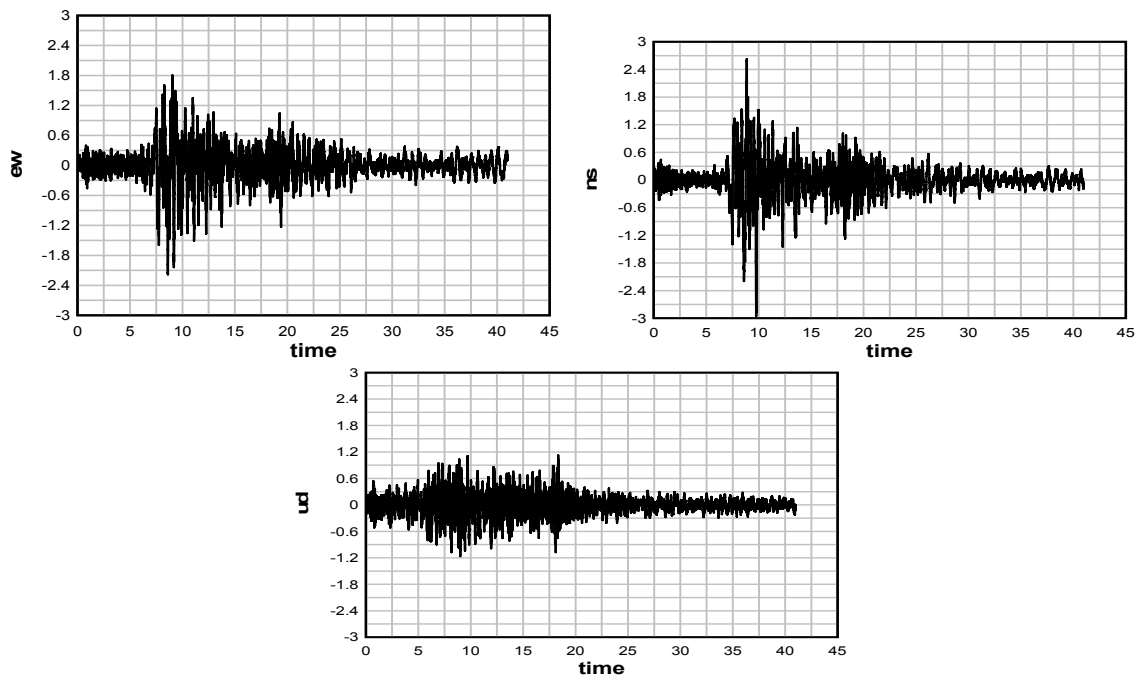


Figure 7 Earthquake Time History data at BUET (18-09-2005)

Figure 8 shows Earthquake (EQ) data recorded by triaxial accelerometer on 5 August 2005. The figure shows that the ground displacement in n-s direction had the highest acceleration of 3.2 cm/s^2 and e-w direction had an acceleration of 1.6 cm/s^2 . The duration of the shaking was 40 seconds. The peak displacement in u-d was 0.8 cm/s^2 .

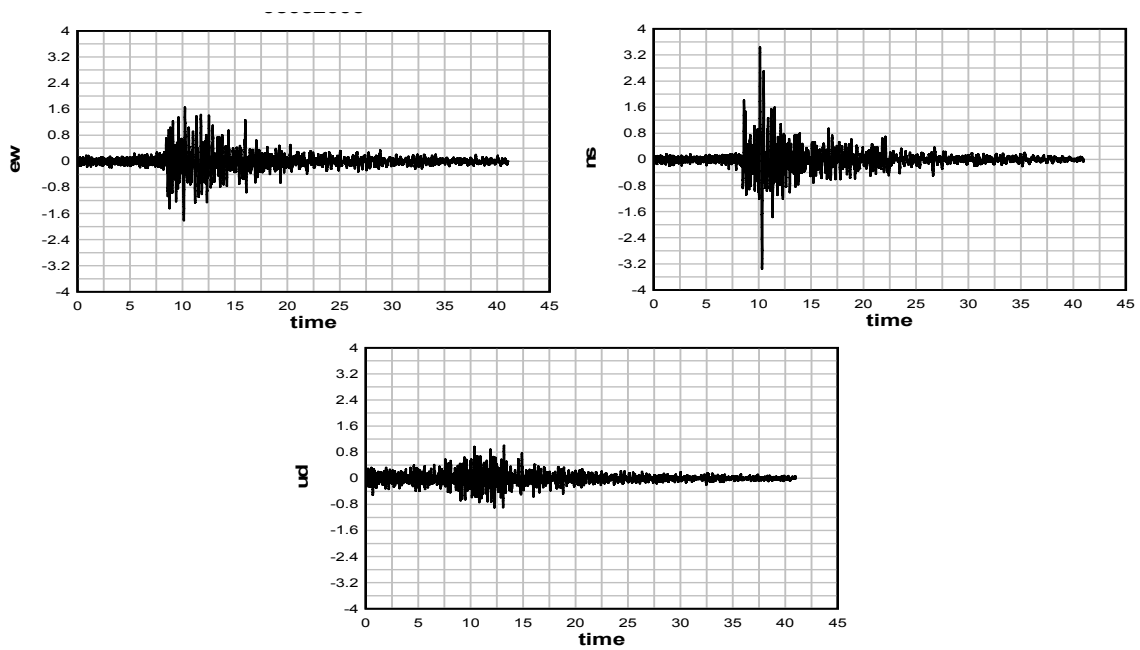


Figure 8 Earthquake Time History data at BUET (05-08-2005)

Figure 9 shows Earthquake (EQ) data recorded by triaxial accelerometer on 09 June 2011. The figure shows that the ground acceleration in n-s direction had a value of 6 cm/s² and e-w direction had a displacement of 5 cm/s². The duration of the shaking was 15 seconds. After that the vibration gradually dissipated. The peak acceleration in u-d was 6 cm/s².

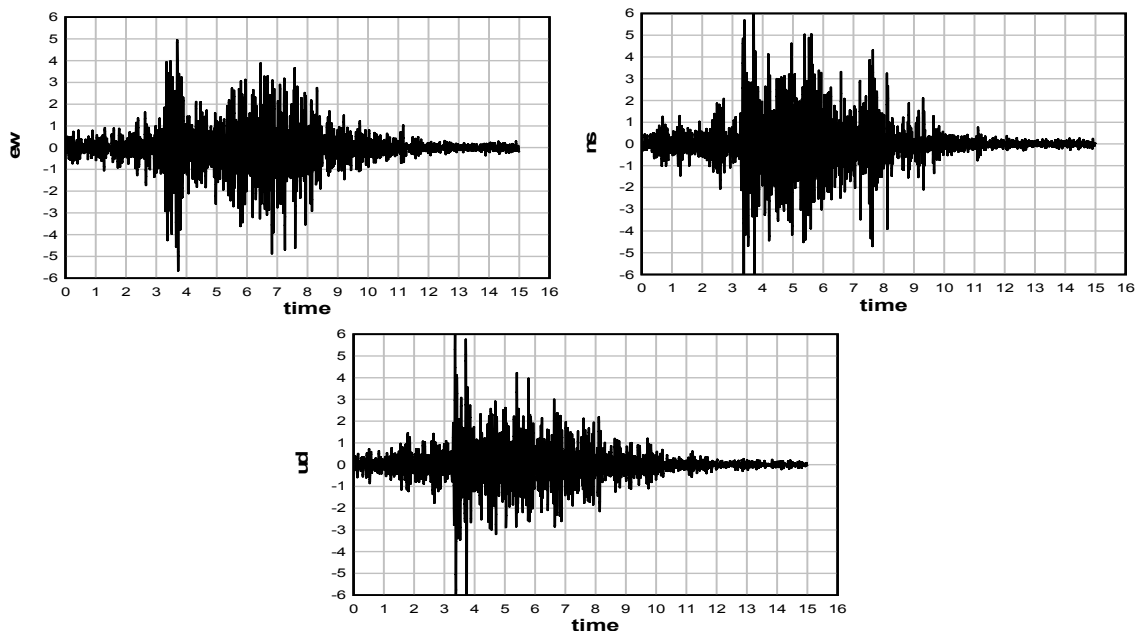


Figure 9 Earthquake Time History data at BUET (09-06-2011)

Figure 10 shows Earthquake (EQ) data recorded by triaxial accelerometer on 18 March 2012. The figure shows that the ground acceleration in both e-w and n-s direction was equal with a value of 20 cm/s^2 . The duration of the shaking was 50 seconds. The peak acceleration in u-d was 12 cm/s^2 .

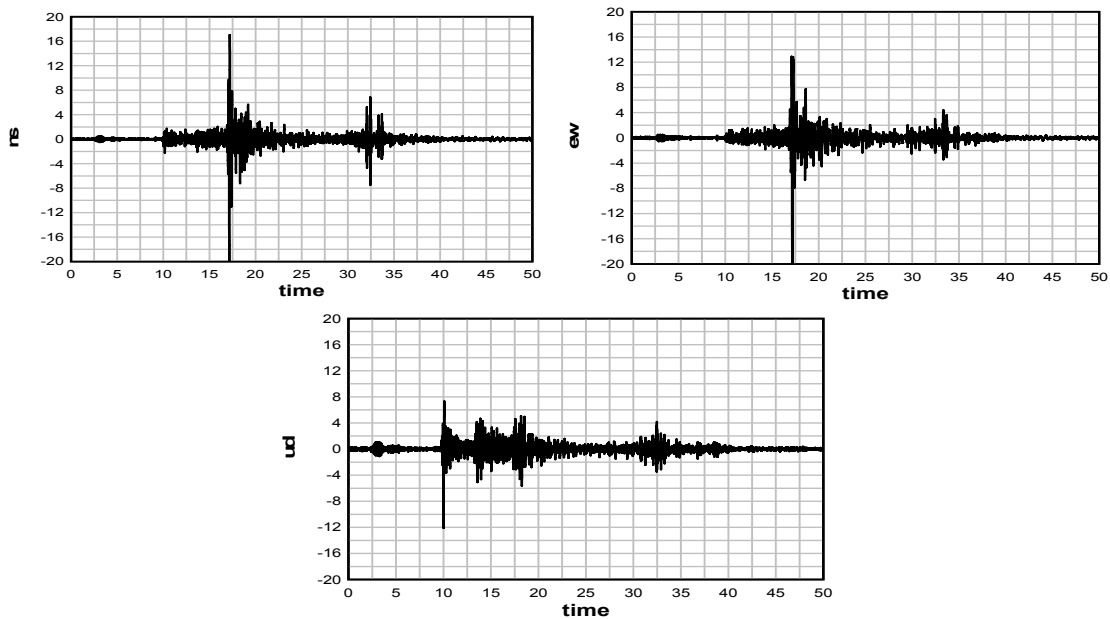


Figure 10 Earthquake Time History data at BUET (18-03-2012)

The following Figure 11 shows time history MT data of three segments with data length of 80 seconds at BUET campus. FFT has been used and compared with actual earthquake data. It shows ground wave velocity recorded in three channels of MT. Peak ground velocity is recorded in ch1 with a value of $120 \mu\text{m/s}$. ch3 recorded a uniform velocity of $2 \mu\text{m/s}$. Later FFT has been used and compared with actual earthquake data.

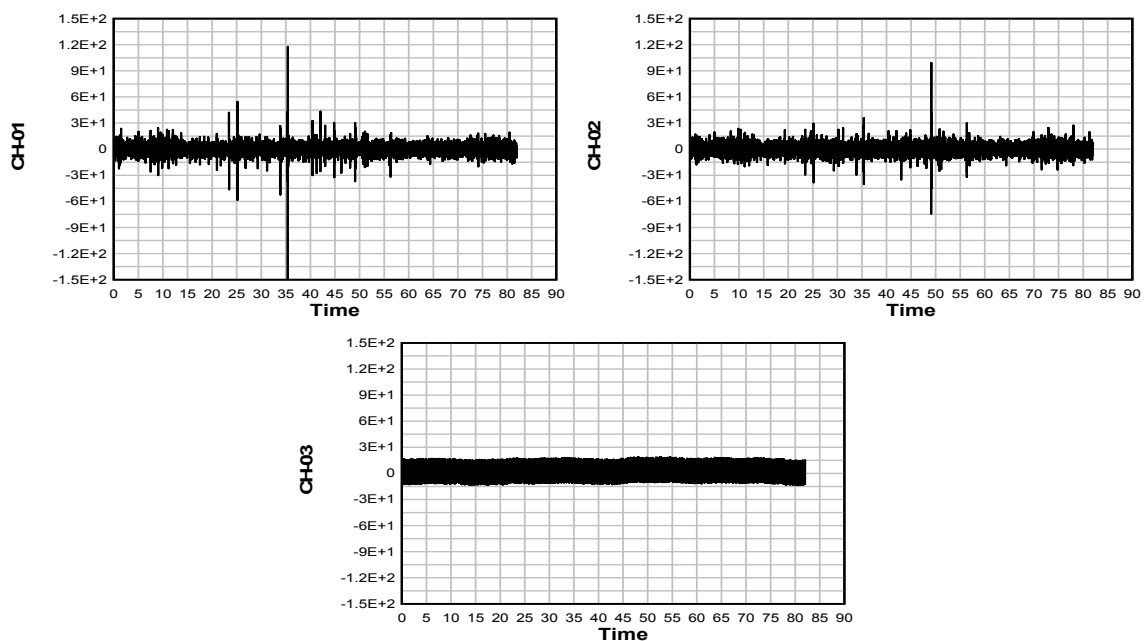


Figure 11 Microtremor Time History data at BUET campus

Figure 12 shows comparison of horizontal to vertical ratio (HVR) of MT and EQ data recorded at BUET campus. HVR of EQ data is average of 4 different earthquakes and HVR of MT is average of 5 data. Comparison of earthquake and MT HVR shows similar overall trend. For EQ predominant frequency ranges between 0.7 to 1 hz. MT recorded data shows predominant frequency between 1 to 2 hz.

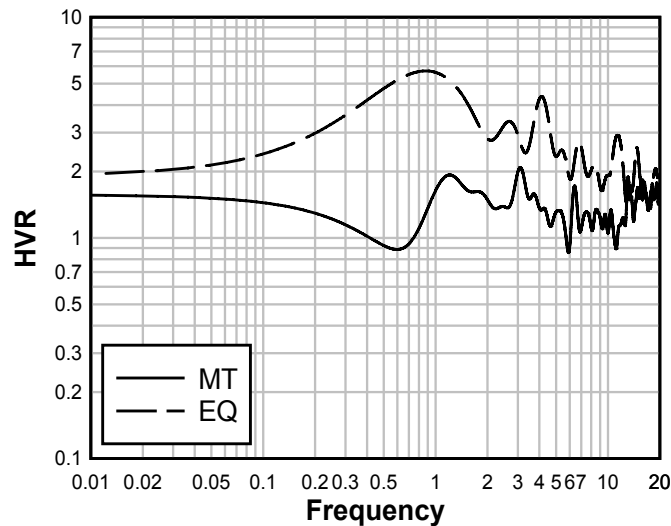


Figure 12 HVR vs Frequency plot of MT and EQ

7.3 EAST SIDE OF JAMUNA BRIDGE

Figure 13 shows Earthquake (EQ) data recorded by triaxial accelerometer on 14 February 2006. The figure shows that the ground acceleration in both e-w and n-s direction was equal with a value of 2.4 cm/s^2 . The duration of the shaking was 70 seconds. The peak acceleration in u-d was 0.6 cm/s^2 .

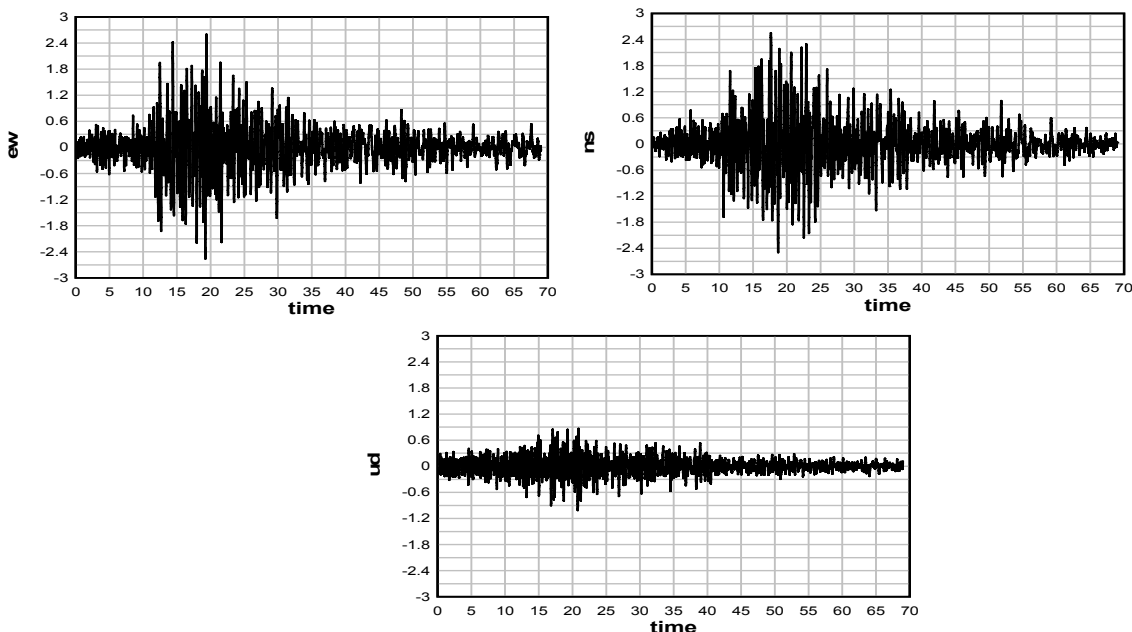


Figure 13 Earthquake Time History data at East Side of Jamuna Bridge (14-02-2006)

Figure 14 shows Earthquake data recorded by triaxial accelerometer on 11 April 2006. The figure shows that the ground acceleration in n-s direction has highest acceleration with a value of 1 cm/s^2 . Acceleration in e-w direction had a value of 0.8 cm/s^2 . The duration of the shaking was 40 seconds. The peak displacement in u-d was 0.2 cm/s^2 .

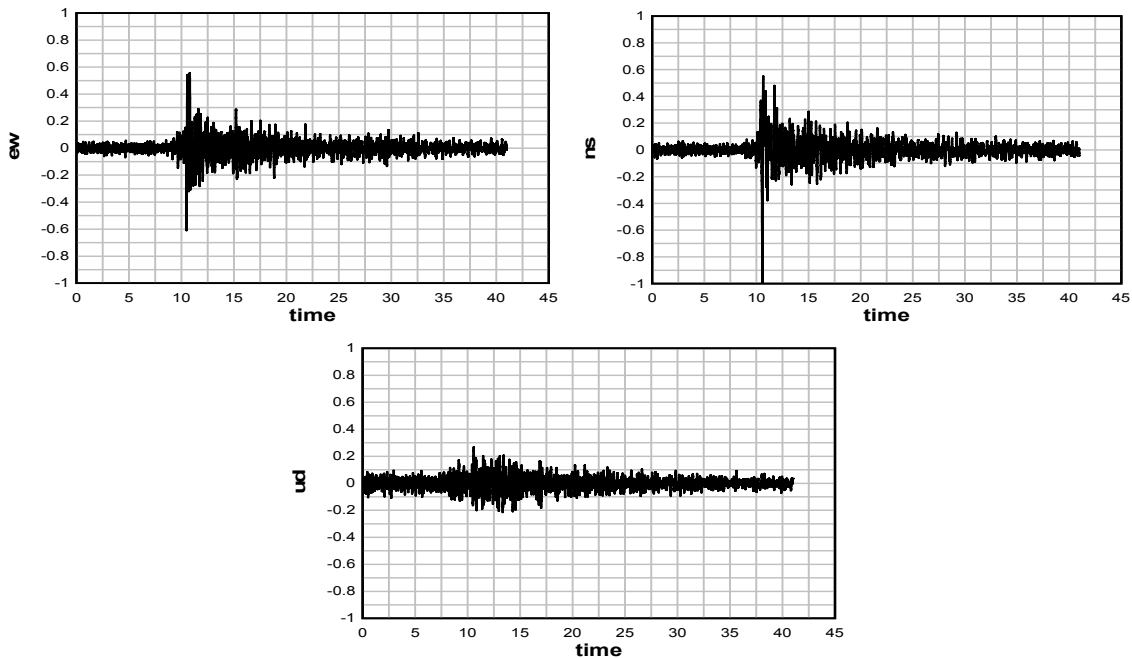


Figure 14 Earthquake Time History data at East Side of Jamuna Bridge (11-04-2006)

Figure 15 shows Earthquake data recorded by triaxial accelerometer on 05 August 2006. The figure shows that the ground acceleration in e-w direction had highest acceleration with a value of 3.2 cm/s^2 . Acceleration in e-w direction had a value of 2.4 cm/s^2 . The duration of the shaking was 65 seconds. The peak acceleration in u-d was 1.6 cm/s^2 .

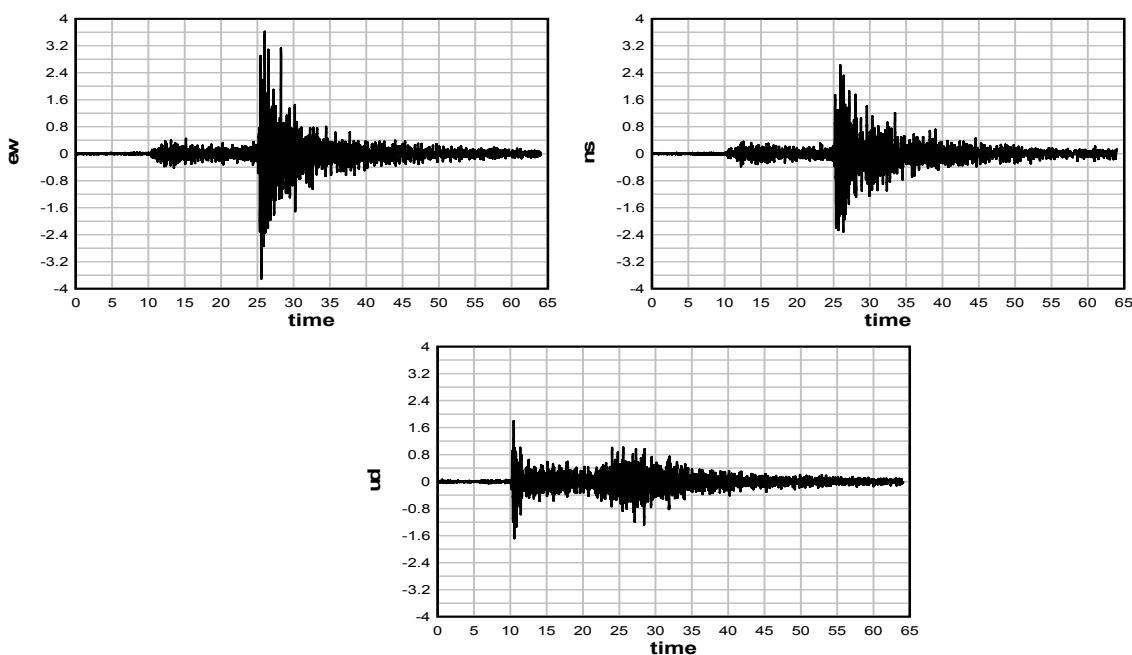


Figure 15 Earthquake Time History data at East Side of Jamuna Bridge (05-08-2006)

Figure 16 shows time history MT data of three segments with data length of 80 seconds at East side of Jamuna Bridge. FFT has been used and compared with actual earthquake data. It shows ground wave velocity recorded in three channels of MT. Peak ground velocity was recorded in ch3 with a value of 24 $\mu\text{m/s}$. Later FFT has been used and compared with actual earthquake data.

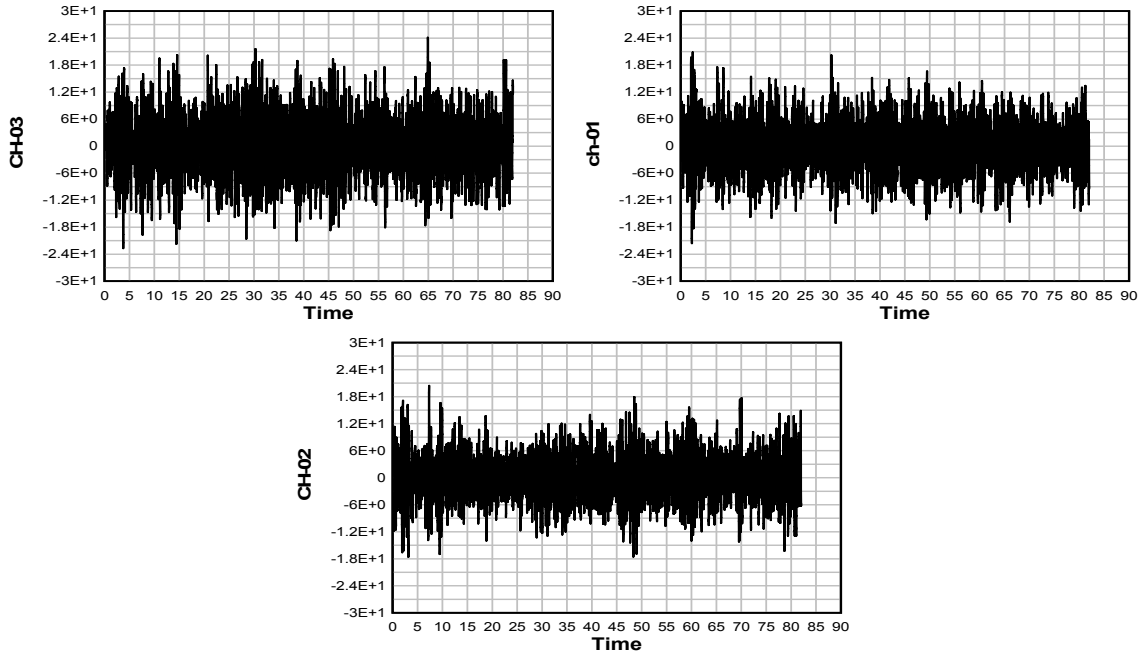


Figure 16 Microtremor Time History data at East Side of Jamuna Bridge

Figure 17 shows comparison of horizontal to vertical ratio (HVR) of MT and EQ data recorded at East side of Jamuna bridge. HVR of EQ data is average of 3 different earthquakes and HVR of MT is average of 5 data. Comparison of earthquake and MT HVR shows similar overall trend with a predominant frequency in the range of 0.7 to 1 hz.

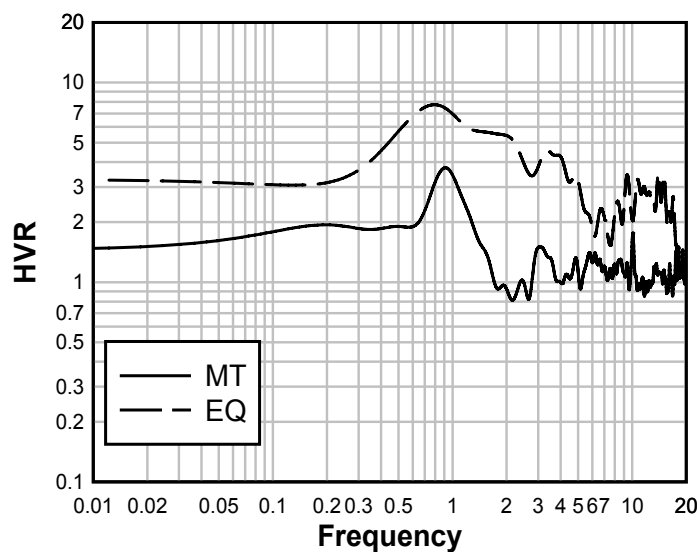


Figure 17 HVR vs Frequency plot of MT and EQ

7.4 WEST SIDE OF JAMUNA BRIDGE

Figure 18 shows Earthquake (EQ) data recorded by triaxial accelerometer on 14 February 2006. Ground acceleration in both e-w and n-s direction was equal with a value of 2 cm/s^2 . The duration of the shaking was 45 seconds. The peak acceleration in u-d was 1.5 cm/s^2 .

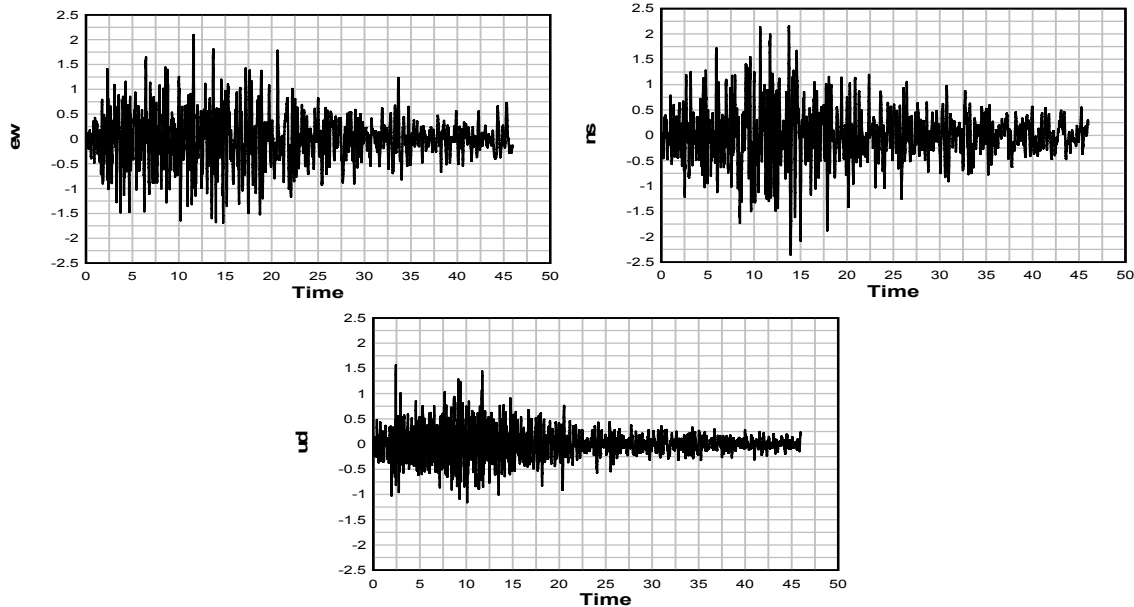


Figure 18 Earthquake Time History data at West Side of Jamuna Bridge (14-02-2006)

Figure 19 shows Earthquake (EQ) data recorded by triaxial accelerometer on 27 July 2008. The figure shows that the ground displacement in e-w direction has the highest acceleration of 4 cm/s^2 and n-s direction has a displacement of 3 cm/s^2 . The duration of the shaking was 60 seconds. The peak displacement in u-d was 1 cm/s^2 .

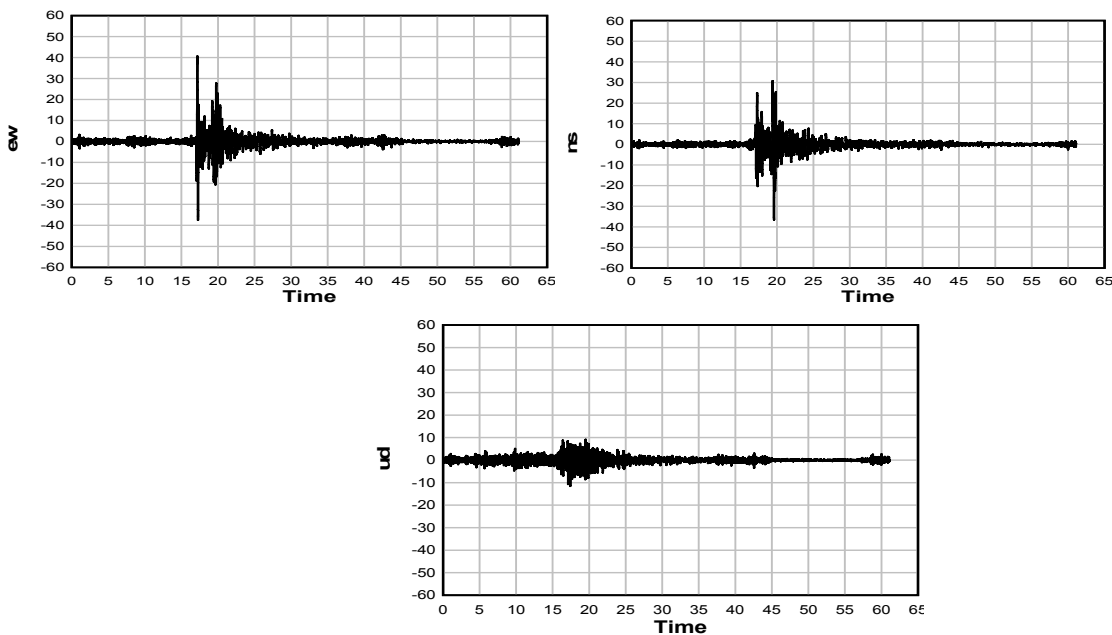


Figure 19 Earthquake Time History data at West Side of Jamuna Bridge (27-07-2008)

Figure 20 shows time history MT data of three segments with data length of 80 seconds at West side of Jamuna Bridge. FFT has been used and compared with actual earthquake data. It shows ground wave velocity recorded in three channels of MT. Peak ground velocity was recorded in ch3 with a value of 500 $\mu\text{m/s}$. Lowest ground velocity was recorded in ch1 with a value of 50 $\mu\text{m/s}$. Later FFT has been used and compared with actual earthquake data.

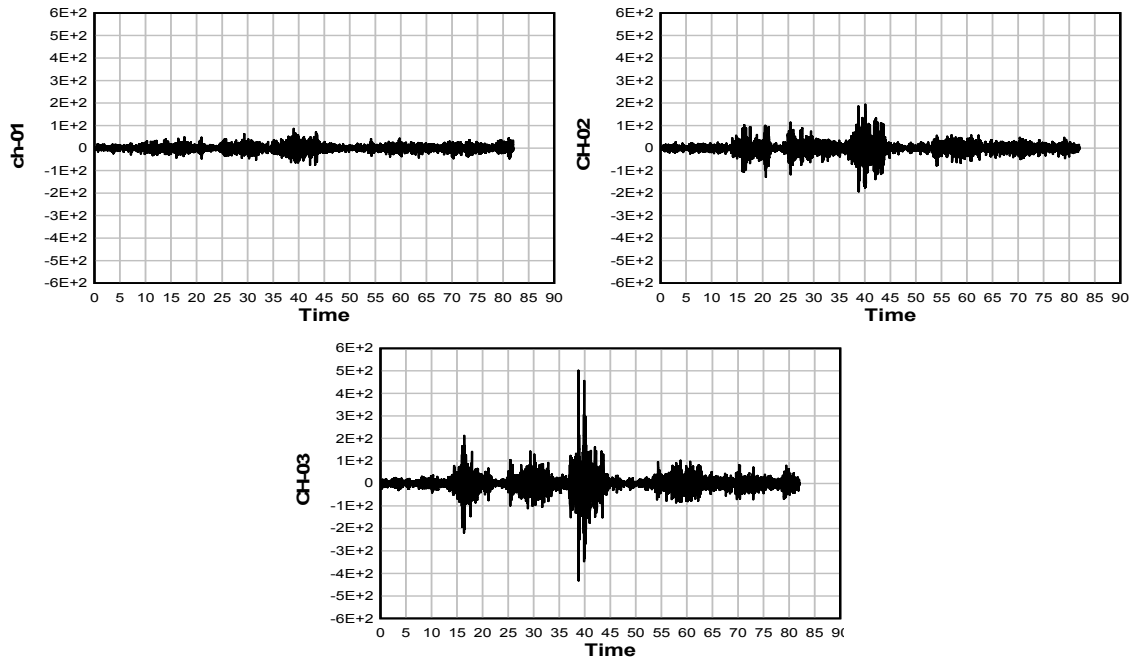


Figure 20 Microtremor Time History data at West Side of Jamuna Bridge

Figure 21 shows comparison of horizontal to vertical ratio (HVR) of MT and EQ data recorded at West side of Jamuna bridge. HVR of EQ data is average of 2 different earthquakes and HVR of MT is average of 5 data. Comparison of earthquake and MT HVR shows similar overall trend. Predominant frequency of EQ is 0.7hz and MT reading shows predominant frequency of 1hz.

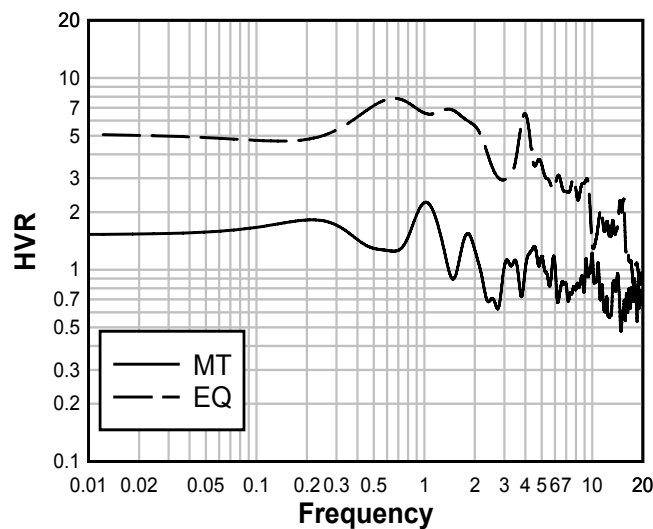


Figure 21 HVR vs Frequency plot of MT and EQ

7.5 POLICE STAFF COLLEGE

Figure 22 shows Earthquake (EQ) data recorded by triaxial accelerometer on 18 September 2011. Ground acceleration in n-s direction had an acceleration of 6 cm/s^2 and e-s direction had an acceleration of 5 cm/s^2 . The duration of the shaking was 40 seconds. The peak acceleration in u-d was 3 cm/s^2 .

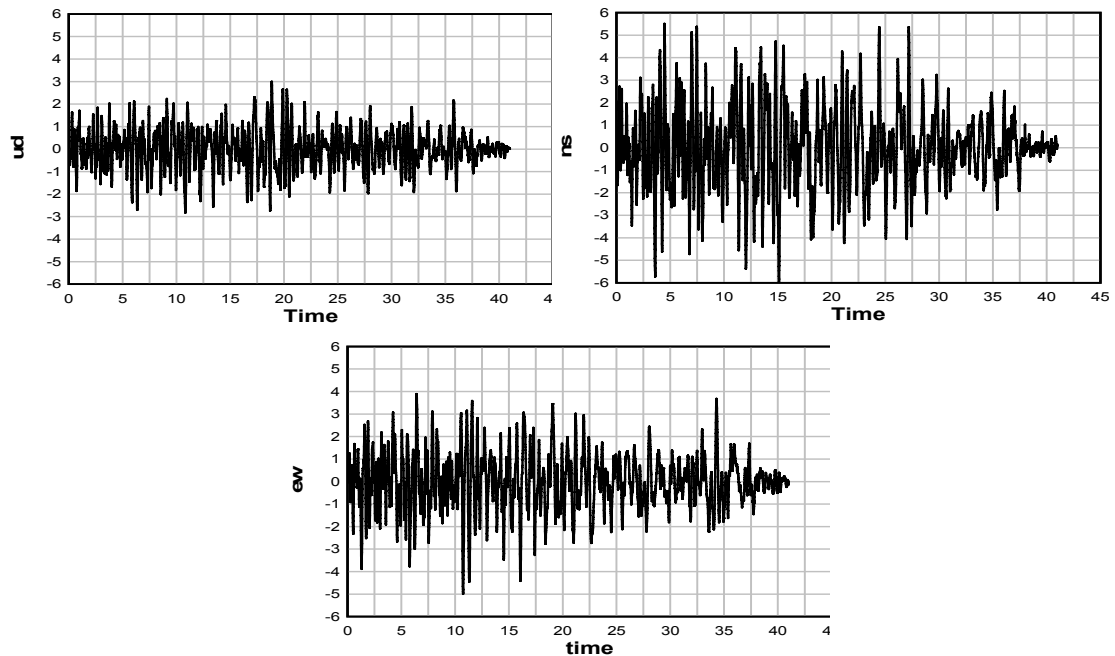


Figure 22 Earthquake Time History data at PSC (18-09-2011)

Figure 23 shows time history MT data of three segments with data length of 80 seconds at Police Staff College. FFT has been used and compared with actual earthquake data. It shows ground wave velocity recorded in three channels of MT. Peak ground velocity was recorded in ch2 with a value of $24 \mu\text{m/s}$. Later FFT has been used and compared with actual earthquake data.

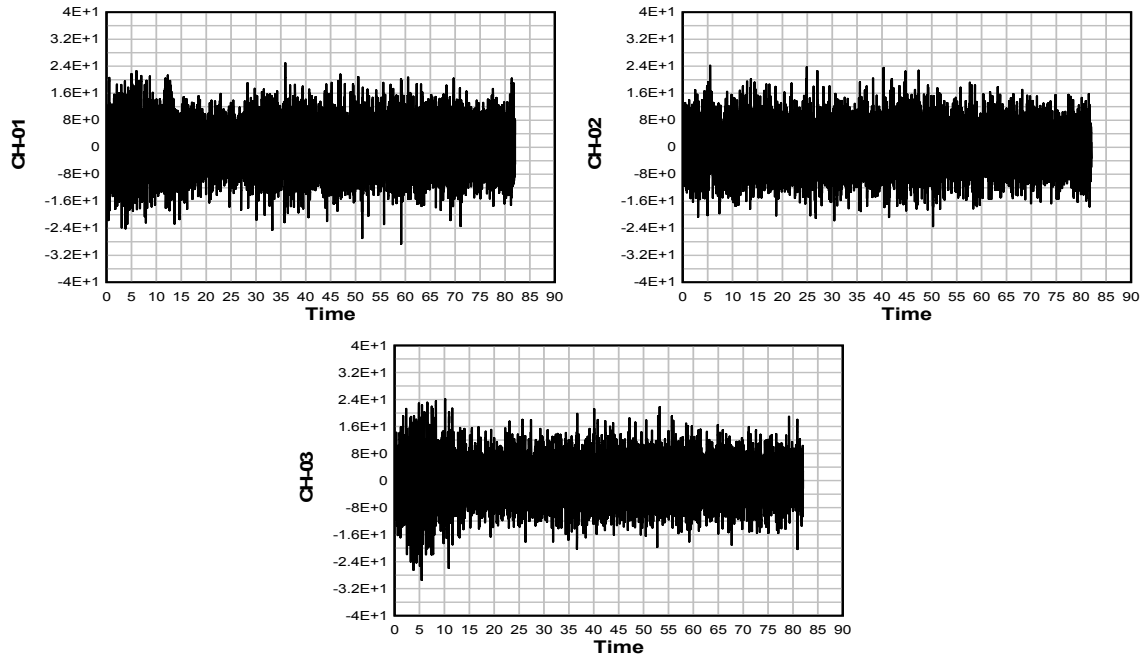


Figure 23 Microtremor Time History data at Police Staff College

Figure 24 shows comparison of horizontal to vertical ratio (HVR) of MT and EQ data recorded at Police Staff College. Comparison of earthquake and MT HVR shows similar overall trend. Predominant frequency of EQ is 0.45hz and MT reading shows predominant frequency around 1 hz.

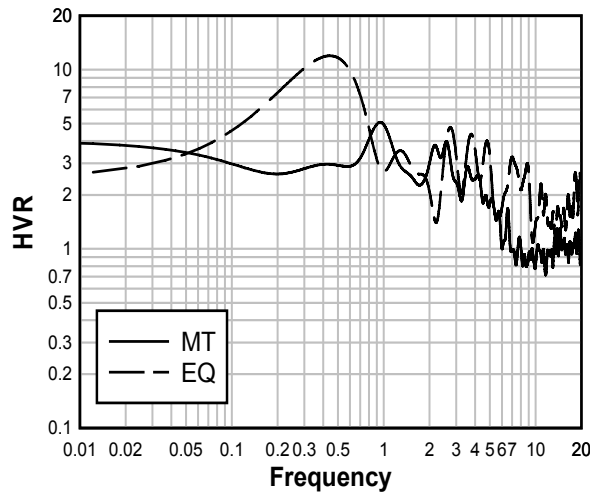


Figure 24 HVR vs Frequency plot of MT and EQ

7.6 HAZI CAMP

Figure 25 shows Earthquake (EQ) data recorded by triaxial accelerometer on 10 September 2010. The figure shows that the ground acceleration in e-w direction had highest acceleration value of 10 cm/s^2 and n-s direction had an acceleration of 6 cm/s^2 . The duration of the shaking was 21 seconds. The peak displacement in u-d was 4 cm/s^2 .

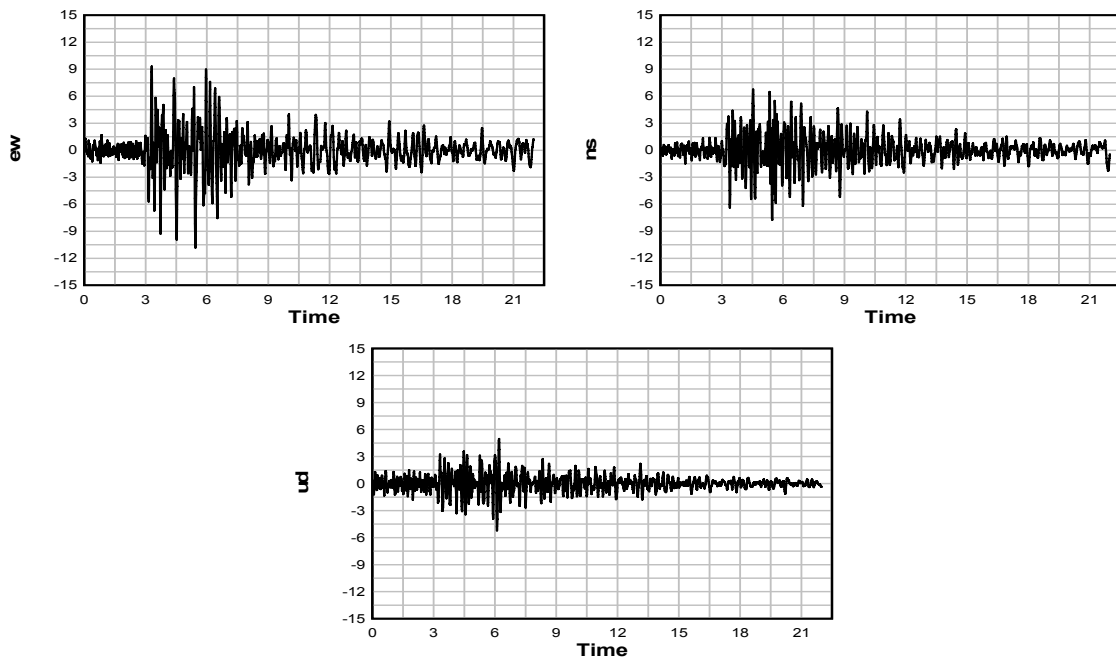


Figure 25 Earthquake Time History data at Hazi Camp (10-09-2010)

Figure 26 shows Earthquake (EQ) data recorded by triaxial accelerometer on 18 September 2011. Ground acceleration in e-w direction had a value of 8 cm/s² and n-s direction had an acceleration value of 4 cm/s². The duration of the shaking was 35 seconds. The peak acceleration in u-d was 2 cm/s²

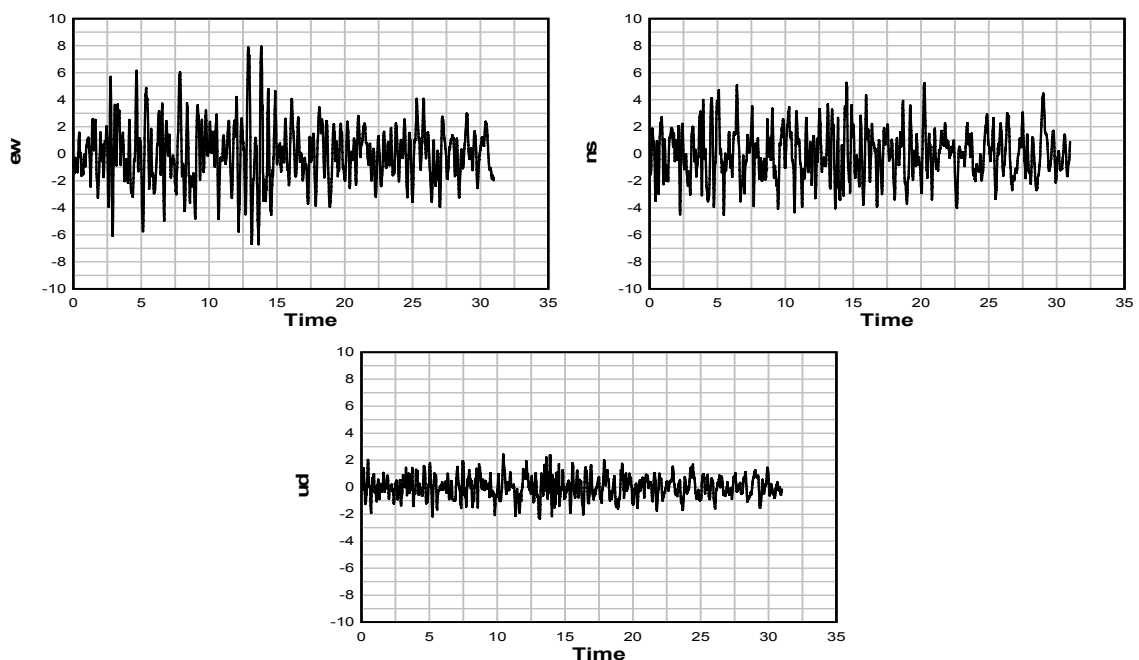


Figure 26 Earthquake Time History data at Hazi Camp (18-09-2011)

Figure 27 shows time history MT data of three segments with data length of 80 seconds at Hazi Camp. FFT has been used and compared with actual earthquake data. It shows ground wave velocity recorded in three channels of MT. Three channels had almost the same ground velocity with a peak value of $30\mu\text{m/s}$. Later FFT has been used and compared with actual earthquake data.

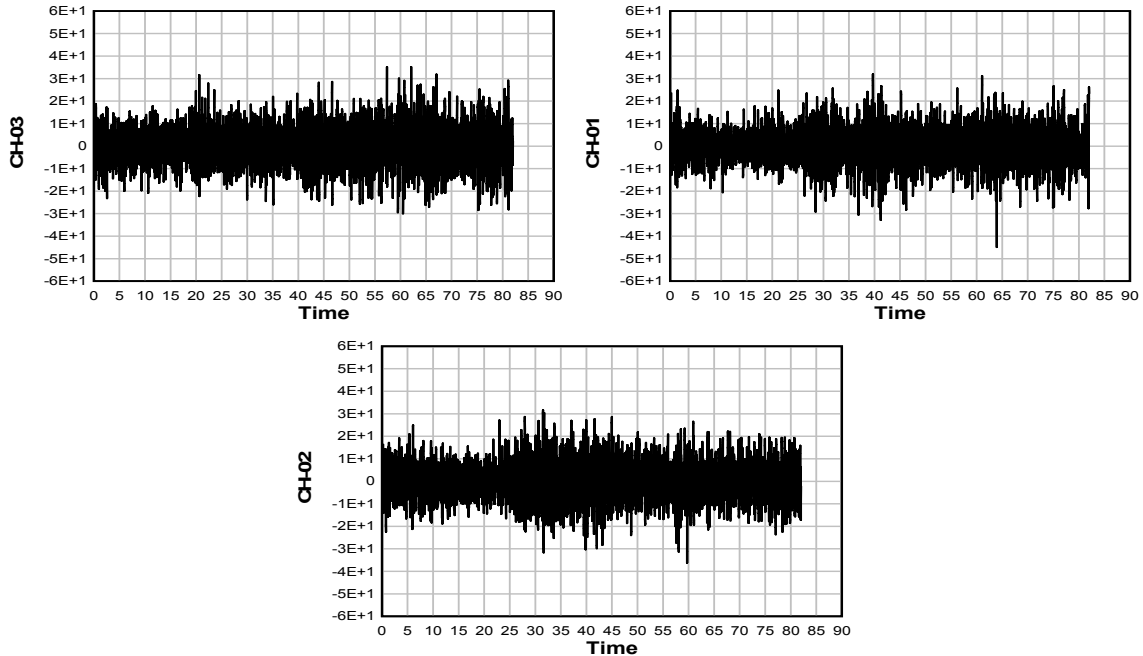


Figure 27 Microtremor Time History data at Hazi Camp

Figure 28 shows comparison of horizontal to vertical ratio (HVR) of MT and EQ data recorded at West side of Jamunabridge. HVR of EQ data is average of 2 different earthquakes and HVR of MT is average of 5 data. Comparison of earthquake and MT HVR shows similar overall trend. Predominant frequency of EQ is 2hz and MT reading shows predominant frequency around 1 hz.

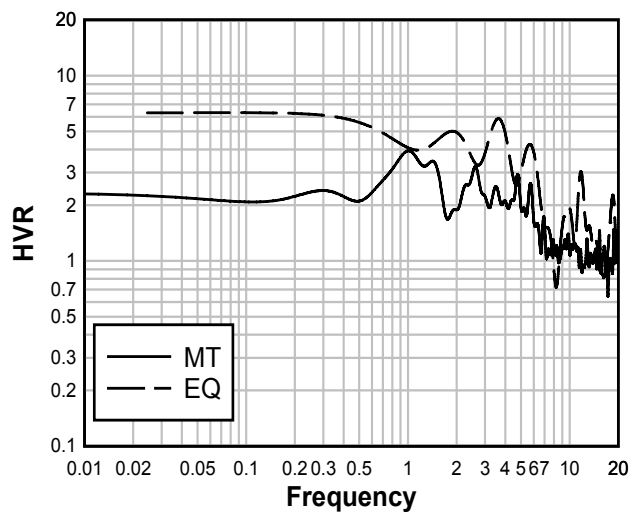


Figure 28 HVR vs Frequency plot of MT and EQ

7.7 NATORE LGED

Figure 29 shows Earthquake (EQ) data recorded by triaxial accelerometer on 14 February 2005. The figure shows that the ground acceleration in both e-w and n-s direction was equal with a value of 2.4 cm/s^2 . The duration of the shaking was 80 seconds. The peak displacement in u-d was 0.6 cm/s^2 .

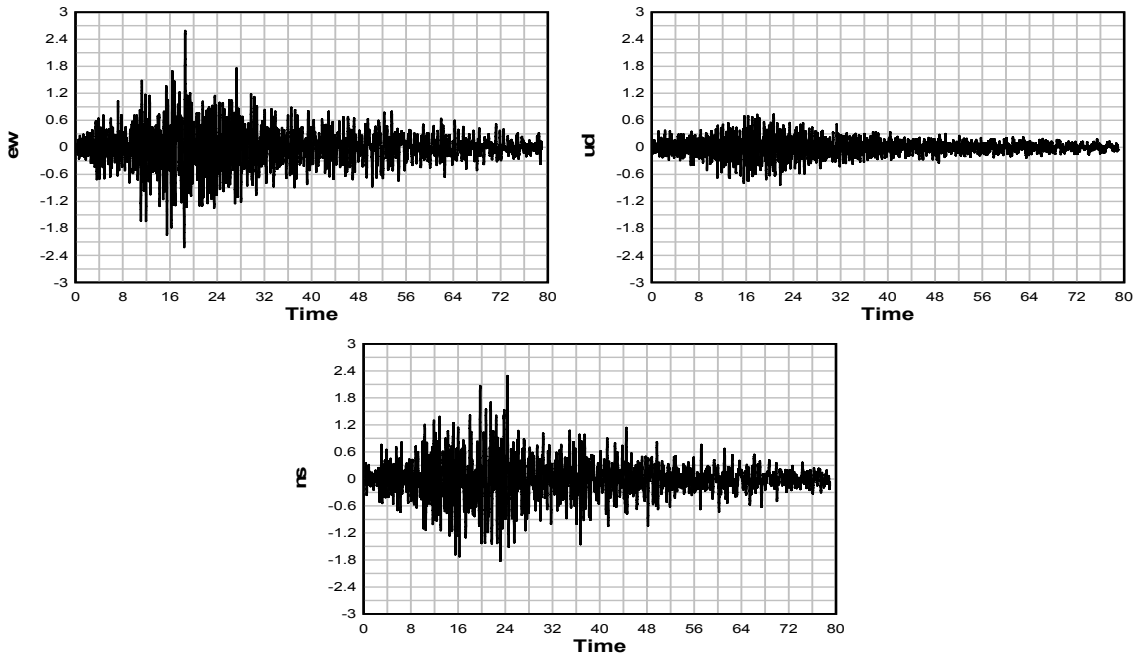


Figure 29 Earthquake Time History data at Natore (14-02-2006)

Figure 30 shows Earthquake (EQ) data recorded by triaxial accelerometer on 23 February 2006. Ground acceleration in n-s direction had a value of 1.6 cm/s^2 and in e-s direction the value is 1.6 cm/s^2 . The duration of the shaking was 45 seconds. The peak displacement in u-d was $.4 \text{ cm/s}^2$

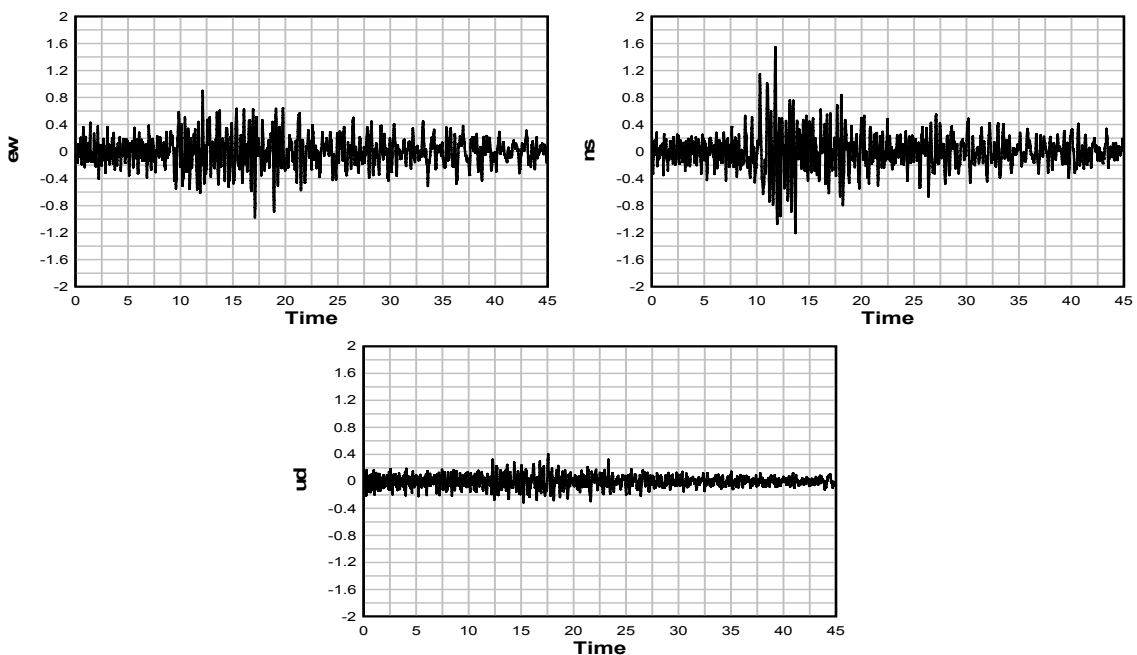


Figure 30 Earthquake Time History data at Natore (23-02-2006)

Figure 31 shows Earthquake (EQ) data recorded by triaxial accelerometer on 05 June 2006. Ground acceleration in both e-w and n-s direction was equal with a value of 1.6 cm/s^2 . Duration of the shaking was 45 seconds. The peak displacement in u-d was 1.2 cm/s^2 .

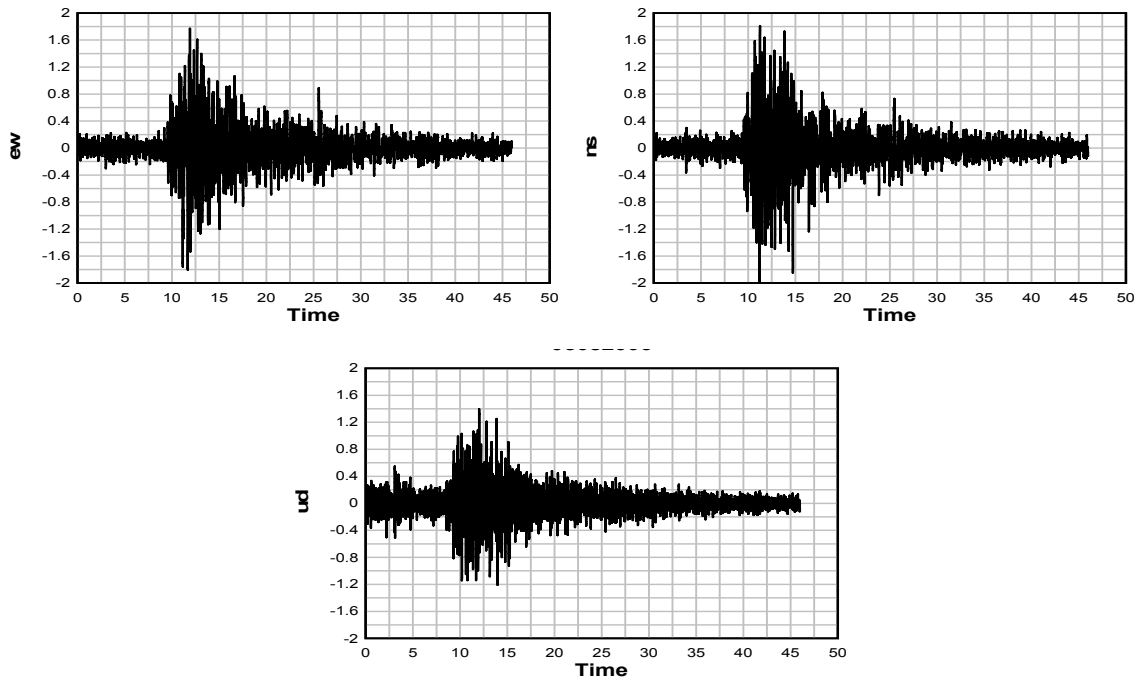


Figure 31 Earthquake Time History data at Natore (05-06-2006)

Figure 32 shows time history MT data of three segments with data length of 80 seconds at Natore LGED. FFT has been used and compared with actual earthquake data. It shows ground wave velocity recorded in three channels of MT. ch3 had recorded the highest ground velocity with a value of $30 \mu\text{m/s}$. Later FFT has been used and compared with actual earthquake data.

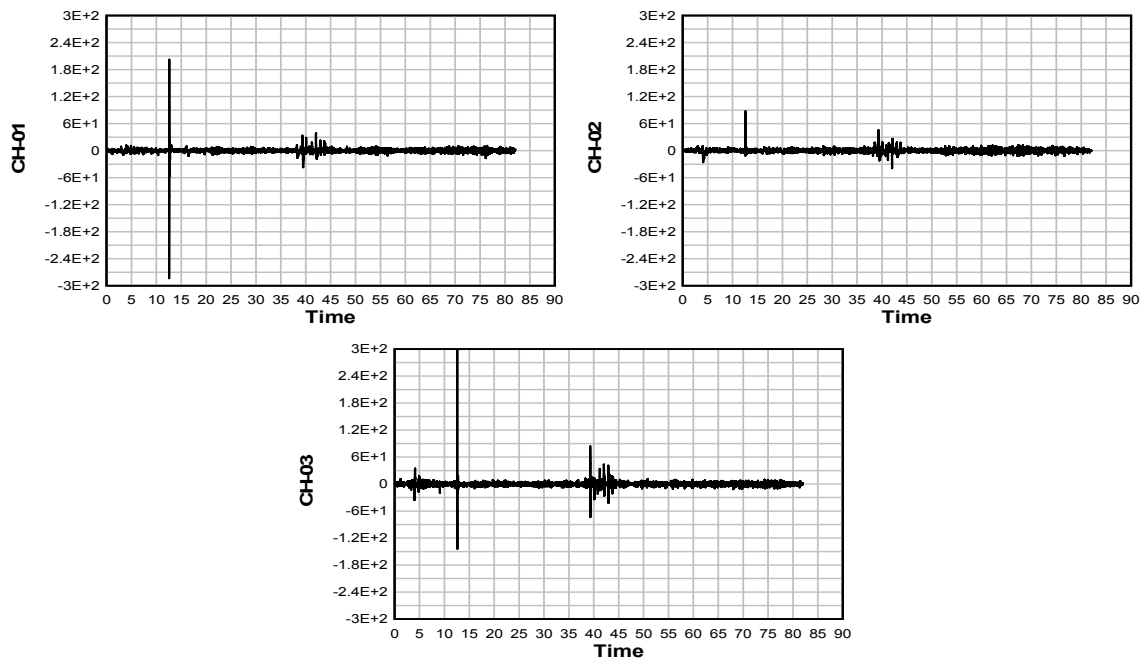


Figure 32 Microtremor Time History data at Natore LGED

Figure 33 shows comparison of horizontal to vertical ratio (HVR) of MT and EQ data recorded at West side of Jamunabridge. HVR of EQ data is average of 2 different earthquakes and HVR of MT is average of 5 data. Comparison of earthquake and MT HVR shows similar overall trend. Predominant frequency is 0.7hz both for EQ and MT.

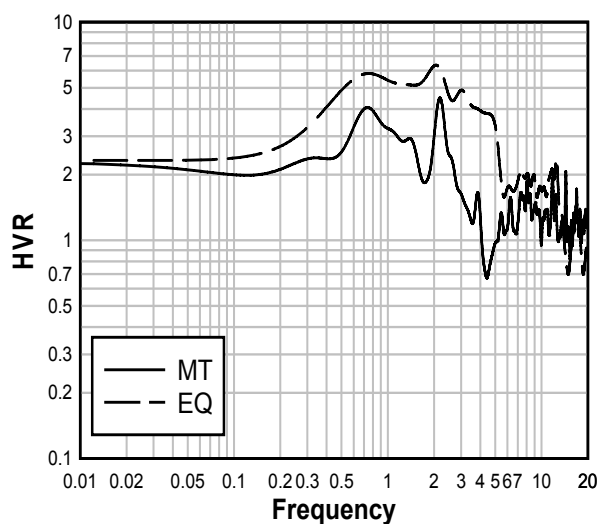


Figure 33 HVR vs Frequency plot of MT and EQ

8. CONCLUSIONS

Microtremor measurement has been carried out in 7 locations where Earthquake data has been recorded for the last 10 years. The overall predominant frequency for these sites range between 0.7 Hz and 1.5 Hz. On the other hand, the overall H/V ratio for these sites range between 1.9 and 5.1. Table 2 summarizes findings of this study. The table also shows average soil conditions of the sites based on V_{s30} . All the sites fall into NEHRP D-class, which is stiff soil ($180 \leq V_{s30} \leq 360$ m/s).

Table 2 Microtremor Test Location, Predominant Frequency, H/V Ratio and V_{s30} for the sites

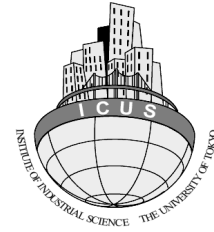
SL. No	Location	Predominant Frequency, F_g (Hz)	H/V Ratio, A_g	V_{s30} (m/s)
1	Bogra LGED	1.5	4.6	270
2	BUET Campus	1.2	1.9	250
3	East Side of Jamuna Bridge	0.9	3.7	280
4	West Side of Jamuna bridge	1.0	2.3	280
5	Police Staff College	1	5.1	280
6	Hazi Camp	1	3.9	220
7	Natore LGED	0.7	4.1	210

REFERENCES

- BUET (2014). Inception Report on Seismic Instrumentation Monitoring of Bangabandhu Bridge, report submitted to JMBA.
- Field, EH and Jacob, KH (1993). The theoretical response of sedimentary layers to ambient seismic noise, *Geophysical Research Letter* 20:2925–2928.
- Kanai, K and Tanaka, T (1954). Measurements of Micro-tremors 1. In: *Bulletin Earthquake Research Institute*, vol 32. Tokyo University, pp 199–210.
- Konno, K and Ohmachi, T (1998). Ground motion characteristics estimated from spectral ratio between horizontal and vertical components of microtremor. *Bull Seism Soc Am* 88(1):228–241.
- Lermo, J and Chavez-Garcia, FJ (1994). Are Microtremors Useful in Site Response Evaluation? *Bull Seism Soc Am* 84:1350–1364.
- Nogoshi, M. and Igarashi, T. (1971). On the Amplitude Characteristics of Microtremor (Part 2) (in Japanese with English abstract)", *Jour. Seism. Soc. Japan*, 24, 26-40.
- Nakamura Y (1989). A method for dynamic characteristics of subsurface using microtremors on the ground surface, *Quick Report of Railway Technical Research Institute*, vol 30, no 1, pp 25–33 (in Japanese).
- Ohmachi, T, Nakamura, Y and Toshinawa T (1991). Ground motion characteristics in the San Francisco Bay area detected by microtremor measurements. In: *Proceedings 2nd International Conference on Recent Advances in Geotech Earth Engand Soil Dyn*, Saint Louis, pp 1643–1648.



**BANGLADESH NETWORK
OFFICE FOR URBAN SAFETY**



PART-XI

MEASUREMENT OF SHEAR-WAVE VELOCITY AT DIFFERENT LOCATIONS OF DHAKA CITY USING SEISMIC REFRACTION



**BANGLADESH NETWORK OFFICE FOR URBAN
SAFETY (BNUS), BUET, DHAKA**

**Prepared By: Abul Khair
Mehedi Ahmed Ansary**

1. Introduction

Seismic refraction is a commonly used geophysical technique to determine depth-to bedrock, competence of bedrock, depth to the water table, or depth to other seismic velocity Boundaries (www.nga.com,20th, April, 2009). The seismic refraction method involves the analysis of the travel times of arrivals that travelled roughly parallel to the upper surface of a layer during their transmission through the subsurface. This method uses the seismic energy that returns to the surface of the earth after traveling along ray paths through the ground, to locate refractors that separate layers of different seismic velocities (Keller et al, 1981).

Seismic refraction methods provide an effective and efficient means to obtain general information about large volumes of the subsurface in the two dimensions of depth and horizontal (or slope) distance. Information provided by seismic refraction includes compression wave (p-wave) velocities within the investigated subsurface profile. Traditionally, these velocities are interpreted to be present within layers or horizons whose depths are also interpreted. Newer interpretation methods are making it possible to interpret velocity changes as gradients as well as discrete layers. Limitations due to subsurface geometries such as thin layers and lower velocity horizons underlying higher velocity horizons must be understood and, if necessary, accounted for. Cross correlation with other exploration methods such as drilling, test pits and geologic mapping, can greatly increase the value of refraction seismic data. In return, refraction seismic data can significantly enhance the value of other exploration data. Both basic field operations and basic interpretations of the resulting data can be performed by properly trained and experienced geotechnical or geological engineering personnel as well as by geophysical specialists.

Seismic refraction measurements are applicable in mapping subsurface conditions for various uses including geological, geotechnical, hydrological, environmental, mineral and archaeological investigations. The calculated seismic wave velocity is related to the type of rock, degree of weathering, and rippability assessment on the basis of seismic velocity and other geologic information.

2. Background of the study

The seismic refraction survey has application in a variety of geological exploration problems, where information on the depth and strength of subsurface materials is required. These surveys provide subsurface information over large areas at relatively low cost; locate critical areas for more detailed testing by drilling and can readily eliminate less favorable alternative sites. Seismic surveys can also

reduce the number of boreholes required to test a particular site and improve correlation between boreholes. The following are the areas, where this method can be used to obtain information

- a) Problems of engineering geology
 - i. Depth to bedrock (thickness of overburden and for weathered rock).
 - ii. Strength of the bedrock (looking for weak zones like fractures, shears and weathering and for faults etc) for foundation studies.
 - iii. Rippability/excavability studies for quarries and dynamic elasticity determination.
 - iv. Location of sink holes and other manmade objects
 - v. Correlation of geological units between boreholes
 - vi. Monitoring of landslides.
- b) Problems in alluvial prospecting
 - i. Indirect search for alluvial deposits.
 - ii. Location of ancient stream channels.
 - iii. Location of thick gravel beds
- c) Problems in hydrogeology
 - i. Thickness of aquifer over lying impermeable bedrock.
 - ii. Detection of water table, mainly in alluvial aquifers.
 - iii. Location of leakage zones.

2.1 Advantages / Disadvantages:

- Difficulty of interpretation in areas morphologically rough or with many underground pipes
- Open spaces is needed for cables and electrodes array, the electrodes must be planted into the ground (can also be applied in paved areas or asphalt, drilling holes).
- Good vertical and lateral stratigraphic resolution.
- For best accuracy, a calibration reference stratigraphy is needed.
- Very useful for discrimination of metal, clay / sand and aquifers

2.2 Literature review:

The refraction method consists of measuring (at known points along the surface of the ground) the travel times of compressional waves generated by an impulsive energy source. The energy source is usually a small explosive charge and the energy is detected, amplified, and recorded by special equipment designed for this purpose. The instant of the explosion, or "zero-time," is recorded on the record of arriving pulses. The raw data, therefore, consists of travel times and distances, and this time-distance information is then manipulated to convert it into the format of velocity variations with depth. The interpretation of this raw data will be developed as we go along. The process is

schematically illustrated in Fig. 1. All measurements are made at the surface of the ground, and the subsurface structure is inferred from interpretation methods based on the laws of energy propagation.

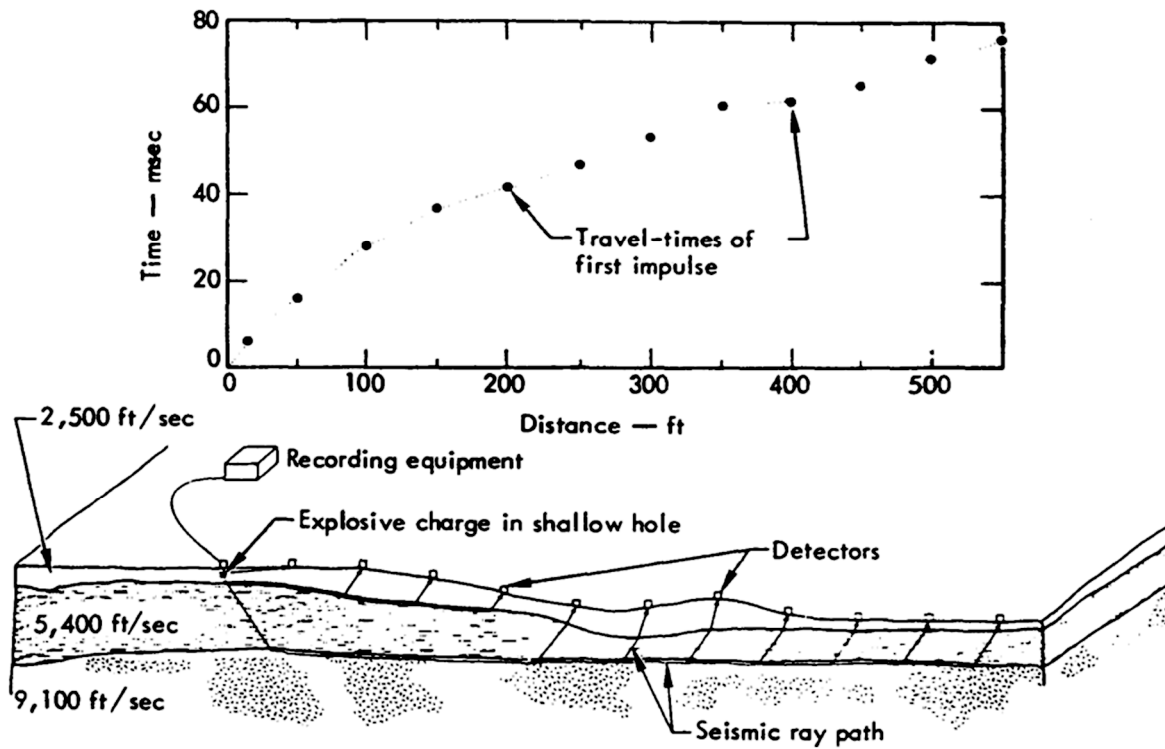


Fig 1: Schematic of seismic refraction survey

The fundamental law that describes the refraction of light rays is Snell's Law (see Fig. 2), and this, together with the phenomenon of “critical incidence,” is the physical foundation of seismic refraction surveys.

A small explosive charge is detonated in a shallow hole at A and the energy is detected by a set of detectors laid out in a straight line along the surface. The arrival times of the impulses are plotted against the corresponding shot-to-detector distances as shown in Fig. 3. The first few arrival times are those of direct arrivals through the first layer, and the slope of the line through these points, $\Delta T/\Delta X$, is simply the reciprocal of the velocity of that layer; i.e., $1/V_1$. At some distance from the shot, a distance called the critical distance, it takes less time for the energy to travel down to the top of the second layer, refract along the interface at the higher velocity V_2 and travel back up to the surface, than it does for the energy to travel directly through the top layer.

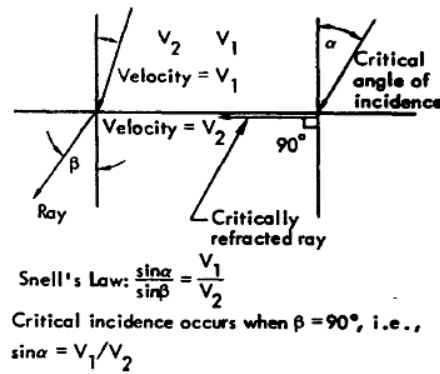


Fig 2: Snell's law and refraction of ray transmitted across boundary between two media with different velocities.

The energy that arrives at the detectors beyond the critical distance will plot along a line with a slope of $1/V_2$. The line through these refracted arrivals will not pass through the origin, but rather will project back to the time axis to intersect it at a time called the intercept time. Because both the intercept time and the critical distance are directly dependent upon the velocities of the two materials and the thickness of the top layer, they can be used to determine the depth to the top of the second layer.

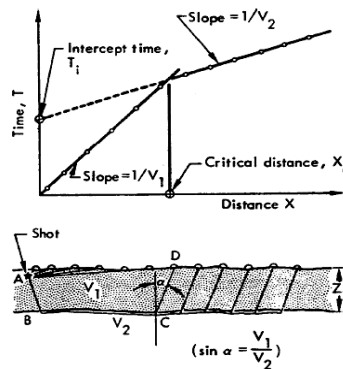


Fig 3: Simple two-layer case with plane, parallel boundaries and corresponding time-distance curve. The rock types can be found to know the seismic velocity transmitted to the soil. The verities of seismic velocity of different layers indicated different types of soil. There is an approximate range to classify rocks depending on seismic velocities (www.Geo2X.com).

Table 1: Approximate seismic velocities for rocks

Rock type	V _p (km/sec)
Unconsolidated sediment	
Clay	1.0-2.5
Sand, dry	0.2-1.0
Sand, saturated	1.5-2.0
Sedimentary Rocks	
anhydrite	6.0
Chalk	2.1-4.5
Coal	1.7-3.4
Dolomite	4.0-7.0
limestone	3.9-6.2
Shale	2.0-5.5
Salt	4.6
sandstone	2.0-5.0
Igneous and metamorphic rocks	
Basalt	5.3-6.5
Granite	4.7-6.0
gabbro	6.5-7.0
Slate	3.5-4.4
Ultramafic rocks	7.5-8.5
Others	
Air	0.3
Natural gas	0.43
Ice	3.4
Water	1.4-1.5
oil	1.3-1.4

In the following articles different methods of depth calculation are described.

2.2.1 Intercept times

Referring to Fig. 3, let us compute the arrival time of the refracted impulse at a detector. Consider the travel path ABCD

$$AB = CD = \frac{Z_1}{\cos \alpha}$$

Where Z_1 is the thickness of the top layer, and a is the critical angle of incidence. The travel time is therefore given by

$$\begin{aligned}
 T &= \frac{AB + CD}{V_1 \cos \alpha} + \frac{BC}{V_2} \\
 &= \frac{2Z_1}{V_1 \cos \alpha} + \frac{X V_2 \tan \alpha}{V_2} \\
 &= 2Z_1 \left(\frac{1}{V_1 \cos \alpha} - \frac{\sin \alpha}{V_2 \cos \alpha} \right) + \frac{X}{V_2} \\
 &= 2Z_1 \left(\frac{V_2 - V_1 \sin \alpha}{V_1 V_2 \cos \alpha} \right) + \frac{X}{V_2}
 \end{aligned}$$

Snell's law defines the critical angle of incidence α , by:

$$\sin \alpha = \frac{V_1}{V_2} \tag{1}$$

and selectively substituting Eq. (1) into the previous equation:

$$\begin{aligned}
 T &= 2Z_1 V_1 \left(\frac{1}{V_1 V_2 \cos \alpha} - \frac{\sin \alpha}{V_1 V_2 \sin \alpha \cos \alpha} \right) + \frac{X}{V_2} \\
 T &= 2Z_1 V_1 \left(\frac{1 - \sin^2 \alpha}{V_1 V_2 \sin \alpha \cos \alpha} \right) + \frac{X}{V_2} \\
 T &= \frac{\cos^2 \alpha}{V_2 \sin \alpha \cos \alpha} + \frac{X}{V_2}
 \end{aligned}$$

And substituting V_1 for $V_2 \sin \alpha$

$$T = \frac{2Z_1 \cos \alpha}{V_1} + \frac{X}{V_2}$$

If we now let $X = 0$, then T becomes the intercept time, T_i , and we can rewrite the last expression as:

i.e.,

$$\begin{aligned}
 Z_1 &= \frac{T_i V_1}{2 \cos \alpha} \\
 Z_1 &= \frac{T_i V_1}{2 \cos(\sin^{-1} \frac{V_1}{V_2})}
 \end{aligned}
 \tag{2}$$

For the situation we have assumed in Fig. 3, everything on the right-hand side of Eq.(2) can be determined from the time distance plot; therefore, the depth to the second layer can be computed. A very important point to bring out at this time is that all depths determined in refraction surveys are measured normal to the boundary between layers and are not necessarily vertical depths beneath the ground surface. The intercept-time analysis can be extended to the case of multiple layers; however, only the resulting formulas will be given here because their derivations are redundant and may be found in a number of references. Fig. 4 schematically illustrates the multiple layer case and corresponding time-distance plots. The intercept times and layer thicknesses have been identified by a subscript corresponding to the number of the layer:

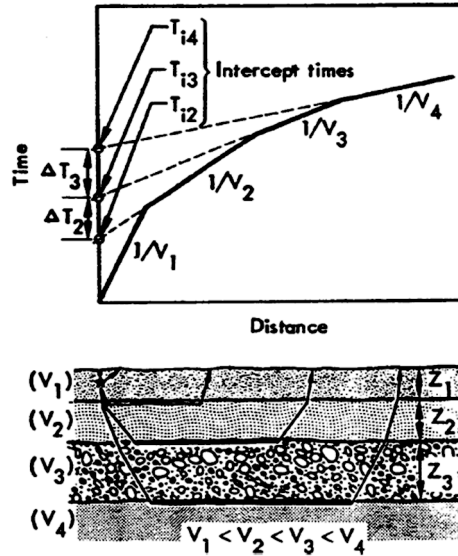


Fig 4: Schematic of multiple-layer case and corresponding time-distance curve.

$$Z_1 = \frac{(T_{i1})V_1}{2 \cos(\sin^{-1} \frac{V_1}{V_2})} + \frac{1}{2} \text{shot depth} \tag{3}$$

$$Z_2 = \frac{\left[\begin{matrix} \cos(\sin^{-1} \frac{V_1}{V_3}) \\ T_{i3} - T_{i2} \frac{\cos(\sin^{-1} \frac{V_1}{V_2})}{\cos(\sin^{-1} \frac{V_1}{V_2})} \end{matrix} \right] V_2}{2 \cos(\sin^{-1} \frac{V_2}{V_3})} \tag{4}$$

$$Z_3 = \frac{\left[\begin{matrix} \cos(\sin^{-1} \frac{V_2}{V_4}) & 2Z_2 \cos(\sin^{-1} \frac{V_2}{V_4}) \\ T_{i4} - T_{i2} \frac{\cos(\sin^{-1} \frac{V_1}{V_2})}{\cos(\sin^{-1} \frac{V_1}{V_2})} - \frac{2Z_2 \cos(\sin^{-1} \frac{V_2}{V_4})}{V_2} \end{matrix} \right] V_3}{2 \cos(\sin^{-1} \frac{V_3}{V_4})} \tag{5}$$

If the velocity contrasts between layers are high enough; say 2 to 1, and only approximate depths are required, then the following formulas can be used:

$$Z_2 = \frac{(\Delta T_2)V_2}{2 \cos(\sin^{-1} \frac{V_2}{V_3})} \tag{6}$$

$$Z_3 = \frac{(\Delta T_3)V_3}{2 \cos(\sin^{-1} \frac{V_3}{V_4})} \tag{7}$$

Where ΔT_2 and ΔT_3 ; are as indicated in Fig. 4. Equations (6) and (7) will give thicknesses that are greater than actual, and it is suggested that thicknesses initially be computed both ways to learn whether the error is significant in a particular situation.

2.2.2 Critical Distance

The critical-distance method for determining depth will receive only brief attention here because it is analogous to the intercept-time method, and offers no advantages significant enough to warrant further detail. Its primary application is to compute the depth of the first layer and to estimate the length of the seismic line required for a particular exploration task. The critical distance is the distance from the shot point to the point at which the refracted energy arrives at the same time as the energy traveling directly through the top layer. The critical distance (X_c) is illustrated in Fig. 3; it is the breakpoint in the graph of arrival times.

By an approach similar to the one used in deriving the intercept-time formulas, it can be shown that the depth of the first layer is given by:

$$Z_1 = \frac{X_c}{2} \frac{(1 - \frac{V_1}{V_2})}{\cos(\sin^{-1} \frac{V_1}{V_2})} \quad (8)$$

Where X_c is the critical distance.

Equation (8) can be used to construct a graph showing the length of a seismic line (relative to the depth of the first layer) required to detect refractions from the underlying layer, as a function of velocity ratios. Figure 5 is a graph of Eq. (8), which can be of use in planning a seismic survey if velocity ratios are assumed. The graph also assists in giving a sense of perspective to the effect of velocity contrasts. For example, assume that there is about 15 feet of overburden with a velocity of 2,500 feet/sec, and that it is underlain by a shale with a velocity of about 5,500 feet/sec. How long should the seismic line be to insure adequate coverage for mapping the overburden thickness? The velocity ratio, V_2/V_1 , is 2.2 so that X_c/Z_1 is approximately 3.25, which means that the critical distance will be about 50 feet. The seismic spread should be at least three times this distance; therefore, a seismic line 150 to 200 feet long would be satisfactory.

2.2.3 Dipping Layer

If the boundaries between interface are not parallel (that is, if they are dipping interfaces), the t-x curve will give only apparent velocities for the refracting layers usage of which can give erroneous depths. Reverse shooting field procedure can provide complete protection against above said errors. Reverse shooting means firing a shot at both ends of the seismic line so that arrival times at each detector are measured from both directions. The case of a dipping boundary and its effect on travel-time plots is as shown in Fig. 4. The condition of reciprocity provides a valuable constraint. The condition of reciprocity states that the total travel time from A to D must be equal to the total travel

time from D to A. The gradients of the travel-time curves of reflected arrivals along the forward and reverse profile lines yield the down dip (VJ and up dip (VJ apparent velocity respectively (see Fig, 4). From the forward direction

$$V_{2d} = \frac{V_1}{\sin(i_{12} + \theta)}$$

And from the reverse direction

$$V_{2u} = \frac{V_1}{\sin(i_{12} - \theta)}$$

Solving for i_{12} and θ

$$i_{12} = \frac{1}{2} \left[\sin^{-1} \left(\frac{V_1}{V_{2d}} \right) + \left[\sin^{-1} \left(\frac{V_1}{V_{2u}} \right) \right] \right]$$

$$\theta = \frac{1}{2} \left[\sin^{-1} \left(\frac{V_1}{V_{2d}} \right) - \left[\sin^{-1} \left(\frac{V_1}{V_{2u}} \right) \right] \right]$$

The perpendicular distances Z and Z' to the interface under the two ends of the profile are obtained from the intercept times t_1 and t_1' the travel-time curves obtained in the forward and reverse direction.

$$Z = \frac{V_1 t_1}{2 \cos i_{12}}$$

By using the computed refractor dip e , the perpendicular depths Z and Z' can be converted into vertical depths h and h' using

$$h = \frac{Z}{\cos \theta}$$

$$h' = \frac{Z'}{\cos \theta}$$

2.3 Methodology

Measurement of subsurface conditions by the seismic refraction method requires a seismic energy source, trigger cable, geophones, geophone cable, and a seismograph. The geophones and the seismic source must be placed in firm contact with the soil or rock. The geophones are usually located in a line, sometimes referred to as a geophone spread. The seismic sources may be a sledge hammer, a mechanical device that strikes the ground, or some other type of impulse source. Explosives are used for deeper refractors or special conditions that require greater energy. Geophones convert the ground vibrations into an electrical signal. This electrical signal is recorded and processed by the seismograph. The travel time of the seismic wave (from the source to geophone) is determined from the seismic wave form.

2.3.1 Study area selection

Over the past 45 years, Dhaka city has experienced a rapid growth of urban population and it will continue in the future due to several unavoidable reasons. Hence, most of the areas of Dhaka city have already been occupied. As a result, different new areas are being reclaimed inside and near Dhaka city by both government and private agencies. General practice for reclaiming such areas is to fill low lands (ditches, lakes etc.). In most cases, the practice for developing new areas is just to fill low land by dredge fill materials. In most cases, the dredged material is almost silty sand with high fines content. The presence of fines in hydraulic fill means greater compressibility and greater difficulty in compaction of the fill. Fines also reduce permeability and hence the rate of drainage is slow. Therefore consolidation rate is also slow. Since Dhaka city exists in seismic Zone II of Bangladesh. This silty sand layer may liquefy if an earthquake of sufficient magnitude occurs in future. As well as, it may cause geotechnical problems.

It is clear that this very soft clay layer, in reclaimed areas demand special attention for designing foundation system on or through it. So, it is felt necessary to carry out research to know the characteristics of the soft organic clay layer of such reclaimed areas.

The different location of Dhaka city is selected as the study area. The location are selected upon some criteria such as free open space, less noisy area, dominating soil characteristics of that region, land use characteristics etc. The table below shows the location of the study area.

Table 2: List of the study points of Dhaka city

Sl. no	Date	Name of the point of study area	Location		City
			Latitude	Longitude	
01	14/11/2014	Garden in front of Civil Building at BUET	23° 43' 19" N	90° 23' 48" E	Dhaka
02	13/11/2014	Vatara, Gulshan	23° 47' 39" N	90° 26' 40" E	Dhaka
03	14/11/2014	Bashaundhara river view, Keranigong	23° 39' 45" N	90° 26' 25" E	Dhaka
04	14/11/2014	New Jail, Keranigong	23° 39' 07" N	90° 23' 03" E	Dhaka



Fig 5: Location of study points within Dhaka city

2.3.2 Data collection and Analysis

Planning and design of a seismic refraction survey should be done with due consideration of the objectives of the survey and the characteristics of the site. These factors determine the survey, design, the equipment to be used, the level of effort, the interpretation method selected, and budget necessary to achieve the desired results. Important considerations include site geology, depth of investigation, topography and access. The presence of noise-generating activities and operational constraints should also be considered. It is a good practice to obtain as much relevant information about the site, prior to planning a survey and mobilization to the site.

The first important consideration in planning a field refraction survey is the spacing between the geophones. The spacing will depend on the desired depth of exploration. Selection of detector spacing is also determined by the required detail of the refractor geometry. This is because the sampling interval of interpretation points on the refractor is approximately equal to the detector

spacing on the surface. Thus, the horizontal resolution of the method for subsurface targets is equal to the detector spacing. Once the spacing between geophones is decided, the “spread” length that is covered by one shot is fixed by the number of channels of the seismic equipment being deployed. Usually, in detailed engineering surveys, a 5m interval between geophones is appropriate. But due to lack of energy 3m interval between geophone is selected to found better result. If the profile length required to get the desired subsurface information is more than one “spread” length, the time-distance information should be collected by overlapping as many spreads as required. In doing so, at least two geophones should be kept overlapping between successive spreads to tie the timings from different shots to make profile continuous. Usually, five to seven shots are required for each spread. The data of the different locations were collected using different combination of seismic impulse source and different spacing of geophones. Some specific softwares based on conventional method were needed to process seismic refraction. WinSism is widely used to analyze the seismic refraction data after collecting field data. The details of data collection and results after processing data are described below:

➤ **Seismic refraction result analysis for BUET ground**

The geophone spread and impulse source is shown in Fig. 6 and Fig. 7 respectively during seismic refraction test at BUET. Five shot points were selected during this test named middle shot, 1st offset shot, 1st end shot, last end shots and last offset shot. The position of two offset shots 23m away from 1st and last geophone, which is half of the total spread length 46m as shown in fig 8. Seven strikes for each offset shot and 5 strikes for rest three shots were taken by tripod hammer. As the noise provides bad data, the strikes were taken when the circumstances seems to be quiet.



Fig 6: Spread of geophones during refraction test at BUET



Fig 7: Using 140lb hammer as impulse source



Fig 8: Layout of shots position during seismic refraction test at BUET

The soil profile of the seismic refraction test is shown in Fig. 9. It shows that the investigation depth of soil profile is about 30m. The seismic velocity ranges is about to 150m/s to 350m/s which range indicates the sub soil is dry sand according to Table 1.

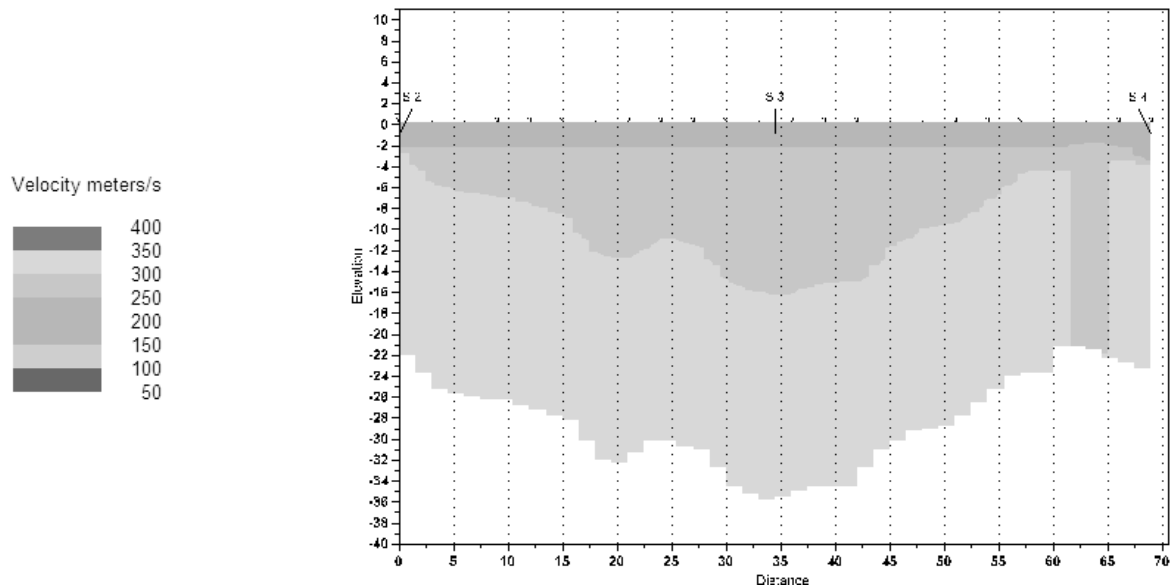


Fig 9: Soil profile at BUET playground using seismic refraction

➤ **Seismic refraction result analysis for Vatara**

The geophone spread and impulse source is shown in Fig. 10 and Fig. 11 respectively during seismic refraction test at Vatara. Five shot points were selected during this test named middle shot, 1st offset shot, 1st end shot, last end shots and last offset shot. The position of two offset shots is 30m away from 1st and last geophone as shown in Fig. 12. Seven strikes for each offset shot and 5 strikes for rest three shots were taken by tripod hammer. As the noise provides bad data, the strikes were taken when the circumstances seems to be quiet.



Fig 10: Spread of geophones during Refraction test at Vatara



Fig 11: Using 140lb hammer as impulse source

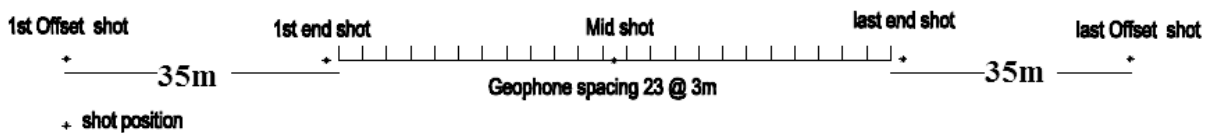


Fig 12: Layout of shots position during seismic refraction test Vatara

Recently this place has filled up by filling materials about 3m in depth. As the filling materials is not compacted properly the energy of impulse source were consume by lose filling. Hence the result may vary from actual one due to lack of energy through the subsoil .The soil profile of the seismic refraction test is shown in Fig. 13. It shows that the investigation depth of soil profile is about 30m. The seismic velocity range is about to 150m/s to 290m/s which range indicates the sub soil is dry sand according to Table 1.

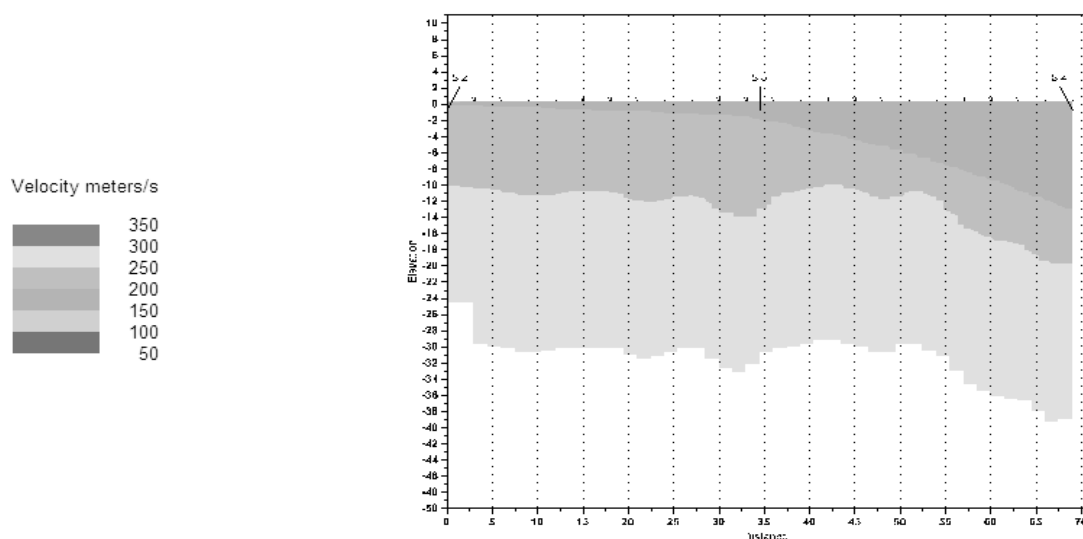


Fig 13: Soil profile at Vatara using seismic refraction

➤ **Seismic refraction result analysis for Bashundhara River view:**

The geophone spread and seismic data collection is shown in Fig. 14 and Fig. 15 respectively during seismic refraction test at Bashundhara river view. Five shot points were selected during this test named middle shot, 1st offset shot, 1st end shot, last end shots and last offset shot. The position of two offset shots 30m away from 1st and last geophone, which is half of the total spread length 69m as shown in Fig. 16. Seven strikes for each offset shot and 5 strikes for rest three shots were taken by tripod hammer. As the noise provides bad data, the strikes were taken when the circumstances seems to be quiet.



Fig 14: Spread of geophones during refraction test at Vatara



Fig 15: Seismic data collection equipment

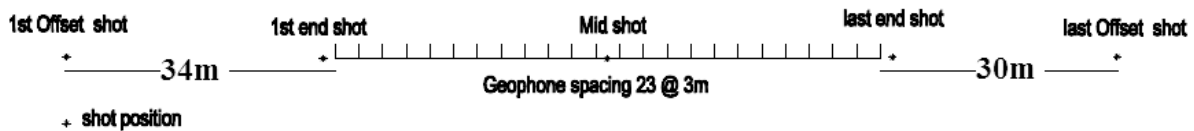


Fig 16: Layout of shots position during seismic refraction test at Bashundhara river view

The soil profile of the seismic refraction test is shown in Fig. 17. It shows that the investigation depth of soil profile is about 35m. The velocity range is about to 50m/s to 250m/s which range indicates the sub soil is dry sand.

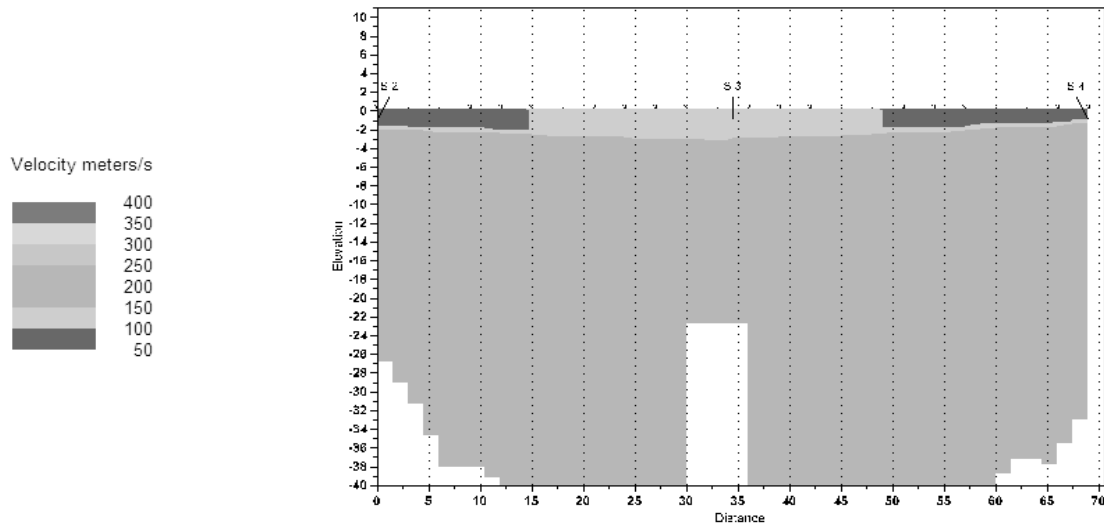


Fig 17: Soil profile of Bashundhara river view

➤ **Seismic refraction result analysis at Outside of New jail**

The geophone spread and impulse source is shown in Fig. 18 and Fig. 19 respectively during seismic refraction test at New Jail. Five shot points were selected during this test named middle shot, 1st offset shot, 1st end shot, last end shots and last offset shot. The position of two offset shots 30m away from 1st and last geophone, which is half of the total spread length 69m as shown in Fig. 20. Seven strikes for each offset shot and 5 strikes for rest three shots were taken by tripod hammer. As the noise provides bad data, the strikes were taken when the circumstances seems to be quiet.



Fig 18: Spread of geophones during refraction test at New Jail



Fig 19: Using 140lb hammer as impulse source

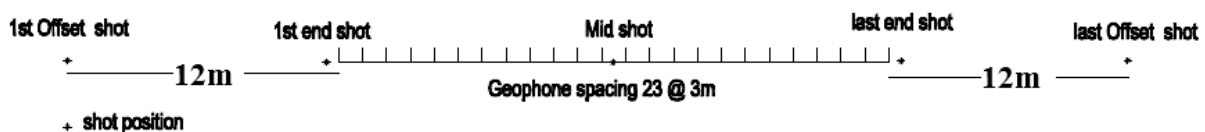


Fig 20: Layout of shots position during seismic refraction test at New Jail

The soil profile of the seismic refraction test is shown in Fig 21. It shows that the investigation depth of soil profile is about 18m. The velocity range is about to 150m/s to 280m/s which range indicates the sub soil is dry sand.

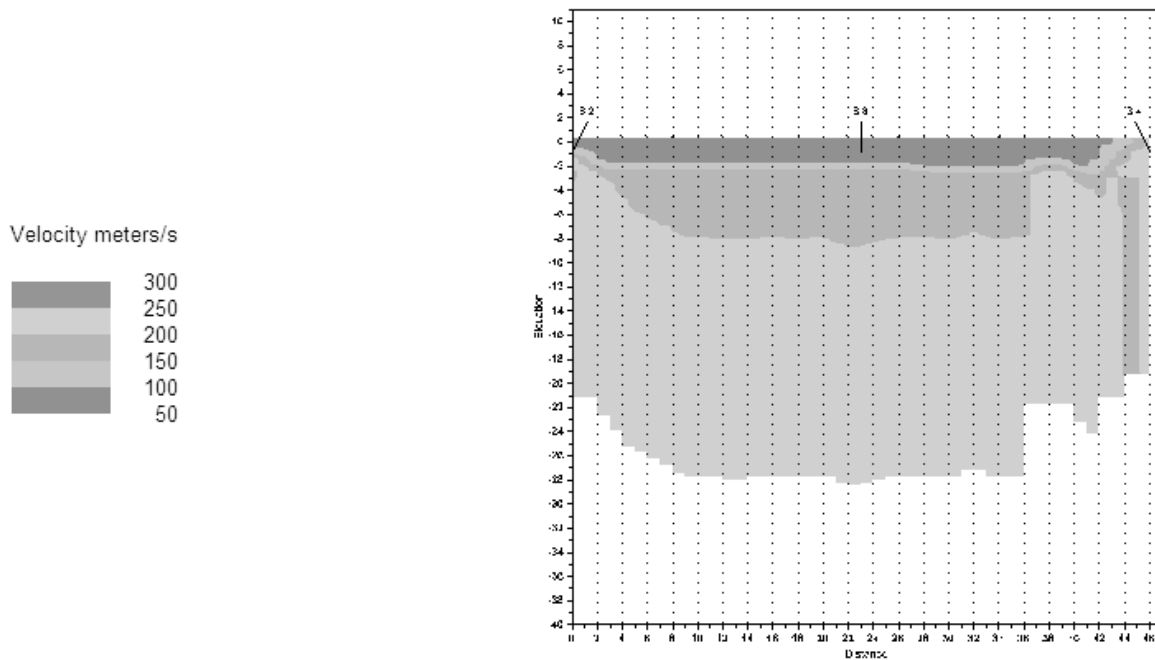


Fig 21: Soil profile beside new jail using seismic refraction

2.3.3 Limitations

A hidden layer, or blind layer, is one that is undetectable by refraction surveying. In practice, there are two different types of hidden layer problem. A layer may simply not give rise to first arrivals, that is, rays traveling to deeper levels may arrive before those critically refracted at the top of the layer in question(see Fig. 22). This may result from the thickness of the layer or from the closeness of its velocity to that of the overlying layer. In such a case, a method of survey involving recognition of only first arrivals will fail to detect the layer. The problem may be overcome by firing a shot in a deep hole so that arrivals from the intermediate layer are recorded at the surface. A more insidious type of hidden layer problem is associated with a low velocity layer, as illustrated in Fig. 23. Rays cannot be critically refracted at the top of such a layer and the layer will, therefore, not give rise to head waves. Hence, a low velocity layer cannot be detected by refraction surveying although the top of the low velocity layer gives rise to wide angle reflections that may be detected during a refraction survey. In the presence of a low velocity layer, the interpretation of travel-time curves leads to an overestimation of the depth to underlying interfaces. Low velocity layers are a hazard in all types of refraction seismology. On a small scale, a peat layer in muds and sands above bedrock may escape detection, leading to a false estimation of foundation conditions and rock depths beneath a construction site.

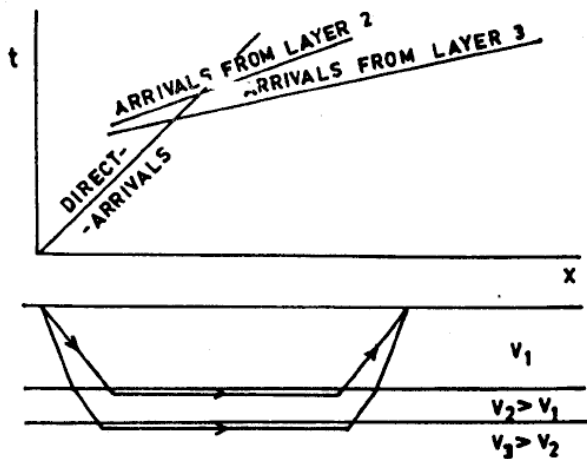


Fig 22: Hidden layer problem in seismic refraction

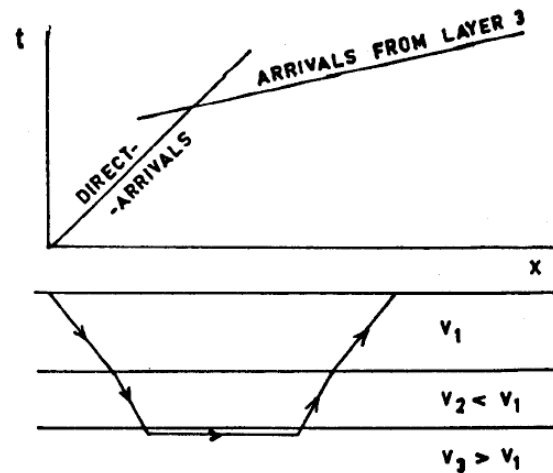


Fig 23: Blind zone problem in seismic refraction

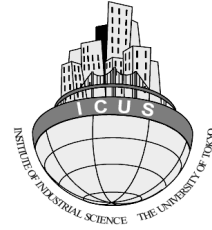
Due to lack of available impulse source the seismic refraction test is difficult in maximum places. To buy and use explosive is difficult in Bangladesh. Hence seismic refraction test is not feasible to investigate subsoil characteristics.

References

1. Alhassan, D. U., Dangana, L.M., Salako, K.A., Jonah, S.A. and Ofor, **seismic refraction investigation of the subsurface structure at the southern part of niger state college of education**, Bayero Journal of Pure and Applied Sciences, 3(2): 56 – 61
2. **Geological exploration by geophysical method (seismic refraction) —code of practice, burau of indian standard, is 15681:2006** , pp.8-15
3. Keller G.R, Sinno Y.A, and Sbar M.L (1981). **Seismic refraction in West and central Arizona**, journal of Geophysical Research, New York, U.S.A, Vol. 86 ,No. 36, PP5023
4. Redpath B. B., A book of “**Seismic refraction exploration for Engineering site investigations**” Explosive Excavation Research Laboratory Livermore, California, May 1973
5. www.geo2X.com

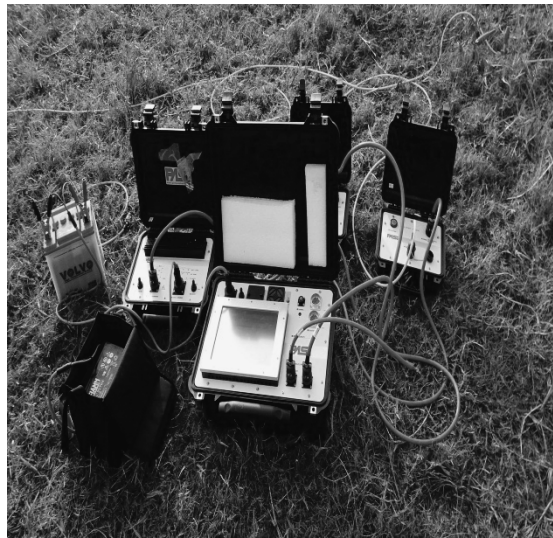


**BANGLADESH NETWORK
OFFICE FOR URBAN SAFETY**



PART-XII

MEASUREMENT OF ELECTRICAL RESISTIVITY AT DIFFERENT LOCATIONS OF DHAKA CITY



**BANGLADESH NETWORK OFFICE FOR URBAN
SAFETY (BNUS), BUET, DHAKA**

**Prepared By: B.S. Pushpendue Biswas
Mehedi Ahmed Ansary**

1. Introduction:

Ground Resistivity survey methods have been widely used in order to solve engineering, archeology, environmental and geological problems in the last decades. Subsurface resistivity distributions are measured by applying electrical current into the ground by using two current electrodes. The potential differences caused by the flow of current between any two points in linear line with the current electrodes are then measured by a pair of potential electrodes. From the measured voltage (V) and current (I) values, the resistance at the specified point in the subsurface can be determined. In homogeneous ground, penetration depth is directly proportional to electrodes spacing, and changing the electrode's separation gives information on sub surface's stratification [1-2].

For 2D resistivity imaging, it is important to have a large set of data recorded along a survey line to effectively map the complex resistivity distribution of subsurface structure. The most practical way to acquire such large amount of data is by using automated multi-electrode data acquisition system. In the interpretation of ground resistivity survey, it is important to differentiate between apparent resistivity and true resistivity. Apparent resistivity can be defined as the volumetric average of a heterogeneous half-space, except that the averaging is not done arithmetically but by a complex weighing function dependent on electrode's configurations [3].

In resistivity survey, true resistivity can only be measured in ideal condition where the ground is homogenous, which is almost never is the case. Advancement in computer forward modeling software (e.g. Res2DINV, Resix) have made it possible to calculate numerous amount of data obtained from 2D resistivity survey in a short amount of time, and minimized the different between true and apparent resistivity for subsurface earth material by subdividing the subsurface into small rectangular cells where each cell has resistivity value close to the true resistivity of subsurface material. The principle is in determining the cell resistivity that provides a model response that fits well with the measured data [4].

However, this assumption is only true theoretically. Uncertainty still remains in the final obtained image even if the inversion is a quasi-automatic process. In practice, there are a lot of factors that can affect resistivity pseudo section imaging. Apparent resistivity is measured instead of trueresistivity due to unknown near surface strata with different resistivity. This affects the conduction of current through earth material and thus affects the resistivity measurement. Most of field resistivity surveys conducted by geophysicist are not always validated by laboratory measurement. The difficulty in obtaining the core sample, where the drillingworks should be preceded by resistivity survey has

made it difficult for geophysicist to analyze samples in laboratory [5]. Figure 1 shows the points (red star marked) of the study area of Dhaka city.



Figure 1: Study Area

2. Background of the study

In the seismic and GPR methods, signals from the source pass through the medium and return to a sensor. They are more ‘direct’ methods, changes in the travel time and characteristics of the signal due to passage through the anomaly give information about it. The electrical method is an ‘indirect’ method; it directly measures the current that passes through the anomaly but it measure distortions in the electrical potential on the ground surface due to changes in the current flow causes by the anomaly. This sometimes makes the interpretation of electrical data more difficult.

Fields of application:

- **Geology:** lithological discontinuities and voids, tectonic lines localization, deposits of gravel and sand, mining plans etc.
- **Hydrogeology:** aquifers surveys, interface freshwater/salt detection etc.
- **Environmental studies:** presence of pollutants in the soil, filling areas, leakage from landfills, trace contaminants in leachate and groundwater
- **Archaeology:** surveys of large buried structures.

Advantages / Disadvantages:

- Difficulty of interpretation in areas morphologically rough or with many underground pipes.
- Open spaces is needed for cables and electrodes array, the electrodes must be planted into the ground (can also be applied in paved areas or asphalt, drilling holes).
- Good vertical and lateral stratigraphic resolution.
- For best accuracy, a calibration reference stratigraphy is needed.
- Very useful for discrimination of metal, clay / sand and aquifers

The electrical resistivity method allows the calculation of the resistivity present in soil. The calculation of resistivity makes it possible to obtain information about the subsoil nature and structure. Applying a potential difference (ΔV) to the two poles of a conductor, in it will pass a current of intensity (I) which is related to the potential difference from Ohm's law:

$$R = \Delta V / I$$

Where,

R = electrical resistance that depends on the nature and geometric characteristics of the conductor.

ΔV = difference of potential measured between M and N [V]

I = current injected into soil [A]

For each acquisition performed in the selected spreading, the following formula is generally applied:

$$\rho = \left(\frac{\Delta V}{I} \right) \cdot K$$

Where,

ρ = apparent resistivity [Ω m]

ΔV = difference of potential measured between M and N [V]

I = current injected into soil [A]

K = geometric coefficient related to the sounding being used

ρ (*spell it 'rho'*) is known as resistivity, is measured in $\Omega \cdot m$ and provides useful elements for identifying the nature of the rock types investigated. The value of this parameter depends on the

mineralogical composition of soils, the presence of fluid saturation, temperature, porosity and degree of cementation.

➤ **Electrical properties of sediments and sedimentary rocks**

The resistivity of sedimentary rocks and sediments/soils depend mainly on the porosity, fluid content and clay content. Most resistivity values range from 10 to 1000 ohm*m. Resistivity decreases with increasing clay content. Most clay has resistivity of 1 to 10 ohm*m. For rocks and sediments with low clay content, the electrical conduction is mainly through the fluids filling the pores of the rock. The relationship between resistivity and porosity is given by Archie's Law:

$$\rho_r = a \rho_w \phi^{-m}$$

($a \approx 1$, $m \approx 2$, ρ_r = rock resistivity, ρ_w = fluid resistivity, ϕ = fraction of the rock filled with fluid). The resistivity of ground water varies from 10 to 100 Ω *m, depending on the concentration of dissolved salts. The resistivity of sea water is about 0.2 Ω *m due to the relatively high salt content.

➤ **Electrical properties of metamorphic and igneous rocks**

Igneous and metamorphic rocks typically have high resistivity values of over 1000 Ω *m. The resistivity of these rocks is greatly dependent on the degree of fracturing, and the percentage of the fractures filled with ground water. A given rock type can have a large range of resistivity, from about 1000 to 10 million Ω *m, depending on whether it is wet or dry. This characteristic is useful in the detection of fracture zones and other weathering features, such as in engineering and groundwater surveys.

➤ **Electrical properties of mineral ores**

Metals, such as iron, have extremely low resistivity values. Metallic sulfides (such as pyrrhotite, galena and pyrite) have typically low resistivity values of less than 1 Ω *m. The resistivity value of a particular ore body can differ greatly from the resistivity of the individual crystals. Other factors, such as the nature of the ore body (massive or disseminated) have a significant effect. Graphitic slate has a low resistivity value, similar to the metallic sulfides, which can give rise to problems in mineral surveys. Most oxides, such as hematite, do not have a significantly low resistivity value. One exception is magnetite.

➤ **Electrode array**

Common array types are-

- Wenner array
- Wenner-Schlumberger array
- Dipole-dipole array
- Pole-dipole
- Multiple gradient array

Wenner array:The Wenner array is an attractive choice for a survey carried out in a noisy area (due to its high signal strength) and also if good vertical resolution is required.

Wenner-Schlumberger array:The Wenner-Schlumberger array (with overlapping data levels) is a reasonable all-round alternative if both good horizontal and vertical resolutions are needed, particularly if good signal strength is also required. This is a combination of the Wenner and Schlumberger arrays. The “n” factor for this array is the ratio of the distance between the C1-P1 (or P2-C2) electrodes to the spacing (“a”) between the P1-P2 potential pair. The geometric factor is proportional to n^2 . Figure 2 given below shows the Wenner- Schlumberger array.

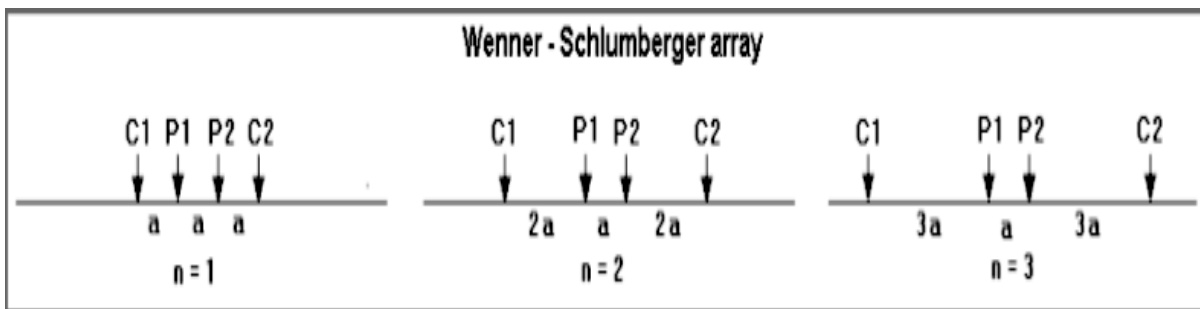


Figure 2: Wenner- Schlumberger array (source: PASI-2010) [17]

Dipole-dipole array: The dipole-dipole array might be a more suitable choice if good horizontal resolution and data coverage is important (assuming your resistivity meter is sufficiently sensitive and there is good ground contact). To use this array, the resistivity meter should have comparatively high sensitivity and very good noise filtering circuitry, and there should be good contact between the electrodes and the ground. A high current output is also desirable. This array has been successfully used in many areas to detect structures such as cavities where the good horizontal resolution of this array is a major advantage. Figure 3 shows the Dipole-dipole array.

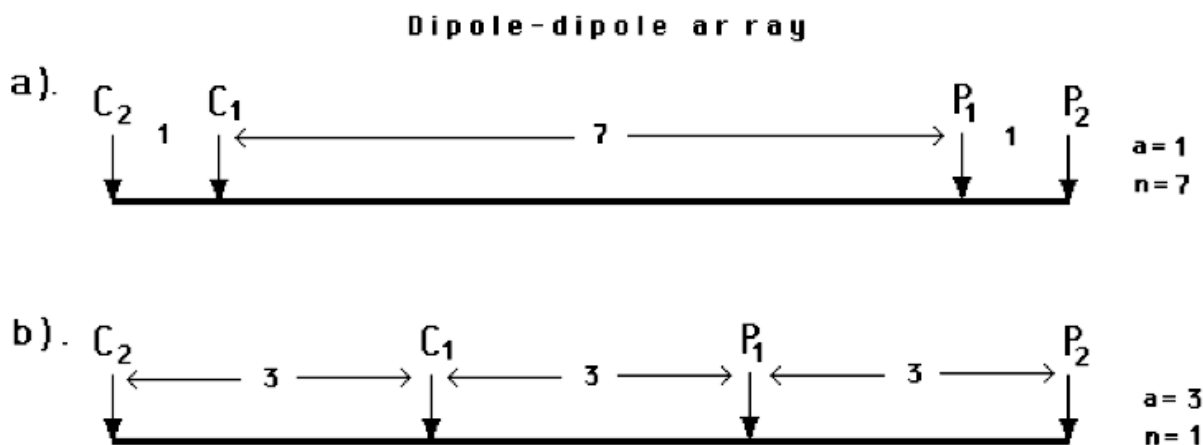


Figure 3: Dipole-dipole array (source: PASI –2010) [17]

Pole-dipole array: If the system is limited with a limited number of electrodes and limited survey line length, the pole-dipole array with measurements in both the forward and reverse directions might be a suitable choice. It is an alternative to the dipole-dipole for IP surveys. Unlike the other arrays, the pole-dipole array is an asymmetrical array.

The pole-dipole array requires a remote electrode, the C2 electrode, which must be placed sufficiently far from the survey line (at least 5 times the maximum C1-P1 distance used). Over symmetrical structures the apparent resistivity anomalies in the pseudo section are asymmetrical. In some situations, the asymmetry in the measured apparent resistivity values could influence the model obtained after inversion. Figure 4(a) and 4(b) shows the Pole-dipole array and Reverse pole-dipole array respectively.

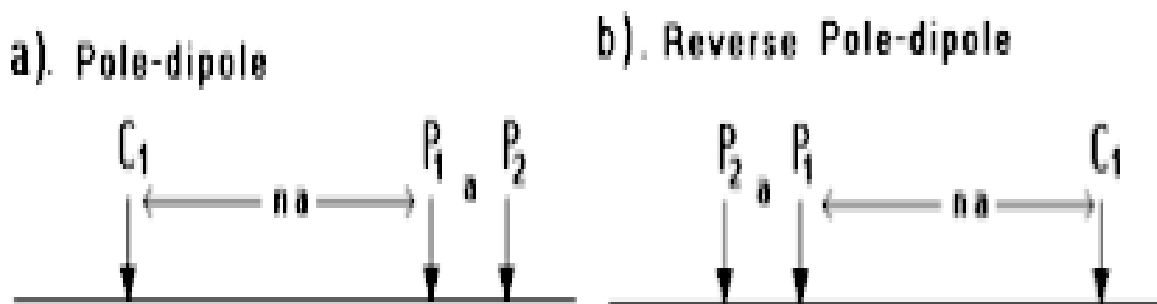


Figure 4: a) Pole-dipole array b) Reverse pole-dipole array (source: PASI – 2010) [17]

One method to eliminate the effect of the asymmetry of this array is to repeat the measurements with the electrodes arranged in the reverse manner. By combining the measurements with the “forward” and “reverse” pole-dipole arrays, any bias in the model due to the asymmetrical nature of this array would be removed. However these procedures will double the number of data points and consequently the survey time.

Multiple gradient array: This is a relatively new array developed primarily for multi-channel resistivity meter systems. In the multiple gradient arrays, different sets of measurements are made with the potential electrodes at different locations for the same current electrodes. As an example, for a system with 32 electrodes, one set of measurements can be made with the current electrodes at nodes 1 and 32. Next, another series of measurements are made with the current electrodes at nodes 1 and 16, as well as another with the current electrodes at 16 and 32. A similar set of measurements can be made with the C1-C2 electrodes at 1-8, 8-16, 16-24 and 2-32. This can be repeated using smaller distances between the current electrodes. Figure 5 shows the Multiple Gradient array.

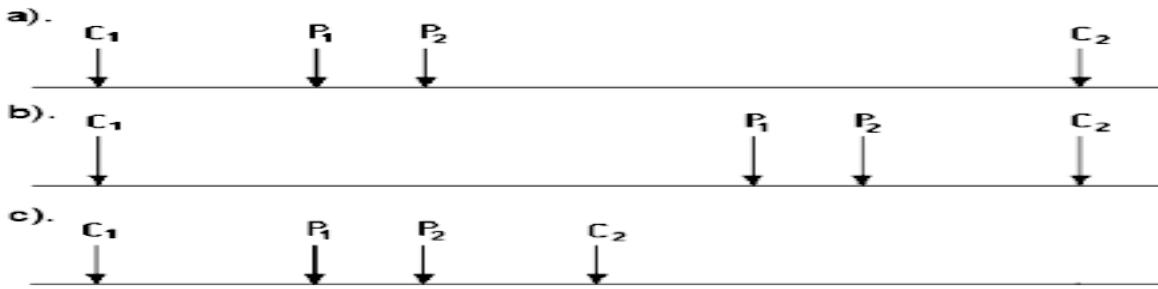


Figure 5: Multiple Gradient array (source: PASI –2010) [17]

Wenner configuration is, on equal terms, the most robust since it allows a greater ΔV signal and therefore less sensitive to environmental noise. This is due to the geometrical factor K , for Wenner is the smallest possible.

Among the characteristics of an array that should be considered are:

- the depth of investigation
- the sensitivity of the array to vertical and horizontal changes in the subsurface resistivity
- the horizontal data coverage
- the signal strength

The Figure 6 below shows the electrode arrays of different methods-

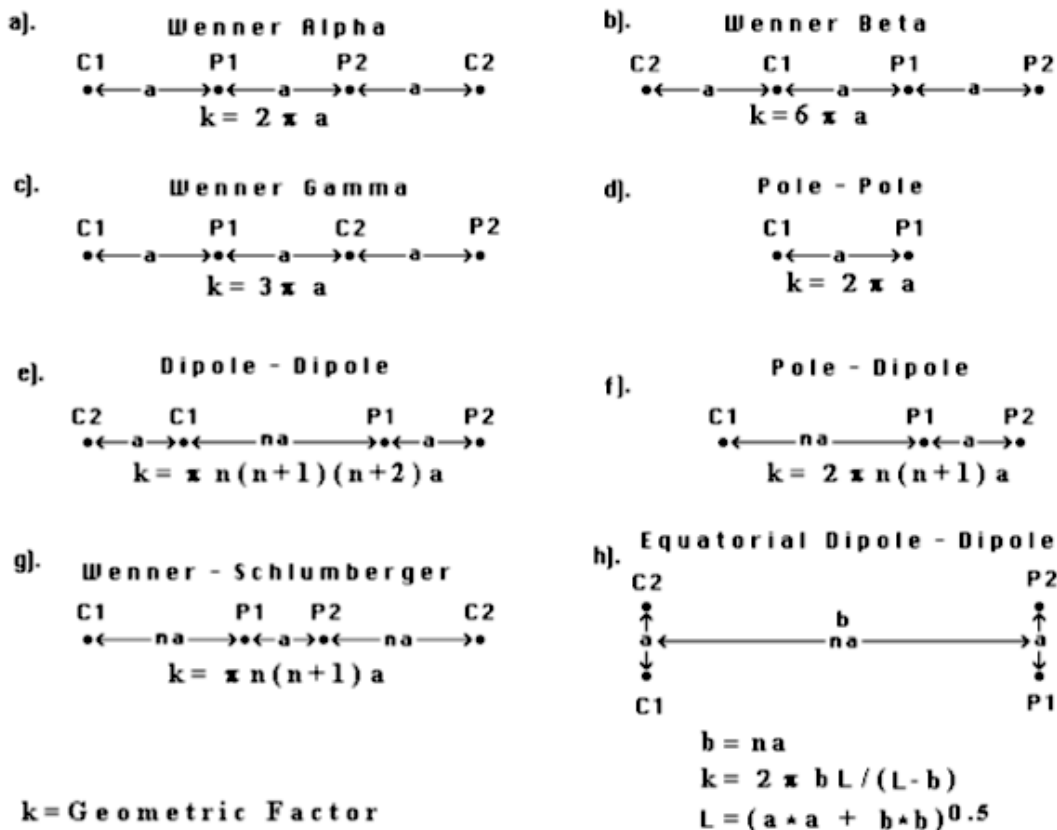


Figure 6: Electrode arrays of different methods (source: PASI – 2010) [17]

The signal strength is an important factor in noisy areas, or when large electrode spacing's are used or for surveys with conductive material. The signal strength is inversely proportional to the geometric factor, so it can be easily estimated. The Wenner (alpha) array has the smallest geometric factor, and thus the highest signal strength. This means surveys with the Wenner alpha array are generally less noisy. The pole-pole array has the same geometric factor but it has higher telluric noise due to the large distance between the potential electrodes. The geometric factor for the dipole-dipole array is proportional to n^3 , thus dipole-dipole surveys tend to have the noisiest data. As a general rule, the maximum 'n' value should not exceed 6. The geometric factors for pole-dipole and Wenner-Schlumberger arrays are proportional to n^2 , thus the signal strength is stronger than the dipole-dipole but weaker than the Wenner. The signal strength for the gradient array is between that of the Schlumberger and pole-dipole arrays.

➤ **Depth of investigation - different arrays**

The "median depth of investigation", z_e , can be easily calculated for different arrays, and the results are listed in the table below. The depths are given as the ratio to the 'a' spacing or the total length 'L' of the array. To calculate the actual depth of investigation, just multiply this ratio by the 'a' spacing or 'L' length used in the field survey. Table 1 shows the combination of depth for different arrays-

Table 1: Combination of depth for different arrays (source: PASI –2010) [17]

Array type	z_e/a	z_e/L	Array type	z_e/a	z_e/L
Wenner Alpha	0.519	0.173	Wenner-Schlumberger		
Wenner Beta	0.416	0.139	n = 1	0.519	0.173
Wenner Gamma	0.594	0.198	n = 2	0.925	0.186
			n = 3	1.318	0.189
Dipole-dipole			n = 4	1.706	0.190
n = 1	0.416	0.139	n = 5	2.093	0.190
n = 2	0.697	0.174	n = 6	2.478	0.191
n = 3	0.962	0.192	n = 7	2.863	0.191
n = 4	1.220	0.203	n = 8	3.247	0.191
n = 5	1.476	0.211	n = 9	3.632	0.191
n = 6	1.730	0.216	n = 10	4.015	0.191
n = 7	1.983	0.220			
n = 8	2.236	0.224	Pole-dipole		
			n = 1	0.519	
Equa. dipole-dipole			n = 2	0.925	
n = 1	0.451	0.319	n = 3	1.318	
n = 2	0.809	0.362	n = 4	1.706	
n = 3	1.180	0.373	n = 5	2.093	
n = 4	1.556	0.377	n = 6	2.478	
			n = 7	2.863	
Pole-Pole	0.867		n = 8	3.247	

The Wenner alpha array is about half the 'a' spacing between the electrodes. The pole-pole array has the deepest depth of investigation. The 'median depth of investigation' for the dipole-dipole array is probably an underestimate, due to the extreme form of the shape of the sensitivity function.

➤ **Types of surveys and models**

In geophysical inversion, the finding is a model that gives a response that is similar to the actual measured data. The model is an idealized mathematical representation of a section of the earth (which is always 3-D). The models used can be classified as 1-D, 2-D and 3-D.

The Figure 7 below illustrates the models-

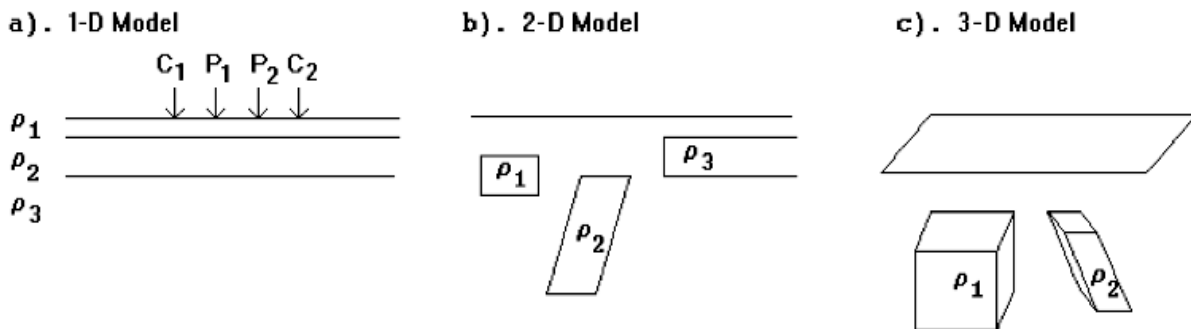


Figure 7: Different resistivity models (source: PASI –2010) [17]

1-D electrical imaging survey: Resistivity only changes in the vertical direction (with depth). 1-D surveys are the simplest to carry out, but interpretation model is too simplistic and not sufficiently accurate in many cases. Traditional 1-D models are probably too inaccurate for most surveys where there are significant lateral variations. Lateral changes might be mistaken for vertical changes in the resistivity.

2-D electrical imaging survey: A 2-D imaging survey is usually carried out with a computer controlled resistivity meter system connected to a multi-electrode cable system. The control software automatically selects the appropriate four electrodes for each measurement to give 2-D coverage of the subsurface. A large variety of arrays and survey arrangements can be used with such a system. Resistivity changes in the vertical direction and one horizontal direction (the x-direction). Assume resistivity does not change in y-direction. 2-D surveys and models are potentially the most accurate, but requires involves higher surveys costs and greater computational resources.

To plot the data from a 2-D imaging survey, the pseudo-section contouring method is normally used. The horizontal location of the point is placed at the mid-point of the set of electrodes used to make that measurement. The vertical location of the plotting point is placed at a distance that is proportional to the separation between the electrodes. For example, the data point measured by electrodes 1, 2, 3 and 4 are plotted at the mid-point between electrodes 2 and 3 in the diagram below. Figure 8 shows an example of the electrodes arrangement and measurement sequence that can be used for a 2-D electrical imaging survey.

Figure 8 below shows the Sequence of measurements to build up a pseudo-section using a computer controlled multi-electrode survey setup

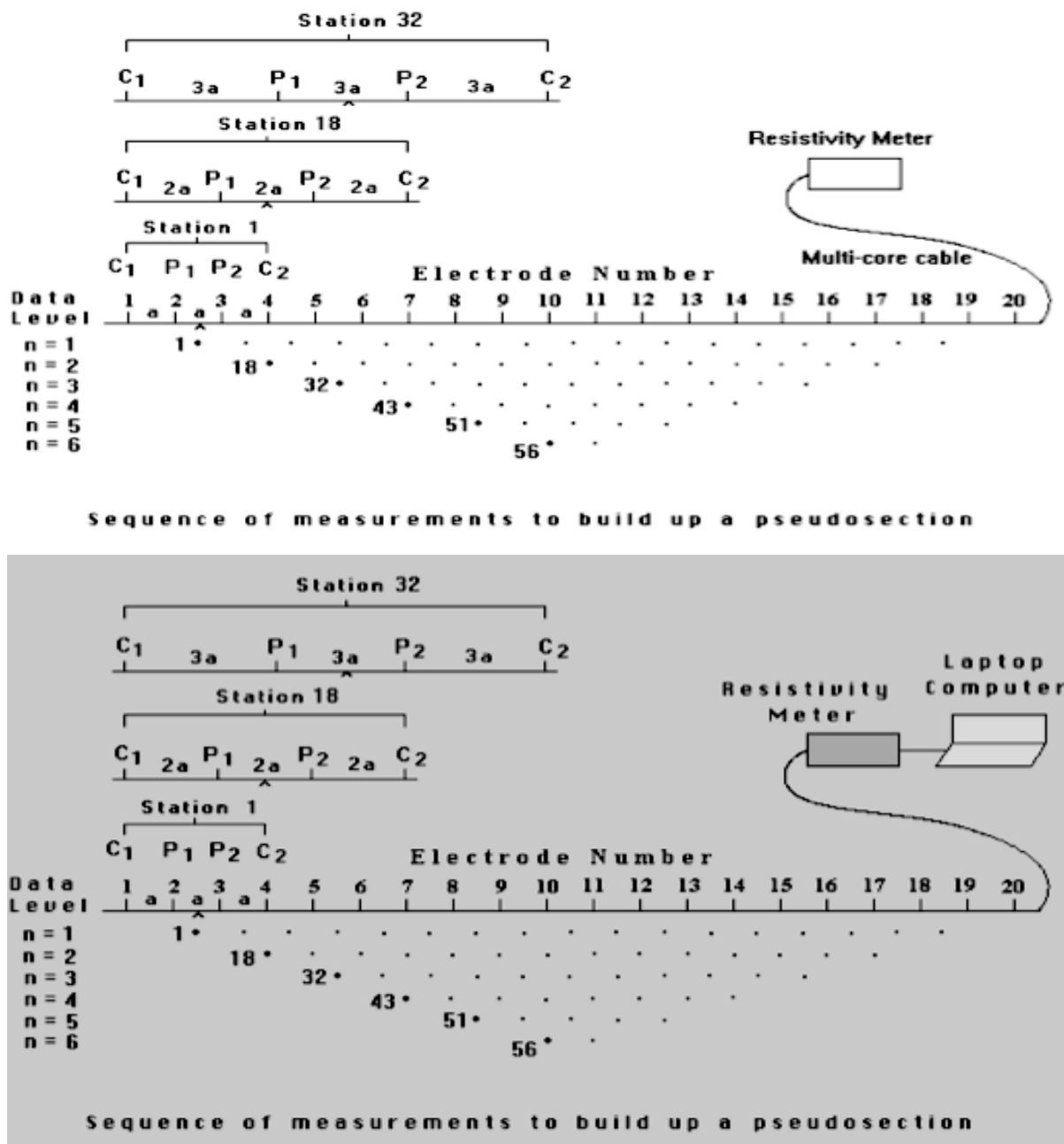


Figure 8: Sequence of measurements to build up a pseudo-section using a computer controlled multi-electrode survey setup(source: PASI –2014) [17]

A 2-D model is used to interpret the data from a 2-D imaging survey. The model usually consists of a large number of rectangular cells. The size and position of each cell is fixed. An inversion program is used to determine the resistivity of the cells from the measured apparent resistivity values. Figure 9 shows the arrangement of model blocks and apparent resistivity datum points-

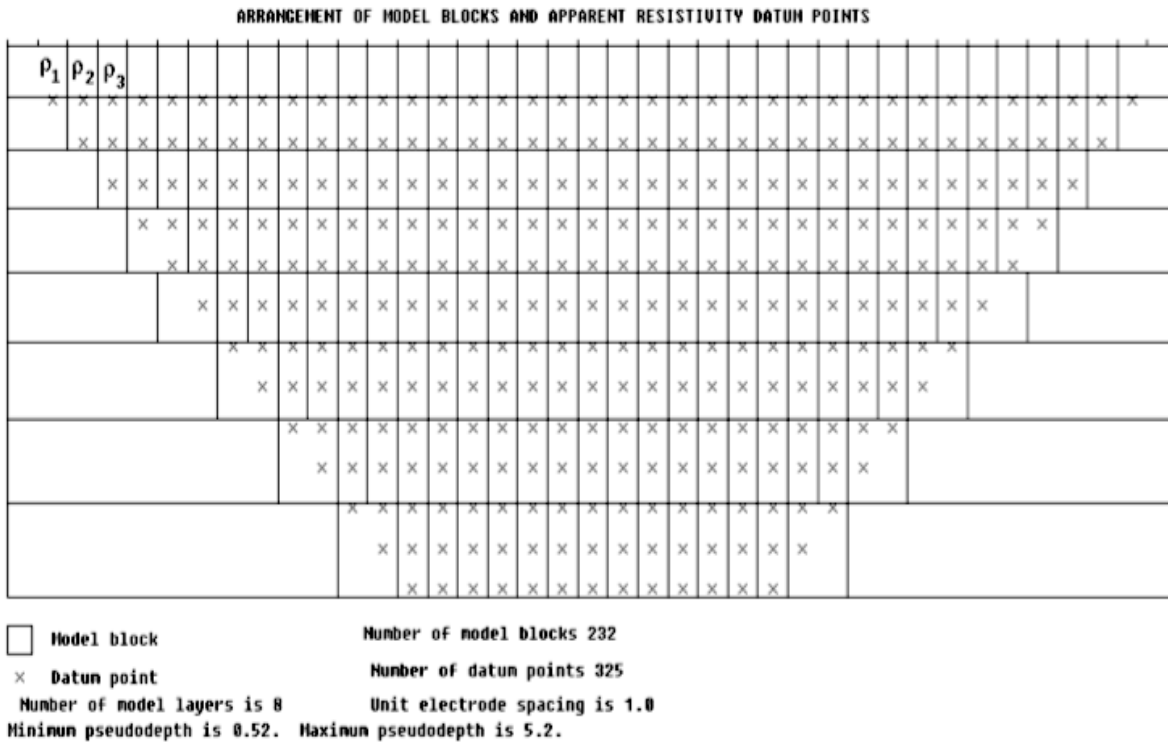


Figure 9: Arrangement of model blocks & apparent resistivity datum points (source: www.geoelectrical.com, 2010) [18]

3-D electrical imaging survey: Resistivity can change in all directions. Probably the best compromise in many situations, particularly over elongated geological structures. For more complex situations, a 2-D (or even a 3-D) survey and interpretation model is required.

➤ **The software RES2DINV**

RES2DINV is a computer program that will automatically determine a two-dimensional (2-D) resistivity model for the subsurface for the data obtained from electrical imaging surveys (Griffiths and Barker 1993) [7]. This program is designed to invert large data sets (with about 200 to 21000 data points) collected with a system with a large number of electrodes (about 25 to 16000 electrodes). The 2-D model used by the inversion program, which consists of a number of rectangular blocks, is shown in Figure 9.

The arrangement of the blocks is loosely tied to the distribution of the data points in the pseudo-section. The distribution and size of the blocks is automatically generated by the program using the distribution of the data points as a rough guide. The depth of the bottom row of blocks is set to be approximately equal to the equivalent depth of investigation of the data points with the largest electrode spacing (Edwards 1977) [8]. The survey is usually carried out with a system where the

electrodes are arranged along a line with a constant spacing between adjacent electrodes. However, the program can also handle data sets with non-uniform electrode spacing.

A forward modeling subroutine is used to calculate the apparent resistivity values, and a non-linear least-squares optimization technique is used for the inversion routine (deGroot-Hedlin and Constable 1990, Loke and Barker 1996a) [9-10]. The program supports both the finite-difference and finite-element forward modeling techniques. This program can be used for surveys using the Wenner, pole-pole, dipole-dipole, pole-dipole, Wenner-Schlumberger and equatorial dipole-dipole (rectangular) arrays. In addition to these common arrays, the program even supports non-conventional arrays with an almost unlimited number of possible electrode configurations. Besides normal surveys carried out with the electrodes on the ground surface, the program also supports underwater and cross-borehole surveys.

The inversion routine used by the program is based on the smoothness-constrained least-squares method (deGroot-Hedlin and Constable 1990, Sasaki 1992) [9, 11]. The smoothness-constrained least-squares method is based on the following equation-

$$(\mathbf{J}^T\mathbf{J} + \mathbf{u}\mathbf{F})\mathbf{d} = \mathbf{J}^T\mathbf{g}$$

Where $\mathbf{F} = \mathbf{f}_x\mathbf{f}_x^T + \mathbf{f}_z\mathbf{f}_z^T$

f_x = horizontal flatness filter

f_z = vertical flatness filter

\mathbf{J} = matrix of partial derivatives

\mathbf{u} = damping factor

\mathbf{d} = model perturbation vector

\mathbf{g} = discrepancy vector

One advantage of this method is that the damping factor and flatness filters can be adjusted to suit different types of data. The program supports a new implementation of the least-squares method based on a quasi-Newton optimization technique (Loke and Barker 1996a). This technique is significantly faster than the conventional least-squares method for large data sets and requires less memory.

3. Literature review

Electrical resistivity is known to be highly variable among other physical properties of rock. In some cases, different in extreme values of a single rock type can differ by a factor approaching several

orders of magnitude. Wide range of rock's resistivity parameter has always been the reason that makes it difficult to distinguish subsurface rock type if no information on the geological surroundings of field survey is available. Electrical current flows through the earth material under subsurface through two methods, which are electrolytic and electronic conduction [12].

Electronic conduction, which is conduction through the rock's mineral compositions, occurs mainly through metallic ore minerals, providing that these minerals exist in dense enough concentration. However, most conducting minerals rarely exist in sufficient quantity in a rock composition, especially granite, to have considerable effect on the electrical properties of host rock. This conduction is controlled by matrix properties (semi conduction, lattice defects, and conductive accessories) which often resulted in very high resistivity values [13].

Thus, for dry rock, it is common to find the resistivity values to be higher than $10^4 \Omega \cdot m$. For most subsurface rock, electrical conduction occurs mainly through groundwater that exists in pores and cracks of the rocks. The flow of current in electrolyte conduction through rock is largely influenced by the porosity of the rock. Generally, for rocks that are still in their original conditions (in situ condition), rock with higher porosity have lower resistivity. Under any normal condition, the porous structure of rock is partly or completely filled with underground water, which usually carries salt solution and thus increasing the moisture content of the rock. It is not unusual for igneous rock to have moisture content less than 1%. However, even that small percentage of water is enough to affect the rock's resistivity considerably [14].

Electrical geophysical methods have proven to be fairly effective in delineating inorganic contaminants in the subsurface. The mechanism and responses are fairly well understood. Their application for mapping organic contaminants in the subsurface, in particular non-aqueous phase liquids is not as well accepted nor the mechanisms as well understood. Various surveys have reported results conducted over subsurface organic contamination; however the actual anomaly associated with the organic contamination has been difficult to ascertain over other factors caused by variations in the porosity, degree of saturation, mineralogy, and structure [15]. For this reason, a number of laboratory studies and controlled spill experiments have been conducted over the past few years in order to evaluate the changes in the physical properties of the geological formations and the associated geophysical responses due the presence of the organic contamination [16].

4. Methodology of the study

The research has been conducted with the following methodology:

4.1 Study design

Over the past 45 years, Dhaka city has experienced a rapid growth of urban population and it will continue in the future due to several unavoidable reasons. Hence, most of the areas of Dhaka city have already been occupied. As a result, different new areas are being reclaimed inside and near Dhaka city by both government and private agencies. General practice for reclaiming such areas is to fill low lands (ditches, lakes etc.). In most cases, the practice for developing new areas is just to fill low land by dredge fill materials. Different filling procedures are in practice to develop such land. One of them is to carry soil by vehicles from remote sources and manually dumped at the filling site. Due to huge traffic congestion, most widely used method is hydraulic filling procedure. In most cases, the dredged material is almost silty sand with high fines content. The presence of fines in hydraulic fill means greater compressibility and greater difficulty in compaction of the fill. Fines also reduce permeability and hence the rate of drainage is slow. Therefore consolidation rate is also slow. Since Dhaka city exists in seismic Zone 2 of Bangladesh. This silty sand layer may liquefy if an earthquake of sufficient magnitude occurs in future. As well as, it may cause geotechnical problems. It is clear that this very soft clay layer, in reclaimed areas demand special attention for designing foundation system on or through it. So, it is felt necessary to carry out research to know the characteristics of the soft organic clay layer of such reclaimed areas. Thereby, objectives of the study were defined to characterize the sub-surface soil profile of Dhaka city. Then methodology of the study was defined based on literature review.

4.2 Study area selection

Four different points of Dhaka city is selected as the study area. The points are selected upon some criteria such as free open space for electrical resistivity test, dominating soil characteristics of that region, land use characteristics etc. The list below shows the points of the study area. Table 2 shows the Geological and Geomorphological classification of the study area.

Table 2: Geological and Geomorphological classification of the study area

Sl. no	Date	Name of the point of study area	Location		City
			Latitude	Longitude	
01	13/10/2014	Kamrangir Char	23° 42' 34" N	90° 22' 04" E	Dhaka
02	16/11/2014	Bosila	23° 44' 32" N	90° 21' 10" E	Dhaka
03	17/11/2014	AftabNagor	23° 45' 38" N	90° 27' 02" E	Dhaka
04	18/11/2014	BUET Play Ground	23° 43' 19" N	90° 23' 48" E	Dhaka

4.3 Data collection

The Electrical Resistivity Tomography consists of the experimental determination of the apparent resistivity ρ of a given material, through joint measurements of electric current intensity and voltage introduced into the subsoil through electrodes, driven in the ground surface. By deploying a linear array and recording the electrical signals for an acquisition time, it is possible to back-figure a 2D pseudo-section, which can be subsequently turned into an actual resistivity section, with an investigated depth of the order of one sixth of the array length; of course, the longer the array, the higher the depth, but increasing the electrode spacing the resolution decreases.

The Electrical Resistivity Tomography data have been gathered through electrodes of length equal to 50 cm, partially driven into the ground. The electrodes were then connected through multichannel cables, adopting the Wenner-Schlumberger array configuration. This type of arrangement is hybrid between the Wenner and Schlumberger arrays: during the acquisition, the wiring is continuously changed so that the spacing a between the 'potential electrodes' remains constant, while that between the 'current electrodes' increases as a multiple n of a .

The data of the four points were collected using different electrode and spacing combination as the geology and the available free spaces of the points were different. The details of the data collection of the points are given below:

I. Kamrangir Char

- Low land area which is situated at a distance of about 500m-600m from the Buriganga River.
- Number of Electrodes used = 32
- Electrodespacing = 1m
- Three data acquisitions were made, two parallel acquisitions @ 5m apart and one cross acquisition across the center of the parallel acquisitions.

Figure 10 and Figure 11 given below illustrates the data acquisition setup in the field and spread of electrodes and ERT arrangement during resistivity test respectively.

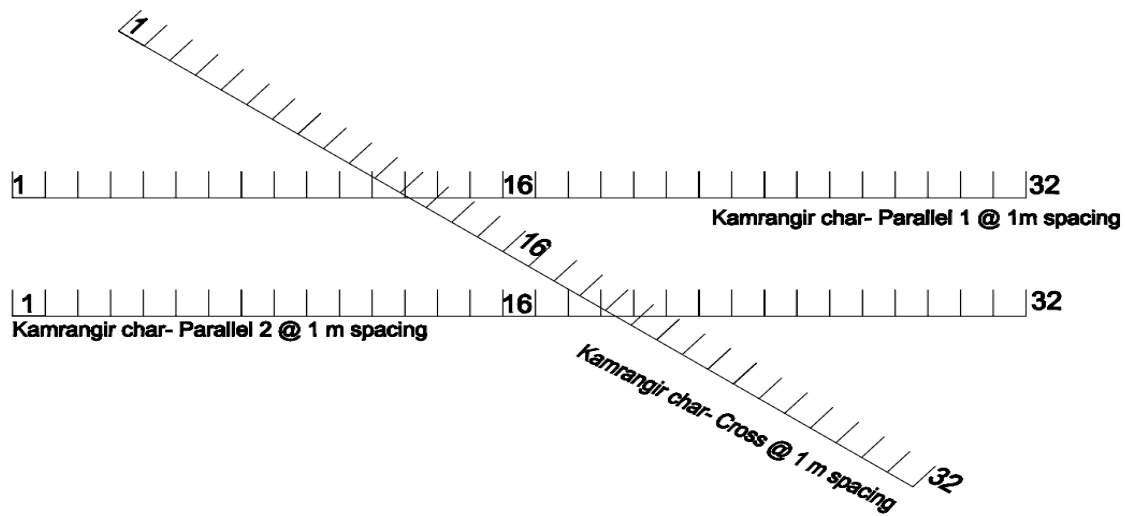


Figure 10: Data acquisition setup in the field

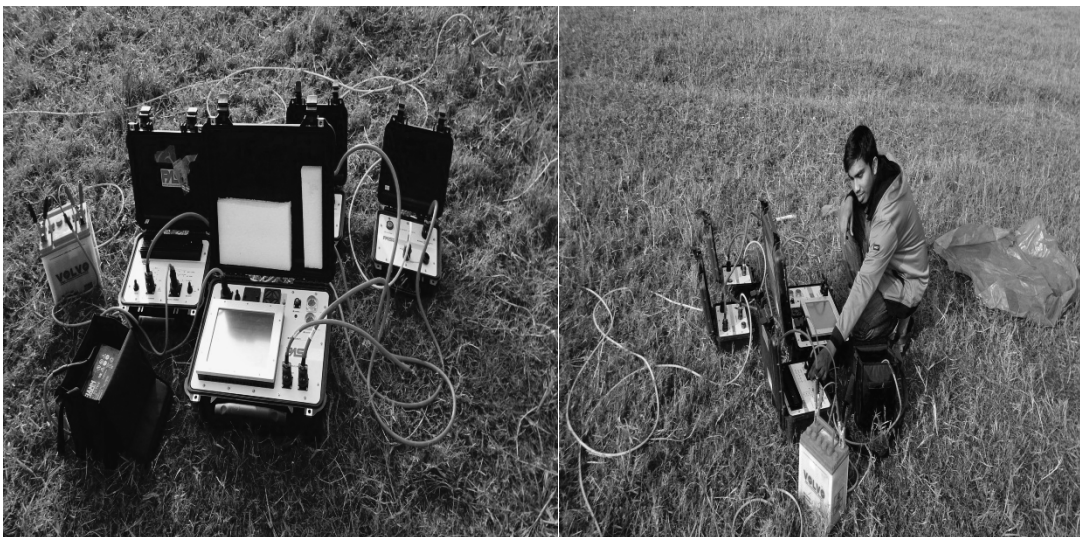


Figure 11: Spread of electrodes and ERT arrangement during resistivity test

II. **Bosila**

- Number of electrodes used = 32
- Two data acquisitions were made, one parallel acquisition and one cross acquisition across the center of the parallel acquisition.
- Spacing between electrodes of parallel acquisition is 2m and spacing between electrodes of cross acquisition is 1.5m

Figure 12 and Figure 13 given below illustrates the data acquisition setup in the field and spread of electrodes and ERT arrangement during resistivity test respectively.

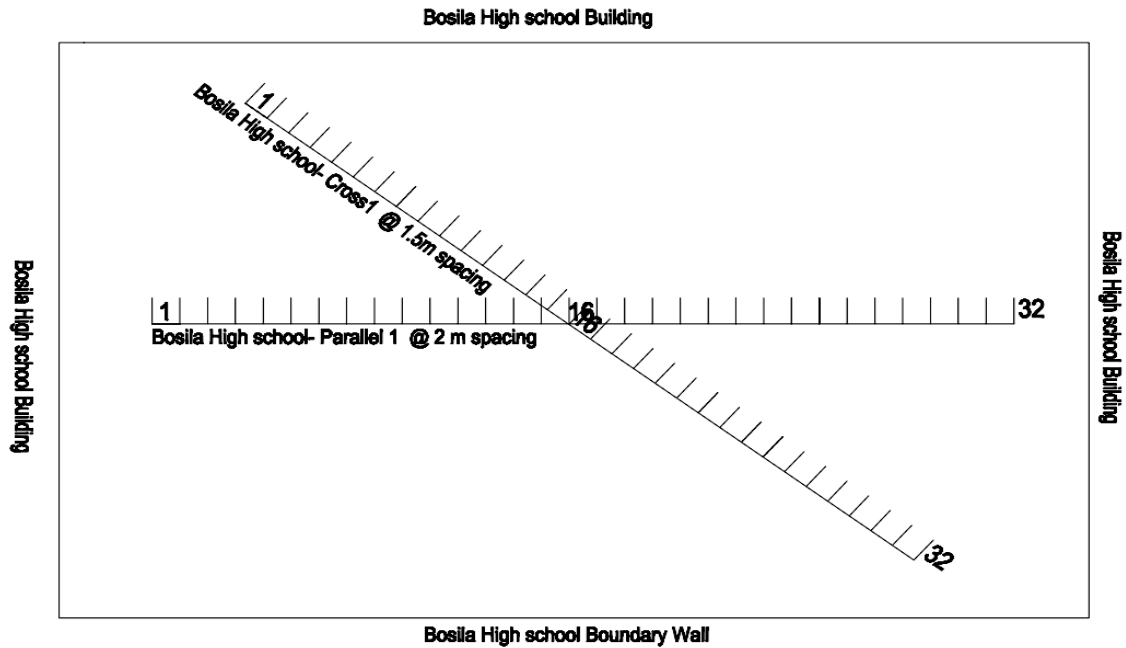


Figure 12: Data acquisition setup in the field



Figure 13: Spread of electrodes and ERT arrangement during resistivity test

III. AftabNagor

- Semi-submerged land during rainy season
- Number of electrodes used = 31
- Electrode spacing = 3m
- Two data acquisitions were made, one parallel acquisition and one cross acquisition across the center of the parallel acquisition.

Figure 14 and Figure 15 given below illustrates the data acquisition setup in the field and spread of electrodes and ERT arrangement during resistivity test respectively.

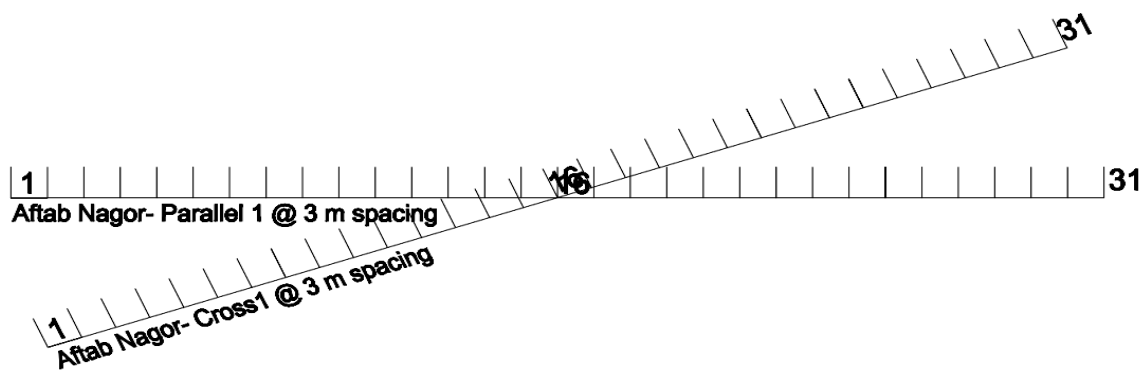


Figure 14: Data acquisition setup in the field



Figure 15: Spread of electrodes and ERT arrangement during resistivity test

IV. BUET Play Ground

- Number of electrodes used = 32
- Electrode spacing = 3m
- Four data acquisitions were made, two parallel acquisitions @ 5m apart and two cross acquisitions @ 5m apart across the center of the parallel acquisition.

Figure 16 and Figure 17 given below illustrates the data acquisition setup in the field and spread of electrodes and ERT arrangement during resistivity test respectively.

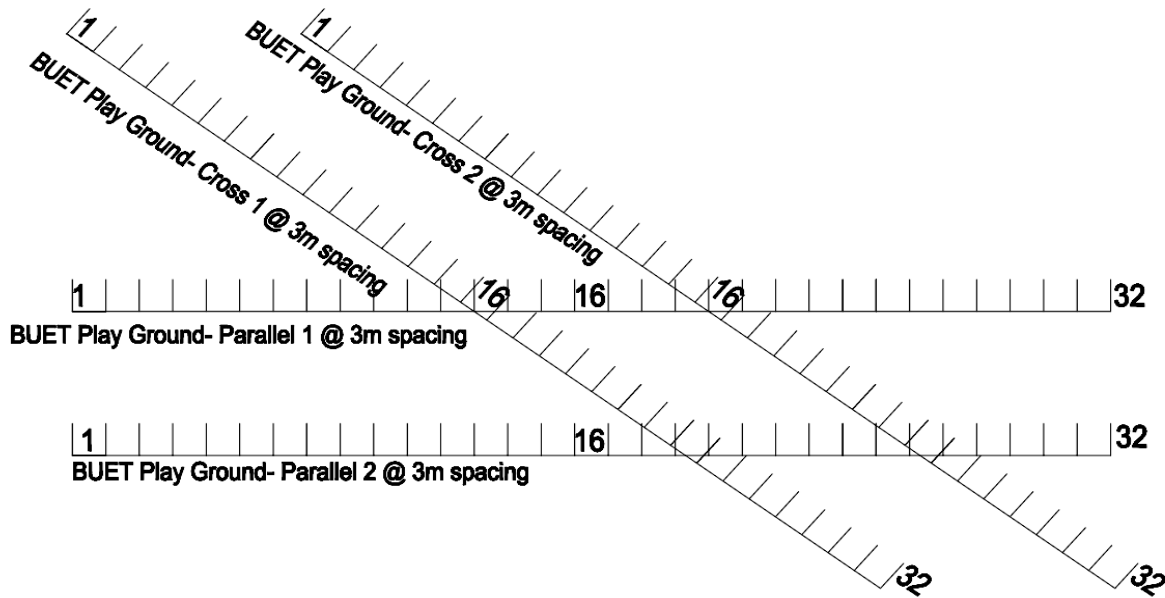


Figure 16: Data acquisition setup in the field



Figure 17: Spread of electrodes and ERT arrangement during resistivity test

4.4 Data processing and analysis

The data collected from the survey have been analyzed with the software RES2DINV. RES2DINV is a computer program that automatically determined a two-dimensional (2-D) resistivity model for the subsurface for the data obtained from electrical imaging surveys.

4.5 Preparation of Final Report

All information and findings were gathered and presented by tables and maps to prepare the final report.

5. Data processing and analysis

Sub-soil analysis is necessary for the dynamic characteristics of soil. The Electrical Resistivity Tomography (ERT) method was under-taken with several different electrode spacing. Wenner-Schlumberger array was used as electrode arrays. Measuring was performed with electrodes

positioned on the surface. Primary data were processed through a 2-D inverse method, using the program Res2DInv. The presented figures are the results of smoothness-constrained inversion; these outputs best fit the situation observed in the sites. The validity of these results is supported by the low RMS error. Sounding was performed with various electrode spacing and configurations according to the purpose and position of the particular site. Data from these profiles were also processed through a 2-D inverse method in the program Res2DInv. Table 3 shows the reference resistivity values table of various materials.

Table 3: Reference resistivity values table of various materials

Type of Soil or Water	Typical Resistivity Ωm	Usual Limit Ωm
Sea water	2	0.1 to 10
Clay	40	8 to 70
Ground well & spring water	50	10 to 150
Clay & sand mixtures	100	4 to 300
Shale, slates, sandstone etc	120	10 to 100
Peat, loam & mud	150	5 to 250
Lake & brook water	250	100 to 400
Sand	2000	200 to 3000
Moraine gravel	3000	40 to 10000
Ridge gravel	15000	3000 to 30000
Solid granite	25000	10000 to 50000
Ice	100000	10000 to 100000

i. Kamrangir Char

The electrode spacing was 1 m. Resistivity tomography's for Kamrangir Char was measured with Wenner–Schlumberger array. The validity of Wenner–Schlumberger ERT section of Kamrangir Char is supported by good low RMS error of 5.6% for the 11th iteration for parallel acquisition and of 4.4% for the 20th iteration for cross acquisition. The depth of the investigation was found of about 5.73 m. The resistivity's along the profile span a range of 1.55-7526 $\Omega\text{ m}$ for parallel acquisition and 8.29-6671 $\Omega\text{ m}$ for cross acquisition. The soil profile of the Kamrangir Char is shown in the Table 4. The analysis for soil profile is made by combining both the parallel and cross acquisition. This

profile exists three soil layers. The top layer exist clayey filling sand from 0 to 2.62 m. The second layer exist organic clay from 2.62 to 4.99 m and the third layer exist clay from 4.99 to 5.76 m. Figure 18 and Figure 19 shows the model resistivity of ERT at Kamrangir Char of parallel acquisition and cross acquisition respectively.

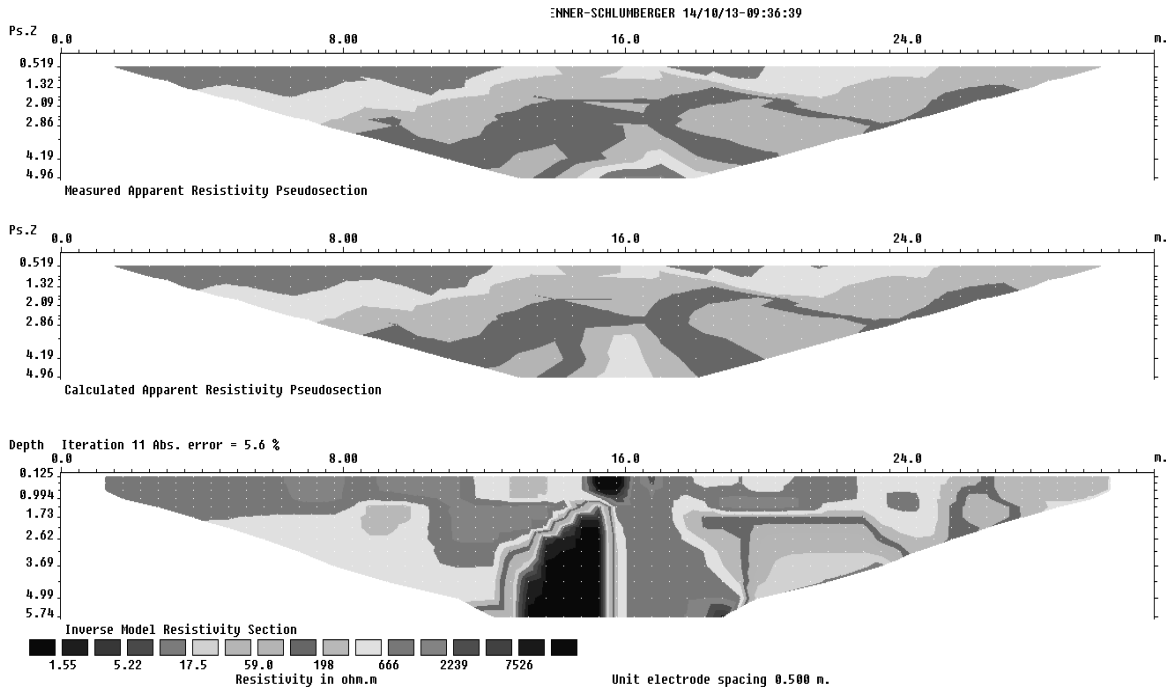


Figure 18: Model resistivity of ERT at Kamrangir Char, parallel acquisition

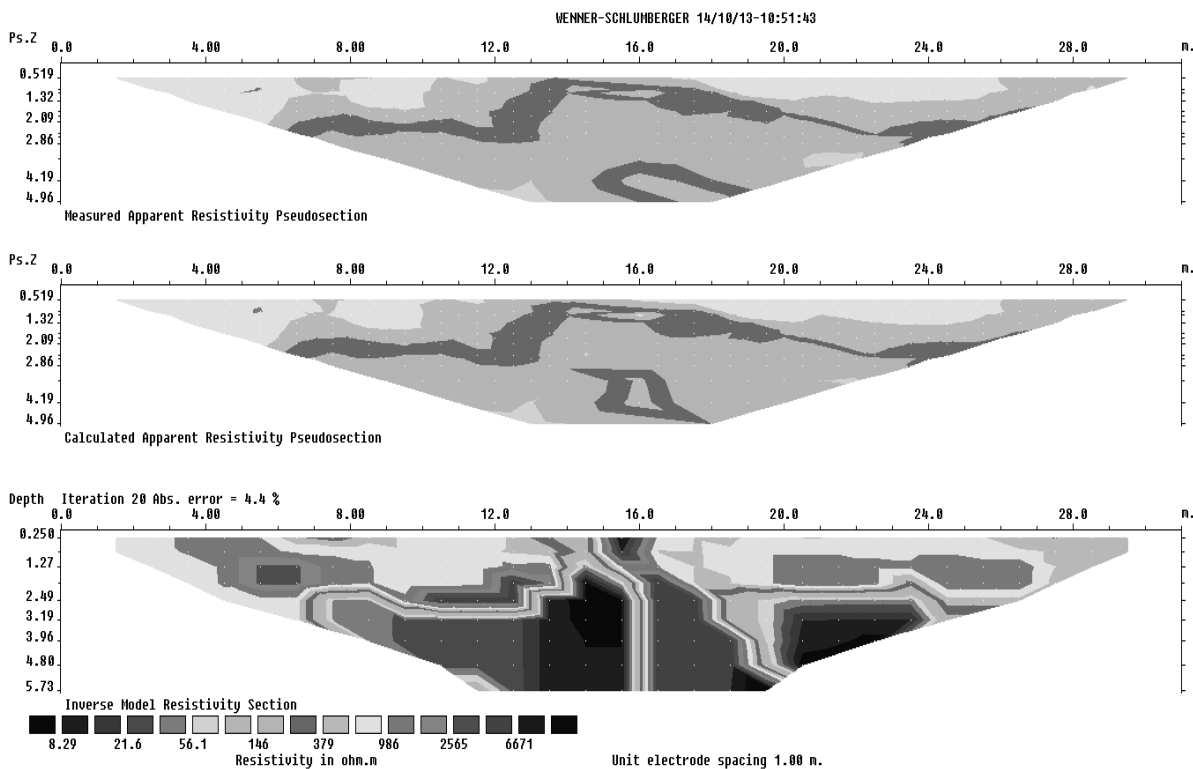


Figure 19: Model resistivity of ERT at Kamrangir Char, cross acquisition

Table 4 given below shows the Electrical Resistivity Tomography (ERT) result at Kamrangir Char-

Table 4: Electrical Resistivity Tomography (ERT) result at Kamrangir Char

Depth (meter)	Soil Description	Resistivity ranges (Ω m)
0 to 2.62	Filling Sand	200-666
2.62 to 4.99	Clay and Sand mixture	10-200
4.99 to 5.76	Sand	198-2239

Kamrangir Char is situated in latitude $23^{\circ} 42' 34''$ N and longitude $90^{\circ} 22' 04''$ E. The upper 2.62 m is filling sand. For better resolution and model images salted water was used outside the periphery of the inserted electrodes to increase the conductivity of electricity as the soil surface was in very dry condition. In the model resistivity of ERT there are some high local resistivity's which is insignificant with respect to local soil profile.

ii. Bosila

The electrode spacing was 2 m and 1.5 m for parallel and cross acquisition respectively. Resistivity tomography's for Bosila was measured with Wenner–Schlumberger array. The validity of Wenner–Schlumberger ERT section of Bosila is supported by good low RMS error of 10.2% for the 22th iteration for cross acquisition and of 33.8% for the 25th iteration for parallel acquisition. The depth of the investigation was found of about 8.00 m. The resistivity's along the profile span a range of 0.047-507 Ω m for cross acquisition and 1.88-1872 Ω m for parallel acquisition. The soil profile of the Bosila is shown in the Table 5. The analysis for soil profile is made by combining both the parallel and cross acquisition. This profile exists four soil layers. The top layer exist filling sand from 0 to 2 m. The second layer exist organic clay from 2 to 4.88 m. The third layer exist clay from 4.88 to 6.75 m and the fourth layer exist sand from 6.75 to 10.5 m. Figure 20 and Figure 21 shows the model resistivity of ERT at Bosila of parallel acquisition and cross acquisition respectively.

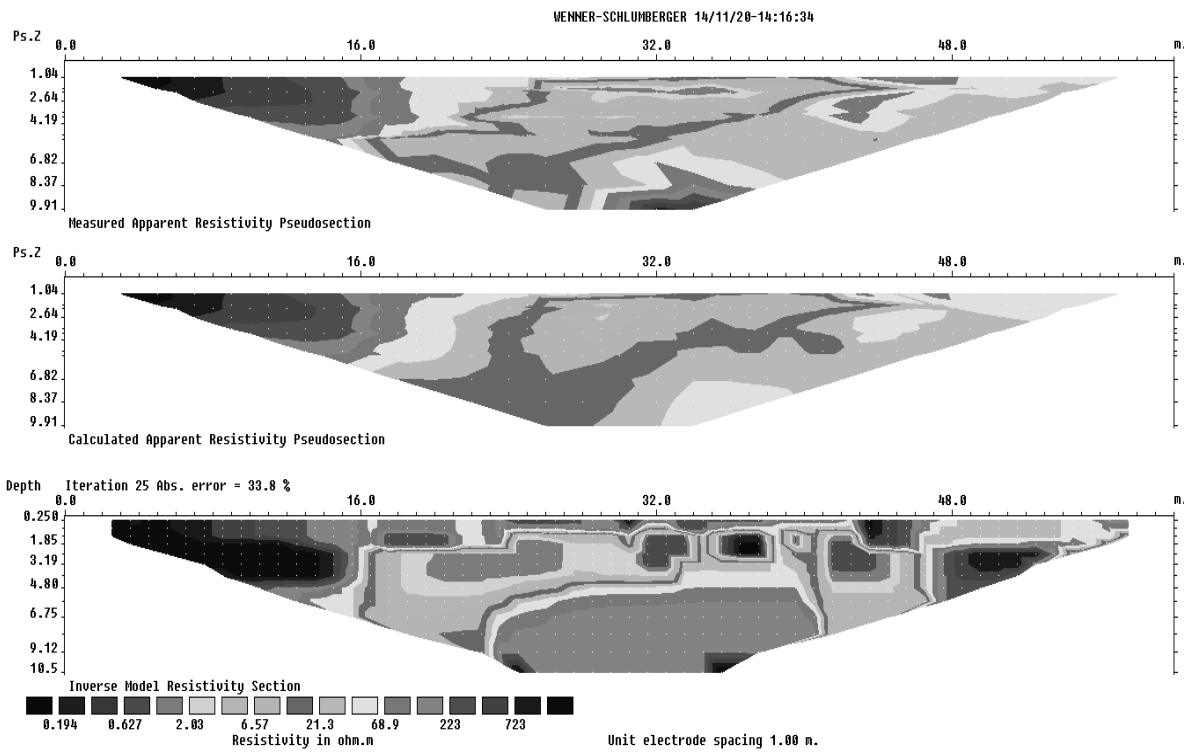
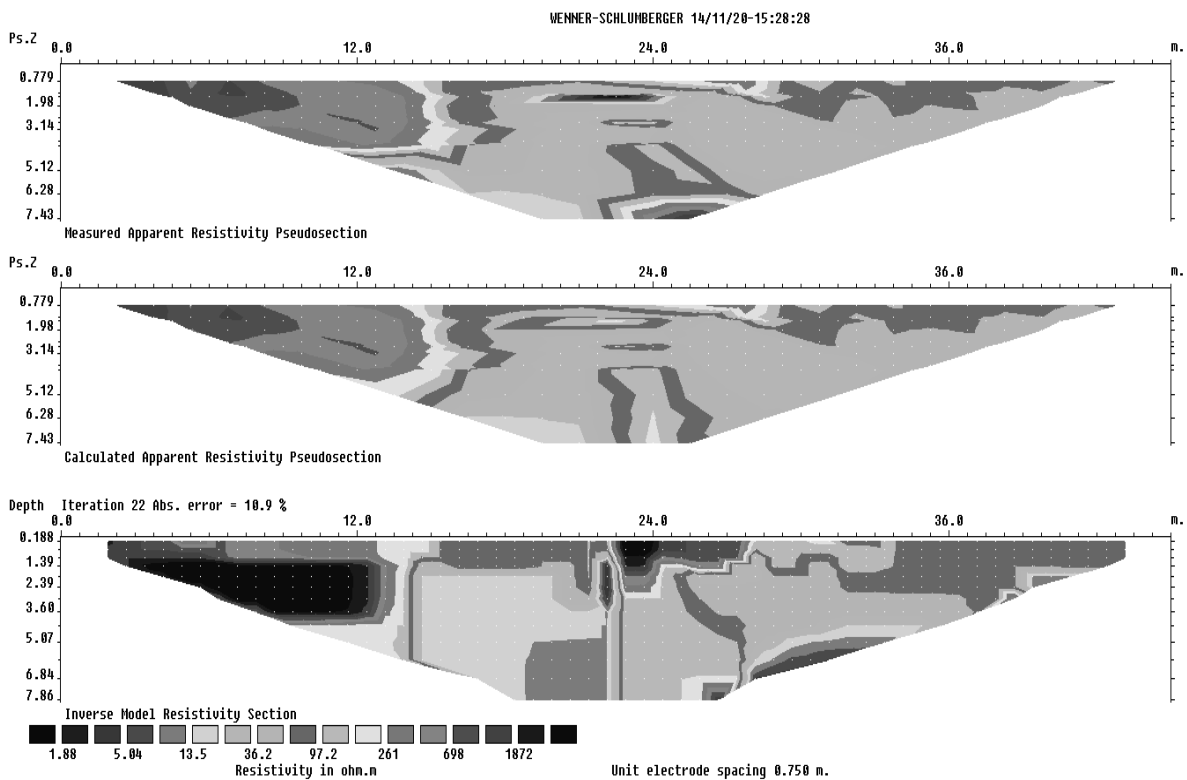


Figure 20: Model resistivity of ERT at Bosila, Parallel acquisition



Figure

21: Model resistivity of ERT at Bosila, Cross acquisition

Table 5 given below shows the Electrical Resistivity Tomography (ERT) result at Bosila-
 Table 5: Electrical Resistivity Tomography (ERT) result at Bosila

Depth (meter)	Soil Description	Resistivity ranges (Ω m)
0 to 2	Filling Sand	68.9-223
2 to 4.88	Clay	1-68.9
4.88 to 6.75	Clay and Sand mixture	68.9-273
6.75 to 10.5	Sand	273-723

Bosila is situated in latitude $23^{\circ}44'32''$ N and longitude $90^{\circ}21'10''$ E. The upper 2 m is filling sand. For better resolution and model images salted water was used outside the periphery of the inserted electrodes to increase the conductivity of electricity as the soil surface was in very dry condition. In the model resistivity of ERT there are some high local resistivity's which is insignificant with respect to local soil profile. In the graph of model resistivity of Bosila, the left side is showing very high resistivity because that side is very adjacent of Bosila High School building. The foundation of the building is very nearby. From this illustration it is clear that the ERT machine is also useful for the investigation of the building foundation and their corresponding depth.

iii. Aftabnagar

The electrode spacing was 3 m for both parallel and cross acquisition. Resistivity tomography's for Aftabnagar was measured with Wenner–Schlumberger array. The validity of Wenner–Schlumberger ERT section of Aftabnagar is supported by good low RMS error of 15.1% for the 18th iteration for parallel acquisition and of 13.0% for the 12th iteration for cross acquisition. The depth of the investigation was found of about 20.4 m. The resistivity's along the profile span a range of 0.434-922 Ω m for parallel acquisition and 0.315-855 Ω m for cross acquisition. The soil profile of the Aftabnagar is shown in the Table 6. The analysis for soil profile is made by combining both the parallel and cross acquisition. This profile exists four soil layers. The top layer exist clayey filling sand from 0 to 2.98 m. The second layer exist sand from 2.98 to 7.28 m. The third layer exist clay from 7.28 to 10.1 m and the fourth layer exit sand from 10.1 to 20.4 m. Figure 22 and Figure 23 shows the model resistivity of ERT at Aftabnagar of parallel acquisition and cross acquisition respectively.

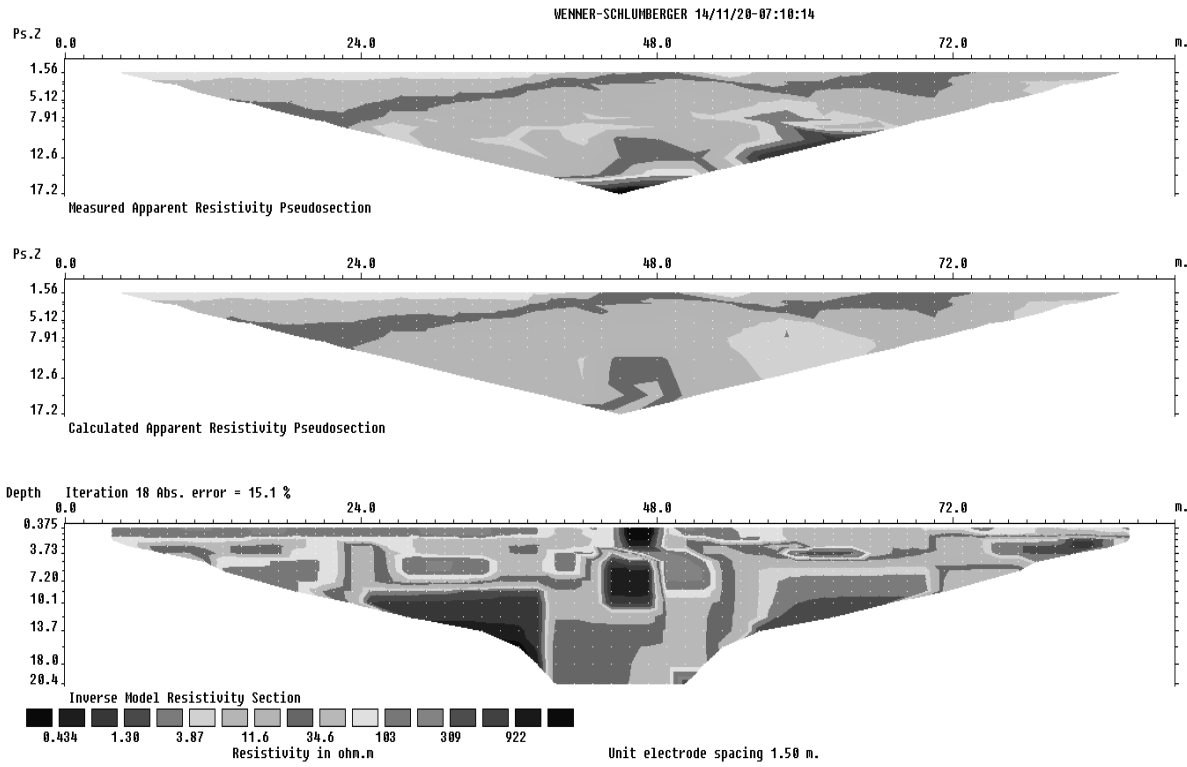


Figure 22: Model resistivity of ERT at Aftabnagar, Parallel acquisition

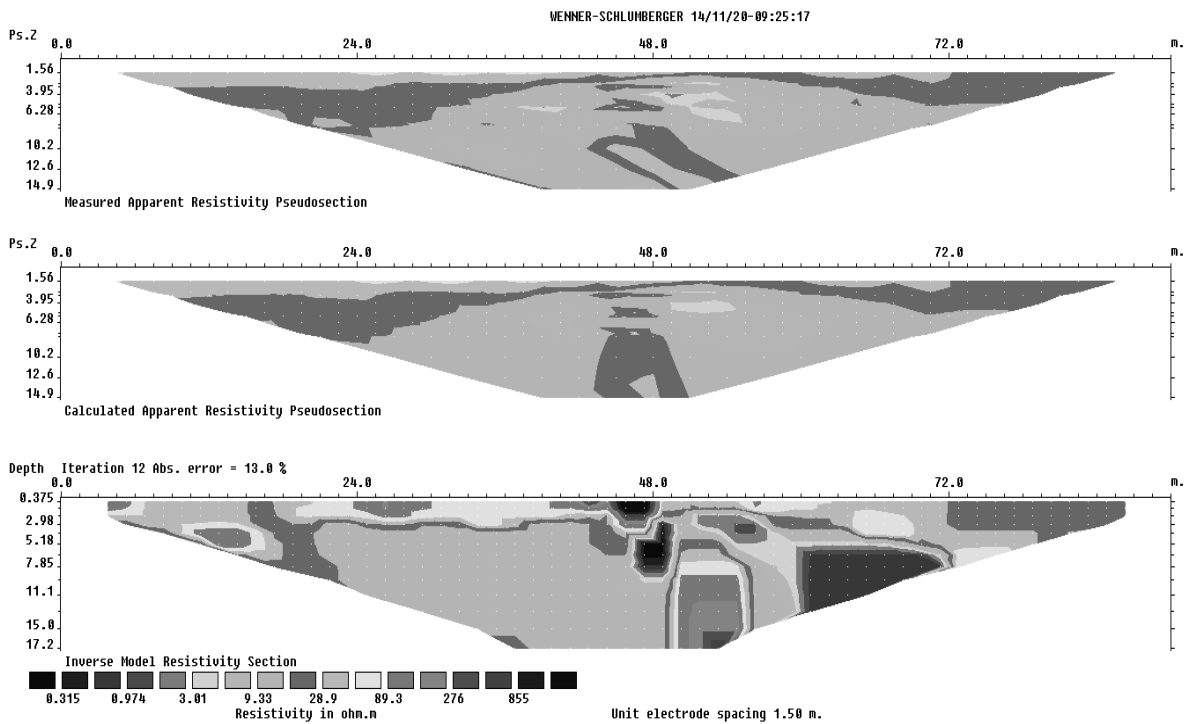


Figure 23: Model resistivity of ERT at Aftabnagar, Cross acquisition

Table 6 given below shows the Electrical Resistivity Tomography (ERT) result at Aftabnagar

Table 6: Electrical Resistivity Tomography (ERT) result at Aftabnagar

Depth (meter)	Soil Description	Resistivity ranges (Ω m)
0 to 2.98	Filling Sand	100-309
2.98 to 7.28	Clay	10-70
7.28 to 10.1	Clay and Sand mixture	10-309
10.1 to 20.4	Sand	309-922

Aftabnagar is situated in latitude $23^{\circ} 45' 38''$ N and longitude $90^{\circ} 27' 02''$ E. The upper 2.98 m is filling sand. For better resolution and model images salted water was used outside the periphery of the inserted electrodes to increase the conductivity of electricity as the soil surface was in very dry condition. In the model resistivity of ERT there are some high local resistivity's which is insignificant with respect to local soil profile.

iv. **BUET Play Ground**

The electrode spacing was 3 m for both parallel and cross acquisitions. Resistivity tomography's for BUET Play Ground was measured with Wenner–Schlumberger array. The validity of Wenner–Schlumberger ERT section of BUET Play Ground is supported by good low RMS error of 15.4% for the 3rd iteration for parallel acquisition and of 14.2% for the 8th iteration for cross acquisition. The depth of the investigation was found of about 19.7 m. The resistivity's along the profile span a range of 2.98-2938 Ω m for parallel acquisition and 03-874 Ω m for cross acquisition. The soil profile of the BUET Play Ground is shown in the Table 7. The analysis for soil profile is made by combining both the parallel and cross acquisition. This profile exists four soil layers. The top layer exist clayey silt from 0 to 5.18 m. The second layer exist clay from 5.18 to 7.85 m. The third layer exist clay and sand mix from 7.85 to 15.8 m and the fourth layer exit sand from 15.8 to 19.7 m. Figure 24 and Figure 25 shows the model resistivity of ERT at BUET Play Ground of parallel acquisition and cross acquisition respectively.

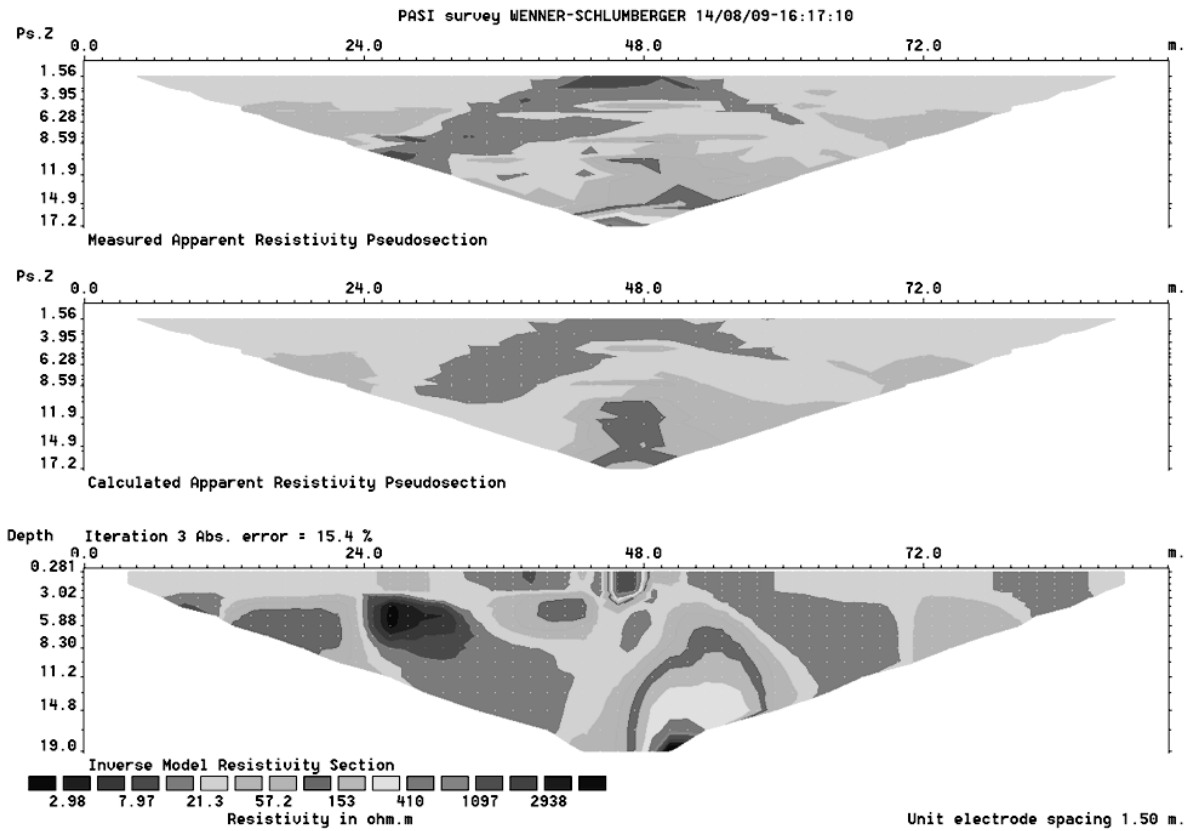


Figure 24: Model resistivity of ERT at BUET Play Ground, Parallel acquisition

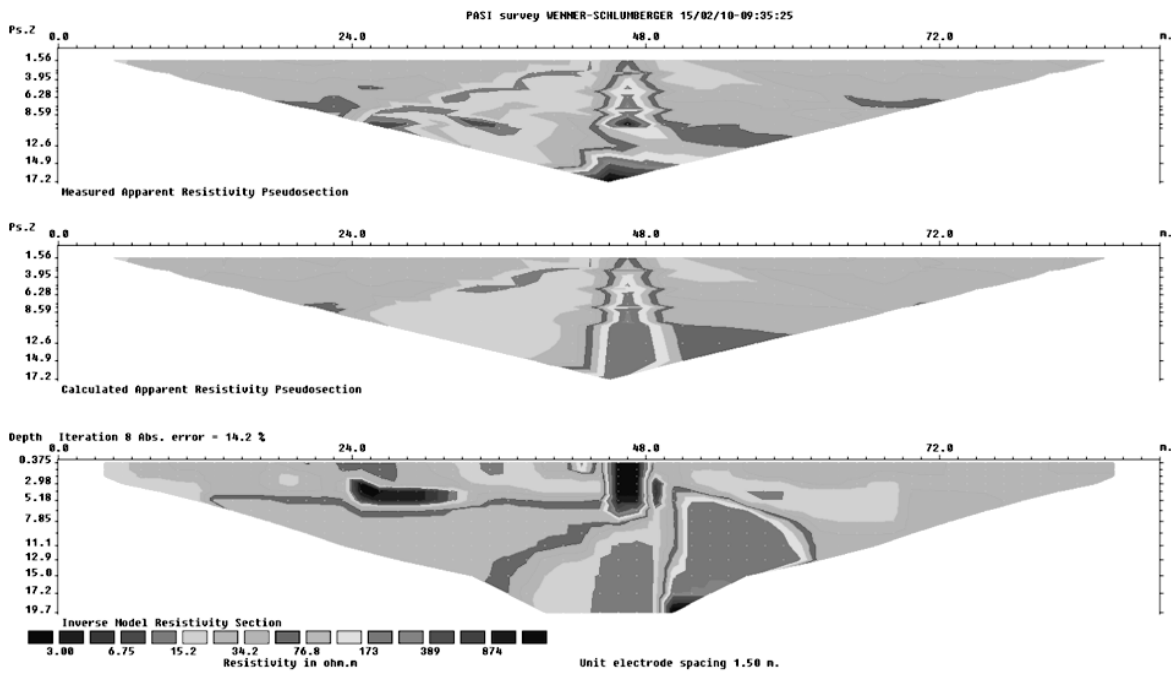


Figure 25: Model resistivity of ERT at BUET Play Ground, cross acquisition

Table 7 given below shows the Electrical Resistivity Tomography (ERT) result at BUET Play Ground.

Table 7: Electrical Resistivity Tomography (ERT) result at BUET Play Ground

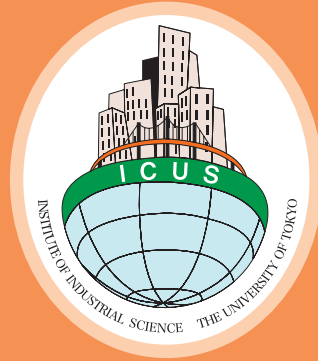
Depth (meter)	Soil Description	Resistivity ranges (Ω m)
0 to 5.18	Clayey silt	3-74
5.18 to 7.85	Clay	34.2-76.8
7.85 to 15.8	Clay and Sand mixture	76.8-389
15.8 to 19.7	Sand	389-1097

BUET Play Ground is situated in latitude 23° 43' 19" N and longitude 90° 23' 48" E. In the model resistivity of ERT there are some high local resistivity's which is insignificant with respect to local soil profile.

References

- [1] Schoor, M.V. "Detection of sinkholes using 2D electrical resistivity imaging," *Journal of Applied Geophysics* 50 (2002),pp. 393–399.
- [2] Osazuwa, I. B. and Chii, C.E., "Two-dimensional electrical resistivity survey around the periphery of an artificial lake in the Precambrian basement complex of northern Nigeria," *Journal of Physical Sciences* Vol. 5(3), pp. 238-245, March 2010.
- [3] Dahlin, T. "The development of DC resistivity imaging techniques" *Computer & Geosciences* 27 (2001), pp. 1019 – 1029
- [4] Compare, V. and Cozzolino, M. "Resistivity probability tomography imaging at the Castle of Zena, Italy," *EURASIP Journal on Image and Video Processing*, Volume 2009
- [5] Nguyen, F. and Garambois, S. "Image processing of 2D resistivity data for imaging faults," *Journal of Applied Geophysics* 57 (2005), pp.260 –277.
- [6] Giao, P.H. and Chung,S.G. "Electric imaging and laboratory resistivity testing for geotechnical investigation of Pusan clay deposits," *Journal of Applied Geophysics* 52 (2003), pp. 157 – 175
- [7] Griffiths D.H. and Barker R.D., 1993, "Two-dimensional resistivity imaging and modelling in areas of complex geology," *Journal of Applied Geophysics*, 29, 211-226
- [8] Edwards, L.S., 1977, "A modified pseudo-section for resistivity and induced polarization: *Geophysics*, 42, 1020-1036
- [9] deGroot-Hedlin, C. and Constable, S., 1990, "Occam's inversion to generate smooth, two-dimensional models from magnetotelluric data," *Geophysics*, 55, 1613-1624.

- [10] Loke M.H. and Barker R.D., 1996, "Rapid least-squares inversion of apparent resistivity pseudo-sections using a quasi-Newton method," *Geophysical Prospecting*, 44, 131-152
- [11] Sasaki, Y., Yoneda, Y. and Matsuo, K., 1992, "Resistivity imaging of controlled-source audiofrequency magnetotelluric data," *Geophysics*, 57, 952-955.
- [12] Loke, M.H. Tutorial, "2-D and 3-D electrical imaging surveys" (2004), pp. 13
- [13] Parkhomenko, E.I. "Electrical Properties of Rocks," Plenum Press, (1967), pp. 121
- [14] Pazdírek O. & Bláha V, "Examples of resistivity imaging using ME-100 resistivity field acquisition system." 58th EAGE conference, Amsterdam, The Netherlands, Extended Abstracts, P050 (1996)
- [15] Pitchford, A.M., A.T. Mazzella, and K.R. Scarbrough, 1989, "Soil-Gas and Geophysical Techniques for Detection of Subsurface Organic Contamination," Final Report, Air Force Engineering and Services Center Report, ESL-TR-87-67, 172 p.
- [16] Greenhouse, John, Brewster, M., Schneider, G., Redman, D., Annan, P., Olhoeft, G., Lucius, J., Sander, K., Mazzella, A., 1993, *Geophysics and Solvents: The Borden Experiment*, The Leading Edge, April 1993, p. 261-267.
- [17] PASI Geophysics, "Geotechnical Resistivity Methods" (2010).
- [18] www.goelectrical.com, "Goelectrical Imaging 2D & 3D" (2010).



International Center for Urban Safety Engineering
Institute of Industrial Science, The University of Tokyo

4-6-1 Komaba, Meguro-ku,
Tokyo 153-8505, Japan

Tel: +81-3-5452-6472

Fax: +81-3-5452-6476

<http://icus.iis.u-tokyo.ac.jp>

E-mail: icus@iis.u-tokyo.ac.jp

ISBN4-903661-72-5

